Master of Science Thesis

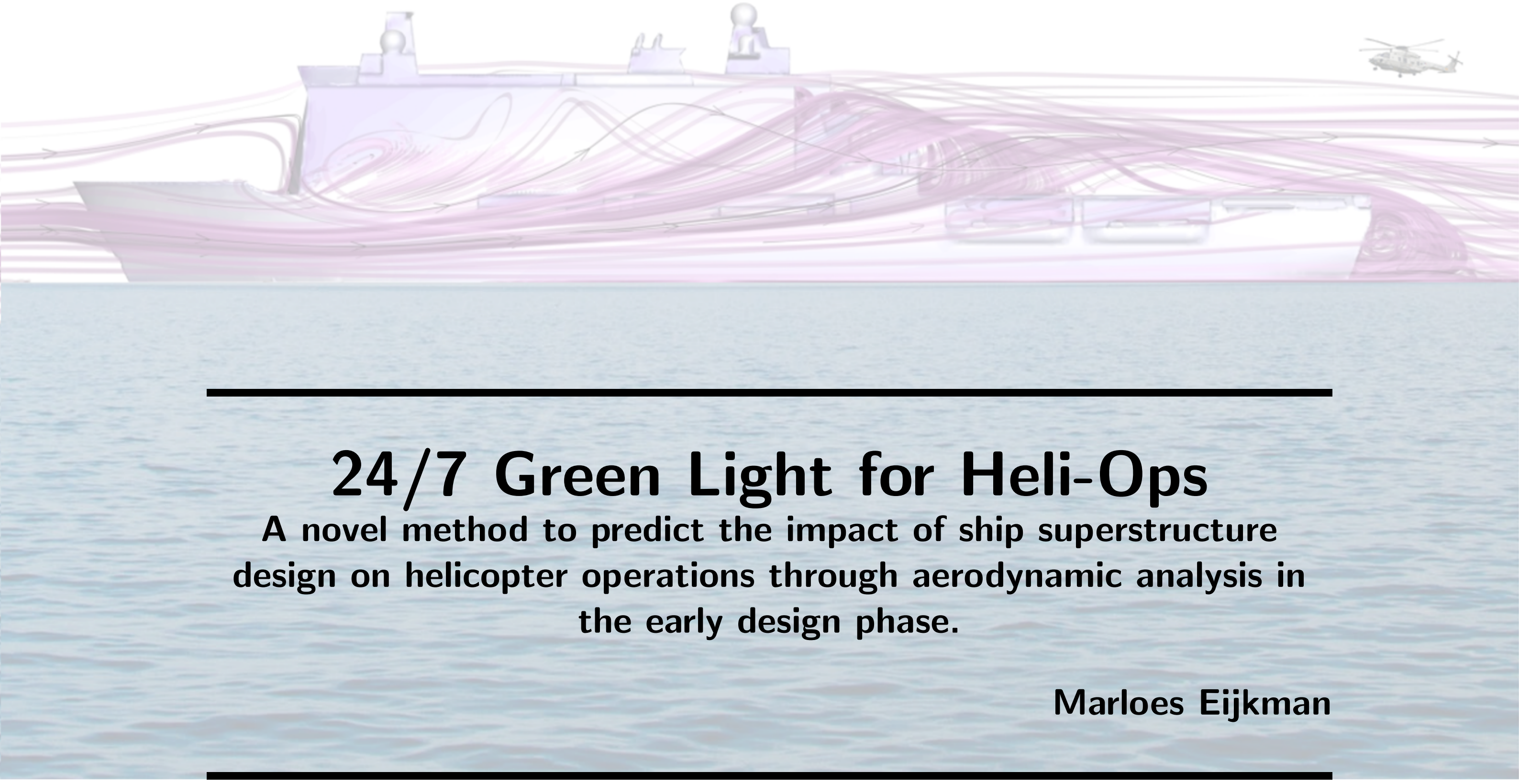

24/7 Green Light for Heli-Ops

A novel method to predict the impact of ship superstructure design on helicopter operations through aerodynamic analysis in the early design phase.

Marloes Eijkman

January 7, 2021

Faculty of Aerospace Engineering

Delft University of Technology

24/7 Green Light for Heli-Ops

A novel method to predict the impact of ship superstructure design on helicopter operations through aerodynamic analysis in the early design phase.

Master of Science Thesis

For obtaining the degree of Master of Science in Aerospace Engineering
at Delft University of Technology

Marloes Eijkman

January 7, 2021

Faculty of Aerospace Engineering · Delft University of Technology

Delft University of Technology

Copyright © Aerospace Engineering, Delft University of Technology
All rights reserved.

DELFT UNIVERSITY OF TECHNOLOGY
DEPARTMENT OF AERODYNAMICS

The undersigned hereby certify that they have read and recommend to the Faculty of Aerospace Engineering for acceptance the thesis entitled **"24/7 Green Light for Heli-Ops"** by **Marloes Eijkman** in fulfillment of the requirements for the degree of **Master of Science**.

Dated: January 7, 2021

Supervisors:

Alexander van Zuijlen

Joost den Haan

Miranti Steijger

Bart van Oers

Preface

Simplicity is the ultimate sophistication.

Leonardo da Vinci

A bachelor in aerospace engineering and my affinity with being on the water, sailing and ships led me to the engineering agency of the navy for my thesis research. Through my fathers Navy stories about his time at sea I have learned some things about the operational side of the Dutch Navy. Spending time working on the thesis that lies before you, I have seen a bit more of the complex and interesting entirety of the Dutch Ministry of Defence. I was lucky, to get the opportunity of experiencing a week aboard a Dutch Navy ship and learn about the life, systems and procedures when at sea. In Utrecht at AMS, I got to know the engineering environment of the Dutch Navy and its friendly and inquisitive people.

My research has put me in touch with people in widely varying lines of work related to the different stages of the procurement of a warship. Something that I take away from my time at DMO is that the sharing of information and experience, and proper communication, is key in such a large and complex organisation. Gathering of relevant information and sources proved a challenge and time-consuming.

I would like to thank Miranti Steijger, who helped me find my way around AMS and through the process of writing the thesis. Your support, directness and hands-on way of doing things is highly appreciated. My gratitude goes to Joost den Haan, for giving me the opportunity of performing this research and his inspiring enthusiasm. I would also like to express my thanks to Bart van Oers, for his valuable practical tips and interest in the subject. A great support during this period was Alexander van Zuijlen, I am grateful for your constant availability to advice me about both the engineering- and the practical elements of this project. I would like to thank Rogier van Kralingen and Jesper van der Waart for their insights into operational aspects of the ship-heli interface. And last but not least, I would like to express my gratitude to Peter Booij and Harmen van der Ven of the NLR, for their support around the use of DeepPurple and answering my ship-heli interface questions.

Summary

> If you can't explain it simply, you don't understand it well enough.
>
> *Albert Einstein*

By 2030, a new amphibious transport ship is to be available for the Dutch Royal Navy. In light of the foreseen rise in airborne operations from the ship, more insight is desired into the impact of ship design choices on helicopter operational availability. Defence Materiel Organisation (DMO) is presently in the early design phase of the ship during which a large number of alternative ship concepts are explored. There is need for a tool to obtain predictive results about the impact of ship design choices on the ship helicopter operational availability. This thesis aims to contribute to an improved ship design for the new amphibious transport ship. This is done by investigating the possibility of developing a tool to provide insight into the impact of ship design on helicopter operations, in the concept exploration phase. With the insights given in this thesis and the proposed prediction methodology, it is aspired to lay the basis for a practical prediction tool. Figure 1 gives an idea of the challenging environment of a ship for the performance of helicopter operations.

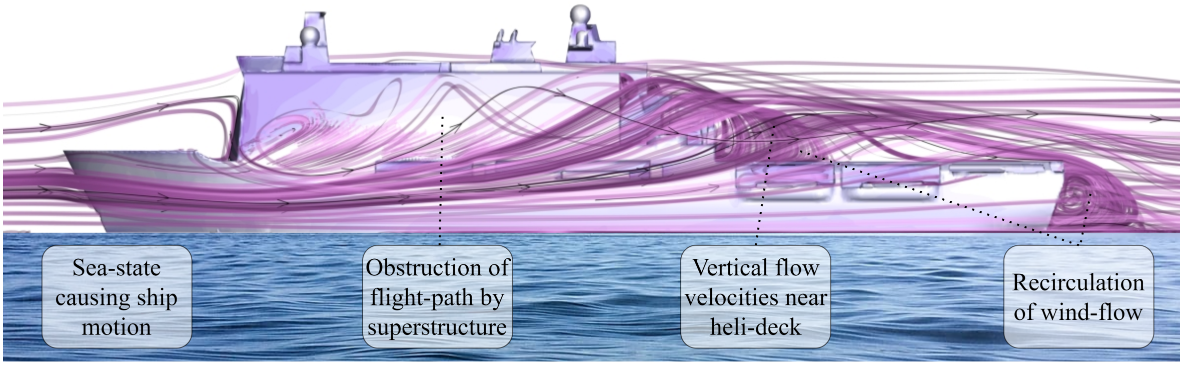
Sea-state causing ship motion
Obstruction of flight-path by superstructure
Vertical flow velocities near heli-deck
Recirculation of wind-flow

Figure 1: Partially visualized streamlines of the flow around a Dutch navy ship, obtained with CFD software *DeepPurple* presenting the challenging ship environment for helicopter operations.

This thesis presents a novel method for the prediction of ship helicopter operational limits (SHOLs) of conceptual ship designs. The method allows for an early analysis of the impact of superstructure design on helicopter operations, which can substantially aid in improved design of navy ships. The accessibility, low computational cost and simplicity of the required inputs are the essence of the methodology. The proposed prediction method relates steady-state information on the ship wind environment to SHOLs. To this end, first a study is performed into the known methodologies for gaining insight into the effect of ship design on the ship wind environment. In addition to this, it is analysed how to gain insight into the impact of the ship wind environment on helicopter operations. Finally, a method is proposed to relate the insights on ship wind environment to shipboard helicopter operations. This leads to the proposal of a tool for the prediction of SHOLs of conceptual ship designs.

Traditionally, insight into the wind environment of a ship is gained by performing wind-tunnel experiments and sea-trial tests, which are both expensive and time-consuming. A more suitable method to apply during the early design phase of the ship is the simulation of the wind environment by means of Computational Fluid Dynamics (CFD). Depending on the CFD method, the level of fidelity and computational cost vary widely. DMO has a software available which is capable of performing CFD simulations based on a RANS method: DeepPurple. A RANS method is characterized by its low computational cost, but is limited in providing detailed results. In the early design phase of a warship, low fidelity information which requires low computational effort is considered valuable for a successful exploration of alternative design concepts, whilst providing enough relevant information. The possibility of using DeepPurple flow information for the investigation of SHOLs is explored in this research.

The extend of the information DeepPurple can provide about the ship wind environment is analysed by performing a verification and validation of the software. From the outcomes, it is anticipated that DeepPurple can provide sufficient information on mean wind flow for the present research. DeepPurple is limited in the modelling of time-varying wind flow. A large part of time-varying flow features are not captured. Considering this, the possibility of relating solely mean wind flow information to the availability of ship helicopter operations is investigated in this study.

Helicopter operational availability is determined by rejection criteria. The criteria are related to the helicopter performance, helicopter attitude, ship motions and the subjective pilot workload rating. A large part of the limits, when considering amphibious transport ships, can be related to the mean wind environment. For these limits, a model is developed which relates mean flow components to rejection criteria. For the development of this model, an analysis is performed of the behaviour of a helicopter in the ship environment by studying helicopter physics, shore-based helicopter hover trials and helicopter sea-trials. A tool *LightPink* is developed which can predict SHOLs for conceptual ship designs.

The capabilities and limitations of LightPink are analysed by a validation and sensitivity analysis of the method. The SHOLs of a Dutch navy ship currently in operation are predicted with LightPink and compared to the existing SHOLs of this ship. It is determined to what extend the tool can capture specific types of limits. It is found that the limits and risk areas (for subjective pilot workload limits) which can be related to mean flow components can successfully be predicted with LightPink for the Dutch navy ship. These

limits determine approximately 85% of the ship helicopter operational envelope of this ship. It became apparent that in specific regions around the flight deck, a number of limits are likely dependent on time-varying flow components and limited visual cues for the pilot. These limits cannot be predicted with the proposed method, and determine approximately 15% of the ship helicopter operational envelope. The limits and risk areas predicted by LightPink have shown to be sufficient to give an outline of the SHOLs for the analysed case. LightPink demonstrates a method, which can potentially be used for performance prediction in the early design phase, whilst the limitations of the predictions are taken into consideration.

This research shows that it is possible to develop a tool to predict the impact of a ship design on helicopter operations in the concept exploration phase. It is advised to validate the tool more extensively in future research and a number of improvements are recommended to implement in the tool for refinement of the outcomes. Amongst others, it is recommended to investigate the possibility of incorporating turbulence intensity data obtained with DeepPurple in the prediction method, to evaluate the possibility of capturing more of the potential SHOLs. Finalizing the thesis, a set of conceptual ship designs is proposed for future research, based on the insights gained. The SHOLs of one of the concepts are predicted with LightPink, to demonstrate the use of the prediction method.

Table of Contents

Preface **v**

Summary **vii**

List of Figures **xv**

List of Tables **xxiii**

Nomenclature **xxv**

Glossary **xxvii**

1 Introduction **1**

1.1 Motivation 1

1.2 Scope 3

1.3 Objectives and Questions 5

1.4 Guide Through the Thesis 9

2 Theoretical Background **11**

2.1 Introduction 11

2.2 The Ship Airwake 12

2.3 Modelling of the Ship Airwake 15

2.4 Fundamentals of Helicopter Physics 17

2.5 Ship-Helicopter Key Concepts 21

2.6 Summary and Conclusions 34

3 Approach 37

3.1 Introduction 37

3.2 Approach Question 1b 38

3.3 Approach Question 3 39

3.4 Main Data Sources 40

3.5 Type of Software 43

4 Verification and Validation of DeepPurple 45

4.1 Introduction 45

4.2 DeepPurple Computational Method 46

4.3 Previous Research with DeepPurple 50

4.4 Verification DeepPurple 52

4.5 Validation DeepPurple 56

4.6 Summary and Conclusions 64

5 Prediction of Ship Helicopter Limits 67

5.1 Introduction 67

5.2 Prediction based on Mean Airflow Data 68

5.3 Mean Flow Components 69

5.4 Prediction of Objective Limits 70

5.5 Prediction of Subjective Limits 80

5.6 Method for Calibration of Criteria 87

5.7 Summary 89

6 Calibration and Validation of LightPink 91

6.1 Introduction . . . 91
6.2 Selection of the Baseline Case . . . 92
6.3 Calibration of Prediction Procedure . . . 94
6.4 Validation of Prediction Procedure . . . 106
6.5 Summary and Conclusions . . . 120

7 Preview Proposed Ship Concepts 121

7.1 Introduction . . . 121
7.2 Impact of Superstructure Design . . . 122
7.3 Proposed Ship Concepts . . . 126
7.4 LightPink Analysis of Concept A . . . 130

8 Conclusions and Recommendations 137

8.1 Conclusions . . . 137
8.2 Recommendations . . . 139

Bibliography 143

A DeepPurple Software Elements 147

A.1 Background . . . 147
A.2 Windows User Interface . . . 147
A.3 Linux Computation Steps . . . 148
A.4 Relevant Files and Locations . . . 150
A.5 Practical Notes on the Use of DeepPurple . . . 152

B Overview NLR Reports - DeepPurple 153

C Additional Validation and Verification of DeepPurple 155

C.1 DeepPurple Validation - Atmospheric Boundary Layer . . . 155
C.2 DeepPurple - RANS Comparison . . . 157

C.3 DeepPurple Verification - Test 2 and Test 3 160

D Sea-Trial Pilot Scales 165

D.1 Deck Interface Pilot Effort Scale 166

D.2 Vibration Assessment Rating Scale 167

D.3 Turbulence Rating Scale 167

E More on Ship Helicopter Physics 169

E.1 Additional Helicopter Physics 169

F Ship Concept Analysis - General Considerations 171

List of Figures

1 Partially visualized streamlines of the flow around a Dutch navy ship, obtained with CFD software *DeepPurple* presenting the challenging ship environment for helicopter operations. vii

2 Red wind and Green wind xxvii

3 Coordinate system xxvii

1.1 A typical SHOL diagram 2

1.2 Zr. Ms. Johan de Witt[1] 2

1.3 Left: helicopter in hover. Middle: helicopter close to the ground. Right: helicopter close to a ship flight deck. 3

1.4 Research structure 8

2.1 Wake flow behind a rearward facing step (Driver et al., 1986) 12

2.2 Wake flow behind a rearward facing step in 3D (Shafer and Ghee, 2005) 13

2.3 Balance of forces top, front and side view 18

2.4 Left: inefficient rotor due to recirculation of disturbed air - Right: efficient rotor due to translational lift. 20

2.5 NH90 NFH rotor rotation directions 21

2.6 NH90 NFH 21

2.7 Fore-aft landing and take-off procedure (Hoencamp, 2015) 22

2.8 Oblique procedure facing starboard (Hoencamp, 2015) 23

2.9 Cross-deck procedure facing starboard (Hoencamp, 2015) 24

2.10 A typical SHOL diagram for the fore-aft procedure 24
2.11 Key factors affecting the SHOLs 25
2.12 Environmental elements affecting SHOLs, and the relation to the superstructure. 28
2.13 AOB 29
2.14 Relative angle between ship and banking helicopter during strong cross-wind . . . 30
2.15 Pitch attitude 30
2.16 Left: forward flight, Right: hover 31
2.17 Torque 31
2.18 Flowchart of SHOL establishment by the Netherlands (Fang and Booij, 2006)(Hoencamp, 2015) 33
2.19 Flow diagram of the determination of subjective limits during sea-trials. 34

3.1 Data flow of proposed procedure for prediction of SHOLs 39
3.2 Turbulence rating 42
3.3 Subjective rating 42
3.4 Partially visualized streamlines around the Dutch amphibious transport ship Zr. Ms. Johan de Witt. 43

4.1 Mesh around SFS2, DeepPurple standard settings 49
4.2 Mesh around *LPD2-Model1*, DeepPurple standard settings 49
4.3 Standard mesh refinement SFS2 50
4.4 Standard mesh refinement *LPD2-Model1* 50
4.5 Prismatic BL 50
4.6 Full scale Simple Frigate Shape 2 Zan (2005), dimensions in [m] and in [**ft**]. . . . 53
4.7 Headwind condition mean velocity of experiment- (Forrest and Owen, 2010) and DeepPurple data for different grids at 50% deck length measured at hangar height with the lateral position normalized by ship beam b and an uniform inflow. . . . 54
4.8 Convergence Plots from DeepPurple for *DP2- Baseline*, *DP2 - Coarse* and *DP2 - Fine* for a headwind. 54
4.9 G45 wind condition mean velocity of experiment- (Forrest and Owen, 2010) and DeepPurple data for different grids at 50% deck length measured at hangar height with the lateral position normalized by ship beam b and an uniform inflow. . . . 55

4.10 Convergence Plots from DeepPurple for *DP2- Baseline*, *DP2 - Coarse* and *DP2 - Fine* for a G45 wind. 55

4.11 Headwind mean velocity of experiment-, DES- (Forrest and Owen, 2010) and DeepPurple data at 50% deck length measured at hangar height with the lateral position normalized by ship beam b and a uniform inflow. 59

4.12 Headwind total turbulence intensity of experiment-, DES- (Forrest and Owen, 2010) and DeepPurple data at 50% deck length measured at hangar height with the lateral position normalized by ship beam b and a uniform inflow. 60

4.13 G45 mean velocity of experiment-, DES- (Forrest and Owen, 2010) and DeepPurple data at 50% deck length measured at hangar height with the lateral position normalized by ship beam b and a uniform inflow. 61

4.14 G45 total turbulence intensity of experiment-, DES- (Forrest and Owen, 2010) and DeepPurple data at 50% deck length measured at hangar height with the lateral position normalized by ship beam b and a uniform inflow. 61

4.15 Headwind condition mean velocity of experiment- (Forrest and Owen, 2010) and DeepPurple data at different Reynolds nr. at 50% deck length measured at hangar height with the lateral position normalized by ship beam b and an uniform inflow. 62

4.16 G45 mean velocity of experiment- (Forrest and Owen, 2010) and DeepPurple data at different Reynolds nr. at 50% deck length measured at hangar height with the lateral position normalized by ship beam b and a uniform inflow. 63

4.17 G45 contour plots of mean velocity component in the y-direction v in [m/s] of DeepPurple data at different Reynolds nr. (*DP* with Re $= 2.26 \cdot 10^7$ left and *DP2* with Re $= 6.58 \cdot 10^5$ right) 64

5.1 Types of base formulas included in the prediction procedure. 68

5.2 Left: Mean flow components used in the LightPink base formulas. Right: Flow components w.r.t. the ship. 69

5.3 Hover Trial: NH90 NFH Angle of Bank attitude versus the relative wind angle for wind velocity 1 (Hoencamp, 2012) 71

5.4 Shore-Based Hover Trial data. Left: angle of bank versus L_{perp}. Right: angle of bank versus U_{tot}. 72

5.5 DeepPurple mean flow data taken in Disk A at wind speed and directions where AOB limits were experienced during sea-trials aboard the LPD2 - for finding the relating of U_{tot} to the angle of bank. 73

5.6 Expected effect of downwash on the angle of bank attitude 73

5.7 Hover Trial: NH90 NFH Angle of Bank attitude versus the relative wind angle for wind velocity 2 (top) and 3 (bottom) (Hoencamp, 2012) 74

5.8 Hover Trial: NH90 NFH Angle of Bank attitude versus the relative wind angle for wind velocity 4 (Hoencamp, 2012) . . . 75

5.9 Hover Trial: NH90 NFH Pitch attitude versus the relative wind angle for wind velocity 2 (top) and 3 (bottom) (Hoencamp, 2012) . . . 76

5.10 Hover Trial: NH90 NFH pedal position versus the relative wind angle for wind velocity 3 (Hoencamp, 2012) . . . 78

5.11 Hover Trial: NH90 NFH torque required versus the relative wind angle for wind velocity 1 (top) and 4 (bottom) (Hoencamp, 2012) . . . 79

5.12 Data obtained from LPD2 Sea-trials Fore-aft Procedure - Left: objective limits, middle: subjective limits, right: subjective rating. . . . 82

5.13 Data obtained from LPD2 Sea-trials Oblique facing port procedure - Left: objective limits, middle: subjective limits, right: subjective rating. . . . 83

5.14 Data obtained from LPD2 Sea-trials Cross facing port procedure - Left: objective limits, middle: subjective limits, right: subjective rating. . . . 84

5.15 Data obtained from LPD2 Sea-trials - Left: Oblique facing starboard procedure, right: Cross facing starboard procedure. . . . 85

5.16 Top view: High pilot workload leeward of the flight deck, for cross winds. . . . 86

5.17 Known helicopter operation limits are correlated to mean flow components computed by DeepPurple to calibrate parameters P. . . . 88

6.1 LPD2-Model1 (developed by the NLR) . . . 95

6.2 LPD2-Model2 (developed for the present research) . . . 95

6.3 Left: situation 1 fore-aft starboard procedure. Right: situation 2 cross facing starboard procedure. . . . 96

6.4 Distribution of 21 data points, taken to determine the average flow velocities in a rotor disk. . . . 97

6.5 Disk A, B and C, port and starboard . . . 98

6.6 Left: data point used for calibration of AoB1. Right: DeepPurple velocity component L_{perp} at Disk A in [m/s]. . . . 99

6.7 Left: data points used for calibration of AoB2. Right: DeepPurple velocity components U_{tot}, L_{perp} and W at Disk A in [m/s]. . . . 100

6.8 Left: data point used for calibration of Pitch1. Right: DeepPurple velocity component U_{head} at Disk B in [m/s]. . . . 101

6.9 Left: data point used for calibration of Pitch2. Right: the DeepPurple velocity component $G30$ at Disk B in [m/s]. . . . 102

6.10 Left: data point used for calibration of Torque1. Right: DeepPurple velocity component L_{perp} at Disk C in [m/s]. 103

6.11 Left: First data point used for calibration of Torque2. Right: DeepPurple velocity components U_{tot}, W and L_{perp} at Disk A in [m/s]. 104

6.12 Left: Second data point used for calibration of Torque2. Right: DeepPurple velocity components U_{tot}, W and L_{perp} at Disk A in [m/s]. 105

6.13 Left: data points used for calibration of the subjective criterion. Right: DeepPurple velocity component W at Disk C in [m/s]. 106

6.14 Top left: existing SHOL fore-aft procedure. Top right: predicted SHOL fore-aft procedure. Bottom: predicted SHOL with exsiting envelope included. Circled in yellow: data points used for calibration. 107

6.15 Top left: existing SHOL oblique procedure. Top right: predicted SHOL oblique procedure. Bottom: predicted SHOL with exsiting envelope included. Circled in yellow: data points used for calibration. 108

6.16 Top left: existing SHOL cross procedure. Top right: predicted SHOL cross procedure. Bottom: predicted SHOL with exsiting envelope included. Circled in yellow: data points used for calibration. 109

6.17 Top left: existing SHOL fore-aft procedure. Top right: predicted SHOL with *calibration1*. Bottom: predicted SHOL with *calibration2*. Circled in yellow: data points used for calibration. Circled in purple: outliers. Blue line: existing SHOL. 114

6.18 Top left: existing SHOL oblique procedure. Top right: predicted SHOL with *calibration1*. Bottom: predicted SHOL with *calibration2*. Circled in yellow: data points used for calibration. Blue line: existing SHOL. 115

6.19 Top left: existing SHOL cross procedure. Top right: predicted SHOL with *calibration1*. Bottom: predicted SHOL with *calibration2*. Circled in yellow: data points used for calibration. Blue line: existing SHOL. 116

7.1 Red: LPD2 SHOL diagrams for the fore-aft, oblique and cross procedure both port and starboard. Yellow: areas for potential improvements in the envelope. 122

7.2 Iterative dialogue for elucidation of requirements and budget, based on Oers et al. (2018) 126

7.3 Blockdiagram conceptual designs with *LPD2-Model2* as baseline and conceptual design A to K. 128

7.4 *LPD2-Model2* as baseline with Concept A to K 3D models. 129

7.5 Concept A: landing- and take-off procedures for Spot 1. 131

7.6 Concept A: LightPink predicted SHOL fore-aft-front port-side and starboard-side (procedure 1 and 2). 132

7.7 Concept A: LightPink predicted SHOL fore-aft-rear port-side and starboard-side (procedure 3 and 4). 132

7.8 Concept A: LightPink predicted SHOL oblique-front and -rear facing port-side (procedure 6 and 8). 133

7.9 Concept A: LightPink predicted SHOL cross facing port-side and starboard-side (procedure 9 and 10). 133

7.10 Top: Front-view of Concept A with partially visualized streamlines for a R50 relative wind angle and 33 kts wind speed. Bottom: Top-view of Concept A with partially visualized streamlines for a R120 relative wind and 31 kts wind speed. 134

7.11 Rear-view of the baseline ship (*LPD2-Model2*) for a R105 relative wind angle and 29 kts wind speed (cross facing port procedure). 135

8.1 Research structure (for full-size refer to thesis introduction). 138

8.2 Data flow of proposed procedure for prediction of SHOLs. 138

A.1 DeepPurple data flow 149

C.1 Headwind (top) and G45 (bottom) mean velocity of experiment- (Forrest and Owen, 2010) and DeepPurple data at different Reynolds nr. at 50% deck length measured at hangar height with the lateral position normalized by ship beam b. . 156

C.2 Modified SFS 2, left: plane L at 9.88 [m] above the flight deck (just below hangar height). Right: plane M at 11.77 [m] above the flight deck (just above hangar height). 157

C.3 Contour plot of x-component of the mean velocity normalised with freestream velocity on the L plane. Left: results from Praveen (2018). Right: DeepPurple results. 158

C.4 Contour plot of z-component of the mean velocity normalised with freestream velocity on the L plane. Left: results from Praveen (2018). Right: DeepPurple results. 158

C.5 Contour plot of turbulence intensity normalised with the freestream velocity on the L plane. Left: results from Praveen (2018). Right: DeepPurple results. 158

C.6 Contour plot of x-component of the mean velocity normalised with freestream velocity on the M plane. Left: results from Praveen (2018). Right: DeepPurple results. 159

C.7 Contour plot of z-component of the mean velocity normalised with freestream velocity on the M plane. Left: results from Praveen (2018). Right: DeepPurple results. 159

C.8 Contour plot of turbulence intensity normalised with the freestream velocity on the M plane. Left: results from Praveen (2018). Right: DeepPurple results. 159

C.9 Convergence Plots from DeepPurple for *DP2- Grid0*, *DP2 - Grid1* and *DP2 - Grid2* for a headwind. 161

C.10 Headwind condition mean velocity of experiment- (Forrest and Owen, 2010) and DeepPurple data for different grids at 50% deck length measured at hangar height with the lateral position normalized by ship beam b and an uniform inflow. . . . 161

C.11 G45 mean velocity of experiment- (Forrest and Owen, 2010) and DeepPurple data for different grids at 50% deck length measured at hangar height with the lateral position normalized by ship beam b and an uniform inflow. 162

C.12 Headwind condition mean velocity of experiment- (Forrest and Owen, 2010) and DeepPurple data for different grids at 50% deck length measured at hangar height with the lateral position normalized by ship beam b and an uniform inflow. . . . 163

C.13 Convergence Plots from DeepPurple for *DP2- Grid0*, *DP2 - Grid1* and *DP2 - Grid2* for a headwind. 163

C.14 45° WOD condition mean velocity of experiment- (Forrest and Owen, 2010) and DeepPurple data for different grids at 50% deck length measured at hangar height with the lateral position normalized by ship beam b and an uniform inflow. . . . 164

E.1 Fully articulated rotor head (Coyle, 1996) 169

E.2 The swashplate (Coyle, 1996) 170

E.3 Cyclic pitch input (Coyle, 1996) 170

E.4 Wake contraction (Bramwell et al., 2001) 170

F.1 NH90 NFH dimensions 171

F.2 LPD 2 flight deck design 172

List of Tables

2.1 A comparison of the properties of computational methods 16

4.1 Simulation used for the Verification of DeepPurple 52
4.2 Simulations used for the Validation of DeepPurple 58

5.1 LightPink base formulas for the prediction of objective limits 89

6.1 Torque required at 10 kts 104
6.2 LightPink formulas for objective limits by calibration 1 113
6.3 LightPink formulas for objective limits by calibration 2 113
6.4 Guidelines for calibration of LightPink formulas. 117
6.5 Limits which are captured and not captured by LightPink 119

7.1 LightPink Analysis details of Concept A 130

A.1 DeepPurple main files and location 151

B.1 NLR Research with DeepPurple: Validation Approaches 153

C.1 Simulations used for the Validation of DeepPurple 157
C.2 Simulation used for the Verification of DeepPurple 160

D.1 Deck Interface Pilot Effort Scale modified from Hoencamp (2015) 166
D.2 Vibration Assessment Rating Scale modified Hoencamp (2015) 167

D.3 Turbulence rating scale modified from Hoencamp (2015) 167

Nomenclature

Abbreviations

AMS	Department of Maritime Systems
AOB	Angle of Bank
BC	Boundary Condition
CFD	Computational Fluid Dynamics
CFE	Candidate Flight Envelope
DMO	Defence Materiel Organisation
FDO	Flight Deck Officer
fr	Frequency
LPD	Landing Platform Dock
NLR	Royal Netherlands Aerospace Centre
OPV	Ocean-going Patrol Vessel
SFS	Simple Frigate Shape
SHOL	Ship Helicopter Operational Limits
SST	Shear Stress Transport
WOD	Wind Over Deck

Coefficients

α	Reference bank attitude of the helicopter in °.
β	Reference pitch attitude of the helicopter in °.
$G30$	Green relative airflow incoming at 30°
L_{perp}	Flow component perpendicular to the longitudinal axis of the helicopter.
$P_{nr.}$	Parameter of LightPink base formula
$R30$	Red relative airflow incoming at 30°
T_{req}	Reference torque required of the helicopter in %.
U	Flow velocity component in the x-direction in [m/s]
U_{head}	Horizontal velocity component flowing directly toward the nose of the helicopter.
U_{tot}	The total horizontal velocity experienced at the rotor disk
V	Flow velocity component in the y-direction in [m/s]
W	Flow velocity component in the z-direction in [m/s]

Glossary

COORDINATE SYSTEM

Figure 3 presents the coordinate system which is used throughout the report. Figure 2 illustrates the following:

Red wind w.r.t. the ship: Wind flowing towards the ship from port side.

Red wind w.r.t. the helicopter: Wind flowing towards the helicopter from the left side of the nose.

Headwind: Wind flowing towards the nose of the ship or the nose of the helicopter.

R30 w.r.t. the ship: A red relative wind flowing 30 degrees from the port side towards the ship.

R30 w.r.t. the helicopter: A relative wind flowing 30 degrees from the left towards the helicopter.

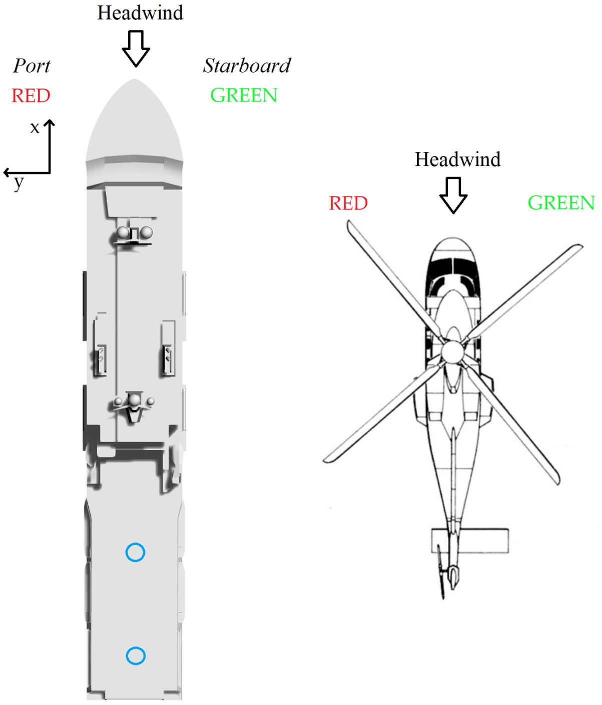

Figure 2: Red wind and Green wind

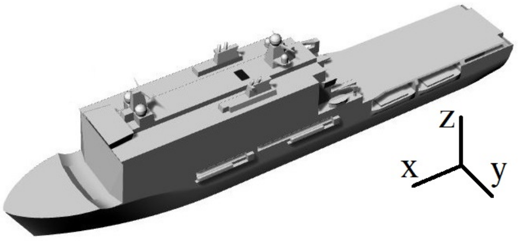

Figure 3: Coordinate system

CONCEPTS

DeepPurple: A DMO in-house software developed by the NLR for investigation of smoke-nuisance aboard navy ships. DeepPurple is a 'shell' with a user-friendly interface which can perform flow computations by running the CFD software *OpenFoam*.

Downwash *or* **Downdraft:** Downwards flowing airflow caused by an object.

Leeward: The side that is sheltered from the wind. Opposite of windward.

OpenFoam: An open-source CFD software.

Operational effectiveness: How effective a design is in terms of the days year-round and the extend of scenarios in which the design can operate successfully.

Relative wind speed: The relative wind speed is the wind speed that the helicopter experiences during a shipboard operation, also called the *apparent wind*. The relative wind speed is the resultant of the environmental wind (true wind) and the ship speed and direction.

Scenario *or* **Operational Scenario:** Entails a collection of environmental and operational factors that compose the situation in which a ship helicopter operation is performed. These factors include for example: relative wind speed and direction, type of ship and helicopter, landing- and take-off procedure, ship roll and pitch motion, daytime or night-time.

Ship helicopter operational availability: The ship helicopter operational availability entails the extend of scenarios in which helicopter take-off and landing procedures can be executed.

Sortie: A sortie is a document which is used during sea-trials to write notes about each trial indicating the turbulence- and DIPES rating given by the test-pilot. Occasionally additional notes are made for a trial about specific experiences of the test-pilot.

Superstructure design features: The superstructure of the ship entails the part of the ship which is above water. The design features include the shape of the superstructure and the overall configuration of the superstructure and flight deck.

Tip path plane: The tip path plane refers to a disk-shaped imaginary plane that is followed by the rotating tip of the helicopter rotor blade.

Weather-cock effect: The tendency of a helicopter to turn head-to-wind.

Windward: The side that is facing the wind. Opposite of leeward.

Chapter 1

Introduction

Motivation
Scope
Objectives and Questions
Research Structure
Guide throught the Thesis

> Remember to look up at the stars and not down at your feet. Try to make sense of what you see and wonder about what makes the universe exist. Be curious. And however difficult life may seem, there is always something you can do and succeed at.
>
> *Stephen Hawking*

1.1 Motivation

Defence Materiel Organisation (DMO) is currently in the starting phase of the replacement of the amphibious transport ships of the Dutch Royal Navy. Currently, there are two amphibious transport ships in operation at the Dutch Royal Navy. These ships are to be replaced by the beginning of 2030. It is expected that in the future, the airborne operations performed aboard the amphibious transport ships will increase drastically. As such, it is desired to include a study of the effects of design choices on the limits of helicopter operations in the early design phase. Traditionally, insight into effects of ship design on airflow around the flight deck and helicopter operations are gained by performing wind-tunnel experiments and sea-trials with helicopters. These are time-consuming and expensive methods which are at the moment mostly related to investigation of existing ship models.

After the ship is designed and build, sea-trials are performed to determine for a helicopter-type a set of limits for different conditions. This set of limits is called a SHOL (Ship Helicopter Operational Limits), see figure 1.1. DMO is in need of a tool to obtain predictive results on the impact of ship design choices on the limits (SHOLs) of a helicopter. To this end the following question is posed by DMO:

Is it possible to develop a method with available resources, to predict the impact of design choices on the operational availability of helicopters, in the early design phase of a new ship?

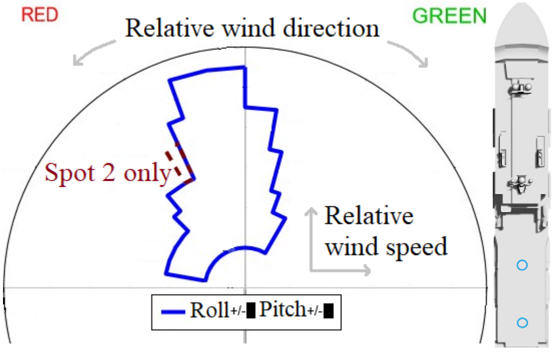

Figure 1.1: A typical SHOL diagram

DeepPurple

For the investigation of the ship wind environment with regard to its impact on helicopter operational availability, DMO would like to explore the possibility of using their in-house software DeepPurple. DeepPurple performs flow computations based on the Computational Fluid Dynamics software "OpenFoam" and is currently used by DMO to evaluate smoke-nuisance aboard ships.

Amphibious Transport Ship

An amphibious transport ship is used to support amphibious operations. During amphibious operations military forces are launched from the ship to execute a mission on land, in airspace or at sea. A landing platform dock (LPD) is a type of amphibious transport ship. Landing platform docks are designed to support transport of helicopters with a flight deck, and landing craft vehicles with a dock. The Dutch navy operates at the moment two landing platform docks: the LPD 1 Zr. Ms. Rotterdam (operational from 1998) and the LPD 2 Zr. Ms. Johan de Witt (operational from 2007). Besides the landing platform dock, there are also other types of amphibious transport ships that are differently equipped. The LPD2 is build by DAMEN[1] and illustrated in 1.2. This ship is approximately 176m long and 27m wide.

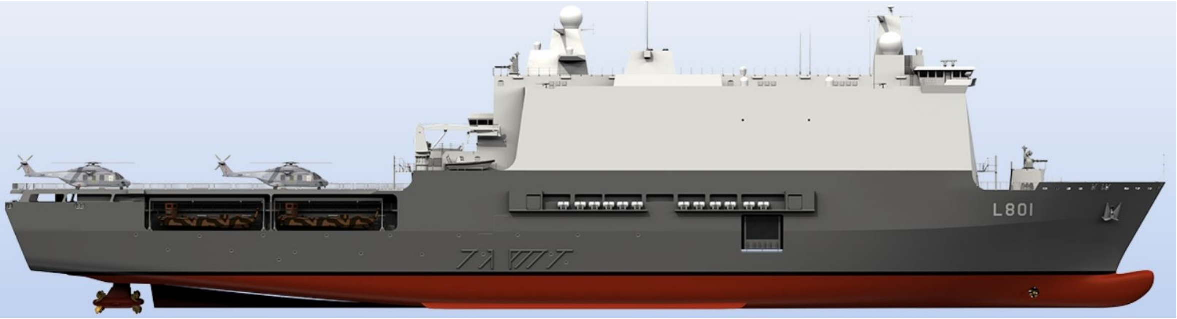

Figure 1.2: Zr. Ms. Johan de Witt[1]

---

[1] https://products.damen.com [cited 25 February 2020]

1.2 Scope

DMO has issued a research into the interaction between the superstructure and flight deck design of an amphibious transport ship and the availability of helicopter operations aboard the ship. Many challenges occur in the ship helicopter interface. An indication of the complexity of the interface is given in figure 1.3. From left to right, the situation in which the helicopter is operating becomes increasingly complex. A growing number of elements affect the helicopter operation when going from mid-air hover, to hover in vicinity of the ground, to hover in the ship environment.

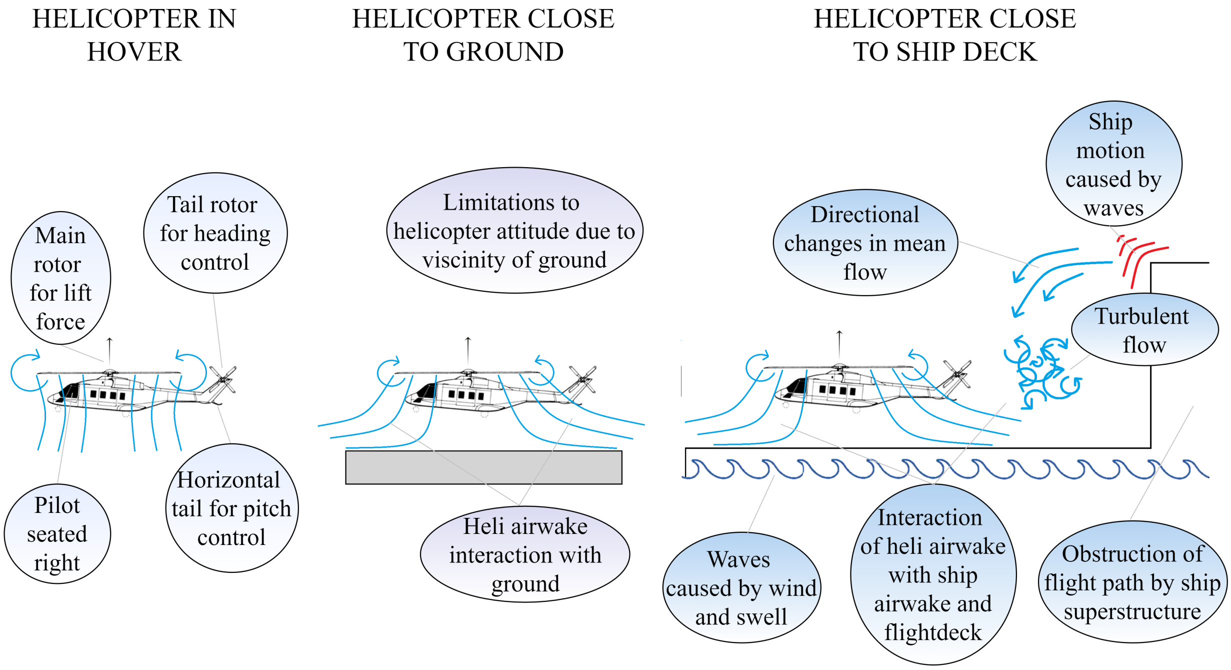
HELICOPTER IN HOVER
HELICOPTER CLOSE TO GROUND
HELICOPTER CLOSE TO SHIP DECK
Main rotor for lift force
Tail rotor for heading control
Pilot seated right
Horizontal tail for pitch control
Limitations to helicopter attitude due to viscinity of ground
Heli airwake interaction with ground
Directional changes in mean flow
Ship motion caused by waves
Turbulent flow
Waves caused by wind and swell
Interaction of heli airwake with ship airwake and flightdeck
Obstruction of flight path by ship superstructure

Figure 1.3: Left: helicopter in hover. Middle: helicopter close to the ground. Right: helicopter close to a ship flight deck.

In order to get a clear picture of the scope of this research, it will shortly be explained what the main subjects and issues are regarding the ship helicopter interface. For more information, refer to the literature survey in Eijkman (2020). Three main subjects of research related to the ship helicopter interface can be distinguished:

- Ship wind environment interaction with helicopters
- Ship-helicopter relative motions
- Air-sea wave interface and ship motions

This research is performed from an aerodynamic viewpoint and focusses on the first of these three: *Ship wind environment interaction with helicopters*. The effect of superstructure and flight deck design on the stability and dynamic behaviour of the ship is not investigated. The effect of ship motions on helicopter operations is briefly discussed, but the air-sea wave interface will not be investigated in the present research.

In the literature survey (Eijkman, 2020), it was discussed which challenges arise when studying the subject of ship wind environment interaction with helicopters. When modelling the ship helicopter interface, choices have to be made with regard to complexity of the model. From the literature survey, it was concluded that considering the purpose of the present research the following simplifications can be made with regard to modelling of the ship airwake:

- The isolated ship airwake is studied in contrast to a coupled ship-helicopter airwake.
- The effect of ship motions on the ship wind environment is not taken into account.

The research will focus in particular on amphibious transport ships, which usually are large and wide ships, significant in height and with multiple helicopter landing spots. The helicopter type that is considered throughout the thesis is the NH90 NFH.

Relevance

In the literature survey, it was found that the subject of superstructure interaction with helicopter operations has two main issues:

1. The (cost) inefficiency of establishment of SHOLs.
2. The (disturbing) effect of the superstructure design on ship helicopter operations.

The first issue leads to research with the aim of increasing the (cost) efficiency of the establishment of SHOLs. The focus in this area lies mostly in the development of an accurate computational helicopter and ship (coupled) airwake model which can reduce the necessary expensive sea-trials for SHOL establishment. An example of a research project on this issue is the recent PhD project for the Dutch Royal Navy by Hoencamp (2015). Hoencamp has developed a tool *SHOL-X* which can determine Candidate Flight Envelopes (a preliminary SHOL). The focus of the predictive tool *SHOL-X* lies in obtaining quantitative results in contrast to finding trends. This results in an accurate model for prediction of limits, requiring accurate inputs about the ship environment (from wind-tunnel tests) and helicopter performance.

For research addressing the second issue, it is generally considered sufficient to use simplified models for (isolated) ship airwake and helicopter performance, in contrast to accurate coupled airwake models. The focus in this area lies in gaining insight about trends, contrary to obtaining quantitative results. This issue is addressed in the present research.

This project is issued by DMO Maritime Systems Devision (AMS) to provide insight into superstructure design impact on helicopter operations. Ideally, the outcomes of this project will contribute to the *concept exploration and definition phase* for the new amphibious transport ship. A wide range of alternative concepts are explored in this phase with regard to the ship layout, systems and performance. There is need for the inclusion of performance prediction of the ship helicopter operational availability into this phase of the ship design process.

The possibility of using a tool in the concept phase, to predict the performance of a concept ship with regard to helicopter operations, is investigated in this study. The relevance of this research lies in the need for a practical research outcome which can contribute to knowledge needed in the early ship design phase. Key for this method is balancing the level of detail with the fidelity of the outcomes. The challenge of this research is to find out to what extend the ship helicopter interface can be simplified whilst giving sufficient information to evaluate the impact of early ship design choices on ship helicopter operations.

1.3 Objectives and Questions

The main objective of the research is formulated below. The first part describes the external goal of the research which is the aim **of** the research and the second part describes how the first part will be achieved which is the internal goal or in other words: the aim **in** the research.

The research objective is to contribute to an improved ship design for the new amphibious transport ship of the Dutch Royal Navy with regard to the ship helicopter operational availability ***by*** *investigating the possibility of developing a method to provide insight on the impact of ship design on helicopter operations in the early design phase, from an aerodynamic viewpoint.*

The main objective requires the clarification of a few terms:

- **Ship design:** The ship design refers to the part of the ship that is above water. This includes the superstructure and the flight deck design.
- **Ship helicopter operational availability:** The ship helicopter operational availability entails the extend of relative wind velocities and directions in which helicopter take-off and landing procedures can be executed.
- **Early design phase:** Many alternative concepts are analysed in this phase of the design process of a warship.
- **Impact on helicopter operations:** This refers to the impact on the extend of the ship helicopter operational availability.
- **Aerodynamic viewpoint:** The focus of the research will lie in aerodynamic aspects of the ship environment that are influenced by the superstructure design.

The main objective states that it will be investigated if a tool can be developed which can be useful in the concept exploration phase. It will be determined what the tool should be able to do, what kind of resources are needed and a first proposal will be made of the tool. The goal is to give insight into the *possibility of developing and applying* such a tool. The main objective breaks-down into three sub-objectives, and one additional objective is formulated:

> **Sub-objective 1:** Gain insight on the methods that can be applied to study the impact of ship design on the wind environment of shipboard helicopter operations.
>
> **Sub-objective 2:** Gain insight on the methods that can be applied to study the impact of the wind environment on a helicopter operating aboard a ship.
>
> **Sub-objective 3:** Gain insight on a method that can be applied to relate the ship wind environment to limits of operation of helicopters aboard a ship.
>
> **Additional objective:** Explore capabilities and limitations of available resources at DMO.

Research Question

The question posed by DMO is as follows: *Is it possible to develop a method with available resources to predict in the early design phase of a new ship what the impact of design choices are on the operational availability of helicopters?* This question is reformulated for the research into:

What is a suitable tool that can be used to predict the impact of a ship design on helicopter operations in the early design phase?

The main research question requires the clarification of one additional term:

- **Suitable tool:** A tool which is suitable in the early design phase is user-friendly and requires simple and low-cost inputs.

The main research question can be divided into the following sub-questions:

> **Sub-question 1:** In what way can insight be gained on the impact of the ship design on the wind environment of shipboard helicopter operations?
>
> > **1a** What is known about the wind environment of ships and methods for measuring and quantifying information of the wind environment?
> >
> > **1b** What is a suitable method for investigation of the wind environment of a ship with regard to helicopter operations in the early design phase?

Sub-question 2: In what way can insight be gained on the impact of the wind environment on a helicopter operating aboard a ship?

2a What are the fundamentals of helicopter physics which determine the functioning of a helicopter?

2b What is known about ship helicopter limits and about the methods applied for the establishment of the limits?

Sub-question 3: In what way can insights on the wind environment be related to the operation of a helicopter aboard a ship?

Research Structure

Figure 1.4 presents the structure of the research which is presented in the form of a flow diagram connecting the objectives and research questions. The sources used to answer the questions are indicated in figure 1.4 as well. The data source *literature* includes research articles, books and reports.

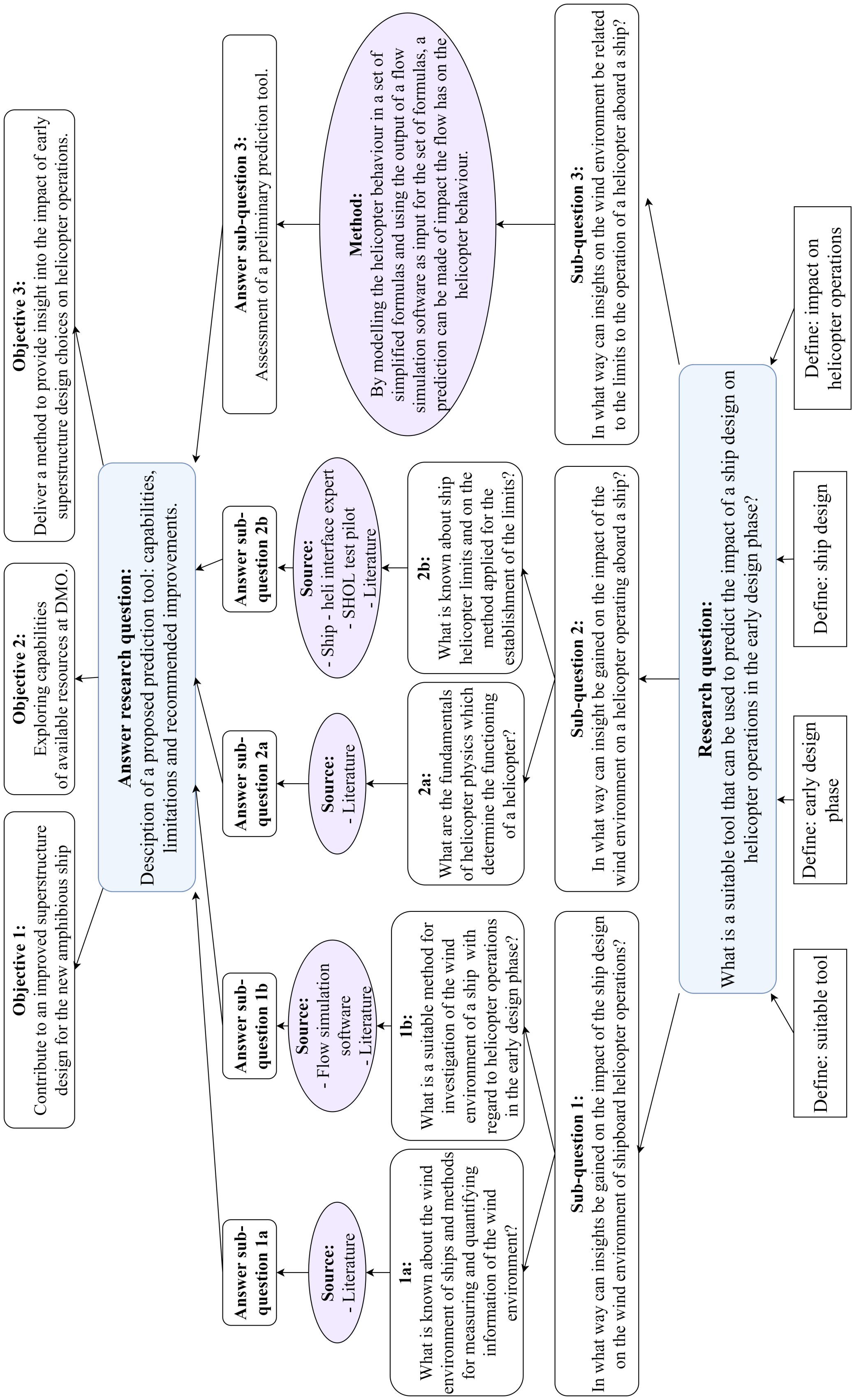
Define: suitable tool
Define: early design phase
Define: ship design
Define: impact on helicopter operations
Research question:
What is a suitable tool that can be used to predict the impact of a ship design on helicopter operations in the early design phase?
Sub-question 1:
In what way can insights be gained on the impact of the ship design on the wind environment of shipboard helicopter operations?
Sub-question 2:
In what way can insight be gained on the impact of the wind environment on a helicopter operating aboard a ship?
Sub-question 3:
In what way can insights on the wind environment be related to the limits to the operation of a helicopter aboard a ship?
1a:
What is known about the wind environment of ships and methods for measuring and quantifying information of the wind environment?
1b:
What is a suitable method for investigation of the wind environment of a ship with regard to helicopter operations in the early design phase?
2a:
What are the fundamentals of helicopter physics which determine the functioning of a helicopter?
2b:
What is known about ship helicopter limits and on the method applied for the establishment of the limits?
Method:
By modelling the helicopter behaviour in a set of simplified formulas and using the output of a flow simulation software as input for the set of formulas, a prediction can be made of impact the flow has on the helicopter behaviour.
Source:
- Literature
Source:
- Flow simulation software
- Literature
Source:
- Literature
Source:
- Ship - heli interface expert
- SHOL test pilot
- Literature
Answer sub-question 1a
Answer sub-question 1b
Answer sub-question 2a
Answer sub-question 2b
Answer sub-question 3:
Assessment of a preliminary prediction tool.
Answer research question:
Description of a proposed prediction tool: capabilities, limitations and recommended improvements.
Objective 1:
Contribute to an improved superstructure design for the new amphibious ship
Objective 2:
Exploring capabilities of available resources at DMO.
Objective 3:
Deliver a method to provide insight into the impact of early superstructure design choices on helicopter operations.

Figure 1.4: Research structure

1.4 Guide Through the Thesis

At the beginning of the thesis, a *glossary* is added where various returning names and terms are explained. This is also where the coordinate system which is used throughout the thesis can be found.

Research questions *1a, 2a and 2b* will be answered in chapter 2[2]. Insight is gained into the wind environment of a ship and the methods for obtaining measurable information of the wind environment. The fundamentals of helicopter physics are discussed, from which an understanding of the functioning of a helicopter is gained. It is outlined what is known about limits for helicopter operations aboard ships and what is known about the establishment of the limits.

By means of the knowledge gained in chapter 2, a methodology can be constructed for answering the remaining research questions. The research methodology is presented in chapter 3.

In chapter 4, an answer is formulated to question *1b* about a suitable method for investigation of the wind environment of a ship. Previous projects performed with DeepPurple, report on verification and validation procedures and results. These are studied and an additional verification and validation is conducted, to test the software for its suitability for the present research.

To answer question *3*, a preliminary method is developed for the prediction of limits to helicopter operations aboard ships. This method uses data obtained with CFD software as input, and gives a predicted SHOL as output. The steps taken to develop the prediction procedure are explained and presented in chapter 5. In chapter 6, the capabilities and limitations of the prediction procedure are tested. This is done by validating the procedure with a baseline case.

Finally, chapter 7 gives a preview of how the knowledge gained in the present research can be applied to contribute to the concept exploration phase of the new amphibious transport ship. In this chapter, an analysis is made of the impact of superstructure design features of an existing amphibious transport ship on its related SHOLs. By means of this analysis a set of conceptual ship designs is presented. These designs are proposed for investigation with the prediction procedure developed in the present research, which is considered valuable for studying the impact of superstructure design choices on the shipboard operational availability of helicopters.

The conclusions and recommendations are presented in chapter 8.

---

[2] In chapter 3 a list of reports which is studied can be found.

Chapter 2

Theoretical Background

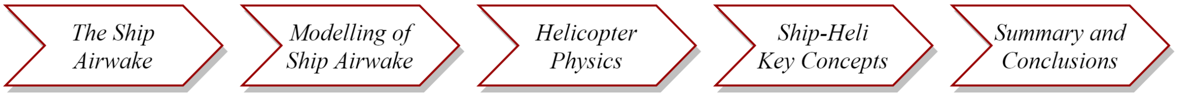
The Ship Airwake
Modelling of Ship Airwake
Helicopter Physics
Ship-Heli Key Concepts
Summary and Conclusions

> Whether outwardly or inwardly,
> whether in space or time, the farther we
> penetrate the unknown, the vaster and
> more marvelous it becomes.
>
> *Charles Lindbergh*

2.1 Introduction

A theoretical background of the research subject is given in this chapter, which involves answering research questions *1a, 2a and 2b*. The answers to these questions lead to the method presented in chapter 3. Additional information can be found in the literature survey (Eijkman, 2020).

1a: *What is known about the wind environment of ships and methods for measuring and quantifying information of the wind environment?*

2a: *What are the fundamentals of helicopter physics which determine the functioning of a helicopter?*

2b: *What is known about ship helicopter limits and about the methods applied for the establishment of the limits?*

The general ship airwake features and methods for controlling the ship airwake are introduced in section 2.2. Section 2.3 focuses on modelling methods of the ship airwake. In section 2.4 the fundamental phenomena and behaviours of helicopters in general are explained. Special attention is given to features of the NH90 NFH. Section 2.5 gives an outline of the key concepts to do with ship helicopter operations, including information about the main landing procedures and information on ship helicopter operational limits. A summary and the main conclusions of this chapter can be found in section 2.6.

2.2 The Ship Airwake

The first part of research question *1a* is discussed: *What is known about the wind environment of ships?* First, generic ship airwake features are described and visualized. This is followed by a short introduction into techniques which can be used to control the airwake.

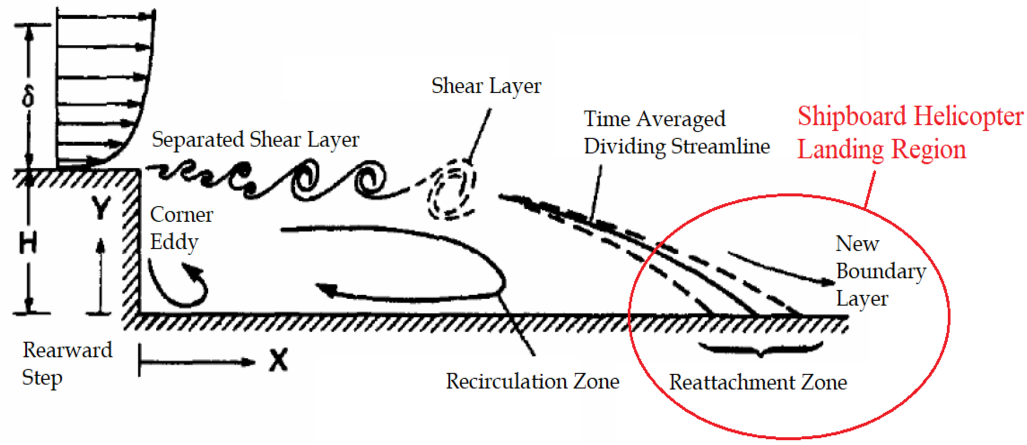

Figure 2.1: Wake flow behind a rearward facing step (Driver et al., 1986)

2.2.1 Ship Airwake Features

The ship airwake resembles the flow around a rearward facing step. A 2D flow over a rearward facing step is presented in figure 2.1 and a visualisation of a 3D flow is presented in figure 2.2. In the flow around a rearward facing step, flow separation and turbulent reattachment occurs. Essential flow features of the flow past the rearward facing step are: unsteady separating shear layers, a significant recirculation region under this separated shear layer and corner vortex structures (Shukla et al., 2019). The flow structures in the shear layer break up before the reattachment which makes the reattachment process chaotic. Shipboard helicopter landings often happen near the chaotic reattachment region which makes the landing procedure difficult. Problematic airwake features for a helicopter include downwash, turbulence, unexpected flow variations and low mean flow velocities. This is discussed into more detail in the literature survey (Eijkman, 2020).

Example: Airwake Features over Frigate Flight Deck

Specific airwake features can be identified in the flow over a frigate flight deck, where the flight deck is placed behind a superstructure. The flow over the flight deck is strongly dependent on the relative wind angle. The following features characterise the flight deck airflow:

- Downdraft in vicinity of the hangar, this is the mean downwards vertical velocity component. The downdraft magnitude measured from experiments and simulation goes upto 30 % of the freestream velocity.
- Turbulent fluctuations with frequencies with the highest intensity occurring in the range 0.1 Hz - 1.5 Hz. The intensity measured in experiments normalized with the freestream velocity occurs in the range of 5 % - 30 % with outshoots to 60%. The magnitude of the intensity obtained from computational modelling is dependent on the method.
- For larger than zero relative angles, an updraft occurs at the flight deck edges. Near the flight deck it is expected that the updraft can be upto 50 % of the freestream velocity. This updraft can cause deck edge vortices which are experienced by the pilot as turbulence and can cause difficulties during the landing of the helicopter.

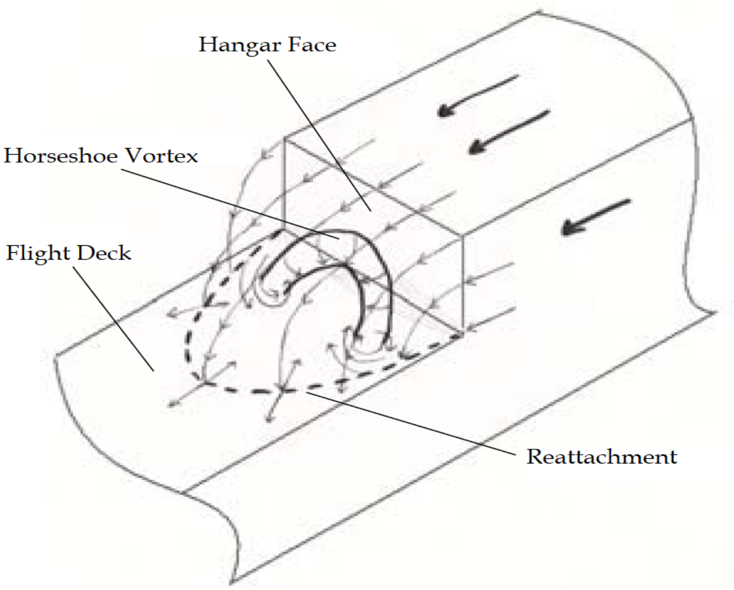

Figure 2.2: Wake flow behind a rearward facing step in 3D (Shafer and Ghee, 2005)

Turbulence

For this research, it is crucial to understand and differentiate the different airwake features which are all ultimately experienced as turbulence. Ultimately, the pilot will experience and react to a combination of disturbances, usually all described by the pilot as *"turbulence"*. In aerodynamic terms, turbulence indicates time variations in velocity components. It should be noted that turbulence experienced by the pilot, can also be caused by regions with (sudden) spacial variations in velocity when moving the helicopter through these regions. Turbulence can be divided into different frequency categories:

- **Turbulence category 1:** fr > 1.6 Hz. High frequency turbulence will vibrate the helicopter, giving an uncomfortable flight and difficulty for the pilot to read the instrumentation, but no large impact on the flight trajectory.
- **Turbulence category 2:** 0.16 Hz > fr > 1.6 Hz. Middle range frequency turbulence will push the helicopter around and increases the pilot workload to keep the helicopter on the correct flight path. Limitations to helicopter performance might be experienced due to peaks in wind speeds.
- **Turbulence category 3:** fr < 0.16 Hz. Low frequency turbulence can significantly impact the flight path and needs large counteracts of the pilot. Limitations to helicopter performance might be experienced due to peaks in wind speeds and *flapback* can become a problem during hover above the flight deck with regard to tail clearance.

2.2.2 Aiwake Control

The techniques for control of the airwake that are considered relevant for the present research are discussed shortly. An extended overview is given in the literature survey (Eijkman, 2020). Three categories were found for airwake control methods: superstructure modification, passive control devices and active control devices[1]. The airwake control methods either aim to reduce the turbulence intensity in the wake, reduce the downwash and/or relocate problematic airwake regions outside of the helicopter path.

For the present research, the following airwake control methods are expected to be relevant:

- Screens (porous) on hangar top and side edges, investigated by Greenwell and Barrett (2006).
- Screens (porous) at flight deck edges, investigated by Greenwell and Barrett (2006).
- Horizontal longitudinal notch in superstructure edges, investigated by Kääriä et al. (2011).
- Porous screen as replacement for flight deck, investigated by Shafer and Ghee (2005).

---

[1] All active flow control methods are not deemed relevant for the present research due to infeasibility and low technology readiness levels.

2.3 Modelling of the Ship Airwake

The second part of research question *1a* is discussed: *What is known about methods for measuring and quantifying information of the wind environment?* First it is shortly explained what can be learned from experimental modelling of the ship airwake. Then different methods of computational modelling of the ship airwake are compared. Lastly choices for assumptions and simplifications of the computations are discussed.

2.3.1 Experimental Modelling

Experimental modelling of the ship airwake refers to wind- or water-tunnel experiments. In short, the following can be learned from experimental ship airwake research:

- Correct atmospheric boundary layer and atmospheric turbulence modelling in the wind tunnel is important for agreement with full-scale data.
- Reynolds number independence is found by multiple researchers which means that results are scalable with the relative wind speed.
- Dynamic velocity data can be scaled to full size with the Strouhal number.

Widely used ship models for investigation of the ship airwake (and modelling techniques) are the Simplified Frigate Shape 1 and 2 (SFS1 and SFS2). These are baseline frigate geometries which were developed in 1985 by The Technical Cooperation Program (TTCP). A lot of data, computational as well as experimental, is available for these models which makes the model suitable for validation purposes.

2.3.2 Computational Modelling

The properties of different computational modelling methods for the ship airwake are compared. Key assumptions and simplifications of computational modelling of the ship airwake are discussed below.

Modelling Methods

The most common computational methods used for the evaluation of the ship airwake are steady and unsteady Reynolds-Averaged Navier-Stokes (RANS and Unsteady RANS) and Detached Eddy Simulation (DES). RANS is used for steady-state simulations and does not resolve any turbulence. Large Eddy Simulation (LES) is a more accurate computational modelling method, which is not used very often for ship airwake analysis because of the high computational cost. DES can be considered as a middle between RANS and LES.

Table 2.1 presents a comparison of the main properties of RANS, URANS and DES methods for ship airwake analysis with regard to ship airwake features. LES is considered infeasible for this research because of the high computational cost and is not included in the comparison. RANS and URANS have low computational cost, one simulation of a ship airwake can be performed in a few hours. DES has a significantly higher computational cost compared to RANS which can amount to a few days for a ship airwake simulation. For a more extended discussion on computational methods for airwake simulation refer to the literature survey (Eijkman, 2020).

COMPUTATIONAL METHOD PROPERTIES			
Method	Turbulence frequency [Hz}	Turbulence intensity [%]	Mean flow [m/s]
RANS	Qualitative (captures trend) Most turbulence frequencies are not captured	Qualitative (captures trend) Most turbulence intensity is not captured	Qualitative and quantitative Captures mean flow
URANS	Qualitative (captures trend) Captures more low frequencies compared to RANS	Qualitative (captures trend) Most turbulence intensity is not captured	Qualitative and quantitative Captures mean flow
DES	Qualitative and quantitative Spectrum very similar to experimental results	Qualitative and quantitative Captures almost all turbulence intensity	Qualitative and quantitative Captures mean flow

Table 2.1: A comparison of the properties of computational methods

From the comparison the following can be deducted:

> **RANS** gives a steady-state solution and is in general considered sufficient for analysing the mean flow patterns of the ship airwake. Steady-state simulations are in general not suitable for the study of unsteady flow features.
>
> **URANS** is similar to RANS in regard to mean flow features and gives some information on unsteady flow features, but of limited accuracy.
>
> **DES** has proved in different studies to be a good middle between RANS and LES and is considered suitable for the simulation of the ship airwake to study mean and turbulent flow features.

Assumptions and Simplifications

The following can be learned about assumptions and simplifications of modelling methods for the ship airwake:

- In order for good agreement with full-scale measurement data, modelling of the atmospheric boundary layer and the atmospheric turbulence is of importance.
- The ship airwake is found in most computations independent of Reynolds number, which means that results can be scaled with relative wind speed.
- The ship airwake is highly dependent on the relative wind angle and so it is crucial to base conclusions of research multiple relative wind angles.
- Multiple studies point out that small geometric features such as communication systems on top of the superstructure do not significantly influence mean flow features of the airwake, but they do impact turbulence levels in the airwake.

When investigating the wind environment of the ship helicopter interface a choice needs to be made about coupling of the ship- and helicopter airwake. As the focus of the present research lies in providing information about ship design in the early design phase, the isolated ship airwake is considered give enough information (Eijkman, 2020). To clarify the impact of 'ignoring' the helicopter airwake in the present research on the results an understanding is gained of the ship- and helicopter airwake coupling types: one-way coupling and two-way coupling. With one-way coupling, the ship airwake and helicopter downwash are first simulated individually and then superimposed. With two-way coupling the ship airwake and the helicopter downwash are modelled dependently (mutual interaction). The interaction effects can be found by studying the difference between one-way coupled and two-way coupled results:

- In the two-way coupled case, the helicopter rotor supervortices are significantly less strong when compared to the one-way coupled case.
- The velocity seen by the rotor in the one-way coupled case is higher than for the two-way coupled case (due to the superstructure of the ship).
- The one-way coupled case over-predicts the inflow in the rotor center and under-predicts the inflow on the sides of the rotor.

2.4 Fundamentals of Helicopter Physics

Research question *2a* will be answered: *What are the fundamentals of helicopter physics which determine the functioning of a helicopter?* The fundamental physics of a helicopter which are presented in this section, are needed to understand how a helicopter behaves in the airwake of a ship. The main principles about the balance of a generic helicopter[2] are briefly explained, followed by an outline of key helicopter phenomena. Lastly, the specifics in the design of the NH90 NFH are discussed and it is explained how these affect the behaviour of the NH90 NFH. More information on the main controls of a helicopter can be found in appendix E.

---

[2] A generic helicopter in this case has a single main rotor and an anti-torque tail rotor.

2.4.1 Balance

The balance of a generic helicopter when looking from the top, the front and the side are discussed below. From the topview, the balance in yaw motion of the helicopter is discussed. From the frontview, the balance in translating and roll motion of the helicopter is discussed. From the sideview, the pitch motion is discussed.

Topview

Looking from the top and assuming the main rotor is turning counter-clockwise, the tail rotor has to exert a force to the right as illustrated in figure 2.3. As the rotor is rotating in the counter-clockwise direction, the fuselage of the helicopter starts to turn clockwise in reaction. To control this yaw-motion the tail rotor exerts a force. The tail thrust to the side has an unsought side effect: translating tendency.

Frontview

When looking from the front, an imbalance in forces can be noted when considering a strictly vertical thrust vector of the main rotor and a sideways thrust vector of the tail rotor as illustrated in the middle of figure 2.3. This imbalance will cause sideslip of the helicopter in the direction of the tail rotor thrust, which is called a translating tendency. To overcome translating tendency, an input can be given to the main rotor to tilt the main thrust vector which in turn will cause a slight angle of bank. In some helicopters this is automated either by the hardware or by an automatic control system.

Sideview

When looking from the side, a balance of forces needs to be created to keep the helicopter from assuming excessive pitch angles in specific conditions. A helicopter has a horizontal tailplane to keep this balance, as illustrated at the bottom of figure 2.3. The tailplane has a negative angle of attack in forward flight, such that during fast forward flight the helicopter will not assume a too extreme pitch-down attitude which would be very uncomfortable for the pilot(s). The faster in forward flight, the more tilt forward of the tip path

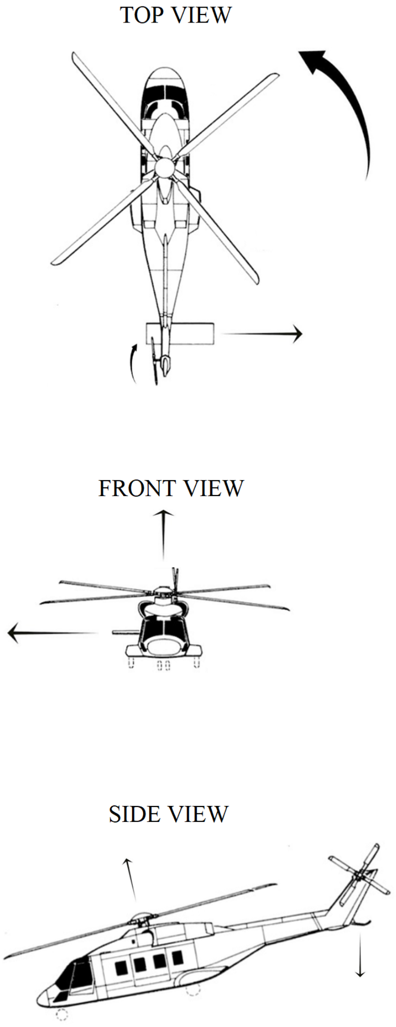

Figure 2.3: Balance of forces top, front and side view

plane is needed. The negative angle of attack of the fixed horizontal tailplane will allow the tip path plane of the helicopter of tilt sufficiently forward for fast flight while keeping the helicopter at an acceptable pitch attitude.

2.4.2 Key Helicopter Phenomena

Below, the key helicopter phenomena are explained of which an understanding is needed when investigating the behaviour of a helicopter in the ship environment.

Gyroscopic Precession

Gyroscopic precession is a phenomenon that has a large effect on the main helicopter rotor. When considering a rotating disk (or rotor blades) and a force is applied to one side to change the rotating plane, the effect of this force is seen 90° later. For example, when you consider a helicopter top-view as in figure 2.3, with counter-clockwise rotating blades and you want to pitch the helicopter nose down, an increase in lift (thus, blade pitch angle) needs to be given at the left side of the rotor disk. In other words, an input that is given to the blade pitch angle (to change lift) will become apparent in the blades tip height 90° later in the cycle.

Dissymmetry of Lift

Dissymmetry of lift occurs when a helicopter experiences an airspeed due to flight speed or wind. In forward flight, the separate main rotor blades will experience different airspeeds, as the blades of the main rotor are rotating. The advancing blade[3], will see a larger airspeed than the retreating blade[4]. The advancing blade will produce more lift than the retreating blade due to the difference in velocity. This is called dissymmetry of lift[5].

Flapback

Flapback is a term used by pilots indicating a sudden pitch-up movement of the helicopter. Flapback is a result of a combination of dissymmetry of lift and gyroscopic precession. This phenomena occurs during wind speed variations from the front which can be either during acceleration of the helicopter or wind gusts. During a wind speed variation from the front of the helicopter, the right side of the rotor disk (topview) will experience a larger lift compared to the left side of the rotor disk. Due to gyroscopic precession the rotor disk will tilt up above the nose of the helicopter and down above the tail of the helicopter causing a pitch-up movement. Whenever these variations are slow, the pilot can adjust controls to avoid excessive pitch-up movements. However when the variations are sudden and strong (gusts) the helicopter will react too quick to respond in time to control the pitch-up movement.

---

[3] The advancing blade is the blade that moves towards the direction of flight.

[4] The retreating blade is the blade that moves away from the direction of flight.

[5] Dissymmetry of lift can be prevented by applying a cyclical change to the pitch of the blades giving the retreating side a higher pitch angle that gives an increase to the lift.

Translational Lift

When the helicopter experiences a relative wind speed the rotor becomes more efficient and less torque is needed to create the same amount of lift. This phenomena is called translational lift. With increasing relative wind speed, the helicopter operates in less disturbed air causing better efficiency of the rotor system. Without a relative wind speed, recirculation of the downwash air occurs causing a loss of efficiency. Due to this phenomenon, some helicopter operations are limited in low relative wind speed conditions. Figure 2.4[6] presents on the left a helicopter in zero relative wind speed with recirculation of airflow and on the right a helicopter experiencing a relative wind speed.

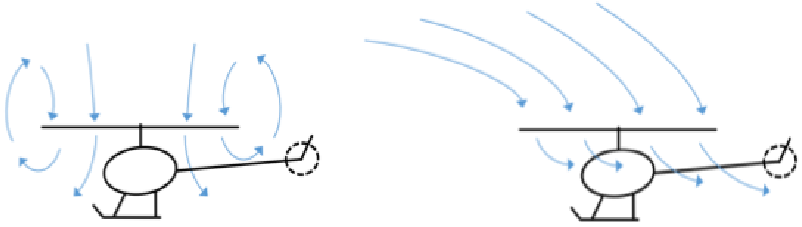

Figure 2.4: Left: inefficient rotor due to recirculation of disturbed air - Right: efficient rotor due to translational lift.

2.4.3 NH90 NFH Specifics

The NH90 has a counter clockwise rotating main rotor and a bottom forward rotating tail rotor. Looking from the top, the lift vector of the tail is pointing to the right as illustrated in figure 3.2[7] to counteract for the clockwise fuselage yaw motion caused by the main rotor. Figure 3.3[8] shows a photograph of the NH90 NFH. It can be seen that the NH90 has an asymmetric horizontal tailplane on the right side of the tail. The horizontal tailplane of the NH90 is not adjustable in angle of attack, it is fixed. This gives the helicopter asymmetric characteristics in pitch motion. Especially at a G30 wind at 30 [kts], the downwash of the main rotor pushed on the horizontal tailplane causing large pitch-up attitudes of the helicopter. The adjustable horizontal tailplane feature for the NH90 NFH was rejected early in the design process of the NH90 NFH. The complex (and heavy) system needed for an adjustable horizontal tailplane such as found on the Seahawk and the Apache is problematic in combination with a foldable tail which is the case with the NH90 NFH.

On the NH90, the deck lock is located almost 5 meters behind the pilot. This distance makes it difficult for the pilot to determine when the helicopter lock is located above the 1.5 meter radius grid on the flight deck where the deck lock needs to be placed during landing. The consequence is that the pilot is limited in choosing a heading of the helicopter with respect to the ship to avoid reference problems. The pilot needs to be able to follow the deck lines and to see the Flight Deck Officer when landing. During the landing procedure, the helicopter should be either aligned with the flight deck, perpendicular to the flight deck or aligned with the 45° deck lines.

---

[6] https://www.thehelicopterstudyguide.com [cited 8 April 2020]
[7] https://www.the-blueprints.com [cited 3 July 2020]
[8] https://www.defensie.nl [cited 23 June 2020]

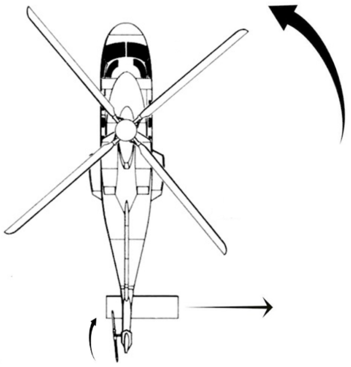

Figure 2.5: NH90 NFH rotor rotation directions

Figure 2.6: NH90 NFH

2.5 Ship-Helicopter Key Concepts

Research question *2b* is the subject of this section: *What is known about ship helicopter limits and about the methods applied for the establishment of the limits?* Before answering this question, first an understanding is needed of the main take-off and landing procedures as used by the Dutch Royal Navy. It is important to note that, the procedures for helicopter operations and establishment of the shipboard limits are not universal. Every *user* (i.e. Navy) have their own procedures for this. To understand more about ship helicopter limits, it will be explained which factors affect these limits. The Dutch Royal Navy uses rejection criteria to assess if a limit is reached in certain conditions. It will be discussed which rejection criteria are important for the present research. At the end of this section, it is described how the ship helicopter limits are determined in practice, by the Dutch Royal Navy[9].

2.5.1 Operational Procedures

Various landing and take-off procedures that are applied during ship helicopter operations by the Dutch Royal Navy are explained, as described by the NATO (Carico et al., 2003). Landing and take-off, ideally happens with nose into the wind, which gives generally the least problems with helicopter performance and attitude. This is not always possible, however to be as close to into the wind as possible there are different landing and take-off procedures. The three procedures used aboard the Dutch amphibious transport ships with the NH90 NFH are the following (Carico et al., 2003) (Hoencamp, 2015): fore-aft procedure, oblique procedure and the cross-deck procedure.

---

[9] Inputs were used from a Dutch Royal Navy ship-helicopter test-pilot.

Fore-aft Procedure

During the fore-aft procedure, the helicopter is aligned with the heading of the ship as illustrated in figure 2.7. The procedure can be performed towards the starboard side or towards the port side. Mostly, due to better visual with the ship, the procedure is carried out towards the port side. The take-off procedure is similar to the landing procedure, but in the opposite order. The climb away from the ship happens usually in a 30° yaw angle as can be seen in figure 2.7. For landing, three main steps can be distinguished:

1. Approach: The helicopter approaches the ship up to the hover wait position which is around 0.75 rotor diameter sideward of the landing spot and 3 meters above the flight deck. In the hover wait position, the nose is aimed into heading direction of the ship.
2. Transition: A sideways flight is made until the helicopter hovers over the landing spot, still 3 meters above the flight deck.
3. Landing: A vertical descend is made to land.

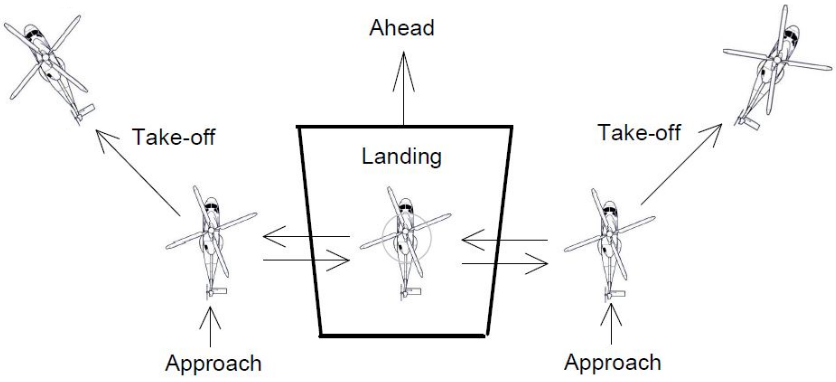

Figure 2.7: Fore-aft landing and take-off procedure (Hoencamp, 2015)

Oblique Procedure

During the oblique procedure, the helicopter is aligned in a 45° angle with the heading of the ship as illustrated in figure 2.8. The procedure can be performed towards the starboard side or towards the port side. The same three steps in landing can be distinguished:

1. Approach: The helicopter approaches the ship up to the hover wait position which is behind the ship at an 45° angle and at a height of around 3 meters above the flight deck.
2. Transition: Flight is proceeded until hover above the landing spot, still 3 meters above the flight deck.

3. Landing: A vertical descend is made to land.

The take-off procedure is similar, but in the opposite order. If there are obstacles in the departure path, then a sideways flight is made until the departure path is clear of obstacles (i.e. superstructure of the ship).

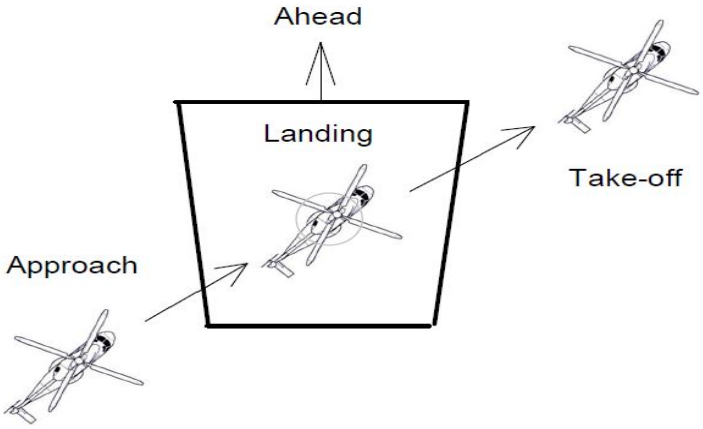

Figure 2.8: Oblique procedure facing starboard (Hoencamp, 2015)

Cross-deck Procedure

During the cross-deck procedure, the helicopter is aligned in a 90° angle with the heading of the ship as illustrated in figure 2.9. The procedure can be performed towards the starboard side or towards the port side. The take-off procedure is similar to the landing procedure but in the opposite order. The same three steps in landing can be distinguished:

1. Approach: The helicopter approaches the ship up to the hover wait position which is sideward of the landing spot, around 3 meters above the flight deck.
2. Transition: The heading of the helicopter is at a 90° angle with the heading of the ship. Flight is proceeded until hover above the landing spot, still 3 meters above the flight deck.
3. Landing: A vertical descend is made to land.

2.5.2 Operational Limits

An understanding is gained on the key facts of ship helicopter operational limits (SHOLs). First a SHOL diagram for the fore-aft procedure is explained as example. Then an outline is given of the environmental elements that affect the SHOLs. Then it is explained what the main criteria are which determine the limits aboard an amphibious transport ship. Lastly, it is explained how the SHOLs are determined in practice by the Dutch Royal Navy.

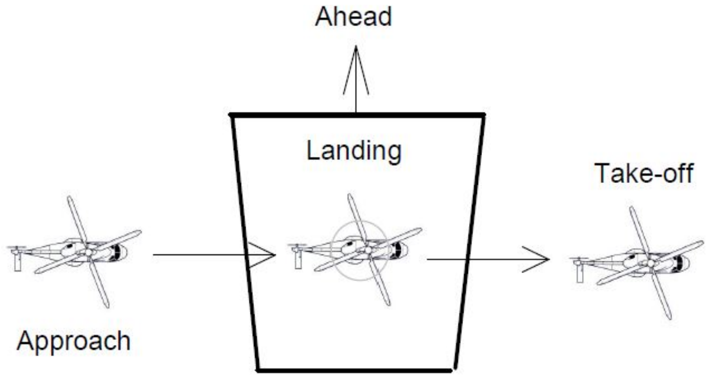

Figure 2.9: Cross-deck procedure facing starboard (Hoencamp, 2015)

Introducing a SHOL Diagram

Every combination of ship and helicopter has its own specific operational envelope, defined by the SHOL diagrams for all landing- and take-off procedures. The establishment of the limitations of helicopter shipboard operations is considered to be the responsibility of the user (the navy). A typical SHOL diagram is presented in figure 2.10[10]. The relative wind speed varies along the horizontal and vertical axes with the lowest velocities in the middle of the circle. The relative wind angle varies along the outside of the circle[11]. In the diagram, it is also indicated what the maximum ship motions are in terms of ship roll and pitch angle.

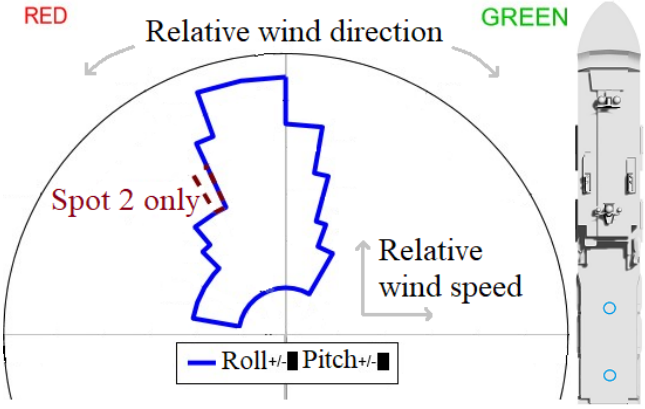

Figure 2.10: A typical SHOL diagram for the fore-aft procedure

Key Factors Affecting Limits

All key factors that affect SHOLs are mapped out in the diagram in figure 2.11. This map can be seen as an overview of all scenarios that can be encountered during ship helicopter operations. For each key factor it will be separately discussed below how it affects the limits.

---

[10] The asymmetry in the SHOL is caused by the asymmetry in the helicopter forces a.o. due to the tail rotor and by the visual cues of the pilot.

[11] Refer to the glossary in for an explanation of the terms used.

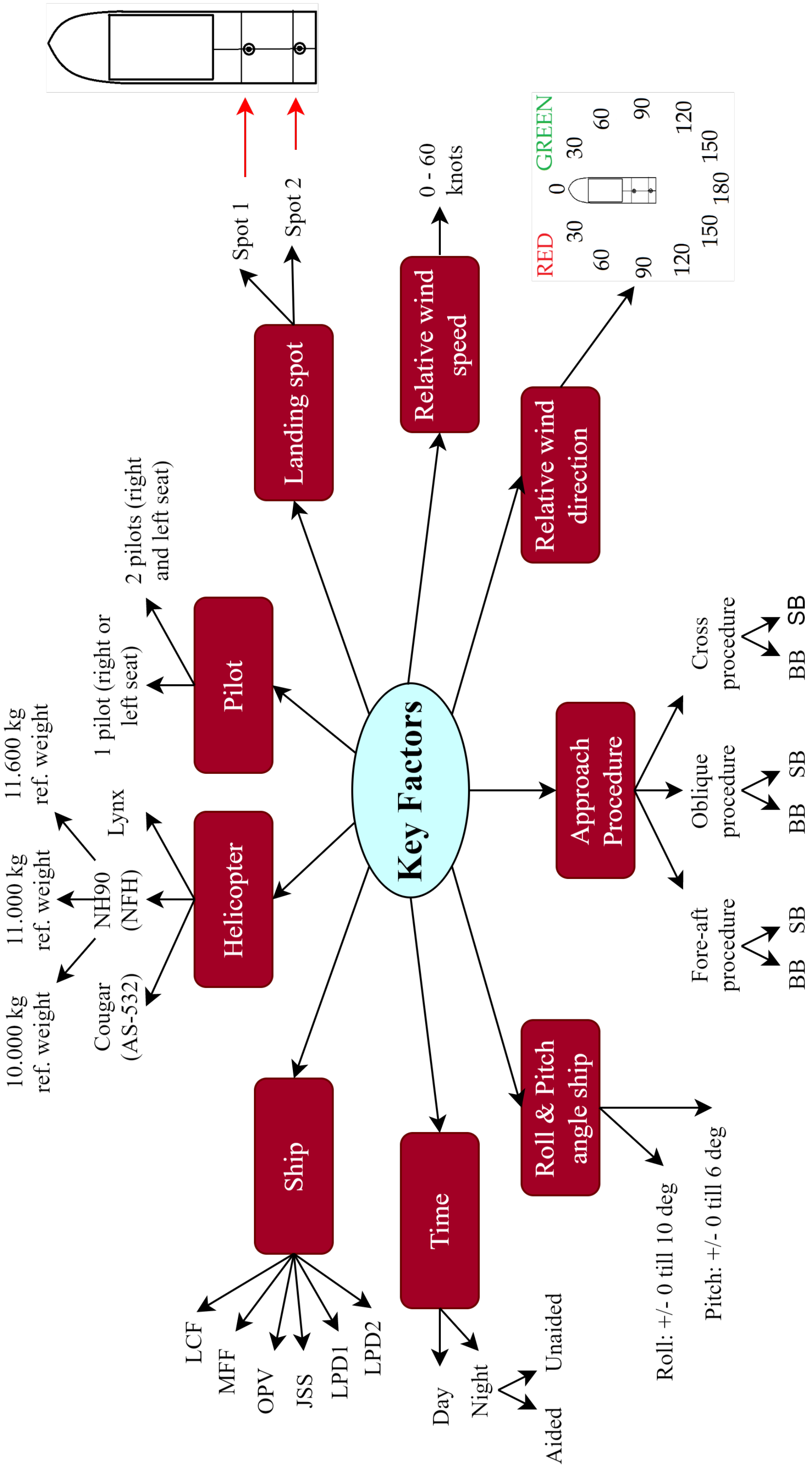
Key Factors
Helicopter
Cougar (AS-532)
NH90 (NFH)
Lynx
10.000 kg ref. weight
11.000 kg ref. weight
11.600 kg ref. weight
Pilot
1 pilot (right or left seat)
2 pilots (right and left seat)
Landing spot
Spot 1
Spot 2
Relative wind speed
0 - 60 knots
Relative wind direction
RED
GREEN
0
30
60
90
120
150
180
Approach Procedure
Fore-aft procedure
Oblique procedure
Cross procedure
BB
SB
Roll & Pitch angle ship
Roll: +/- 0 till 10 deg
Pitch: +/- 0 till 6 deg
Time
Day
Night
Aided
Unaided
Ship
LCF
MFF
OPV
JSS
LPD1
LPD2

Figure 2.11: Key factors affecting the SHOLs

Ship and Helicopter

The present research concerns an amphibious transport ship. An amphibious transport ship is in general a large and wide ship, with a significant height and at least 2 helicopter spots. The type of ship affects the limits due to the influence on the wind environment of the helicopter during ship operations, the ship motions and the feasible approach procedures. The helicopter type determines the helicopter reaction to the wind environment and significantly affects the SHOLs.

Weight

For the NH90 NFH, different SHOLs are determined for the reference weights: 10.000 kg, 11.000 kg and 11.600 kg. The reference weight of the helicopter is determined according to the corrected mass. The helicopter has an operational mass, which is corrected with a mass ranging from -1500 kg to $+1500$ kg depending on the outside temperature and atmospheric pressure. The SHOLs become more strict for increasing weight.

Landing Spot

The location of the landing spot determines the wind environment along the flight path of the helicopter during shipboard operations. For the current Dutch amphibious transport ships, spot 1 and spot 2 have almost identical SHOLs as is also the case in figure 2.10. Near landing spot 1 more problematic wind variations are experienced compared to spot 2, which makes the SHOLs in some cases slightly more strict compared to the SHOLs for spot 2.

Pilot

Regarding the helicopter pilot, there are two scenarios possible. Scenario 1 is operating in the presence of only 1 pilot, seated on the right side of the helicopter. Scenario 2 is operating in the presence of a second deck qualified pilot in the left seat or operating with only 1 pilot seated on the left side. Having scenario 1 or 2 will affect the operational availability for the three procedures as follows, depending on the type of ship:

- *Fore-aft Procedure:* For most ship types, the port fore-aft procedure is allowed for both red and green winds and the starboard fore-aft procedure is only allowed for green winds and in presence of a deck qualified pilot in the left seat[12]. This means that in this case, the operational availability is not affected by the pilot scenario.

  However, for the larger and wider ships such as the amphibious transport ships, the port fore-aft procedure may only be performed for red winds, and the starboard fore-aft procedure may only be performed for green winds and in presence of a deck qualified pilot in the left seat[13]. Thus, presently for the large wide ships (LPD 1, LPD 2, JSS), the pilot scenario influences the operational availability.

- *Oblique Procedure:* For all ship types, the oblique procedure facing port-side is only allowed for red winds. The oblique procedure facing starboard is only allowed for green winds and in the presence of a deck qualified pilot in the left seat. This means that for the oblique procedure, the pilot scenario always influences the operational availability.

---

[12] When approaching the ship from starboard, limited visual for the pilot from the right seat will become problematic.

[13] This is caused by the large and wide superstructure of these ships. The leeward side of the superstructure contains strong downwash regions from the superstructure. The helicopter path cannot cross these regions.

- *Cross Procedure:* Similar to the oblique procedure, the cross procedure facing port is only allowed for red winds. The cross procedure facing starboard is only allowed for green winds and in the presence of a deck qualified pilot in the left seat. This means that for the cross procedure, the pilot scenario always influences the operational availability.

Relative Wind Speed

The relative wind speed affects the wind environment of the ship and has a strong effect on the SHOL.

Relative Wind Direction

The relative wind speed affects the wind environment of the ship and has a strong effect on the SHOL[14].

Approach Procedure

The feasible approach procedures have a large effect on the SHOLs as they determine the flight path taken by the helicopter during ship operations. The relative wind direction usually dictates which procedure is used.

Ship Motions

Ship motions affect the SHOLs mainly in two different ways.

- There is a limit given for each ship-helicopter combination per landing-procedure for the maximum roll and pitch angle of the ship in a period short before the helicopter operation.
- The ship motions can cause limits to the operational envelope through subjective rejection criteria (to do with the pilot workload).

For each SHOL diagram, a maximum is given for the ship motions in pitch and roll angle. This allowable magnitude depends amongst others on the design of the ship and helicopter flight deck. For example when a landing spot is located on the longitudinal axis of the ship, a roll movement of the ship will not have a large impact on the movement of the landing spot. However when the landing spot is not located on the longitudinal axis of the ship, a roll movement of the ship will cause large movements of the landing spot.

The limits to ship motions indicate the maximum allowable roll and pitch angles measured with an inclinometer when the ship is steady on helicopter recovery course (Hoencamp and Kralingen, 2014) during a time span of 2 minutes before the landing procedure. The ship motions during helicopter operations is monitored from the command centre in a digital diagram comparable to the SHOL diagrams. In practice, these limits to the ship motion in itself are often *not* the cause of limits to helicopter operations. Extreme ship motions are most often experienced during strong wind speeds. In these conditions, the strong and fluctuating wind environment is often more critical for helicopter operations than the ship motions in itself. However, ship motions can also cause limits to the ship-helicopter envelope through subjective rejection criteria. The motions of the ship can quite significantly contribute to limits of the SHOL through subjective limits, depending strongly on the ship and helicopter type.

---

[14] The relative wind speed is also called the *apparent wind*. The relative wind speed is the resultant of the environmental wind (true wind) and the ship speed and direction.

Environmental Elements Affecting Limits

There are a number of environmental elements affecting the limits of the ship helicopter operations. A distinction can be made between limiting elements that can be affected by the aerodynamic design of the superstructure and the elements which cannot be affected by the superstructure design.

Figure 2.12 presents the main environmental elements affecting the SHOLs. Each element can cause either an objective limit or a subjective limit. An objective limit is related to the helicopter performance or attitude. A subjective limit is related to the pilot workload, which is indicated according to the Deck Interface Pilot Effort Scale (DIPES) which can be found in appendix D. Each type of limit has a related rejection criterion, indicating when a limit is experienced.

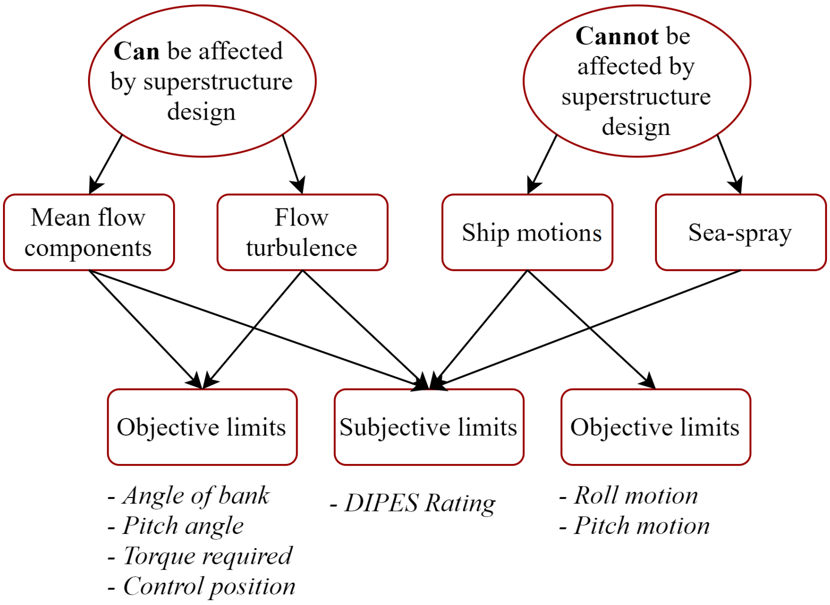
Can be affected by superstructure design
Cannot be affected by superstructure design
Mean flow components
Flow turbulence
Ship motions
Sea-spray
Objective limits
Subjective limits
Objective limits
- *Angle of bank*
- *Pitch angle*
- *Torque required*
- *Control position*
- *DIPES Rating*
- *Roll motion*
- *Pitch motion*

Figure 2.12: Environmental elements affecting SHOLs, and the relation to the superstructure.

2.5.3 Rejection Criteria

A detailed description of a number of rejection criteria is given below. After a brief study of existing SHOLs for amphibious transport ships, it was found that the following rejection criteria are of relevance. These criteria play a role in the operational limits of the NH90 NFH aboard an amphibious transport ship ánd can be affected by superstructure design as illustrated in figure 2.12:

Angle of bank (Category: Helicopter attitude rejection criteria)

Pitch attitude (Category: Helicopter attitude rejection criteria)

Torque required (Category: Helicopter performance rejection criteria)

Pedal control[15] (Category: Control position rejection criteria)

Subjective rating (Category: Subjective rejection criteria)

Angle of Bank Rejection

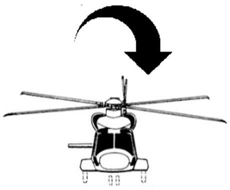

Figure 2.13: AOB

The angle of bank (AOB is the angle that the helicopter is rolled around the longitudinal axis. When hovering above the flight deck during cross-wind, tilting of the main rotor tip path plane[16] is needed to remain at the correct location. The tilting of the tip path plane will induce an angle of bank. So, drifting to the side is avoided by tilting the lift vector of the main rotor. During landing aboard ships during cross-winds, often in addition to a necessary helicopter angle of bank, the relative angle between the deck and the helicopter will be augmented by the ship motion. Cross-winds will cause the ship to lie under a roll angle opposite to the angle of bank of the helicopter during the fore-aft procedure, this is illustrated in figure 2.14. The sailing velocity of the ship partially stabilizes the ship (roll) motions. These motion interactions are not taken into account here.

Reason for limit: There is a maximum acceptable relative angle between the flight deck and the helicopter main wheels as one main wheel will touch the flight deck earlier than the other during the landing[17]. This causes a rejection criteria for the angle of bank of the helicopter.

Difference between green and red winds: The force produced by the tail causes a difference in angle of bank for green wind scenarios and red wind scenarios. The tail force is pointed to the right so in green winds less angle of bank is needed to counter drifting to the side as the tail force helps with countering the drift. In red winds a larger angle of bank is needed as the tail force augments the drift. Limits due to angle of bank will be experienced earlier in red winds compared to green winds.

---

[15] The pedal control position criteria is not taken into account in the present research as the impact of this criteria to the SHOLs is negligible.

[16] Tilting of the tip path plane is induced by a *cyclic input*.

[17] This can give structural problems or may cause a bounce of the flight deck.

Location of limit: This limit only plays a role right before landing, so during hover above the landing spot.

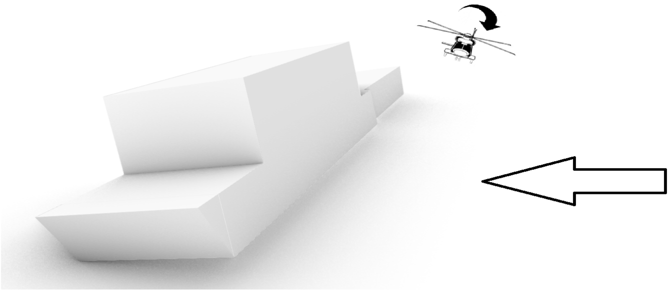

Figure 2.14: Relative angle between ship and banking helicopter during strong cross-wind

Pitch Angle Rejection

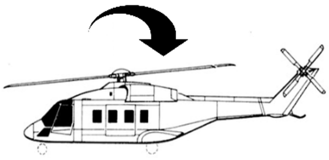

Figure 2.15: Pitch attitude

Pitch attitude indicates a nose-up or a nose-down attitude of the helicopter. The pitch attitude is affected by multiple phenomena. First of all in forward or backward flight, the tip path plane has to be tilted, which induces a pitch-up or pitch-down angle. Secondly, a slight tilt forward of the rotor shaft w.r.t. the helicopter fuselage is applied in the design of most helicopters, including the NH90 NFH[18], which causes a slight pitch-up attitude of the helicopter in low wind-speed conditions as illustrated in figure 2.16. Thirdly, a phenomena called *Flapback*[19] by pilots, can causes sudden excessive pitch-up angles in changing wind speeds (gusts). Lastly, the fixed horizontal tail of the NH90 NFH can cause excessive pitch-up attitudes when the rotor downwash pushes on the tailplane. This last effect occurs most strongly in green winds at a relative wind angle of 30°.

Reason for limit: An excessive pitch-up angle of the helicopter causes a loss of visual with the ship for the pilot and there is risk of a tail strike in neighbourhood of flight deck. A nose-down angle causes in practice no limitations to the envelope.

Difference between green and red winds: Due to the fixed horizontal tailplane, the pitch attitude limit for NH90 NFH is more severe for green winds compared to red winds. This causes the landing and take-off envelope to be more restricted for green winds in the fore-aft procedure.

Location of limit: The loss of visual with the ship is relevant during the entire procedure. The risk of tail strike is relevant as soon as the helicopter moves above the flight deck. In practice, mainly the risk of tail strike causes limits to the envelope which makes this rejection criterion relevant as soon as the helicopter is above the flight deck during the landing procedure.

---

[18] A build-in forward tilt of the rotor shaft is done to reduce the uncomfortable pitch-down attitude during forward cruise flight.

[19] Flapback is caused by a combination of dissymmetry of lift and gyroscopic precession. For more information refer to 2.4.2.

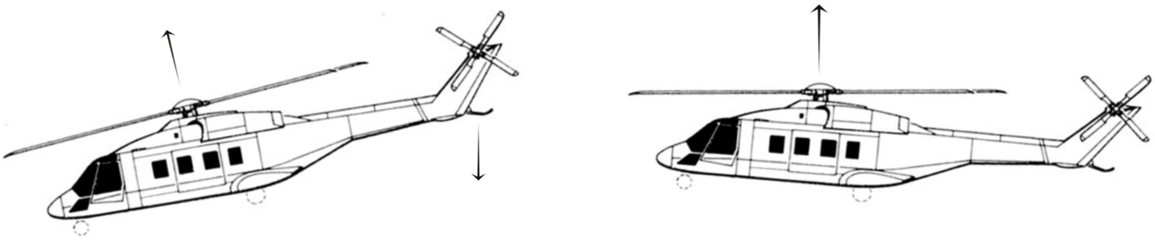

Figure 2.16: Left: forward flight, Right: hover

Torque Required Rejection

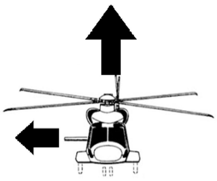

Figure 2.17: Torque

The torque required entails the combination of both the torque required at the main rotor and the torque required at the tail rotor. Main rotor torque is needed to keep the helicopter in level flight, and tail rotor torque is needed to keep the helicopter heading as described in subsection 2.4.1. Multiple elements affect the required torque. First of all, in low wind speeds, more total rotor torque is needed due to the translational lift effect as explained in subsection 2.4.2[20]. Secondly, regions with strong downwash will increase the torque required. Third, the weather-cock effect[21] needs to be countered by the tail torque which makes green winds more restricting than red winds[22].

Reason for limit: There are two limitations for the torque required (Hoencamp, 2015):

- The all engine operatives maximum continuous power may not exceed the safety margin of 98% torque
- The all engine operatives maximum transient power may not exceed 113% torque

Difference between green and red winds: As the tail thrust points to the right when looking at the top view, green winds are more restricting for the torque limitation than red winds.

Location of limit: There are two types of scenarios that cause a torque limit. The first type occurs in low wind speeds and/or strong downwash, this limit will occur in the airwake of the superstructure. The second type occurs during strong green winds, which will occur most likely outside of the airwake of the superstructure where there is no shielding from the environmental wind.

---

[20] In low wind speeds, more main rotor torque is needed due to the inefficiency of the rotor, which causes a higher tail rotor torque necessary to keep heading.

[21] The weather-cock effect indicates the tendency of the helicopter to turn head-to-wind.

[22] In this case, green wind and red wind indicate the relative wind direction w.r.t. the helicopter.

Subjective Rejection

The subjective rejection criterion entails that whenever a scenario is rated with a DIPES higher than 3, a limit is experienced. The DIPES rating is analysed during the sea trials. There are three different scales that are used during sea-trials:

1. Vibration Assessment Rating Scale (VAR)
2. Turbulence Rating Scale
3. Deck Interface Pilot Effort Scale (DIPES)

The test pilot indicates on these three scales what is experienced per specific test condition, the scales are included in appendix D. During sea-trials the DIPES rating, turbulence rating and additional notes are indicated on so-called "sorties".

On the VAR the severity of the vibrations experienced during the test is indicated and on the turbulence rating scale the severity of the turbulence experienced is indicated. On the DIPES the pilot effort can be indicated from "Slight" to "Dangerous" (scale 1 to 5). Whenever the test pilot indicates on the DIPES either 4 or 5, this specific test condition is excluded from the flight envelope. Also, the test conditions where a "Severe" turbulence is indicated by the test pilot by day are excluded from the final nighttime flight envelope. The pilot workload, indicated on the DIPES, is besides *turbulence* and *ship motions* also influenced by *visual cues*[23]. The only difference between daytime and nighttime envelopes is due to the visual cues (Carico et al., 2003).

2.5.4 SHOL Establishment

To develop a SHOL, different countries use different procedures. Below the procedure applied in practice by in the Netherlands is described. The flowchart presented in figure 2.18 Fang and Booij (2006) shows the steps that are applied for establishing SHOLs. The steps are explained below.

First, the ship environment and the helicopter are assessed individually. The scale windtunnel tests are validated by measurements on the full-scale ship using anemometers. Combining the information of the ship aerodynamics and the helicopter shore-based capabilities a "Candidate Flight Envelope" (CFE) is established. The candidate flight envelope is presented in the same type of diagram as the final SHOLs and functions as the starting point of the sea trials. In the CFE, no information about subjective limits is included. The objective of the sea trials is to validate the CFE and to evaluate the pilot workload caused by ship motions, visual references and turbulence. When enough confidence is acquired in the CFE, this will become the SHOL for the particular helicopter-ship combination. Note that the wind tunnel measurements only

---

[23] E.g. with a strong tail wind, the helicopter needs to approach the ship with a nose-up attitude which strongly limits the field of view of the pilot.

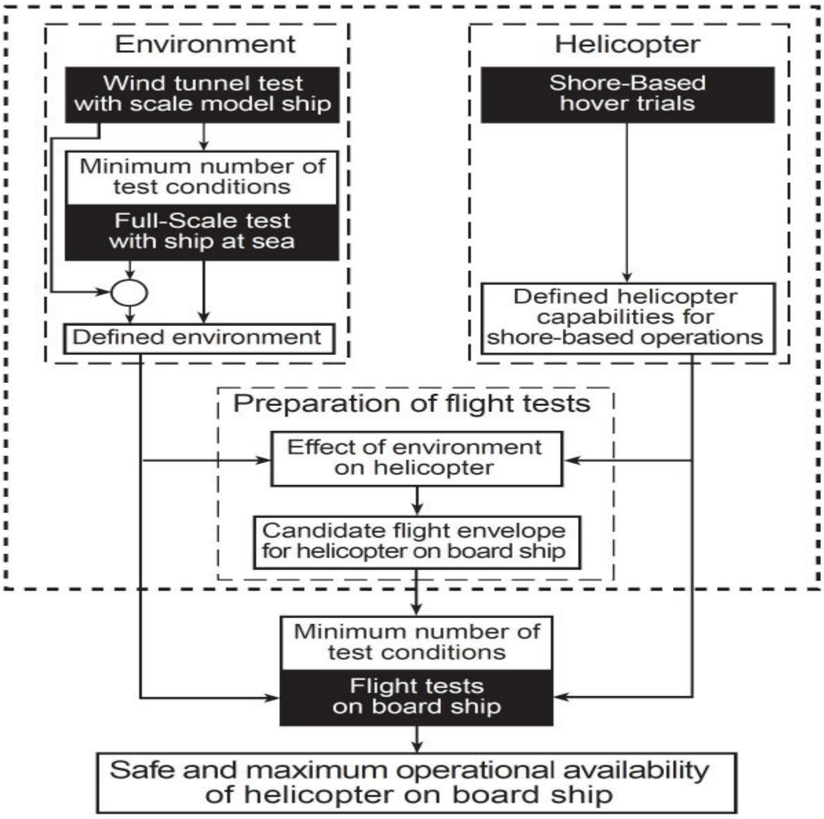
Environment
Wind tunnel test with scale model ship
Minimum number of test conditions
Full-Scale test with ship at sea
Defined environment
Helicopter
Shore-Based hover trials
Defined helicopter capabilities for shore-based operations
Preparation of flight tests
Effect of environment on helicopter
Candidate flight envelope for helicopter on board ship
Minimum number of test conditions
Flight tests on board ship
Safe and maximum operational availability of helicopter on board ship

Figure 2.18: Flowchart of SHOL establishment by the Netherlands (Fang and Booij, 2006)(Hoencamp, 2015)

predict the average airwake of the ship which means that there are no accurate predictions from the wind tunnel tests on turbulence levels. Evaluation of turbulence in the airwake is done during the sea trials by subjective inputs of the pilot.

Determining Subjective Limits

The establishment of subjective limits in practice is not as straightforward as determining objective limits. Subjective limits are determined during sea-trials on basis of the pilot DIPES rating.

Figure 2.5.4 shows a flow diagram describing roughly the steps that are taken to determine subjective limits during sea-trials. Especially for the cross and oblique procedure, the sea-trial test points are mainly executed for red winds. Most of the subjective limits for green winds will be deducted from the limits established for red winds. There are two main reasons for the fact that green winds are not extensively tested during sea-trials:

1. The airflow during the cross and oblique procedure has almost no interaction with the superstructure, only with the flight deck edges. For this reason, it is safe to assume that most DIPES rating for green winds will be almost identical to the DIPES ratings

for red winds.

2. To perform an oblique- or cross facing starboard procedure, the pilot needs to land the helicopter from the left seat of the helicopter. As in general operations are performed in single pilot concept with the pilot in the right seat, the procedures facing starboard are considered of less importance to test extensively during sea-trials.

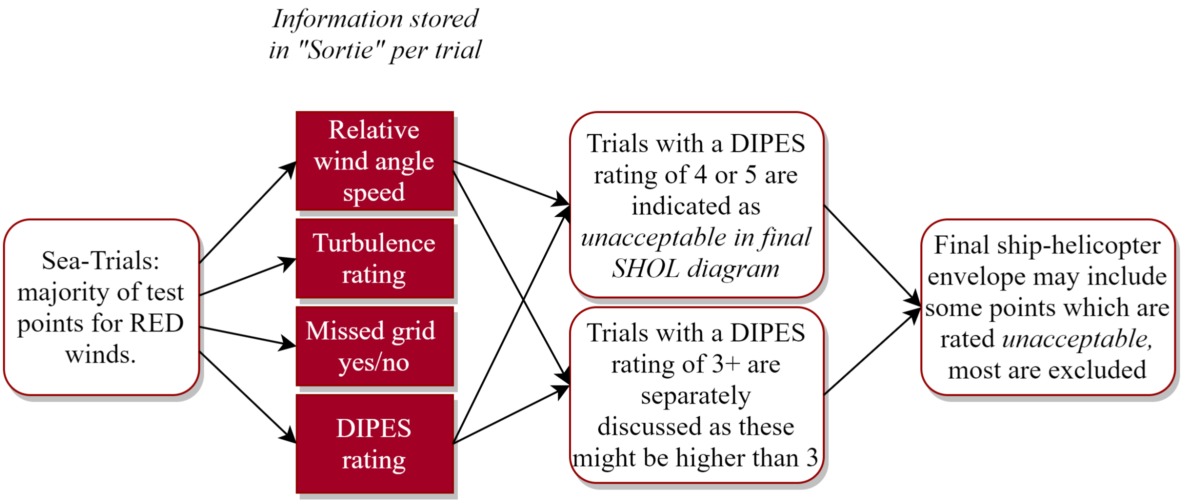
Information stored
in "Sortie" per trial
Sea-Trials: majority of test points for RED winds.
Relative wind angle speed
Turbulence rating
Missed grid yes/no
DIPES rating
Trials with a DIPES rating of 4 or 5 are indicated as unacceptable in final SHOL diagram
Trials with a DIPES rating of 3+ are separately discussed as these might be higher than 3
Final ship-helicopter envelope may include some points which are rated unacceptable, most are excluded

Figure 2.19: Flow diagram of the determination of subjective limits during sea-trials.

2.6 Summary and Conclusions

Information was presented to gain a thorough understanding of the research subject *ship-helicopter interface* from which conclusions can be drawn that lead to the methodology presented in chapter 3. Research questions *1a, 2a and 2b* were answered.

1a: *What is known about the wind environment of ships and methods for measuring and quantifying information of the wind environment?*

2a: *What are the fundamentals of helicopter physics which determine the functioning of a helicopter?*

2b: *What is known about ship helicopter limits and about the methods applied for the establishment of the limits?*

The wind environment of ships is extensively discussed in literature. The main ship airwake features are regions of strong upwash and downwash, and regions of turbulent flow. The problematic airwake features for helicopter operations are mostly considered to be: high intensity turbulence, unexpected changes in flow velocities, downwash regions and low mean horizontal flow velocities. Methods for measuring and quantifying information of the wind environment are traditionally ship helicopter sea-trials and wind-tunnel experiments. More recently, computational methods are used as well for studying the wind environment of ships. Wind-tunnel tests and sea-trials are not considered suitable for the early design phase of a ship. As the objective of the present research is to find a method which is suitable to apply in the early design phase, the focus in the answer to research question *1a* lies in computational methods.

RANS, URANS and DES are the most common computational methods used for simulation of the ship airwake. RANS and URANS are suitable for the investigation of mean flow components in the ship airwake. RANS and URANS methods can give information about trends in turbulence intensity, but cannot accurately quantify turbulent features. DES requires significantly more computation time compared to RANS and provides very accurate results for mean flow components as well as for turbulence. In the early design phase of a ship, methods which are low in computational cost are most useful. Considering this, it is expected that a RANS computational method is most suitable for the early design phase. It has to be tested in the further course of the research if a RANS computation can provide enough useful information on the ship wind environment for the investigation of impact on helicopter operations.

To answer question *2a*, the fundamentals of helicopter physics are briefly discussed in this chapter. The balance of a helicopter is controlled by the main rotor, the tail rotor and the (fixed) horizontal tailplane. Key helicopter phenomena that affect helicopter behaviour are: gyroscopic precession, dissymmetry of lift, flapback and effective translational lift. Specific design features of different types of helicopter can significantly affect their behaviour. The NH90 NFH has a number of design aspects that significantly influence its behaviour. The major design aspect of the NH90 NFH of importance for its behaviour is the fixed horizontal tailplane which can cause excessive pitch-up attitudes for G30 winds towards the helicopter.

Before discussing the answer to research question *2b*, the ship-helicopter landing- and take-off procedures as applied by the Dutch Royal Navy are explained in this chapter. The procedures which apply at the current Dutch amphibious transport ships are: fore-aft procedure, oblique procedure and cross procedure. In answer to research question *2b*, the factors which affect ship helicopter operational limits are mapped. Key factors include: the ship type, the helicopter type, the relative wind environment, the ship motions and the time of day. Limits to the operation of helicopters aboard ships are determined by means of rejection criteria. The procedures for establishing the limits is for each user (navy) different. The Dutch Royal Navy uses rejection criteria for the helicopter attitude, the helicopter performance, the subjective rating, the control positions and the ship motions to determine SHOLs. The SHOLs are established by testing these criteria during sea-trials. The SHOLs are highly dependent on the landing and take-off procedure for which they apply.

Chapter 3

Approach

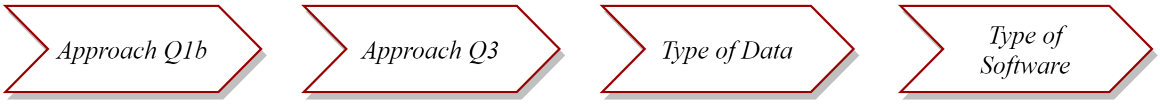

> We are all interested in the future, for that is where you and I are going to spend the rest of our lives.
>
> *Woody Allen*

3.1 Introduction

With the knowledge outlined in chapter 2, the focus can now be put on the core of the research: the development of a tool where insights on the wind environment are related to the operation of a helicopter. The approaches for questions *1b and 3* are described in this chapter:

1b: *What is a suitable method for investigation of the wind environment of a ship with regard to helicopter operations in the early design phase?*

3: *In what way can insights on the wind environment be related to the operation of a helicopter aboard a ship?*

The approaches for questions *1b* and *3* are described in section 3.2 and 3.3. Section 3.4 describes the main data sources used throughout the research and section 3.5 gives an outline of the software tools used.

3.2 Approach Question 1b

The answer to question *1b* will be a computational method or software for modelling of the ship wind environment, which is anticipated to be applicable when studying the ship helicopter interface in the early design phase. The following can be said about the features that a method needs to have in order to be considered suitable for the early design phase:

- The method will allow for quick investigation of the wind environment of many alternative ship designs in different environmental wind conditions.
- The method will provide enough information to be able to study the effect of the ship wind environment on helicopter operations.
- Ideally, the method is part of the resources available for the present research.

In essence, this states that a balance needs to be found between the level of detail of the method and the fidelity of the outcomes while preferably using available resources at DMO. DMO is in possession of a flow simulation software DeepPurple, which is currently used to investigate smoke nuisance aboard ship. The in-house software DeepPurple is user-friendly and can perform quick computations. An assessment is made on the extend that DeepPurple can provide useful information for this research, and what type of prediction tool would suit to the outputs given by DeepPurple. After the exploration of the capabilities and limitations of DeepPurple, it can be anticipated if this software is suitable for investigation of the ship wind environment for the present research.

A number of research reports which were studied for the present research include verification and validation steps performed for DeepPurple. Additionally, a specific verification and validation of DeepPurple is performed in this research to formulate a detailed answer to question *1b*. The assessment of DeepPurple will be done according to the following steps:

STEP 1. The computational method, boundary conditions and assumptions of DeepPurple are studied.

STEP 2. Research reports which include verification and validation procedures of DeepPurple are looked into and the main conclusions about the DeepPurple computational method are extracted.

STEP 3. A verification of DeepPurple is performed by doing a mesh refinement study. The effect of the mesh properties on the mean flow results and residuals and convergence of the solution is analysed.

STEP 4. A validation of DeepPurple is performed by comparing mean flow information and turbulent flow information obtained with DeepPurple to results found in literature. The results found in literature are obtained with different types of computational methods and with wind-tunnel tests.

3.3 Approach Question 3

The answer to question 3 consists of a proposed procedure to relate flow data of a ship wind environment to the behaviour of a helicopter in this environment. With this procedure, a prediction of ship helicopter operational limits will be made. It is investigated if this prediction tool can provide information which can be used for the investigation of ship design impact on helicopter operations.

The data flow of the proposed procedure is presented in figure 3.1. The predictive tool will consist of a set of formulas which define simplified relations between the ship wind environment and specific helicopter shipboard limits. The input for the prediction tool is local flow data obtained with a suitable Computational Fluid Dynamics method.

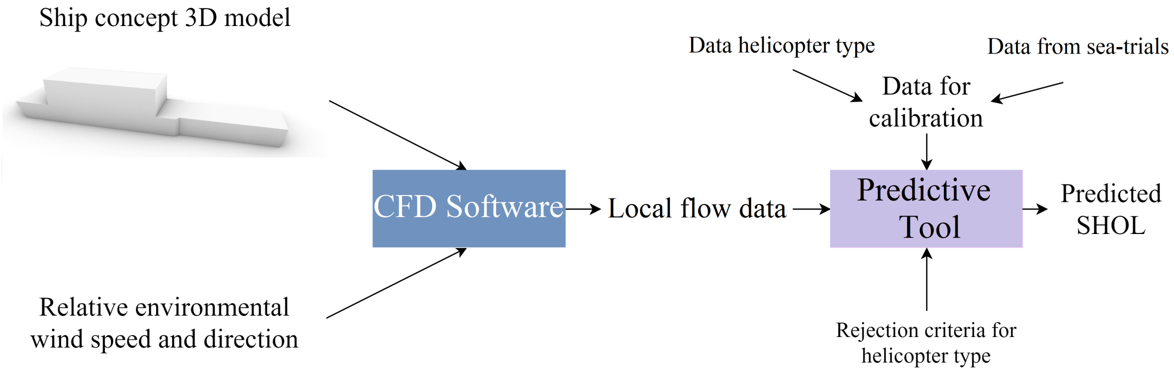
Ship concept 3D model
Relative environmental wind speed and direction
CFD Software
Local flow data
Data helicopter type
Data from sea-trials
Data for calibration
Predictive Tool
Predicted SHOL
Rejection criteria for helicopter type

Figure 3.1: Data flow of proposed procedure for prediction of SHOLs

The tool will have to be calibrated for a specific helicopter type, which in this research is the NH90 NFH. Information on the NH90 NFH flight characteristics from shore-based hover trials, and information from sea-trials with the NH90 NFH are used for calibration. The rejection criteria of the helicopter type have to be specified in the prediction tool as well, which consist of a location in the domain and a maximum magnitude for each criteria. An example of a rejection criteria is: *When in hover above the flight deck, a limit is experienced when the pitch-up attitude of the helicopter exceeds 10°.*

The predictive tool is developed on basis of the anticipation that flow data obtained with the CFD software can be related to the majority of the ship helicopter operational limits. The correctness of this assumption will be evaluated after the validation of the predictive tool. The following steps are taken to develop and validate the tool:

- A set of *prediction base formulas* are created on basis of knowledge gained on the physics of a specific type of helicopter and measured behaviour[1] of this helicopter during shore-based hover trials. Each base formula defines a relationship between flow components in the ship airwake and the behaviour of the helicopter.

- Each base formula is calibrated to an existing combination of a ship and helicopter. This calibration is done by correlating the base formulas to data from shore-based hover trials and sea-trials. Through this, the simplified relations will obtain a predictive function.

- After the calibration of the predictive tool, a validation is performed. The SHOLs of the existing combination of ship and helicopter will be predicted by the tool and compared to the existing SHOLs. The amount of data points used for the calibration is limited to allow for a relevant validation.

- To complete the validation of the tool, a sensitivity analysis is performed. In this analysis, it is assessed what the sensitivity is of the outcome of the predictive tool to the data points used for the calibration.

- An assessment is made of the suitability of the tool for relating the ship wind environment to helicopter operations. It is discussed to what extend the predictive tool is expected to provide useful predictions for new ship designs. Finally, recommendations are made for improvements of the tool.

3.4 Main Data Sources

Inputs Dutch Royal Navy Operational Service

Inputs from a flight deck officer (FDO) and an Air Controller were gathered in the course of the research. The FDO is the person on the helicopter flight deck who guides the helicopter pilot during the final phase of landing on deck. The Air Controller is the person who guides the helicopter from the Command Centre of the ship during the approach of the ship. The Air Controller evaluates the relevant SHOL diagrams and advices on the most suitable approach and landing procedure as well as possible ship heading and velocity changes. Both gave insight into their specific tasks and experiences.

Interview Dutch Royal Navy Test Pilot

At the start of the research, following the literature study, an interview was conducted with a Dutch Royal Navy helicopter pilot. This pilot has extended experience operating different types of helicopters (including the NH90 NFH) on Dutch navy ships. In addition to this, he flies during the sea-trial tests to establish in collaboration with the NLR(Royal Netherlands Aerospace Centre) the ship helicopter operational limits. He shared his experiences of flying ship helicopter operations and establishing the limits over the course of the research.

---

[1] Helicopter behaviour includes: helicopter performance behaviour and helicopter attitude behaviour.

Inputs Royal Netherlands Aerospace Centre

Over the course of the research, continuous personal contact with a helicopter-ship interface specialist from the Royal Netherlands Aerospace Centre (NLR) significantly contributed to the detailed understanding of specific helicopter limit aspects encountered during the research. Besides sharing knowledge on small details related to helicopter behaviour in the ship airwake, also specific reasoning behind various ship design details were clarified.

DeepPurple Documentation

Three documents from the NLR were used, containing information about the computational method of DeepPurple and about the software components of DeepPurple.

- *Physical modelling of the wind climate around ships for the purpose of the preliminary design* (Ven et al., 2012)
- *Calculation method for the determination of the wind climate around ships during the preliminary design* (Ven et al., 2013)
- *Use of a calculation method for the determination of the wind climate around ships during the preliminary design* (Ven and Baalbergen, 2019)

DeepPurple is validated using data acquired from research articles that investigate the SFS2 (Simple Frigate Shape 2). This data includes simulations with CFD methods RANS and DES and experimental (wind-tunnel) data.

Documents and Reports Royal Netherlands Aerospace Centre

The in-house software DeepPurple is developed and installed at DMO by the NLR. For the present research, various research reports related to the use of DeepPurple - provided by the NLR - were studied. The two subjects studied in these research reports, with DeepPurple, are smoke nuisance aboard navy ships and the ship helicopter interface. The following reports were studied for their insights into the use and capabilities of DeepPurple:

- InHolland thesis: *Influence of ship design variation on wind climate around the ship* (Holstein, 2014)
- InHolland thesis: *The effects of cfd modelling on helicopter flight envelopes* (Kamp, 2015)
- NLR intern report: *The use of cfd modelling of a ship's air wake for the generation of candidate flight envelopes* (Booij et al., 2016)
- TU Delft thesis: *Assessment of fidelity of candidate flight envelopes developed using computational fluid dynamics* (Wit, 2017)
- TU Delft internship report: *Comparison of computational fluid dynamics generated aerodynamic ship data against wind tunnel data* (Oliveira, 2017)

General SHOL Regulations

"Voorschrift CZSK Algemeen 010 Opereren met helikopters aan boord van CZSK-eenheden" (translated from Dutch: *Regulations CZSK General 010 Operating helicopters aboard CZSK-units*)(Hulsker, 2019) contains all SHOL diagrams currently in use for the Dutch navy ship-helicopter combinations and additional information on operational procedures.

Sea-Trial Data of the LPD2

The report "NH90 NFH sea trials LPD2 "Zr.Ms. Johan de Witt" (Hoencamp and Kralingen, 2014) contains information on the sea-trail tests performed for the NH90 NFH - LPD 2 helicopter ship combination to establish the SHOL's. In the report, the SHOL diagrams that were obtained for this helicopter-ship combination are presented with specific data points where limits were experienced. It is documented for multiple scenarios whether a limit is experienced, what type of limit this is (i.e. rejection criteria), how much turbulence is experienced and if the scenario is rated acceptable or unacceptably based on the pilot workload rating[2]. This information is presented in the form of SHOL diagrams for each landing procedure and separately for Green and for Red wind. Figures 3.2 and 3.3 show respectively: the turbulence rating (<4, <=5, >5) and the subjective rating (acceptable/unacceptable).

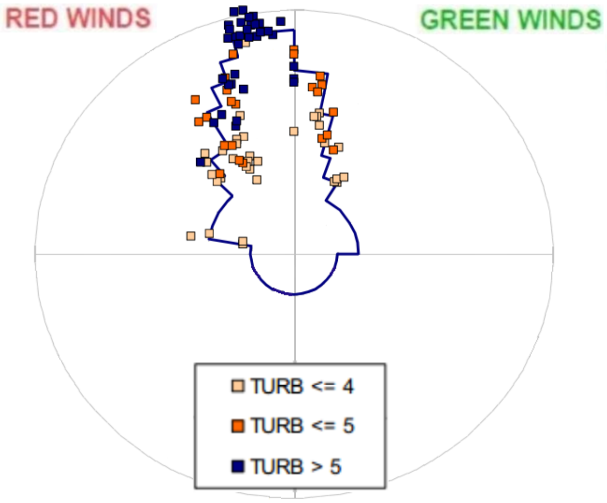

Figure 3.2: Turbulence rating

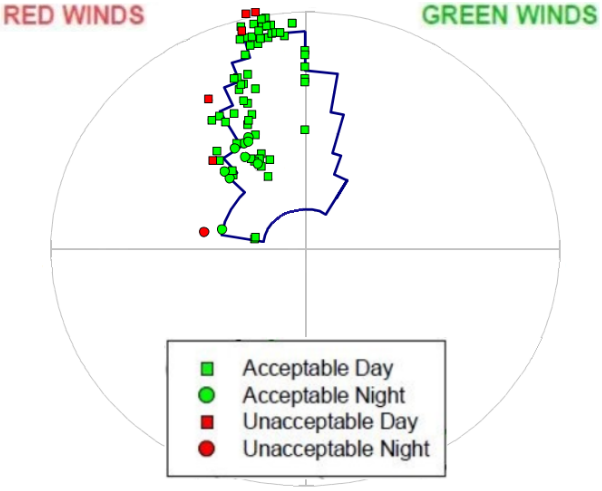

Figure 3.3: Subjective rating

Shore-Based Hover Trials

The report "NH90 NFH Shore-Based Hover Trials Hot Heavy" (Hoencamp, 2012) contains information on the hover trials performed with the NH90 NFH. The data from the hover-trials was combined with ship airwake data establish the Candidate Flight Envelope. During the hover-trials, the behaviour of the NH90 NFH is tested ashore, including attitude behaviour (angle of bank and pitch angle) and performance behaviour.

---

[2] The pilot workload is rated according to the Deck Interface Pilot Effort Scale (DIPES).

3.5 Type of Software

DeepPurple

DeepPurple is a software program developed by the NLR for DMO for the purpose of investigating smoke nuisance aboard navy ships to aid in the preliminary design phase of ships. Information about the computational method of DeepPurple can be found in chapter 4 and detailes on how DeepPurple is structured and how it is installed at DMO can be found in appendix A.

Rhino

DeepPurple evaluates flow around ship designs. These ship design have to be uploaded in DeepPurple as an .STL-file. For the present research, 3D drawing of the ship geometries was done in Rhino 6. The ship models were saved from Rhino 6 to .STL-files and uploaded into DeepPurple for analysis.

Excel

LightPink is developed in Excel. Excel allows for ease of storing, handling and (re)viewing flow velocity data. For future research, a version of LightPink could be developed in Matlab or Python which might give more robustness to the tool.

Tecplot

The software Tecplot is used for the post-processing of DeepPurple flow simulations. TecPlot Macros are developed during the research and used to automate part of the post-processing. For this, the TecPlot manual ("TecPlot.360 2013 User's Manual") (Tecplot, 2013a) and Scripting Guide ("TecPlot.360 2013 Scripting guide") (Tecplot, 2013b) were used. Figure 3.5 presents an example of the type of figures which can be obtained with Tecplot.

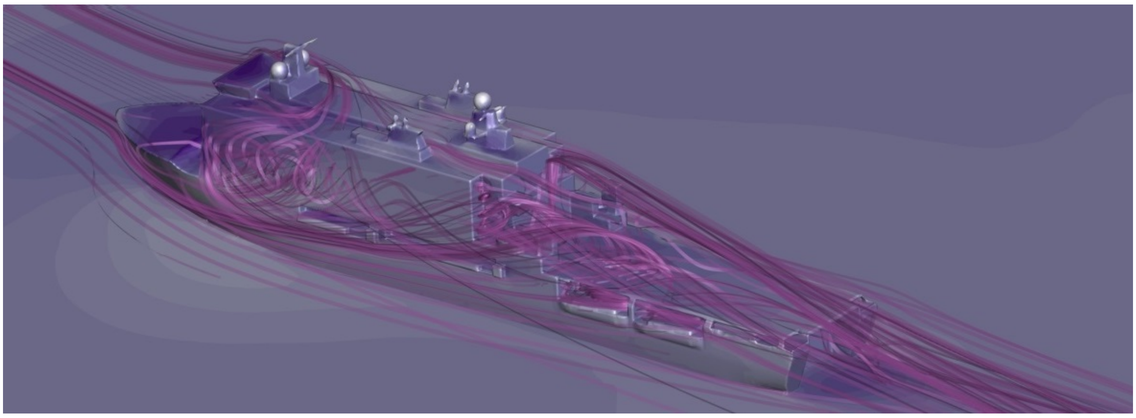

Figure 3.4: Partially visualized streamlines around the Dutch amphibious transport ship Zr. Ms. Johan de Witt.

Chapter 4

Verification and Validation of DeepPurple

DeepPurple Computation Method
Previous research with DeepPurple
Validation of DeepPurple
Verification of DeepPurple
Summary and Conclusions

> Je gaat het pas zien als je het doorhebt.
> - *You will see it once you understand it.*
>
> *Johan Cruijff*

4.1 Introduction

Central in this chapter is research question *1b: What is a suitable method for investigation of the wind environment of a ship with regard to helicopter operations in the early design phase?* As explained in chapter 3, a low-fidelity computational method is considered suitable for acquiring data during the early design phase of a ship. DMO is in possession of software which can make fast and low-fidelity computations for the ship wind environment, *DeepPurple*. In this chapter, an understanding is gained of the capabilities and limitations of DeepPurple. It will be clarified what DeepPurple can and cannot capture with respect to data relevant for helicopter operations. For this, results from previous projects performed with DeepPurple are evaluated and a specific validation for the present study is performed.

Section 4.2 describes the computational method used in DeepPurple. Section 4.3 presents the main conclusions which can be drawn from previous research performed with DeepPurple. Then section 4.4 discusses the verification results and 4.5 the validation results. Finally a summary and the conclusions are presented in section 4.6.

4.2 DeepPurple Computational Method

DeepPurple is a shell that controls simulations in OpenFoam. A standard set of equations, assumptions and boundary conditions is used to set up the calculations in OpenFoam. The solver is described in subsection 4.2.1. Subsection 4.2.2 discusses the boundary conditions and subsection 4.2.3 explaines how DeepPurple meshes the domain.

4.2.1 DeepPurple Solver

DeepPurple runs a RANS (Reynolds-Averaged Navier-Stokes) computation in OpenFoam. In RANS computations, the unsteady flow features are not resolved, all turbulence is modelled. DeepPurple uses a k-ω turbulence model. The OpenFoam solver *buoyantBoussinesqSimpleFoam* is used. This is a steady-state solver for buoyant, turbulent incompressible flow: this solver uses the RANS equations and the Boussinesq approximation. Besides solving for flow velocity and pressure, the buoyantBoussinesq simpleFoam solver in DeepPurple also solves equations for heat transfer and exhaust flow concentration in the ship airwake.

Simple Foam

The OpenFoam solver simpleFoam uses the SIMPLE algorithm to solve incompressible steady-state Navier Stokes equations (RANS equations). SIMPLE is short for Semi-Implicit Method for Pressure-Linked Equations. SimpleFoam uses a finite volume discretization method. SimpleFoam solves the discretized momentum equation and pressure correction equation implicitly (hence iterations are needed), and the velocity correction is solved explicitly. Equations for pressure are derived from the momentum and continuity equations by a pressure-velocity coupling algorithm. The Poisson equation 4.1 is used to calculate the pressure correction at each iteration.

An under-relaxation term is needed in the Simple Foam algorithm to prevent divergence of the solution. Under-relaxation of the iterations means that the pressure and velocity corrections applied per iteration are reduced by multiplying with an under-relaxation factor. Under-relaxation makes the calculations more stable and prevents divergence of the solution, however it slows down convergence of the solution. The SIMPLE algorithm solves the incompressible continuity equation 4.2 and the momentum equation 4.3, where velocity u, kinematic pressure p, stress tensor R and momentum source S_u.

$$\nabla^2 p = -f \tag{4.1}$$

$$\nabla \cdot u = 0 \tag{4.2}$$

$$\nabla \cdot (u \times u) - \nabla \cdot R = -\nabla p + S_u \tag{4.3}$$

Turbulence Model

The solver used in DeepPurple does not resolve any turbulence. All turbulence is modelled by a Shear Stress Transport (SST) k-ω-model. This is a two-equation model for the turbulence kinetic energy k and the turbulence specific dissipation rate ω. This model is able to capture flow separation [1]. The turbulence specific dissipation rate is given by the equation 4.4. The turbulence kinetic energy is given by equation 4.5 and the kinematic eddy viscosity by equation 4.6. Here, D is the effective diffusivity, S is a source term, G indicates the turbulent kinetic energy production rate, γ is the intermittency factor. The intermittency factor determines the percentages of time the flow is turbulent/laminar.

$$\frac{D}{Dt}(\rho\omega) = \nabla \cdot (\rho D_\omega \nabla\omega) + \frac{\rho\gamma G}{\nu} - \frac{2}{3}\rho\gamma\omega(\nabla \cdot u) - \rho\beta\omega^2 - \rho(F_1 - 1)CD_{k\omega} + S_\omega \tag{4.4}$$

$$\frac{D}{Dt}(\rho k) = \nabla \cdot (\rho D_k \nabla k) + \rho G - \frac{2}{3}\rho k(\nabla \cdot u) - \rho\beta^*\omega k + S_k \tag{4.5}$$

$$\nu_t = a_1 \frac{k}{max(a_1\omega, b_1 F23S)} \tag{4.6}$$

Buoyant Bousssinesq Approximation

Buoyancy driven flows occur when density (and temperature) varies in the flow, such as in the case of exhaust air in the ship environment. The Boussinesq approximation is used for incompressible buoyancy-driven flows and approximates flows with temperature differences without solving the compressible Navier-Stokes. The Boussinesq approximation is accurate when used for heat-transfer flows where density and temperature differences are small. DeepPurple uses the Boussinesq approximation 4.7 to determine the exhaust flow for smoke nuisance aboard ships. In 4.7, ρ_k indicates the effective (the driving) density, β is the thermal expansion coefficient and T indicates the temperature in Kelvin.

$$\rho_k = 1 - \beta(T + T_{ref}) \tag{4.7}$$

4.2.2 Boundary Conditions

DeepPurple specifies the initial conditions and boundary conditions for the inflow plane, the outflow plane, the ship surface and the exhausts/inlets (when present). The following variables are specified at the boundaries: velocity (U), pressure (p), turbulent kinetic energy (k), turbulent time scale (ω), temperature (T), turbulent viscosity (ν_t), turbulence thermal diffusivity (α_t), pressure excluding hydrostatic pressure (p_{rgh}), exhaust gas concentration ($conc$) and effective turbulent diffusion for exhaust gases ($DconcEff$).

At the inlet, an atmospheric boundary layer is imposed to the velocity, the ABL is discussed below. Around the ship, the *nutKwallFunction* determines α_t and ν_t, the wall function is discussed below. All other variables are defined at the boundaries either by a fixedValue condition or a zeroGradient condition.

---

[1] https://www.openfoam.com/documentation [cited 28 June 2020]

Atmospheric Boundary Layer

At the inlet, the velocity is defined by an atmospheric boundary layer condition *atmBoundaryLayerInletVelocity*. The velocity and relative wind angle which were given as input to DeepPurple by the user determine together with the atmospheric boundary layer condition, the velocity profile at the inlet. The boundary layer is programmed into DeepPurple to have a height of 10 [m] when simulating at $\frac{1}{4}$ scale (full scale 40 [m]).

Wall Function

Completely resolving the boundary layer at the ship geometry would require a very fine resolution near the geometry (y+ = 1). When using wall functions to approximate the boundary layer solution, the grid at the boundary can be much coarser (y+ = 100). The wall distance in boundary layer areas is usually indicated in a dimensionless measure $y+$ by 4.11 where y indicates the wall-normal height and ν_w is the kinematic viscosity of fluid near a wall. DeepPurple makes use the *nutkWallFunction*, of which the model expression is presented in equation 4.8 with equations 4.9, 4.10 and 4.11. Here f_{blend} is the wall-function blending operator, ν_t is the turbulent viscosity, $\nu_{t_{vis}}$ and $\nu_{t_{log}}$ indicate ν_t computed by the viscous sublayer and inertial sublayer assumptions. E is the wall roughness parameter. Whenever the grid near the wall is too fine, the wall function will give erroneous results so a sufficiently coarse boundary layer resolution is needed (Ven et al., 2012).

$$\nu_t = f_{blend}(\nu_{t_{vis}}, \nu_{t_{log}}) \tag{4.8}$$

$$\nu_{t_{vis}} = 0 \tag{4.9}$$

$$\nu_{t_{log}} = \nu_w\left(\frac{y^+\kappa}{ln(Ey^+)} - 1\right) \tag{4.10}$$

$$y^+ = C_\mu^{\frac{1}{4}} y \frac{\sqrt{k}}{\nu_w} \tag{4.11}$$

4.2.3 Mesh

DeepPurple generates automatically an unstructured grid for the input geometry (in the form of a STL file). Structured grids usually generate more accurate results, however it is difficult to create structured grids automatically for complex geometries such as ships. In some situations, the DeepPurple grid generator can alter the geometry slightly. Increasing the resolution of the STL file helps to avoid this. The DeepPurple grid, and size and shape of the flow domain is set to calculate flows for small relative wind angles. DeepPurple will be less able to calculate results for larger relative wind angles.

SnappyHexMesh

The unstructured gridgenerator snappyHexMesh of OpenFoam is used to create the mesh around the ship model. Three variables are specified by DeepPurple which dictate what the mesh will look like:

- Domain size and total number of elements along x, y and z
- Refinement level of grid towards the ship model and the water surface
- Prismatic boundary layer on ship and water surface

The size of the domain and the total number of elements are dependent on the length of the ship model. Near concave corners, SnappyHexMesh will cannot create a prismatic boundary layer grid. The refinement levels towards the ship geometry are of a higher order than the refinement levels towards the water surface. Figure 4.1 presents a slice of the mesh around the SFS2 model and figure 4.2 presents the mesh around the NLR-developed LPD2 model: *LPD2-Model1*. For these grids the same standard settings of DeepPurple were used[2].

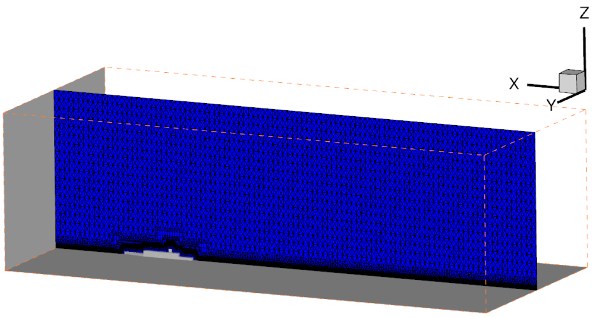

Figure 4.1: Mesh around SFS2, DeepPurple standard settings

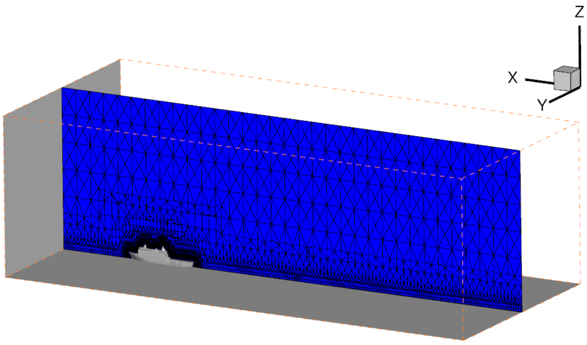

Figure 4.2: Mesh around *LPD2-Model1*, DeepPurple standard settings

Standard Grid Settings DeepPurple

The main script of DeepPurple, that runs the OpenFoam CFD simulations dictates the mesh settings. The domain size is dependent on the ship longitudinal length as can be seen in figures 4.1 and 4.2. The total number of elements per ship length is defined by 4.12.

- Domain size in x: 7 ship lengths
- Domain size in y: 3 ship lengths
- Domain size in z: 2 ship lengths

$$Nr_{elem} = L_{ship}/16 \tag{4.12}$$

The main script of DeepPurple also specifies two refinement regions. The first region is in the neighbourhood of the ship, as can be seen in figure 4.3 for the SFS2 and in figure 4.4 for the *LPD2-Model1*. The second refinement region propagates towards the water surface. This refinement consists of less refinement levels compared to the refinement towards the ship.

---

[2] As the SFS2 model in figure 4.1 is full scale and the *LPD2-Model1* in figure 4.1 is $\frac{1}{4}$ scale, the size of the domain for the SFS2 is larger, resulting in a higher total number of elements.

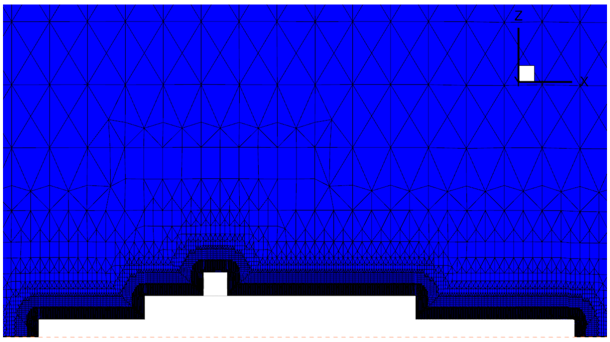

Figure 4.3: Standard mesh refinement SFS2

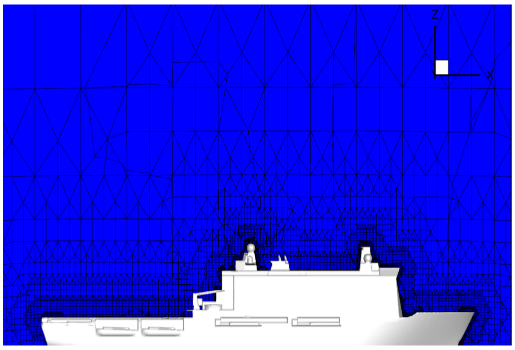

Figure 4.4: Standard mesh refinement *LPD2-Model1*

The prismatic boundary layer on the ship surface and water surface are defined the same and can be seen in figure 4.5. SnappyHexMesh aims to create a prismatic boundary layer around the entire ship model, however at certain concave corners it will not succeed. At these corners no prismatic boundary layer grid is created Ven et al. (2013).

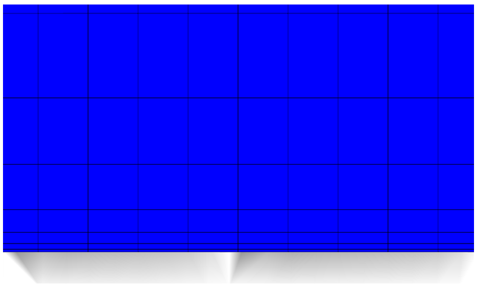

Figure 4.5: Prismatic BL

4.3 Previous Research with DeepPurple

Since the development of DeepPurple by the NLR, several (thesis) studies have been performed with DeepPurple and each study includes a number of validation and verification steps. In this section, the key findings are evaluated. In appendix B, an overview is presented of the reports involving research by the NLR with DeepPurple. Three of the reports Kamp (2015) Booij et al. (2016) Wit (2017) involve the investigation of the potential of using DeepPurple for establishment of the Candidate Flight Envelopes (preliminary SHOLs) instead of using wind tunnel data for CFE establishment which is the conventional method.

4.3.1 Verification and Validation Approaches

The early validations (Ven et al. (2012) and Ven et al. (2013)) are based on qualitative comparisons of velocity contour plots and streamline plots from PIV measurements and exhaust gas concentration visual data. Here, a limited number of relative flow angles were validated. The other reports show are large difference between the extend of their validation steps, however each validation (except Oliveira (2017)) is done for the range of 0 to 360 degrees of relative flow angle. The reason for this is that the key subject of investigation for these reports is the prediction of CFEs (for SHOL establishment), for which information is needed of all possible relative flow angles.

The data which was validated concerned the velocity coefficient (ratio of local flow velocity and relative flow velocity) and the flow deviation angles in both the vertical and horizontal direction at different specific locations on the flight deck. The convergence of the solution is analysed by Booij et al. (2016) by evaluating the residuals per timestep/iteration step and per region in the domain for both the DeepPurple computation and the computation with another solver (AcuSolve). Wit (2017) performed grid refinement studies for DeepPurple and evaluated the effect of grid refinement on the results for the flow velocity coefficient and flow deviation angles.

4.3.2 Effect of Finer Grid (by NLR)

The NLR has tested different settings for the resolution of the grid in DeepPurple. As DeepPurple is developed for the investigation of smoke nuisance above the flight deck, the refinement of the grid resolution around the ship model is originally defined on the basis of the height of the superstructure in front of the flight deck as this is determines the size of the flow structures. As rule of thump, 20 to 30 cells per flow structure should be taken (Ven et al., 2012), so a superstructure with a height 5 [m] will results in a grid width of 0.167 [cm]. The NLR has tested a resolution above the flight deck which is according to this rule of thumb, and one twice as high. It was found that the higher resolution does not give any significant changes in the solution.

4.3.3 Main Conclusions of previous Verification and Validation

The research by Booij et al. (2016) has pointed out that DeepPurple flow information (using standard smoke-analysis settings), is not suitable to replace wind-tunnel mean flow measurements for the purpose of predicting Candidate Flight Envelopes[3]. It is anticipated that for the present research, DeepPurple can still be suitable. DeepPurple data in the present research will be used for a different purpose. The purpose of the predictive tool is to identify trends, in contrast to obtaining quantitative results. Furthermore, the following main conclusions can be drawn about DeepPurple in comparison with wind-tunnel data:

- The mean flow velocity and direction prediction by DeepPurple generally become less accurate closer to the flight deck Wit (2017) Kamp (2015).
- The standard grid used by Wit (2017) in DeepPurple comprised $3.3 \cdot 10^6$ cells. Refinement of the grid does not show consistent improvements (Kamp, 2015), more often the finer the grid, the less similarity with experimental results.
- Averaging of the last 100 iterations in DeepPurple show improved results Wit (2017). The difference between results at a different number of iterations (e.g. 900 iterations and 1000 iterations) is significant, which proves that the solution is actually unsteady and will not convergence neatly to a steady-state solution.

---

[3] Refer to 2.5.4 for more information on CFEs.

- A refined grid resolution 1 mm above the flight deck shows better flow velocity and direction results Booij et al. (2016).
- DeepPurple underestimates the recirculation region behind the hangar Booij et al. (2016).
- A resolution at the boundary layer of y+ = 10 results in non-fysical solutions, a y+ of 100 is more suitable for the grid at the boundary layer (Ven et al., 2012).

4.4 Verification DeepPurple

Previous verification steps performed by the NLR have pointed out the effects of adjusting the grid settings in DeepPurple. The NLR has shown that the standard settings in DeepPurple as used currently at DMO (*Baseline Grid*) are suitable for investigation of the ship environment. For confirmation, in this research a number of verification steps were performed. Results obtained with the current grid settings are compared to results obtained with slightly adjusted grids.

The influence of the grid settings are evaluated by performing a solution convergence study and mesh independence study. It is explained how DeepPurple (with OpenFoam) determines residuals and convergence plots and what is considered an acceptable residual level for the computation to be considered converged. DeepPurple results for mean flow velocities are evaluated for different grid settings. It is analysed how the solution converges for different settings and how the results compare to experimental results found in literature. The verification steps are limited due to the fact that DeepPurple is limited in the freedom of altering mesh settings. The following settings are varied and evaluated with the simulations presented in table 4.1:

- Total number of elements (*Test 1*)
- Refinement levels towards the ship geometry (*Test 2*)
- Settings (thickness and refinement) of prismatic boundary layer (*Test 3*)

Verification Simulations					
Name	Model	Scale	Reynold Nr.	Nr. of Elements	Test
EXP	SFS2	1:100	$6.58{\cdot}10^5$	-	-
DP2 - Baseline	SFS2	Full	$6.58{\cdot}10^5$	9071370	Baseline
DP2 - Coarse	SFS2	Full	$6.58{\cdot}10^5$	1903852	Test 1
DP2 - Fine	SFS2	Full	$6.58{\cdot}10^5$	19100062	Test 1
DP2 - Grid3	SFS2	Full	$6.58{\cdot}10^5$	2780492	Test 2
DP2 - Grid4	SFS2	Full	$6.58{\cdot}10^5$	7624442	Test 3

Table 4.1: Simulation used for the Verification of DeepPurple

The ship model used for the verification is the Simple Frigate Shape 2 (SFS 2) which is presented in figure 4.6. Test 1 is discussed here. The discussion of Test 2 and 3 can be found in appendix C. The main conclusions that be drawn from Test 1, 2, and 3 are discussed in 4.4.3.

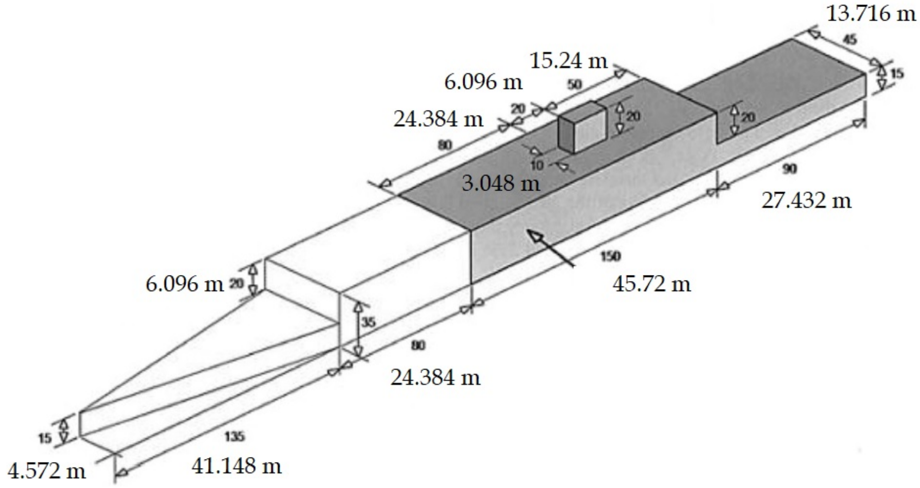

Figure 4.6: Full scale Simple Frigate Shape 2 Zan (2005), dimensions in [m] and in [**ft**].

4.4.1 Residuals and Convergence

DeepPurple uses the simpleFoam iterative algorithm to come to a steady-state solution of the flow around a shipmodel. The convergence of the iterative process is evaluated by plotting solution residuals against the number of iterations. The residual of a variable is a measure of the imbalance of the solution during an iterative process. In other words, the residual indicates the difference between the solution of a variable in a control volume at two subsequent iterations. The residuals are normalised such that they are independent of the magnitude of the variable solutions. For a converging solution, the root mean square of the normalised residuals of the control volumes will decrease with an increasing number of iterations. Usually, a solution tolerance is set which indicates the maximum allowable normalised residual before the solution is considered converged. In the standard settings of DeepPurple, the tolerance is set to a value of: 10^{-4}. No adjustments are made to this level. DeepPurple generates for each computation a convergence plot which presents the velocity and pressure residuals against the number of iterations.

4.4.2 Test 1: Total Number of Elements

Figure 4.7 presents the normalized mean flow velocity (y-axis), measured at different locations above the flight deck (x-axis). It can be seen that for a headwind condition, the *coarse grid* compares worse to the experimental data compared to the *baseline grid*. It can be seen that the *fine grid* gives results close to the *baseline grid*. From the convergence plots in figure 4.8 it can be seen that the *coarse grid* converges slightly slower than the *fine grid* and the *baseline grid*, but to a smaller final residual. The convergence differences are negligible.

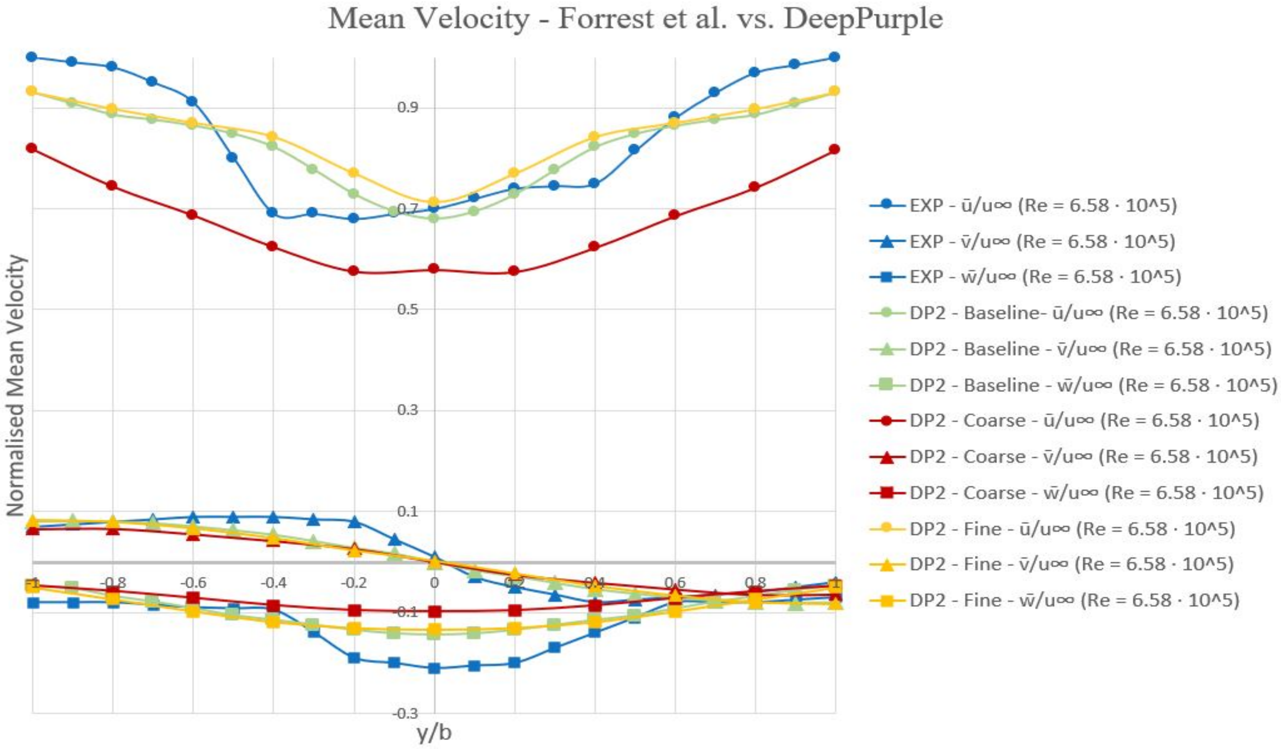

Figure 4.7: Headwind condition mean velocity of experiment- (Forrest and Owen, 2010) and DeepPurple data for different grids at 50% deck length measured at hangar height with the lateral position normalized by ship beam b and an uniform inflow.

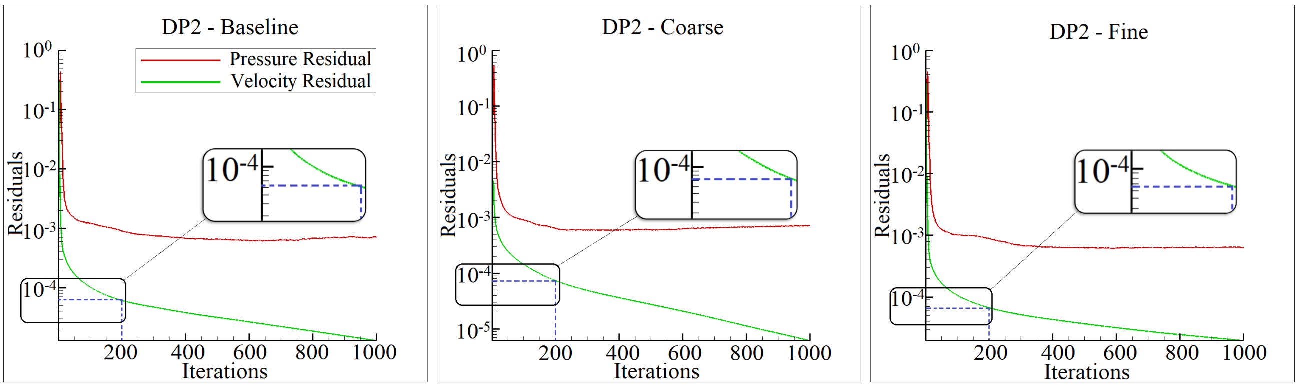

Figure 4.8: Convergence Plots from DeepPurple for *DP2- Baseline*, *DP2 - Coarse* and *DP2 - Fine* for a headwind.

In figure 4.9 it can be seen that for a 45° wind condition, the *coarse grid*, the *fine grid* and the *baseline grid* show quite varying results. This is as expected as the magnitudes of the flow data taken for the graphs significantly depend on the location of the recirculation region. Mind that the x-y axis-ratio is different from 4.7. From the convergence plots in figure 4.10 it can be seen that the *coarse grid* converges slightly faster than the *fine grid* and the *baseline grid* and to a smaller final residual. The *fine grid* is slowest to converge.

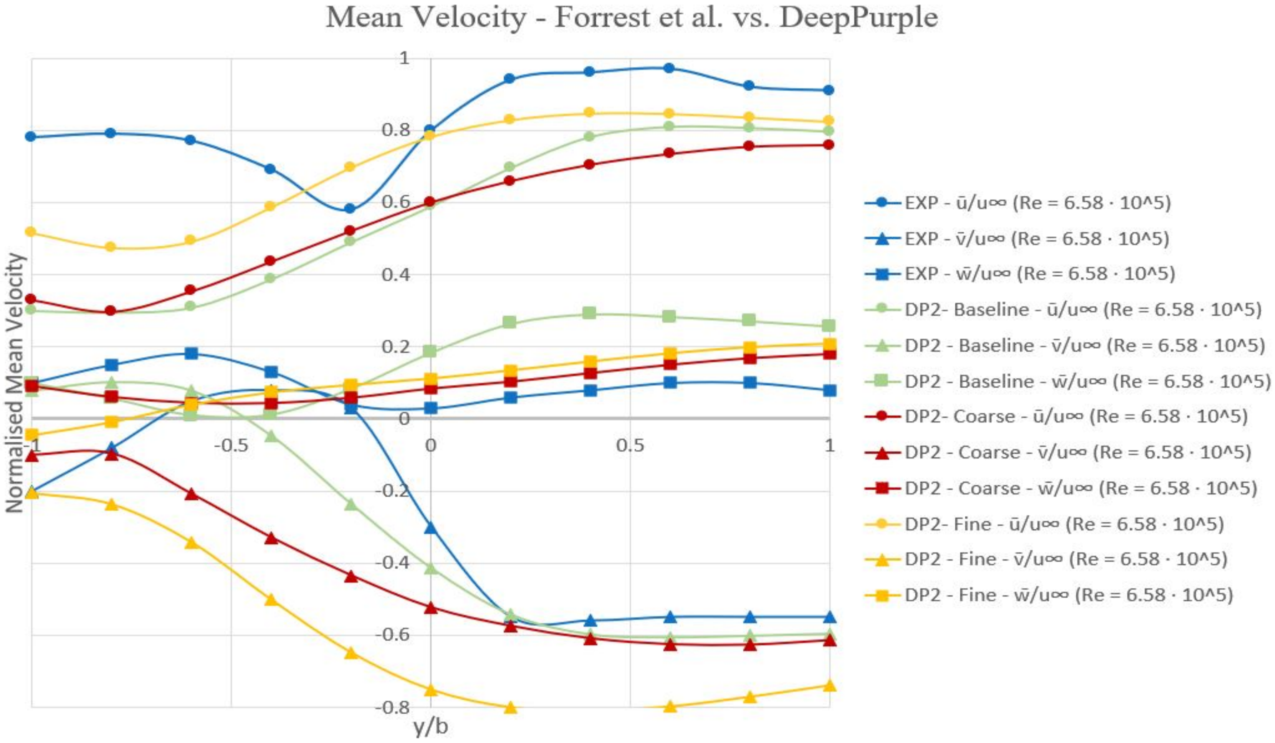

Figure 4.9: G45 wind condition mean velocity of experiment- (Forrest and Owen, 2010) and DeepPurple data for different grids at 50% deck length measured at hangar height with the lateral position normalized by ship beam b and an uniform inflow.

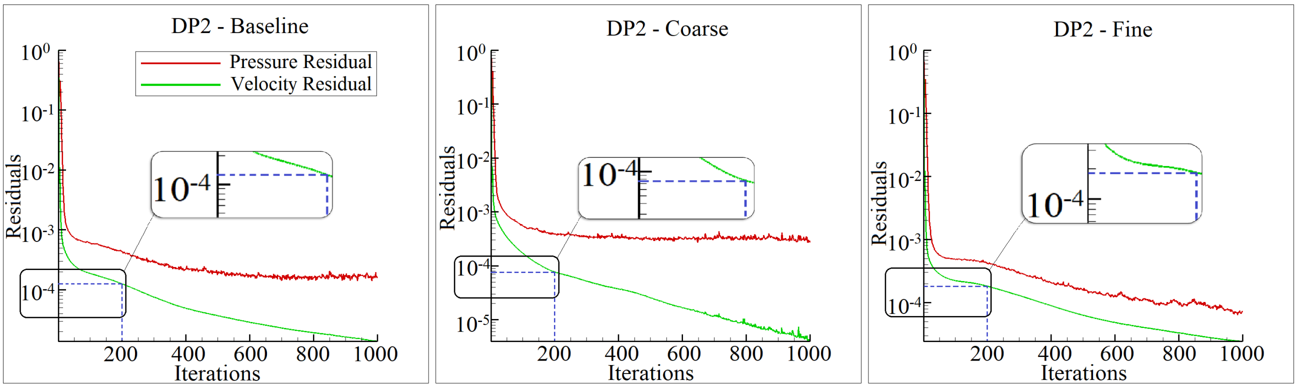

Figure 4.10: Convergence Plots from DeepPurple for *DP2- Baseline*, *DP2 - Coarse* and *DP2 - Fine* for a G45 wind.

4.4.3 Conclusions Verification

The conclusions that can be drawn from *Test1*, *Test2* and *Test3* are presented below. Ideally, for *Test2* and *Test3*, more different grids were compared. However, for a refinement to the ship of a degree higher than the baseline grid either the mesh could not be generated by SnappyHexmesh or the solution did not converge.

- The total number of elements has a visible effect on the mean flow results. The total number of the baseline grid presents most suitable as the *coarse grid* results show more deviation from experimental data whereas the *fine grid* only presents slight improvements compared to experimental data. This conclusion is based on headwind data, for a G45 wind the results are too sensitive to the location of the recirculation region such that the grids cannot properly compared. The convergence of the solutions do not show significant differences for the different grids in *Test1*.
- The refinement level of the grid towards the ship has a visible effect on the mean flow results. In *Test2* the *grid3* with a refinement of a lesser degree was compared to the *baseline grid*. The mean flow solution of *grid3* compares less accurately with experimental data than the *baseline grid* solution. The convergence of the solution with *grid3* is slightly faster than the convergence of the solution with the *baseline grid*.
- The difference between the mean flow solution obtained with *grid4* and obtained with the *baseline grid* is very small which indicates that one level of refinement less in the boundary layer does not influence the mean flow solution significantly when taking data at hangar height at 50% of the flight deck. The convergence plots of these solutions do not differ significantly.

4.5 Validation DeepPurple

By comparing results obtained with DeepPurple to results from wind-tunnel tests and other types of computational methods, conclusions can be drawn about the capabilities of the software. It is important to find out to which extend DeepPurple can predict the problematic airwake features for helicopters, which were discussed briefly in 2.2. A Reynolds number independence study is also of importance as well as an evaluation of the impact of an atmospheric boundary layer inflow in contrast to an uniform inflow. The standard grid settings (*Baseline Grid*) are used during the validation.

4.5.1 Validation Approach

Wind-tunnel data, results obtained with Detached Eddy Simulations and RANS results found in literature, are compared to DeepPurple results. A suitable validation approach is developed, based on the type of information that is looked for from DeepPurple simulations for the objective of this study. Airwake features above the flight deck which are relevant for the present research were identified in section 2.2. This lead to the following airwake variables to be validated (in the helicopter path):

- Mean velocity components
- Turbulence intensity
- Turbulence spectrum (intensity per frequency)

For validation purposes, most research found in literature normalize the mean velocity components with the freestream velocity [U_∞].

For validation purposes, the turbulence intensity [I] is in most cases defined as the root mean squared of the turbulent fluctuations [*u', v', w'*] divided by a reference velocity [U]. The reference velocity can be the freestream velocity [U_∞] or the local mean velocity [$\bar{u}$]. The root mean squared of the fluctuations can be related to the kinetic energy [KE], see equation 4.13. The local turbulence intensity can be calculated by taking into account fluctuations in all directions (x, y, z) or seperately for fluctuations in only one direction [I_x, I_y, I_z], see equation 4.14, 4.15 and 4.16.

$$I = \frac{\sqrt{\frac{1}{3}\sum(u'^2 + v'^2 + w'^2)}}{U_\infty} = \frac{\sqrt{\frac{2}{3}KE}}{U_\infty} \tag{4.13}$$

$$I_x = \frac{\sqrt{\sum u'^2}}{U_\infty} \tag{4.14}$$

$$I_y = \frac{\sqrt{\sum v'^2}}{U_\infty} \tag{4.15}$$

$$I_z = \frac{\sqrt{\sum w'^2}}{U_\infty} \tag{4.16}$$

To ensure a proper comparison of results, the following items are important to clarify per data set which is used to compare results from DeepPurple to:

- **Type of inflow condition:** Two options for the inflow are an atmospheric boundary layer or a uniform inflow. Other item to pay attention to are the flow velocity and angle at which the data set is obtained and the atmospheric turbulence included in the inflow (intensity and frequency).
- **Ship model:** Which model is used for the data set, and is this model scaled down or full scale.
- **Presenting of the results:** What are the units used to present the data, which reference velocities are used for normalization and at which locations is data retrieved.

The ship model used for the validation is the Simple Frigate Shape 2 (SFS 2) which is presented in figure 4.6. The cases presented in table 4.2 are used to validate DeepPurple results. A comparison of DeepPurple results to results from a RANS simulation found in literature (using a different turbulence model) is presented in appendix C.

Validation Simulations						
Name	Model	Scale	Reynold Nr.	Inflow	Rel. Wind Angle	Method
EXP	SFS2	1:100	$6.58 \cdot 10^5$	Uniform	0 and G45	Wind-tunnel
DES	SFS2	Full	$2.26 \cdot 10^7$	Uniform	0 and G45	DES
DP	SFS2	Full	$2.26 \cdot 10^7$	Uniform	0 and G45	RANS
DP2	SFS2	Full	$6.58 \cdot 10^5$	Uniform	0 and G45	RANS
DP ABL	SFS2	Full	$2.26 \cdot 10^7$	Atmospheric BL	0 and G45	RANS

Table 4.2: Simulations used for the Validation of DeepPurple

The cases *EXP* and *DES* are from Forrest and Owen (2010). *DP* refers to DeepPurple simulations performed during this study. It should always be kept in mind that full-scale measurement and wind-tunnel measurements can never be accepted as *reality*. In wind-tunnel testing, there are always measurement errors and other effects that affect the measurement data (such as the blockage effect in wind-tunnels). Wind-tunnel data is used for validation (and not sea-trial data) as there is a lot of data available from wind-tunnel tests.

4.5.2 Validation with Experimental and DES Results

In the article by Forrest and Owen (2010), S. Forrest et al. describe their comparison of SFS 2 airwake data of a DES simulation with the airwake data from their wind-tunnel experiment. Both the airwake data from the DES simulation and, the data from the wind-tunnel experiment of Forrest et al. are compared to DeepPurple results. The cases can be found in table 4.2.

It is chosen to recreate the DES case in DeepPurple[4] instead of the experimental case. The SFS 2 in DeepPurple is for each simulation modelled at full scale as DeepPurple has trouble meshing small models. A higher Reynolds number is selected than the wind-tunnel experiment of Forrest et al. to allow the choice of a realistic temperature and flow velocity when using the full scale SFS 2 model. It is expected that the results are Reynolds number independent since the SFS 2 is a bluff body, as was found from literature Eijkman (2020). To test the Reynolds number independence, the case from Forrest and Owen (2010) is also tested at the Reynolds number of the wind-tunnel experiment, by using the full scale SFS 2 model with a lower freestream velocity.

---

[4] A Reynolds number of $2.26 \cdot 10^7$ in DeepPurple is obtained by a temperature of 15∘C which gives a kinematic viscosity ν of $1.470 \cdot 10^{-5}$ and with a flow velocity of 24.22 [m/s].

Validation - Mean and Turbulent Flow Components

Figure 4.11 presents the normalized mean flow velocity (y-axis), measured at different locations above the flight deck (x-axis). The flow data (for all following graphs), are taken at hangar height along the width of the flight deck, at lengthwise halfway the flight deck. The following can be observed:

- DeepPurple mean flow results show good comparison with DES and experimental results for a headwind condition.
- The DeepPurple graphs are smoother than the DES and experimental results which is to be expected from a RANS calculation.

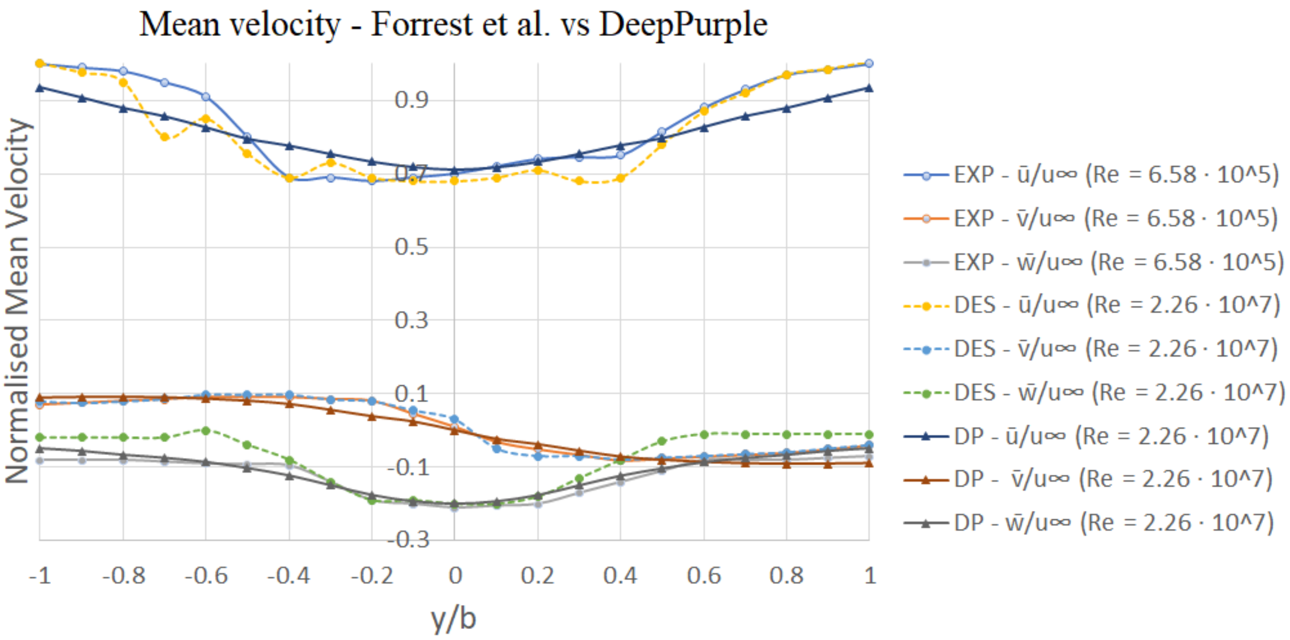

Figure 4.11: Headwind mean velocity of experiment-, DES- (Forrest and Owen, 2010) and DeepPurple data at 50% deck length measured at hangar height with the lateral position normalized by ship beam b and a uniform inflow.

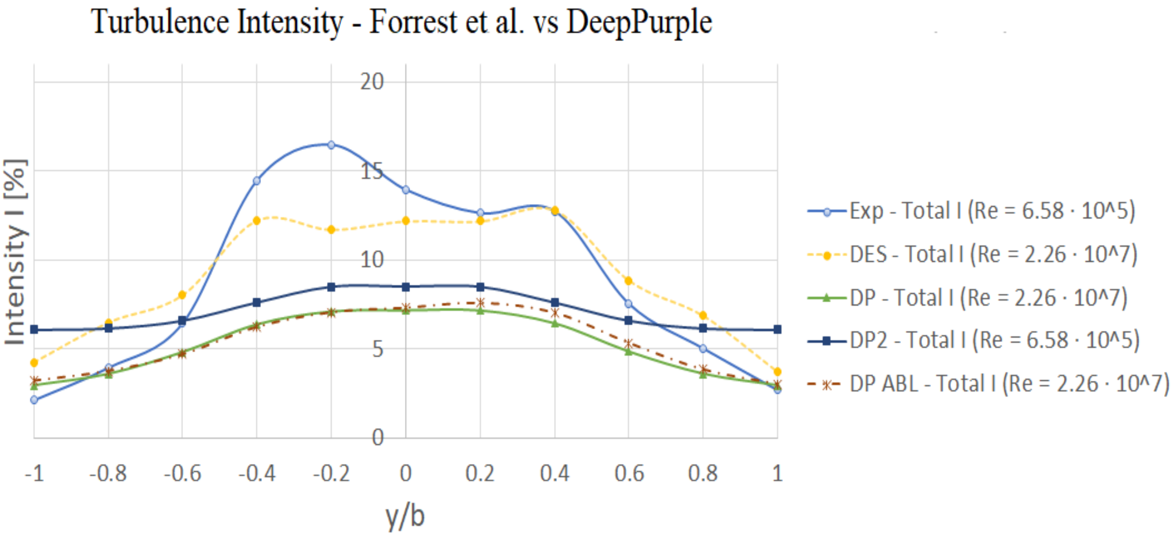

Figure 4.12: Headwind total turbulence intensity of experiment-, DES- (Forrest and Owen, 2010) and DeepPurple data at 50% deck length measured at hangar height with the lateral position normalized by ship beam b and a uniform inflow.

Figure 4.12 includes three DeepPurple graphs, *DP2* is run at a different Reynolds number and *DP ABL* is run with an atmospheric boundary layer. The following can be observed:

- DeepPurple significantly underestimates the turbulence intensity.
- DeepPurple captures the shape of the DES and experimental turbulence intensity graphs to an extend.

From figure 4.13 the following can be observed and concluded:

- Large deviations occur in the graphs when comparing DeepPurple to the experimental (and DES) data, especially in the lateral region y/b -0.8 to y/b -0.2[5].
- The large deviations point out that the DES and wind-tunnel results from figure 4.13 lie ı́n the airwake region on the left side of the flight deck whereas the DeepPurple results lie óutside of the airwake region (due to underestimation of the airwake region) on the left side of the flight deck. To visualize this, refer to the left figure in 4.17.
- This DeepPurple simulation underestimates the airwake compared to DES and wind-tunnel results and/or has the airwake slightly more left compared to the DES and wind-tunnel results.

---

[5] It is important to note here that, as the graphs only show results at a few specific locations in the airwake, large deviations which might occur in the graph do not necessarily mean large errors in a simulation, the location might just be slightly different

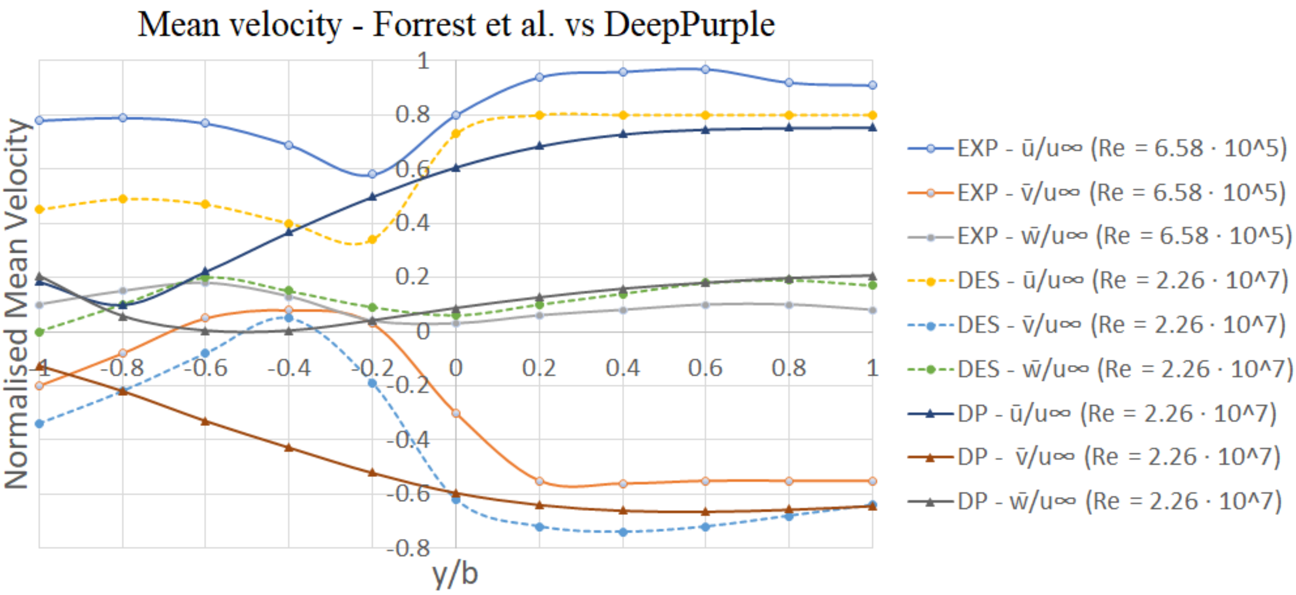

Figure 4.13: G45 mean velocity of experiment-, DES- (Forrest and Owen, 2010) and DeepPurple data at 50% deck length measured at hangar height with the lateral position normalized by ship beam b and a uniform inflow.

Figure 4.14 presents three DeepPurple graphs, *DP2* is run at a different Reynolds number and *DP ABL* is run with an atmospheric boundary layer. It can be seen that DeepPurple significantly underestimates the turbulence intensity. Also, *DP* does not compare well to the shape of the graphs of the DES simulation and the wind-tunnel experiment on the left side of the flight deck (due to underestimation of the recirculation region). *DP2* compares better to the graphs of the DES simulation and the wind-tunnel experiment on the left side of the flight deck (most likely, now the recirculation region is not underestimated).

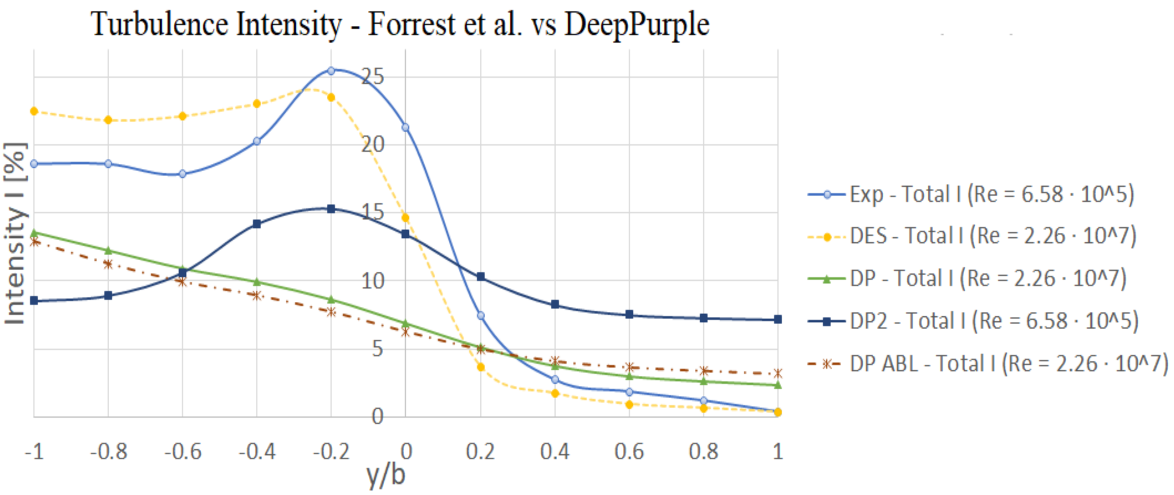

Figure 4.14: G45 total turbulence intensity of experiment-, DES- (Forrest and Owen, 2010) and DeepPurple data at 50% deck length measured at hangar height with the lateral position normalized by ship beam b and a uniform inflow.

Validation of Reynolds Number Independence

Information obtained from literature indicates that the flow topology of the ship airwake is independent of the Reynolds number. To test this theory DeepPurple results for the Reynolds number of the experiment (*DP2:* $6.58 \cdot 10^5$) are compared to DeepPurple results at the Reynolds number of the DES simulation (*DP:* $2.26 \cdot 10^7$) for a headwind condition and a G45 wind. A Reynolds number of $6.58 \cdot 10^5$ at a flow temperature of 15°C with a full scale ship model results in a flow velocity of 0.705 [m/s], see equation 4.17. It is chosen to keep the ship model at full scale and adjust the flow velocity, as DeepPurple has trouble meshing the 1:100 scale SFS 2 model.

$$Re = \frac{V_{DP2} \cdot l}{\nu_{DP2}} \longrightarrow 6.58 \cdot 10^5 = \frac{V_{DP2} \cdot 13.716}{1.470 \cdot 10^{-5}} \tag{4.17}$$

From figure 4.15 the following can be observed and concluded:

- There is no large difference between the DeepPurple results at the different Reynolds numbers, *"DP"* seems to be a bit closer to the wind-tunnel data than *"DP2"*.
- These results indicate Reynolds number independence at a headwind condition.

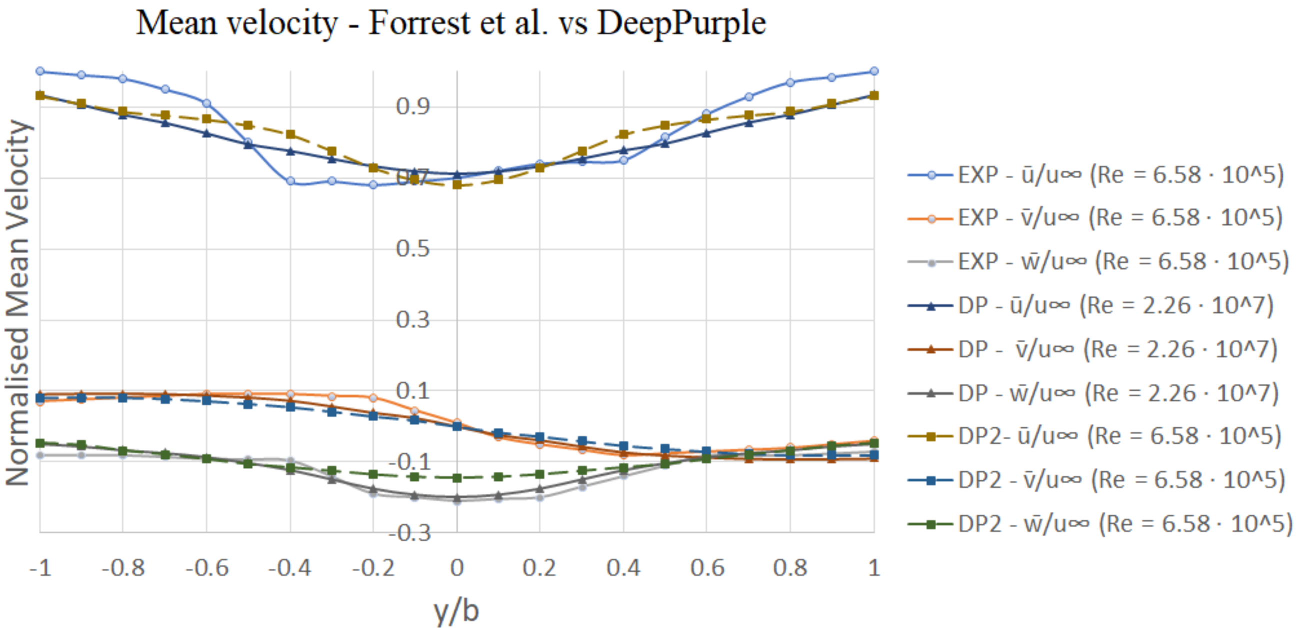

Figure 4.15: Headwind condition mean velocity of experiment- (Forrest and Owen, 2010) and DeepPurple data at different Reynolds nr. at 50% deck length measured at hangar height with the lateral position normalized by ship beam b and an uniform inflow.

From figure 4.16 the following can be observed:

- Large differences occur for the DeepPurple results at the two different Reynolds numbers.
- For the mean velocity component in the y-direction, *DP2* is a lot closer to the experimental data than *DP*. This indicates that *DP2* does not underestimate the recirculation as much as *DP* which can also be seen in figure 4.17.
- These results do not indicate Reynolds number independence for a GREEN45 relative wind angle.

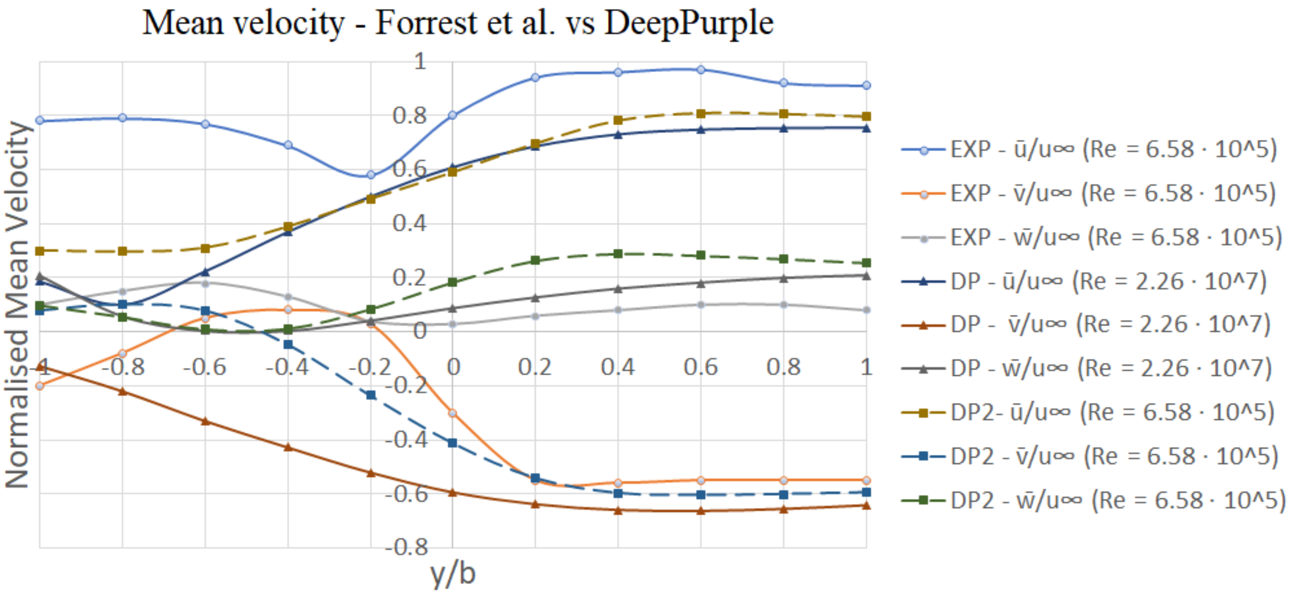

Figure 4.16: G45 mean velocity of experiment- (Forrest and Owen, 2010) and DeepPurple data at different Reynolds nr. at 50% deck length measured at hangar height with the lateral position normalized by ship beam b and a uniform inflow.

In figure 4.17 the recirculation regions are illustrated for the simulations at the different Reynolds numbers. The black rectangle indicates the flight deck, the red line is the location where the data was obtained for the graphs and the ship is oriented with the front to the right. The following can be observed and concluded from figure 4.17:

- The recirculation region in the right contour plot (*DP2*) extends to the red line where the data was obtained for the graphs.
- The recirculation region in the left contour plot (*DP*) is smaller than the region in the right plot and does not extend to the red line.
- The size of the recirculation region simulated by DeepPurple is in better agreement with experimental data when running the simulation at the same Reynolds number as the experiment.

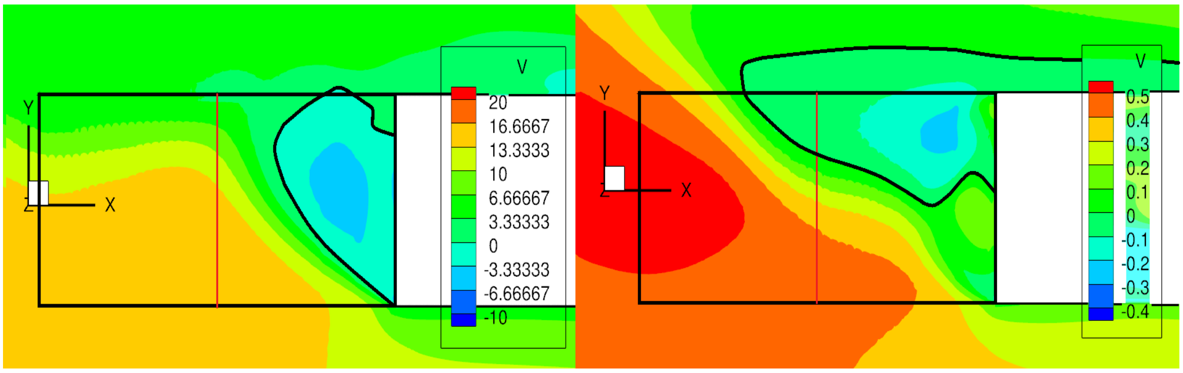

Figure 4.17: G45 contour plots of mean velocity component in the y-direction v in [m/s] of DeepPurple data at different Reynolds nr. (*DP* with Re $= 2.26 \cdot 10^7$ left and *DP2* with Re $= 6.58 \cdot 10^5$ right)

4.5.3 Conclusions Validation

Various validation steps have pointed out that DeepPurple underestimates the recirculation region which is in accordance with the findings from the NLR-reports. DeepPurple smooths out spatial velocity fluctuations as compared to DES and experimental results. DeepPurple can capture the trend[6] of turbulence intensity, but significantly underestimates the turbulence intensity magnitude. Reynolds number independence at headwind conditions (0 degrees relative wind angle) is found, however DeepPurple does not show Reynolds number independence at G45 winds, when comparing results for a Reynolds number of $2.26 \cdot 10^7$ to results for a Reynolds number of $6.58 \cdot 10^5$. Furthermore, using the atmospheric boundary layer with DeepPurple standard settings for the reference height (10 [m]) as inflow condition does not have a significant effect on the mean flow results. The mean flow velocities are slightly lower when including an atmospheric boundary layer compared to a uniform inflow. The graphs supporting this conclusion can be found in appendix C.

4.6 Summary and Conclusions

Research question *1b* is studied by verifying and validating DeepPurple: *What is a suitable method for investigation of the wind environment of a ship with regard to helicopter operations in the early design phase?*

DeepPurple is based on OpenFoam and uses the SIMPLE algorithm to solve incompressible steady-state Navier Stokes equations (RANS equation). Unsteady flow features are not resolved, all turbulence is modelled by a Shear Stress Transport k-ω turbulence model.

Results from DeepPurple are compared to data found in literature to verify and validate the model. A simple frigate shape is used. Testing a simple shape is useful, as DeepPurple will ultimately be used to provide flow information about simple concept ship designs. Mean and turbulent flow components are validated at rotor height during hover above the landing spot. DeepPurple results are compared to outcomes found in literature from wind-tunnel experiments and Detached-Eddy Simulations.

---

[6] DeepPurple can identify approximately where regions are with high or low turbulence intensity.

The verification of DeepPurple in this study points out that the total number of elements in the domain is of importance. Using less than the *standard grid* gives a less accurate solution for the mean flow, using more does not show significant improvements of the solution. Also, using less refinement of the grid towards the ship gives a significantly less accurate mean flow solution. It was found that refining the grid from the *baseline grid* is not always possible as the mesh generator either cannot mesh too fine grids or the solution does not converge.

The following conclusions can be drawn about the DeepPurple computational method:

- DeepPurple underestimates the recirculation region (confirms conclusions from previous research projects with DeepPurple).
- DeepPurple captures the trend of turbulence intensity, but significantly underestimates the magnitude of the turbulence intensity.
- Reynolds number independence is found at headwinds, but not at a G45 wind[7].
- The mean flow results of DeepPurple using an atmospheric boundary layer as inlet condition do not show any significant differences compared to the mean flow results using an uniform inflow.

It is expected that DeepPurple is suitable for the investigation of the ship environment for the present research, however the software is restricted in the information it can give. Learned in chapter 2, shipboard helicopter operations are influenced by the ship wind environment and ship motion. A distinction can be made between flow features that influence helicopter operations: turbulent flow features and mean flow features. The accuracy of the captured mean flow components by DeepPurple is expected to be sufficient for the purpose of identifying trends with the prediction method. It is expected that the underestimation of the recirculation region will not pose large problems during the investigation of the shipboard helicopter operations. It is questionable if the influence of turbulent flow features on helicopter operations can be studied using data from DeepPurple.

For the reasons described above, it is decided to base the predictive tool developed in this research on mean flow information only. In the course of the research, it is investigated if the predictive tool can provide enough relevant information when purely based on mean flow data. If this is not the case, a further validation should be performed with existing data of turbulence experienced by pilots during ship helicopter operations to determine if the turbulence intensity which is modelled by DeepPurple can give relevant information. Then, possibilities of incorporating turbulent flow information in the model can be explored.

---

[7] This is based on a comparison between results at Reynolds numbers differing with a factor 10^2. Low differences in Reynolds number are not expected to influence results.

Chapter 5

Prediction of Ship Helicopter Limits

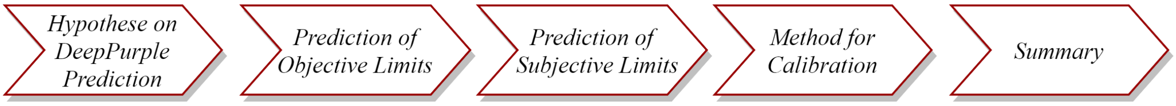
Hypothese on DeepPurple Prediction
Prediction of Objective Limits
Prediction of Subjective Limits
Method for Calibration
Summary

> You cannot cross the sea merely by standing and staring at the water.
>
> *Rabindranath Tagore*

5.1 Introduction

This chapter concentrates on research sub-question *3*: *In what way can insights on the wind environment be related to the operation of a helicopter aboard a ship?* A procedure for the prediction of ship helicopter operational limits, on basis of DeepPurple outputs, is introduced. The prediction procedure *LightPink* is developed for a combination of the NH90 NFH helicopter with an amphibious transport ship on the basis of computed mean flow velocities. LightPink consists of a set of formulas which define a simplified relation between mean flow components and helicopter shipboard limits. In this chapter the basis of these formulas is constructed. In chapter 6 these formulas are calibrated and tested.

The relations between mean flow components and the helicopter limits are based on shore-based hover trails of the NH90 NFH and a number of known limits found during sea-trials. Also incorporated in the base formulas is the mean downwash in the ship environment. In the shore-based hover trials there is no data about the helicopter behaviour in downwash. The relation between downwash and helicopter limits is anticipated based on theory about helicopter physics.

A distinction can be made between LightPink formulas for objective limits and LightPink formulas for subjective limits. Section 5.2 explains in short what is expected of a prediction based on mean flow data. The mean flow components that affect the NH90 NFH are presented in section 5.3 and illustrated in figure 5.2. Section 5.4 discusses LightPink base formulas for objective limits and section 5.5 discusses the LightPink base formula subjective limits. The method which is proposed for calibration of the LightPink base formulas is presented in section 5.6. Finally section 5.7 gives a summary of the chapter.

5.2 Prediction based on Mean Airflow Data

As explained in chapter 2, SHOLs are determined by objective rejection criteria and subjective rejection criteria. The most relevant rejection criteria for limits on board amphibious transport ships are for: the angle of bank (AoB), the torque required, the pitch attitude and the subjective ratings. It is expected, through a study of the existing SHOL diagrams for multiple types of navy ships, that the SHOLs for amphibious transport ships are in practice mainly defined by objective rejection criteria. This is in line with the statement of A. Hoencamp in his PhD research (Hoencamp, 2015) about a method for efficient establishment of SHOLs ”The objective rejection criteria are generally more consistent and restrictive in defining the boundaries of the operational envelopes determined during the sea trials than the subjective ratings given by the test pilots involved” (A. Hoencamp, 2015, p. 153). It is anticipated that a large part of the objective limits can be related to mean flow, when using a correlation method, which will be tested in chapter 6. From chapter 4 it is anticipated that DeepPurple can capture the mean flow well enough for the investigation of helicopter limits, but the turbulent flow components might not be captured accurately enough.
Based on these expectations it is anticipated that with mean airflow data, enough objective limits can be predicted to determine the outline of a SHOL. Objective limits that are caused by turbulent airflow components will not be predicted, which are expected to be mainly limits due to a pitch attitude. Subjective limits likely cannot be predicted with mean airflow data, however it will be tested if a relation can be found between mean flow components and some subjective limits. For this, an analysis of subjective limits and the causes performed with the LPD2 as reference ship. Figure 5.2 gives an overview of the types of base formulas which are developed in this chapter.

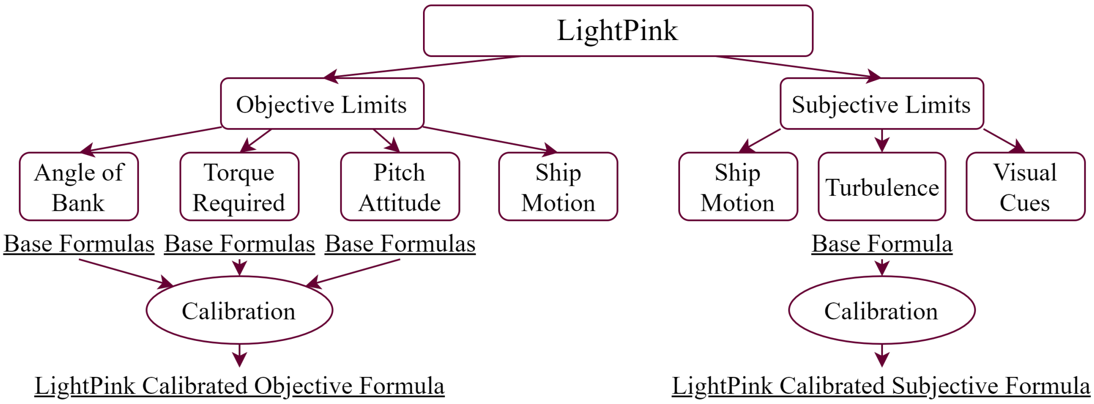
LightPink
Objective Limits
Subjective Limits
Angle of Bank
Torque Required
Pitch Attitude
Ship Motion
Ship Motion
Turbulence
Visual Cues
Base Formulas
Base Formulas
Base Formulas
Base Formula
Calibration
Calibration
LightPink Calibrated Objective Formula
LightPink Calibrated Subjective Formula

Figure 5.1: Types of base formulas included in the prediction procedure.

5.3 Mean Flow Components

Below, the flow components obtained from DeepPurple and used in the LightPink base formulas are presented. The flow components are also illustrated in figure 5.2. Whenever a notation $(-)$ is added to a component in the further course of this chapter, it indicates that a negative value for this component is expected, $(+)$ indicates an expected positive value.

- **U:** Flow velocity component in the x-direction in [m/s]. In DeepPurple, a negative U-component flows from a relative wind angle of 0° towards the ship.
- **V:** Flow velocity component in the y-direction in [m/s]. In DeepPurple, a positive V-component flows from right to left (starboard of the ship to port of the ship).
- **W-component:** Flow velocity component in the z-direction in [m/s]. A negative W-component indicates downwash, which is downward flow.
- **Total horizontal velocity U_{tot}:** The total horizontal velocity experienced at the rotor disk: $\sqrt{U^2 + V^2}$.
- **G30-component:** The horizontal velocity component in the Green 30° direction w.r.t. the helicopter longitudinal axis.
- **R30-component:** The horizontal velocity component in the Red° direction w.r.t. the helicopter longitudinal axis.
- **Headwind-component U_{head}:** The horizontal velocity component that flows directly toward the nose of the helicopter.
- **Perpendicular component to longitudinal axis L_{perp}:** The flow component that is perpendicular to the longitudinal axis of the helicopter. A positive perpendicular component to the longitudinal axis indicates flowing towards the right side of the helicopter.

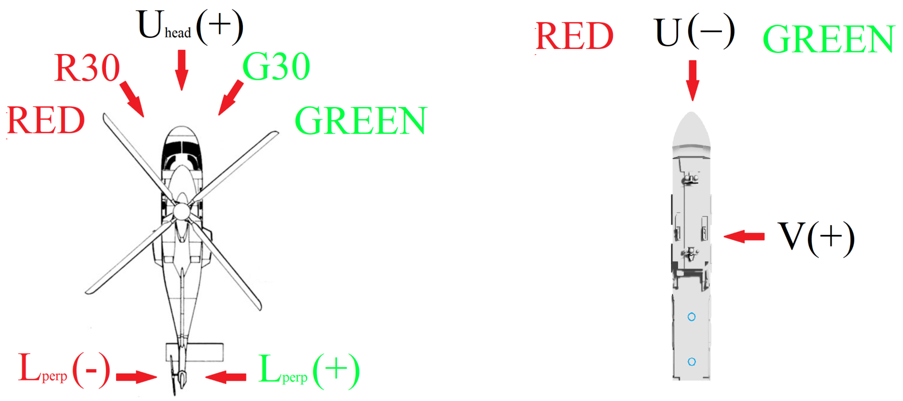

Figure 5.2: Left: Mean flow components used in the LightPink base formulas. Right: Flow components w.r.t. the ship.

5.4 Prediction of Objective Limits

This section describes how LightPink base formulas are developed. A selection is made of objective rejection criteria that will be included in the prediction method. These are the criteria that cause in practice the largest part of the limits aboard amphibious transport ships. The selection consists of objective rejection criteria for:

- Angle of bank attitude (AoB α)
- Torque required (Torque T_{req})
- Pitch attitude (Pitch β)

For each type of criterion (types: AoB, Pitch, Torque), a set of LightPink base formulas is developed. The base formulas describe the relation between mean flow components in the ship environment and the type of objective rejection criterion. Parameters P, in the formulas, need to be calibrated to a scenario using known data points. The base formulas are created in accordance with knowledge outlined in chapter 2, data from shore-based hover trials with the NH90 NFH (Hoencamp, 2012) and a study of existing limits on the LPD2 (Hoencamp and Kralingen, 2014).

5.4.1 Angle of Bank Base Formulas

Two base formulas are developed for the angle of bank attitude α: AoB1 and AoB2. Both the base formulas have to do with an excessive bank angle to the left. As can be seen from the graphs in figures 5.3, 5.7 and 5.8, GREEN winds w.r.t. the helicopter are never critical for the angle of bank attitude in contrast to RED winds. From the theory described in 2.5.3 it is expected that the angle of bank is influenced by the following flow components: U_{tot}, L_{perp} and $(-)W$.

Base for AoB1

> *The base formula in 5.1 indicates a maximum P_1 to the velocity of the RED perpendicular flow component to the helicopter (i.e. $(-)L_{perp}$). For the NH90 NFH rotor system, P_1 will be negative which has to do with the direction of the flow component.*

$$L_{perp} < P_1(-)\ [m/s] \tag{5.1}$$

The graph in figure 5.3 presents the angle of bank attitude of the NH90 NFH for a varying relative wind angle. It can be seen that the peak in the angle of bank occurs at a relative wind angle R90. The angle of bank to the left becomes smaller when wind rotates away from R90 in a sinusoidal manner. This is accordance to theory, as a strong side-wind to the helicopter requires an angle of bank to counter for sideslip as explained in subsection 2.5.3. These observations lead to the expectation that AoB attitude limits due to too strong RED winds w.r.t. the helicopter can be found by the base formula AoB1 in 5.1. P_1 indicates the parameter for the maximum RED L_{perp} velocity.

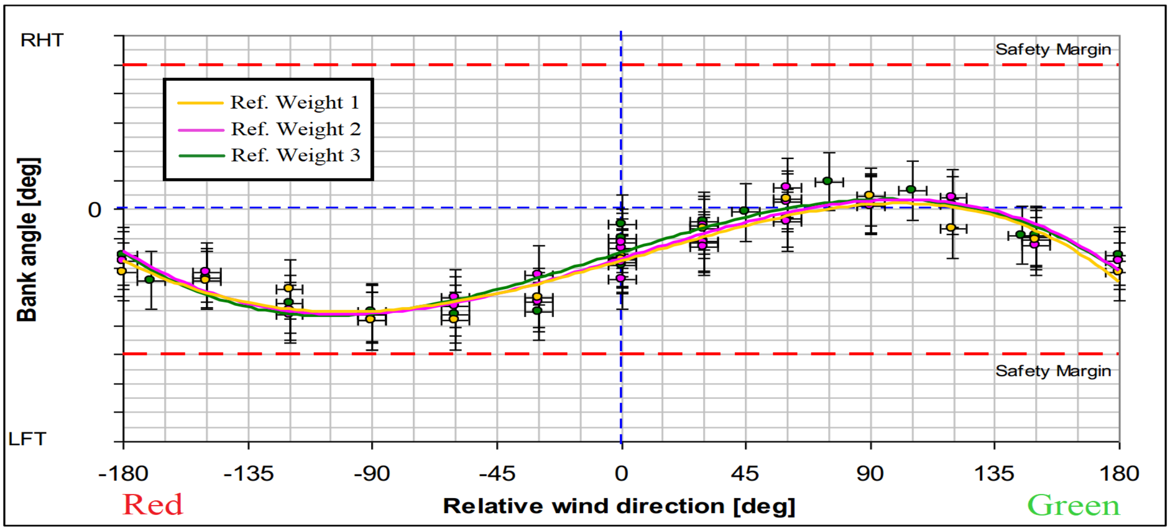

Figure 5.3: Hover Trial: NH90 NFH Angle of Bank attitude versus the relative wind angle for wind velocity 1 (Hoencamp, 2012)

Base for AoB2

> *The base formula in 5.2 is only used when* $\boldsymbol{W} < \boldsymbol{0}$. *For the NH90 NFH rotor system,* P_3 *will be negative which has to do with the direction of the flow component. The base formula indicates that a combination of low wind velocity, a RED perpendicular flow component to the helicopter (i.e.* $(-)L_{perp}$*) and a strong downwash can cause an excessive angle of bank to the left. It is expected that* U_{tot}, L_{perp} *and* $(-)W$ *can be related to a reference*[1] *angle of bank.*

$$P_2 \cdot \frac{1}{U_{tot}} + P_3 \cdot L_{perp} + |W|^{P_4} > \ \alpha_{max} \ [^\circ] \tag{5.2}$$

The graphs presented in figure 5.3, 5.7 and 5.8 present the relation between the angle of bank of the NH90 NFH and the relative wind angle for different velocities. Velocity 1, 2, 3 and 4 indicate an increasing velocity. From these graphs, the following can be observed:

- The angle of bank peak at a R90 wind is approximately directly proportional to the wind speed as can be seen in the left plot in figure 5.4. For each step in velocity increase, the peak of the angle of bank increases with a proportional step. This suggest a directly proportional relationship of L_{perp} to the angle of bank.

---

[1] A reference value indicates that the magnitude in reality might be different.

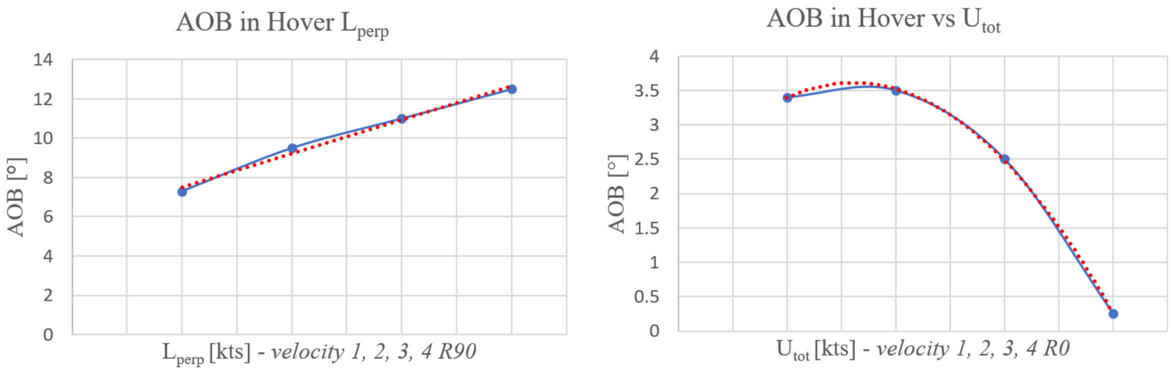

Figure 5.4: Shore-Based Hover Trial data. Left: angle of bank versus L_{perp}. Right: angle of bank versus U_{tot}.

- Looking at the angle of bank for headwinds it can be seen that with decreasing wind speed, this angle increases. The relation between α and U_{tot} is presented on the right in figure 5.4. This is supported by the theory from subsection 2.5.3; for low wind speeds more main rotor torque and consequently tail torque is needed, inducing an increased side-drift which needs to be countered by an angle of bank. It is not considered suitable to formulate the contribution of U_{tot} to the angle of bank in AOB2 purely on data from shore-based hover trials. It is expected that in the ship environment a number of other factors affect the relative angle of bank between the ship and helicopter which are not experienced in shore-based hover.

With the resources at hand, it is considered most suitable to formulate the contribution of U_{tot} by looking at known limits from sea-trials. The known limits can be related to mean flow data that DeepPurple computes above the landing spot. The four data points presented in figure 5.5 are taken at wind directions where W is considered to have a negligible contribution to the angle of bank and where low wind velocities are expected above the landing spot. The graph in figure 5.5 is constructed assuming that L_{perp} is linearly related to the angle of bank and the contribution of U_{tot} to the angle of bank can be determined by equation 5.3[2]. From 5.5 this relation is expected to be in the form of $P_2 \cdot \frac{1}{U_{tot}}$.

$$\alpha_{by:Utot} = 10.5 + L_{perp} \tag{5.3}$$

---

[2] For clarification on the choice of 10.5° refer to 6.3.2. The exact magnitudes are not relevant yet as these steps are purely to find the relation between U_{tot} and the angle of bank for the AOB2 criterion.

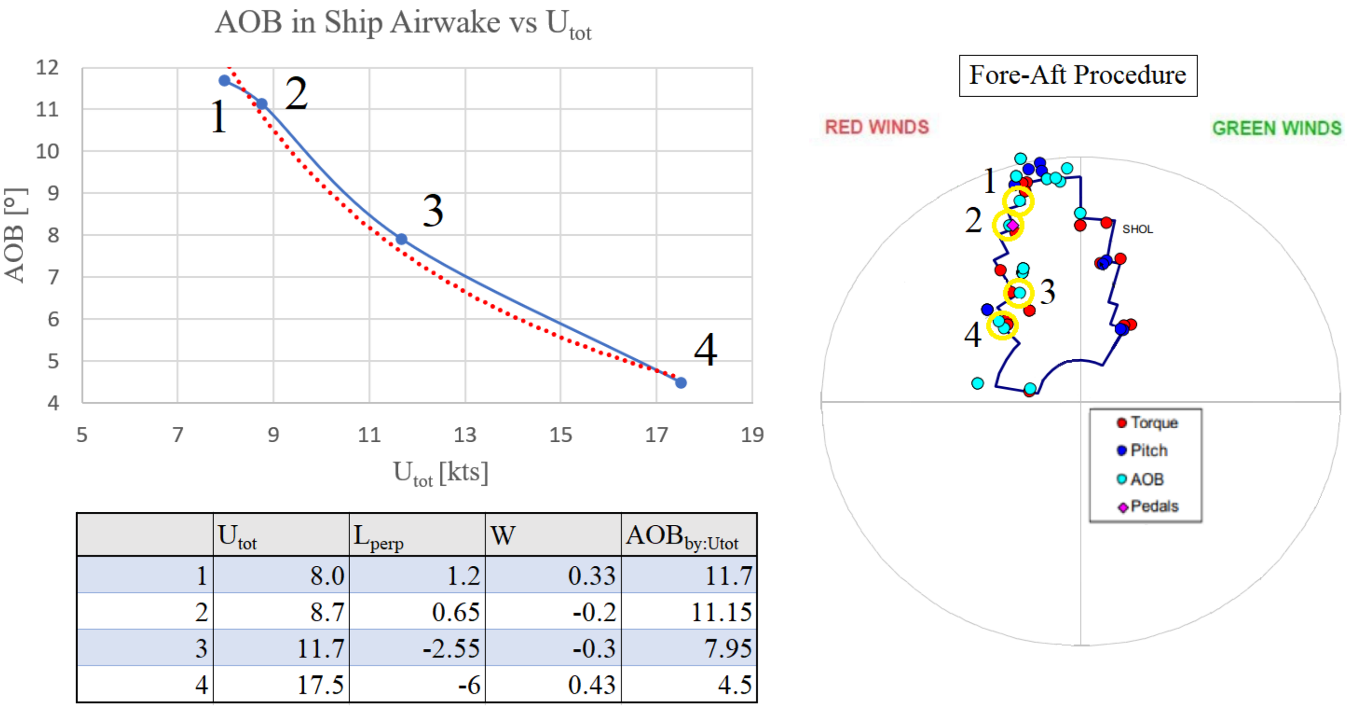

	U_{tot}	L_{perp}	W	$AOB_{by:Utot}$
1	8.0	1.2	0.33	11.7
2	8.7	0.65	-0.2	11.15
3	11.7	-2.55	-0.3	7.95
4	17.5	-6	0.43	4.5

Figure 5.5: DeepPurple mean flow data taken in Disk A at wind speed and directions where AOB limits were experienced during sea-trials aboard the LPD2 - for finding the relating of U_{tot} to the angle of bank.

Discussion AOB2 Base Formula

The inverse relation of U_{tot} to the reference angle of bank is restricted in applicability. This relation is not valid for U_{tot} values below $+/-$ 8 [kts] as can be seen in figure 5.5. This is not considered to pose problems in the prediction procedure as for these wind speeds often 'torque required limits' already pose boundaries to the envelope. However, whenever there is a case where an AOB2 limit occurs in a scenario where $U_{tot} < 8\ kts$ then this limit has to be removed from the prediction. The linear relation of L_{perp} will be less suitable for strong wind speeds as in reality the angle of bank will not continue to increase linearly with increasing L_{perp} but there will be a certain maximum angle of bank to be reached. For this reason, the AOB2 base formula is considered to be sufficiently valid only in the airwake of the superstructure where low wind speeds occur, hence the condition of $W < 0$ to the AOB2 base formula.

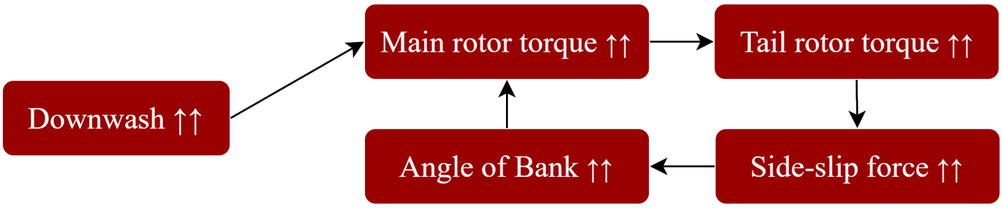

Figure 5.6: Expected effect of downwash on the angle of bank attitude

- During the hover trials, no downward flow components $(-)W$ are encountered, so the relation between the angle of bank and downwash is based on the theory described in subsection 2.5.3. When the helicopter encounters a downwash region, more main rotor torque is needed to achieve a rate of climb to keep level flight. The increased main rotor torque requires a higher tail rotor torque, which causes a side-slip force which needs to be countered by an angle of bank. This effect is expected to be of such magnitude, that the induced angle of bank in turn requires again a slight increase in main rotor torque due to the tilting of the main lift vector, this circle is illustrated in figure 5.6. A power function is expected to indicate the relation between the angle of bank α and the downwash W where P_4 indicates the power.

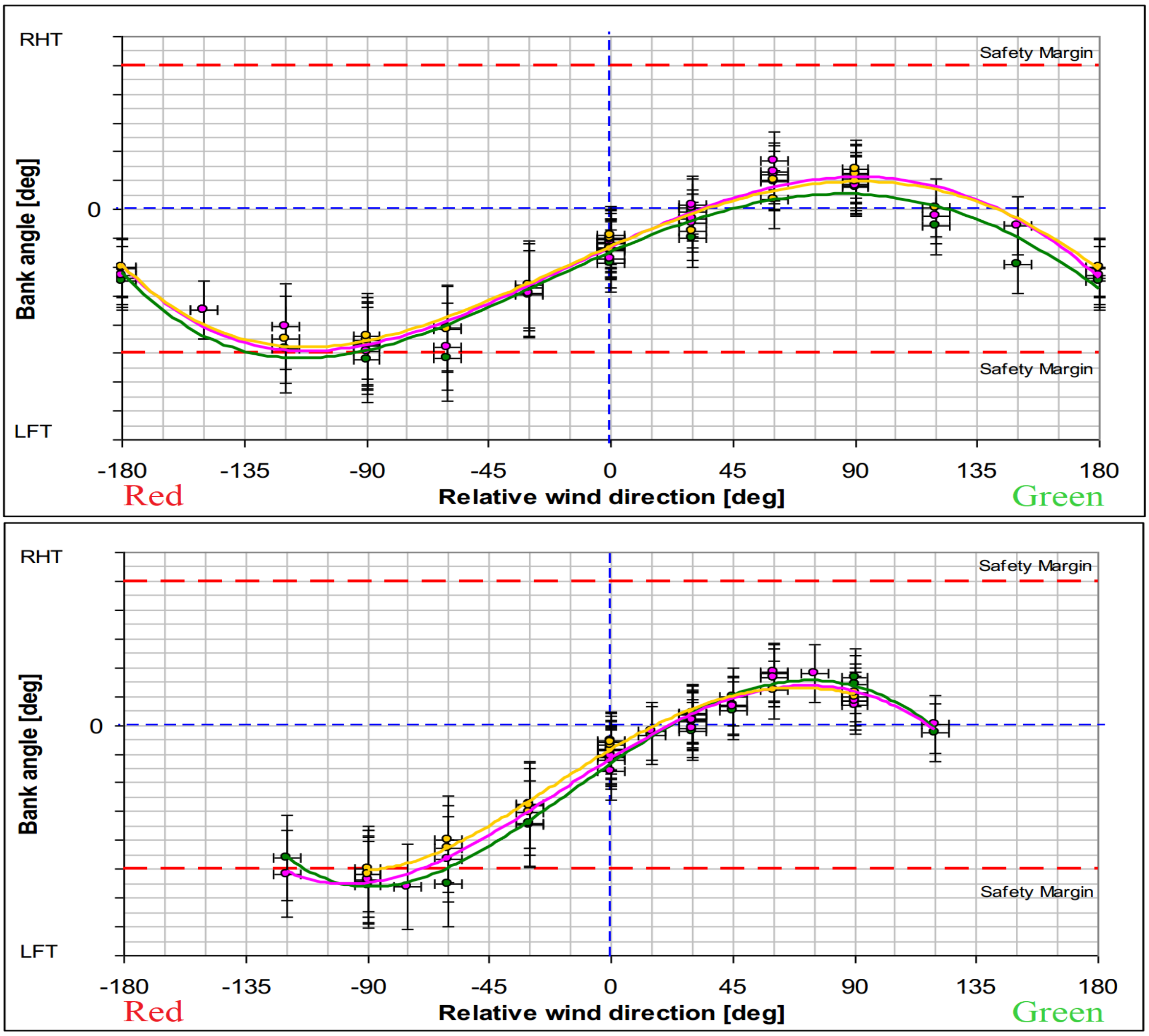

Figure 5.7: Hover Trial: NH90 NFH Angle of Bank attitude versus the relative wind angle for wind velocity 2 (top) and 3 (bottom) (Hoencamp, 2012)

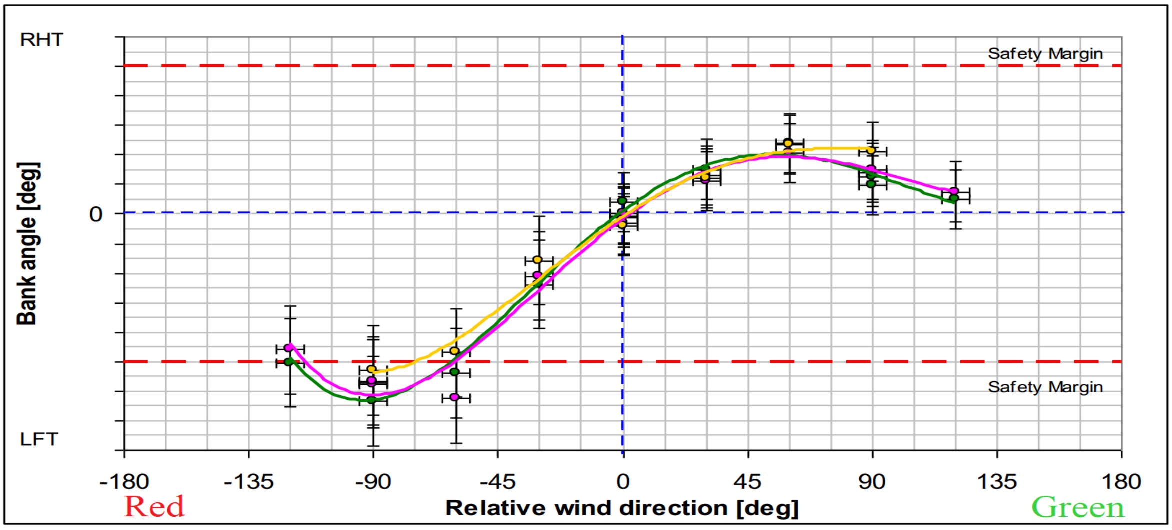

Figure 5.8: Hover Trial: NH90 NFH Angle of Bank attitude versus the relative wind angle for wind velocity 4 (Hoencamp, 2012)

5.4.2 Pitch Attitude Base Formulas

Two LightPink base formulas are developed for the pitch attitude β: Pitch1 and Pitch2. Both the base formulas indicate when an excessive pitch-up attitude occurs. As can be seen from the graphs in figure 5.9, GREEN winds (w.r.t. the helicopter) are more critical for the pitch-up attitude in contrast to RED winds and a nose-down attitude is never critical. Three flow components are expected to affect the pitch-up attitude based on theory explained in subsection 2.5.3: U_{head}, wind from $G30$ and wind speed variations.

The component U_{head} is expected to induce a pitch-up angle due to the normal effect of the horizontal tailplane. Wind from $G30$ is expected to induce an extra pitch-up attitude due to downwash of the main rotor which pushes on the horizontal fixed tailplane. Wind speed variations[3] toward the front of the helicopter can cause *flapback*. *Flapback* can cause pitch-up peaks. DeepPurple cannot predict wind speed variation accurately so this phenomena cannot be taken into account in the base formulas for pitch. This means that pitch-up limits caused by wind speed variations will not be predicted.

Base for Pitch1

> *The base formula in 5.4 is only valid during* ***RED wind (w.r.t. the helicopter)*** *and indicates that there is a maximum* P_5 *for the helicopter headwind.*

$$U_{head} > P_5 \; [m/s] \tag{5.4}$$

---

[3] In this case: low frequency, high intensity turbulence.

From the graphs in figure 5.9 it can be seen that with increasing velocity, the peak for the pitch-up angle also increases. For RED winds, no extreme outliers in pitch-up angle are observed from the graphs. It is expected that pitch-up attitude limitations during RED winds w.r.t. the helicopter can be found by the base formula Pitch1 in 5.4, where P_5 indicates the maximum acceptable headwind velocity.

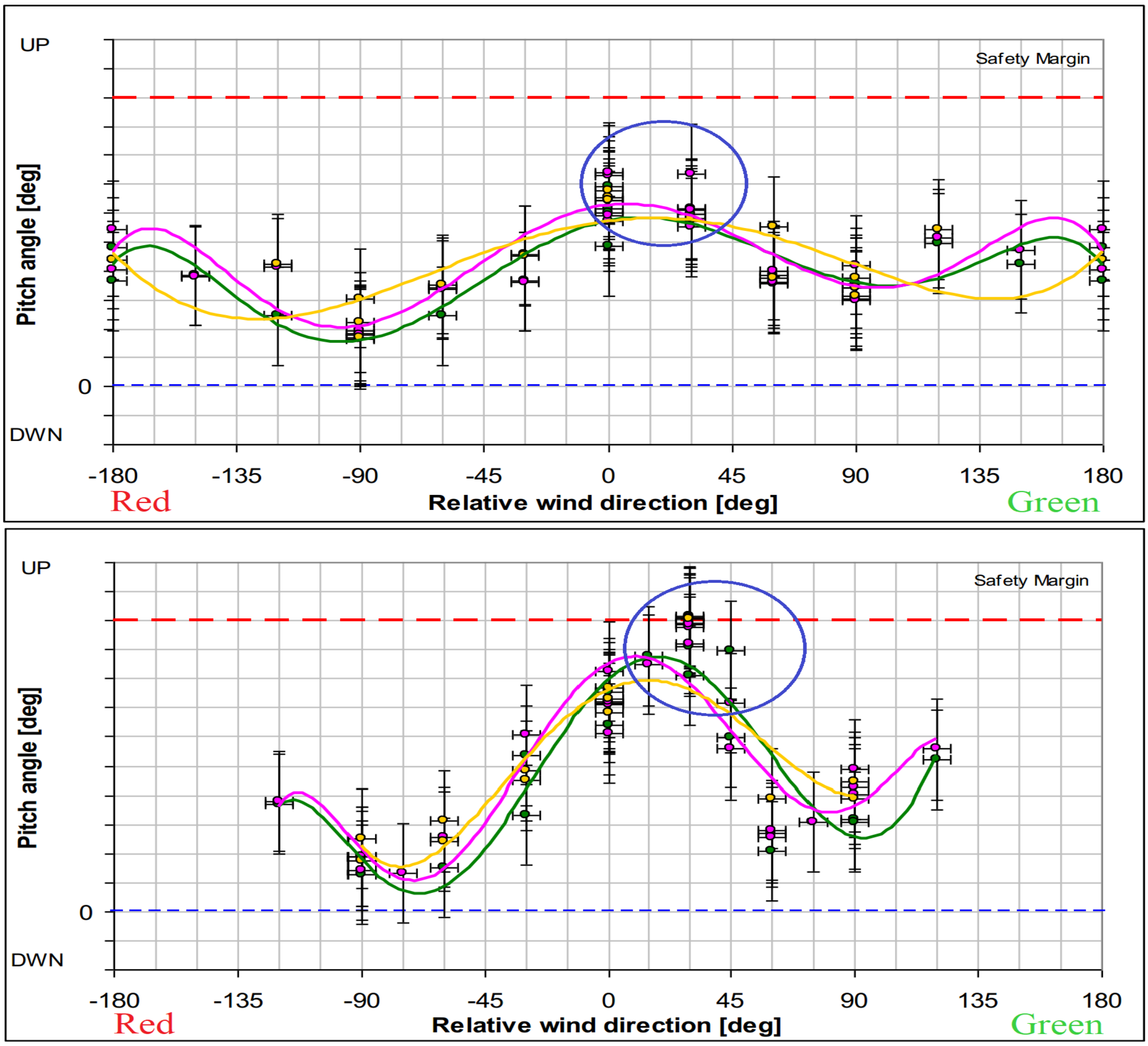

Figure 5.9: Hover Trial: NH90 NFH Pitch attitude versus the relative wind angle for wind velocity 2 (top) and 3 (bottom) (Hoencamp, 2012)

Base for Pitch2

> *The base formula in 5.5 is valid during* ***GREEN wind (w.r.t. the helicopter)*** *and indicates a maximum P_7 for the helicopter wind component from G30. In addition to this, the effect of a G30 flow component becomes more critical when the relative wind direction comes closer to the G30 direction (severity is indicated by parameter P_6).*

$$\left(\frac{G30}{U_{tot}}\right)^{P_6} \cdot G30 > P_7 \; [m/s] \tag{5.5}$$

From the graphs in figure 5.9 it can be seen that the pitch-up peak lies between G0 and G30. It can also be observed that between G0 and G30 outliers (circled in blue) can be found. For higher velocities (here, velocity 3), these outliers are especially occurring for a G30 wind direction. The outliers suggest that some of the pitch-up limits in practice are caused by unsteady phenomena as is supported by the theory described in 2.5.3. It is expected that the pitch-up limits caused by GREEN winds (w.r.t. the helicopter) can be for the greater part found by the base formula Pitch2 in 5.5.

5.4.3 Torque Required Base Formulas

Three LightPink base formulas are developed for the torque required T_{req}: Torque1, Torque2a and Torque2b. Torque1 has to do with the tail rotor required torque. Torque2a and torque2b have to do with the total torque required which includes both the main rotor and the tail rotor torque required. From the theory described in 2.5.3 it is expected that the torque required percentage is influenced by the following flow components: U_{tot}, L_{perp} and $(-)W$.

Base for Torque1

> *The base formula in 5.6 is related to the torque required of the tail rotor only. This formula indicates that there is a maximum P_8 to the velocity of the RED perpendicular flow component to the helicopter (i.e. $(-)L_{perp}$) and a maximum P_9 to the velocity of the GREEN perpendicular flow component to the helicopter (i.e. $(+)L_{perp}$)*

$$P_8(-) > L_{perp} > P_9(+) \; [m/s] \tag{5.6}$$

From the theory described in subsection 2.5.3 it is learned that a crosswind to the helicopter causes a higher tail rotor torque required to keep the correct heading. This can be attributed to the weathercock effect and this effect is larger for GREEN winds compared to RED winds due to the direction of the tail rotor force. This theory suggests that there is a maximum to the perpendicular flow velocity to the tail (i.e. L_{perp}) after which problems will be experienced in keeping the correct heading. This is supported by the graph presented in figure 5.10 where it can be observed that peaks in pedal position occur when the relative wind angle approaches G90 or R90 with the (negative) peak at G90 more severe than the peak at R90. This leads to the base formula presented in 5.6 where it is expected that $|P_8| > |P_9|$.

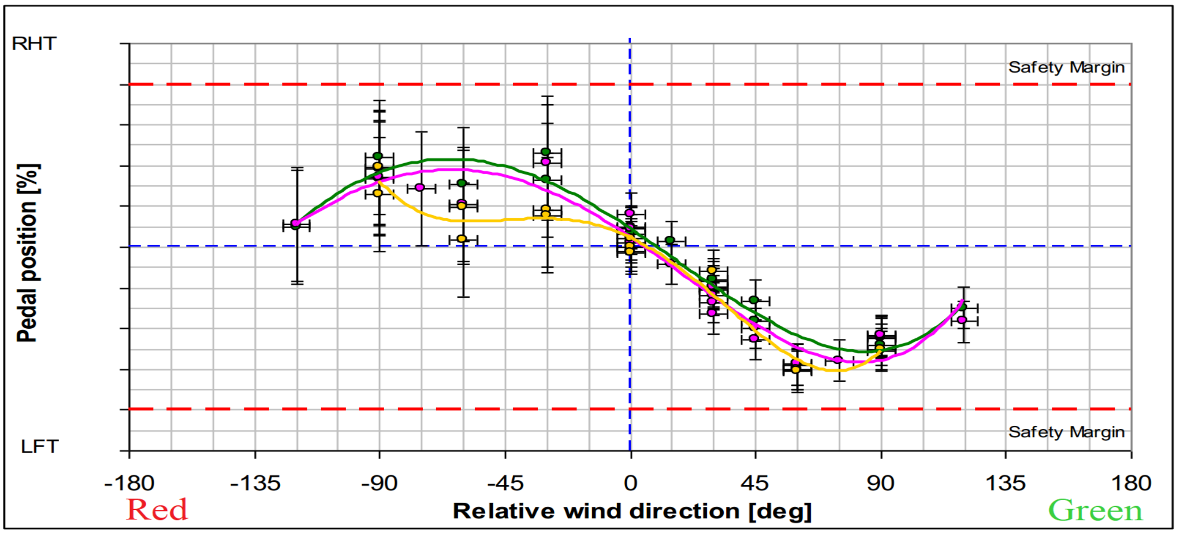

Figure 5.10: Hover Trial: NH90 NFH pedal position versus the relative wind angle for wind velocity 3 (Hoencamp, 2012)

Base for Torque2

The LightPink base formula for the Torque2a is presented in 5.7 and for Torque2b in 5.8. The only difference between the two criteria is that Torque2a is valid in downwash regions and includes the flow component $(-)W$. Torque2b is the same formula, but excludes the $(-)W$ component and can be related to different maximum values depending on the situation.

The base formula in 5.7 is valid when $\boldsymbol{W} < \boldsymbol{0}$ *and related to the torque required of the main rotor and tail rotor combined. This formula indicates that a combination of low wind speed with a strong downwash and a GREEN perpendicular flow component to the helicopter (i.e.* $(+)L_{perp}$*) causes a high* T_{req} *[%].*

$$P_{10} \cdot \frac{1}{U_{tot}^{P_{11}}} + P_{12} \cdot |W|_{13}^{P} + P_{14} \cdot L_{perp} + P_{15} > T_{req,max}\ [\%] \tag{5.7}$$

The base formula in 5.8 is valid when $\boldsymbol{W} >= \boldsymbol{0}$ *and related to the torque required of the main rotor and tail rotor combined. The base formula is the same as Torque2a excluding the W component.*

$$P_{10} \cdot \frac{1}{U_{tot}^{P_{11}}} + P_{14} \cdot L_{perp} + P_{15} > T_{req,max}\ [\%] \tag{5.8}$$

In the graphs in figure 5.11 the torque required indicates the total torque (main rotor + tail rotor). The following can be observed:

- The torque required is strongly dependent on the reference weight of the helicopter.
- Lower wind speed causes higher torque required which is in line with the theory from subsection 2.5.3 related to the effect of translational lift.
- When the rotor is most efficient, i.e. for higher wind speeds, there is a minimum required torque percentage (in the range of 50%-80%) depending on the weight of the helicopter. This can be seen from the bottom graph in figure 5.11.
- In general a GREEN cross wind causes a higher T_{req} than a RED cross wind.

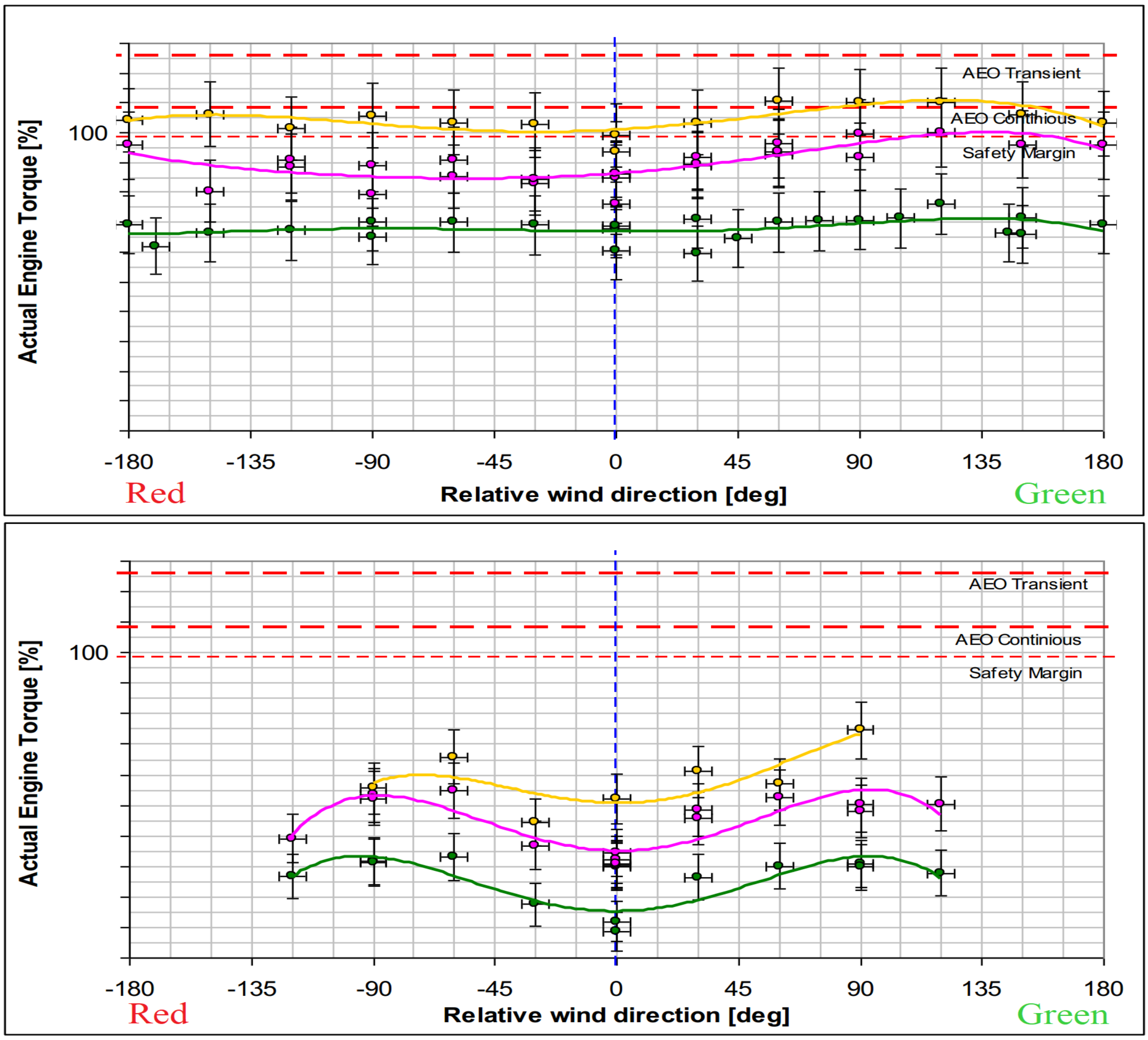

Figure 5.11: Hover Trial: NH90 NFH torque required versus the relative wind angle for wind velocity 1 (top) and 4 (bottom) (Hoencamp, 2012)

These observations in combination with the theory discussed in subsection 2.5.3 result in the base formula presented in 5.7. The relation between U_{tot} and the torque required is expected to be in the form of a negative power function. The relation of downwash to the torque required is expected to be in the form of a power function and the relation to L_{perp} is expected to be directly proportional. The minimum torque required when the rotor is most efficient (due to translational lift) is indicated by P_{15}.

5.5 Prediction of Subjective Limits

This section describes how a base formula for one type of subjective rejection criterion is developed. It is also discussed which subjective limits are expected to be missed with the LightPink prediction of SHOLs. Subjective limits are less straightforward to predict than objective limits and even more difficult to relate to mean flow components. As stated at the beginning of this chapter in 5.2, it is expected that subjective limits cannot be accurately predicted by LightPink. In this section it is tested if a relationship can be found between mean flow components and subjective limits.

Based on the conclusions the analysis presented in this section, the base formula in 5.9 is expected to be able to predict some of the subjective limits with mean flow data. This base formula is only valid in the **approach path** towards the flight deck and will not indicate exact scenarios in which a limit is experienced such as the LightPink base formulas for objective limits, but will indicate regions where there is a high risk of the occurrence of subjective limits.

$$Risk\ Region\ when\ \rightarrow\ |W| > P_{16} \tag{5.9}$$

Subsection 5.5.1 will present a detailed analysis of regions in existing SHOLs of the LPD2 where subjective limits cause boundaries to the envelope. Subsection 5.5.2 presents the conclusions which can be drawn from the analysis that lead to the base formula presented in relation 5.9.

5.5.1 Regions in SHOL with Subjective Limits

An analysis is presented which explains which parts of the boundaries of the LPD2 SHOLs are caused by subjective limits. It will be discussed what factors in the ship environment are attributed to the cause of the subjective limits by SHOL test pilots[4]. Explained in subsection 2.5.3, subjective limits can be caused by various factors such as the ship movement, turbulence experienced by pilots and restricted visual cues. To find out if some of the subjective limits can be correlated to mean flow components and which ones, a detailed analysis is performed of the regions in the existing SHOLs of the LPD2 where subjective limits occur.

---

[4] This information is obtained using inputs from a test pilot and a study of documented *sorties*.

Figures 5.12, 5.13, 5.14, 5.15 and 5.14 present per procedure the objective limits and the subjective limits obtained from sea-trial tests. In each diagram where the subjective limits are indicated, regions are circled in yellow where either subjective limits occur or where boundaries to the ship helicopter envelope are not supported by objective limits nor indicated by subjective limits. The circled regions are numbered and an explanation is given of the reason for the boundary to the envelope.

Clarification of Diagrams

The sea-trial report (Hoencamp and Kralingen, 2014) includes SHOL diagrams where the ”acceptable” and the ”unacceptable” points are indicated[5]. These diagrams can be found in the middle of figures 5.12, 5.13 and 5.14 and on the right of figures 5.15 and 5.14. For the purpose of this research, the original *sorties* of the LPD2 sea-trials were studied [6]. The DIPES ratings which are 3+, 4 or 5 are plotted in SHOL diagrams which can be found on the right in figures 5.12, 5.13 and 5.14. For the oblique and cross facing starboard procedures, less trials have been performed as explained in section 2.5.4, for these procedures there are no trial points with a DIPES rating of > 3, hence this is not included in figures 5.15 and 5.14. The DIPES and turbulence rating scale can be found in appendix D.

Analysis of LPD2 Subjective Limits

> **Region 1.** Subjective limits occur with a DIPES rating of 4 both at spot 1 and 2 in circled region 1 in figure 5.12. The cause for an excessive pilot workload here is attributed by pilots to *turbulence*[7], created by the superstructure. Turbulence ratings in this area go up to 7 and 8, on basis of the scale presented in in appendix D. Before the sea-trials, it was expected by the test-team that the turbulence in this region would play already a role for lower velocities, as this was the case during the sea-trials for the LPD1. It is expected that the higher superstructure of the LPD2 caused the envelope to extend to larger velocities (Dutch Royal Navy SHOL test-pilot, personal communication, 7 Oct 2020).

---

[5] A DIPES rating of 1-3 results in an acceptable data point. A DIPES rating of 4 or 5 results in an unacceptable data point which is in general removed from the ship-helicopter envelope.

[6] The sorties contain for each sea trial the DIPES rating, turbulence rating and sometimes additional notes.

[7] This is based on the *experience* of the helicopter pilot during a sea-trial. It is not defined which kind of turbulence causes the workload, there is only the turbulence rating on basis of the scale in appendix D. Sometimes additional notes taken during the sea-trials specify further where the turbulence was experienced.

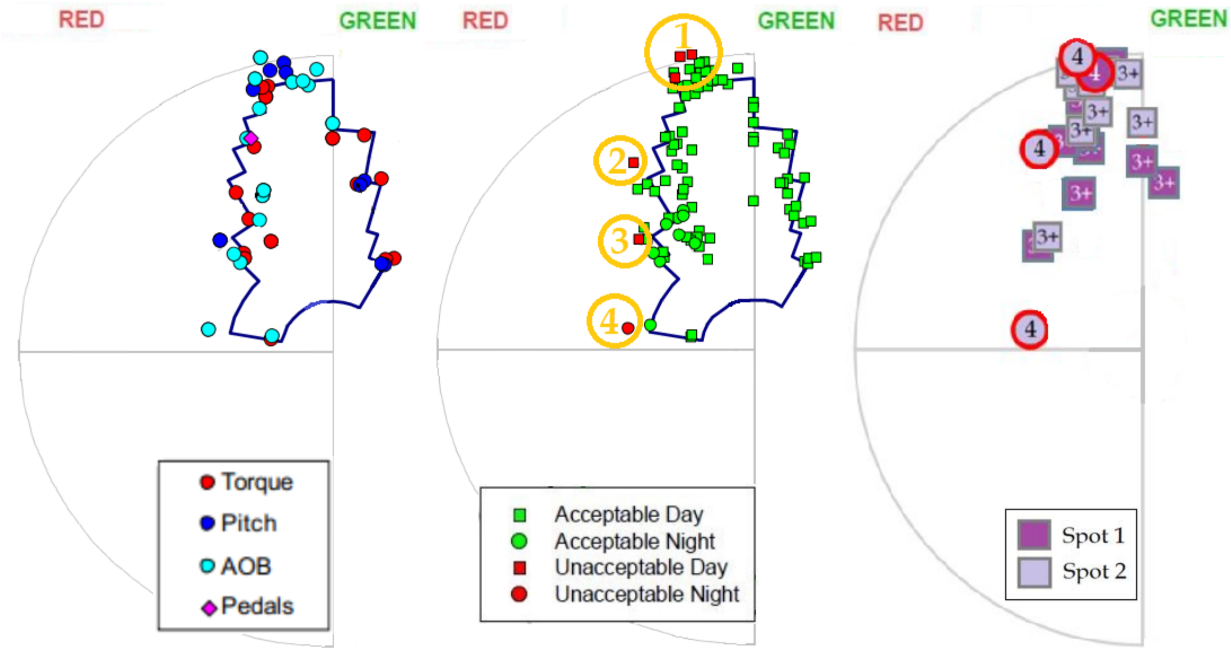

Figure 5.12: Data obtained from LPD2 Sea-trials Fore-aft Procedure - Left: objective limits, middle: subjective limits, right: subjective rating.

Region 2. A subjective limit is experienced with a DIPES rating of 4 at spot 2. The cause of an excessive pilot workload here is attributed to the *restricted visual cues* due to an excessive angle of bank. The objective limit for the angle of bank for this relative wind angle is much more strict as can be seen on the left of figure 5.12.

Region 3. A subjective limit is experienced with a DIPES rating of 3+ at spot 1 and 2. As indicated in the sorties, the cause of an excessive pilot workload here is the *ship attitude* in combination with the helicopter angle of bank. The roll angle of the ship here went to 5° (to the right) during the sea-trials.

Region 4. A subjective limit is experienced with a DIPES rating of 4 at spot 2. The cause of an excessive pilot workload, relevant by night only, is most likely due to *restricted visual cues* due to an excessive angle of bank.

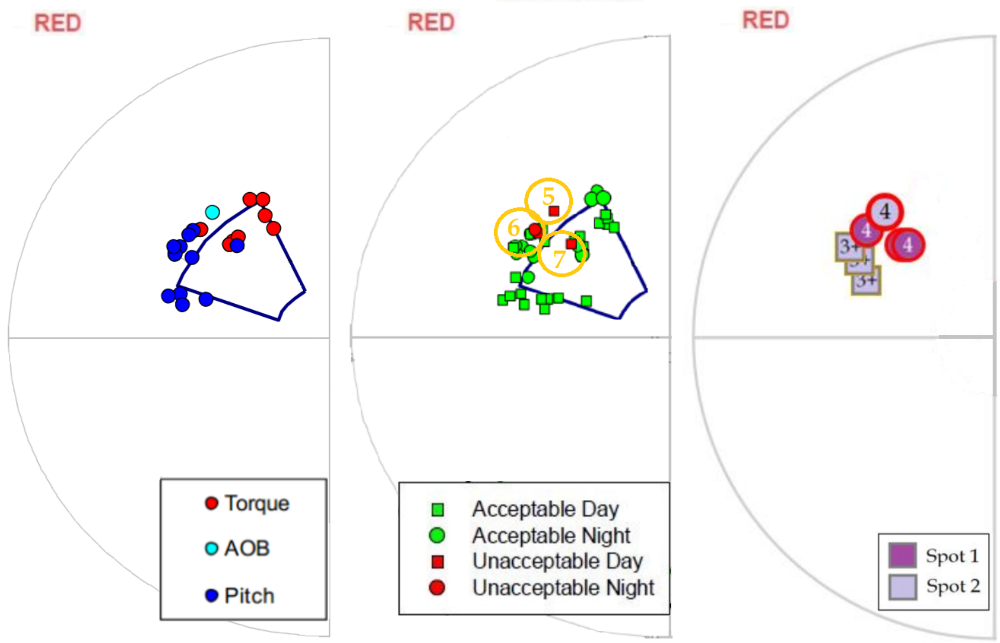

Figure 5.13: Data obtained from LPD2 Sea-trials Oblique facing port procedure - Left: objective limits, middle: subjective limits, right: subjective rating.

Region 5. A subjective limit is experienced with a DIPES rating of 4 in the approach path towards spot 2. The cause of an excessive pilot workload is attributed by test-pilots to *turbulence*, most likely caused by the upwash and downwash over the flight deck. Note that spatial change in mean velocity, can be experienced by pilots as turbulence when moving through these regions. A turbulence rating of 7 was given in this area.

Region 6 and 7. Subjective limits are experienced with a DIPES rating of 4 at spot 1. The cause of an excessive pilot workload is attributed to *turbulence* most likely caused by the upwash and downwash over the flight deck. A turbulence rating of 6 and 7 were given in these areas, in the approach path towards spot 1[8].

---

[8] For spot 1, with relative wind angles between R30 and R50 an excessive turbulence is experienced in the approach path. Above the grid the turbulence is not problematic according to notes in the *sorties*.

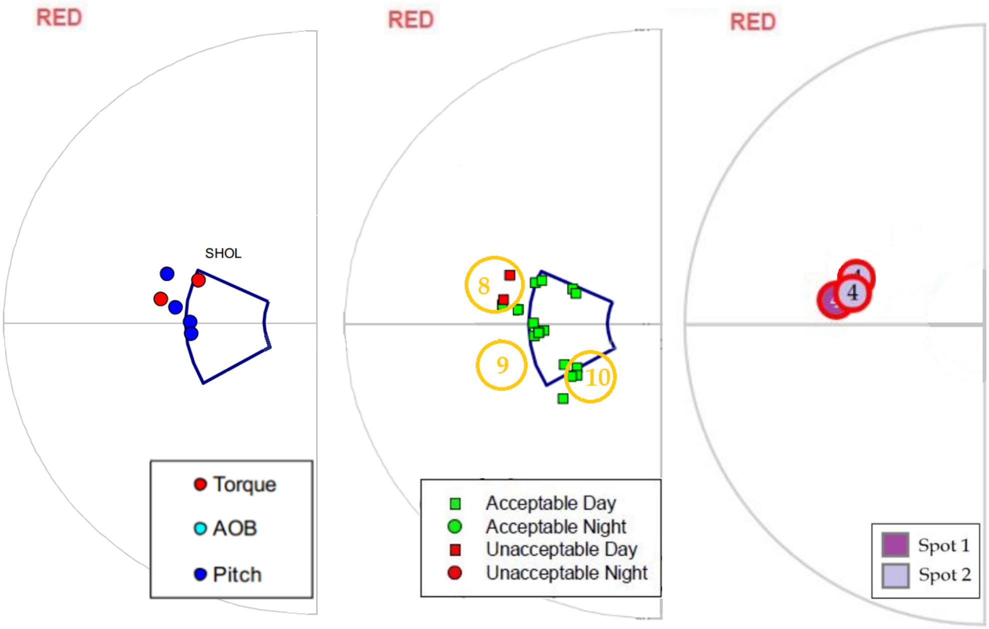

Figure 5.14: Data obtained from LPD2 Sea-trials Cross facing port procedure - Left: objective limits, middle: subjective limits, right: subjective rating.

Region 8. Subjective limits are experienced with a DIPES rating of 4 at spot 1 and 2. The cause of an excessive pilot workload is attributed to *turbulence*, most likely caused by the upwash and downwash over the flight deck. A turbulence rating of 7 was given in this area.

Region 9. Subjective limits are expected[9] similar to those experienced in region 8 at spot 1 and 2.

Region 10. Subjective limits are expected. The cause of an excessive pilot workload most likely due to a combination of *turbulence* caused by the upwash and downwash over the flight deck and *restricted visual cues* due to the heading and attitude (angle of bank) of the helicopter towards the ship.

---

[9] These relative wind angles and speed are not explicitly tested during sea-trials as subjective limits here are easy to predict on basis of the subjective limits in region 8.

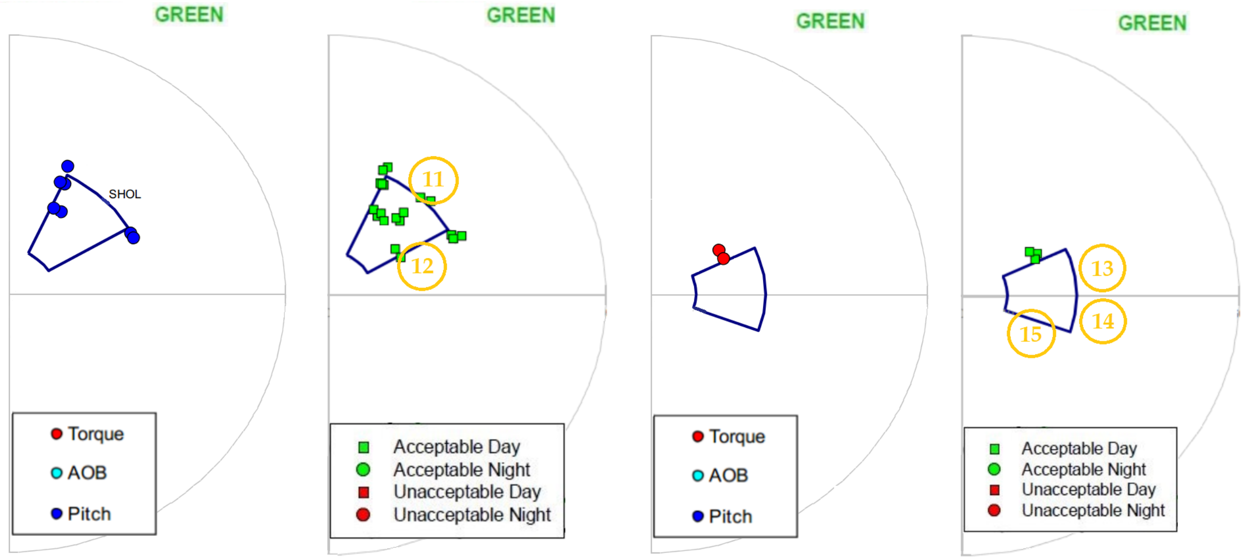

Figure 5.15: Data obtained from LPD2 Sea-trials - Left: Oblique facing starboard procedure, right: Cross facing starboard procedure.

Region 11. Subjective limits are expected similar to the oblique procedure facing port (region 5, 6 and 7). The cause of an excessive pilot workload likely due to *turbulence* experienced by the pilot caused by the upwash and downwash over the flight deck.

Region 12. Objective limits here are expected similar to the oblique procedure facing port. The cause of objective limits here is the *torque required* (due to the tail), the yaw control will become inadequate for larger relative wind angles. Also, *restricted visual cues* are expected in this area due to the helicopter heading and attitude (angle of bank).

Region 13 and 14. Subjective limits are expected similar to the cross procedure facing port (region 8 and 9). The cause of an excessive pilot workload likely due to *turbulence* experienced by the pilot caused by the upwash and downwash over the flight deck.

Region 15. Subjective limits are expected. The cause of an excessive pilot workload is likely due to *turbulence* experienced by the pilot caused by the upwash and downwash over the flight deck and *restricted visual cues* due to the heading and attitude (angle of bank) of the helicopter towards the ship. In addition to this, also the pilot has to fly the helicopter here from the left seat and the yaw control will become inadequate for increasing relative wind angles which makes this region slightly more restricted than region 10.

5.5.2 Conclusions on Subjective Limits

From the analysis presented in subsection 5.5.1, two main causes for subjective limits can be identified which affect the ship-helicopter envelope: turbulence in approach and restricted visual cues. It is expected that turbulence in the approach path as experienced by pilots can be mainly attributed to a spatial change of mean vertical velocity. When flying through strong spatial changes in mean flow, the pilot can experience this as turbulence. Considering this, it is anticipated that subjective limits attributed to turbulence in the approach can be correlated in most cases to a mean vertical flow component. Restricted visual cues however, are expected to be difficult to relate to mean flow data. LightPink will include a base formula for the prediction of subjective limits due to turbulence in the approach path. Subjective limits due to restricted visual cues will not be included in LightPink. Below, the two main causes for subjective limits are discussed.

Turbulence in Approach

Multiple subjective limits are attributed to an excessive turbulence in the approach path of the helicopter (refer back to subsection 2.2.1 to recap what exactly can be considered as turbulence). The cause of the excessive turbulence experienced by the pilot in the approach path is most likely the occurrence of spatial changes in mean vertical flow velocity. These strong spatial changes in mean vertical flow velocity can, for large wind angles, occur due to the interaction of the undisturbed wind with the flight deck. This causes strong upwash and downwash regions in the helicopter flight path. The approach path of the helicopter during the cross and oblique procedures at the LPD2 coincide with the leeward region where these downwash and upwash flows occur. In figure 5.16, the top-view of a simplified LPD2 model is presented with several visualized streamlines. This figure is obtained with DeepPurple for a G50 relative wind of 31 [kts]. In the leeward region of the ship during crosswinds, the pilot can experience great difficulty in keeping the helicopter heading. Strong downwash regions near the edge of the flight deck can cause the helicopter to be pushed downwards into the flight deck edge. It is expected that the leeward region of the ship during crosswinds, where subjective limits occur attributed to turbulence in approach, can be correlated to a mean vertical flow component in DeepPurple which leads to the base formula 5.9.

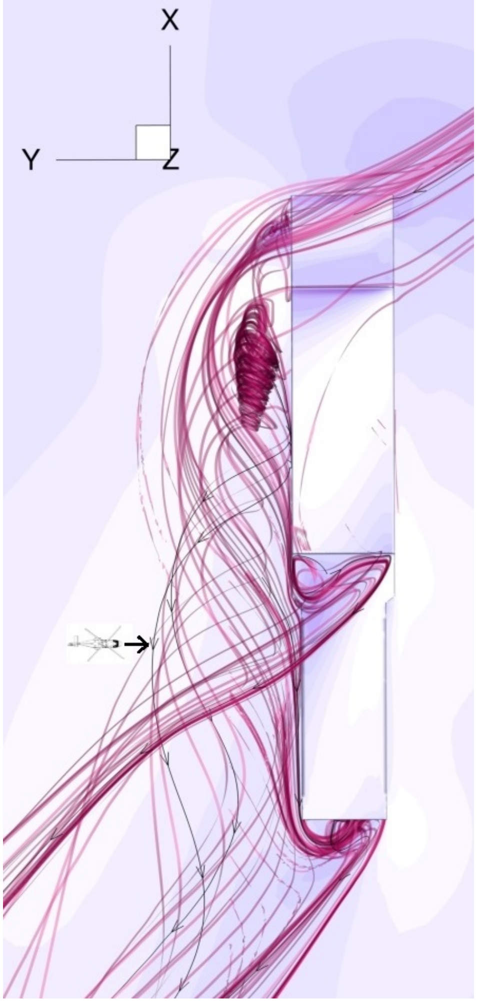

Figure 5.16: Top view: High pilot workload leeward of the flight deck, for cross winds.

Restricted Visual Cues

Some subjective limits are caused by restricted visual cues, usually in combination with other causes of high pilot workload such as inadequate yaw control and turbulence. This type of subjective limit is difficult to predict without performing sea-trials, as a lot of different factors add to the pilot workload. These subjective limits will not be included in LightPink.

5.6 Method for Calibration of Criteria

In this section, it will be explained which methods can be used for the calibration of the base formulas. This will be applied in chapter 6 for a baseline case. The base formulas presented in section 5.4 and 5.5 contain parameters P. The magnitude of the parameters will be determined for a specific set of scenarios. The calibration of parameters P will be done in one of two methods: calibration by hover-trial data or calibration by correlation to sea-trials. The two calibration methods are discussed in subsection 5.6.1 and 5.6.2.

5.6.1 Calibration by Hover-Trial Data

From the shore-based hover trials with the NH90 NFH (Hoencamp, 2012), a lot of data is available on the behaviour and limitations of the NH90 NFH during shore-based hover in different wind speeds and directions. From these trials, some of the parameters P can be determined after selecting a specific weight of the helicopter. The parameters which are dependent on features which are characteristic for ship environment (such as downwash), cannot be found with shore-based hover trial data. For the angle of bank attitude, pitch attitude and the torque required, it is indicated in multiple graphs where safety margins lie which give an indication of the scenarios (i.e. wind direction and speed) where a limitation to the operational envelope can be expected. The following parameters can be determined by the hover-trials which are all part of the Torque2b base formula: P_{10}, P_{11}, P_{14} , P_{15}.

5.6.2 Calibration by Correlation

The parameters which are strongly dependent on characteristic features of the ship environment (such as downwash) are determined from mean flow data obtained with DeepPurple simulations. An existing set of SHOLs - where various data points indicate a relative wind angle and speed where a limit occurs - is needed to calibrate by correlation. Per type of limit, one or multiple data points are selected to calibrate the base formulas to. These data points indicate a relative wind angle and speed which is simulated in DeepPurple to obtain mean flow information. This information is used to find the parameters of the base formula. This is illustrated in figure 5.6.2.

There are various methods which can be used to determine parameters from experimental data. These methods all entail in the basis a 'curve fitting' to data points obtained from experiments, which in this context refers to computational data. For the AOB2 and Torque2 base formulas, a least-squares parameter estimation technique is used to determine specific parameters. In chapter 6 this is applied to a baseline case.

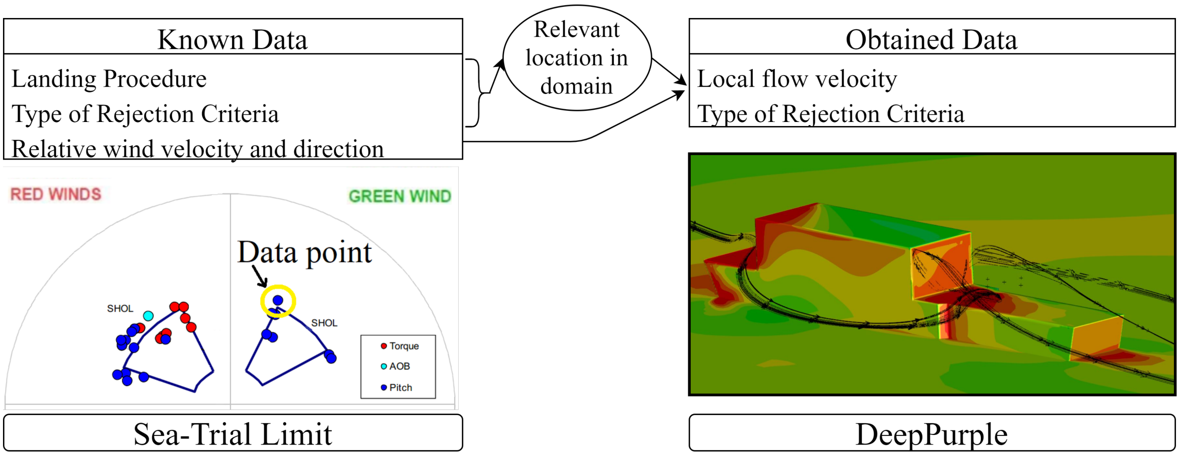
Known Data
Landing Procedure
Type of Rejection Criteria
Relative wind velocity and direction
Relevant location in domain
Obtained Data
Local flow velocity
Type of Rejection Criteria
RED WINDS
GREEN WIND
Data point
SHOL
SHOL
Torque
AOB
Pitch
Sea-Trial Limit
DeepPurple

Figure 5.17: Known helicopter operation limits are correlated to mean flow components computed by DeepPurple to calibrate parameters P.

Least-Squares Methods

There are several least-squares methods known which can be used to estimate parameters from experimental data. A least-squares method estimates parameters by minimizing the the squared differences of experimental data compared to their expected values. A distinction can be made between least-squares methods for linear problems and for non-linear problems. In addition to this, the method can be iterative or non-iterative. The base functions pose non-linear problems, so a non-linear method is needed to find the parameters of the base functions. A few examples of iterative algorithms for non-linear problems are: the Gauss-Newton method, the Nelder-Mead simplex method and the Levenberg-Marquardt method (Johnson and Faunt, 1992). The Gauss-Newton method uses first derivatives, but ignores second derivatives which can be difficult to compute. The Levenberg-Marquardt method is adjusted Gauss-Newton method and uses second derivatives. The Nelder-Mead simplex method is a derivative-free method and can estimate a local optimum of a problem with n variables in a multidimensional space.

The Nelder-Mead simplex method is deemed most suitable for the present research. A derivative-free method such as the Nelder-Mead method will converge faster compared to a method using derivatives, and is more robust with respect to noisy and sparse data. The data points which are available for the calibration by correlation are 'noisy' and sparse. Least-squares methods that use derivatives, such as the Gauss-Newton and Levenberg-Marquardt method, are not suitable for noisy data sets as they will take a lot of iterations to converge to a solution for the parameters or will not be able to converge at all.

5.7 Summary

A procedure is introduced for the prediction of SHOLs for a combination of the NH90 NFH with an amphibious transport ship, *LightPink*. This procedure will predict a set of ship helicopter limits, on the basis of mean airflow information. LightPink base formulas form the core of the prediction procedure. The base formulas include parameters P which need to be calibrated using shore-based hover trial data and a number of existing (sea-trial established) limits. A distinction can be made between a LightPink base formula to predict an objective limit and a LightPink base formula to predict a subjective limit.

The base formulas consist of relations between mean flow components and helicopter behaviour. These relations are based on theoretical knowledge which is presented in chapter 2, shore-based hover-trial data and sea-trial data. The calibration of these formulas can be done using shore-based hover-trial data and by correlating computed mean flow data to existing SHOLs. It is anticipated that on basis of LightPink calibrated formulas, a large part of the objective limits and risk areas for subjective limits can be predicted.

The final LightPink base formulas for objective limits are presented in table 5.1. If a rejection criteria is *true*, a *limit* occurs. The condition indicates when the rejection criterion is used and the GREEN and RED wind are with respect to the helicopter.

LightPink Base Formulas for Objective Limits			
Type	Name	Condition	Base Formula
Angle of Bank	AoB1	-	$L_{perp} < P_1(-)\ [m/s]$
	AoB2	W <0	$P_2 \cdot \frac{1}{U_{tot}} + P_3 \cdot L_{perp} + \lvert W \rvert^{P_4} > \alpha_{max}[^\circ]$
Pitch Attitude	Pitch1	RED wind	$U_{head} > P_5[m/s]$
	Pitch2	GREEN wind	$\frac{G30}{U_{tot}}^{P_6} \cdot G30 > P_7[m/s]$
Torque Required	Torque1	-	$P_8(-) > L_{perp} > P_9(+)\ [m/s]$
	Torque2a	W <0	$P_{10} \cdot \frac{1}{U_{tot}^{P_{11}}} + P_{12} \cdot \lvert W \rvert^{P}_{13} + P_{14} \cdot L_{perp} + P_{15} > T_{req,max}[\%]$
	Torque2b	W >= 0	$P_{10} \cdot \frac{1}{U_{tot}^{P_{11}}} + P_{14} \cdot L_{perp} + P_{15} > T_{req,max}[\%]$

Table 5.1: LightPink base formulas for the prediction of objective limits

Chapter 6

Calibration and Validation of LightPink

Selection of the Baseline Case
Calibration of LightPink
Validation of LightPink
Assessment of LightPink
Summary and Conclusions

> Focus on signal over noise. Don't waste time on stuff that doesn't actually make things better.
>
> *Elon Musk*

6.1 Introduction

The base formulas for the prediction procedure which were introduced in chapter 5 are calibrated and validated in this chapter for a known case. It will be investigated to what extend the procedure can predict SHOLs by means of mean flow data from DeepPurple. The calibration will be performed by relating the base formulas to data from trials. It is chosen to calibrate by combining information from shore-based hover-trials and sea-trials with the NH90 NFH. By basing most of the calibration on data from sea-trials, elements of the ship environment (which are not experienced on shore) are incorporated in the LightPink model. In this chapter, the LightPink base formulas are calibrated to a selected number of limits from the existing SHOLs of a *baseline case.* LightPink will be validated and assessed by comparing predicted limits to the complete set of existing SHOLs. As part of the validation, an analysis is performed on the sensitivity of LightPink to the selected limits used for calibration.

In section 6.2 a baseline case is selected. In section 6.3 the LightPink base formulas are calibrated to the selected baseline case. In section 6.4 the prediction procedure is validated with existing SHOLs. Section 6.5 gives a summary and presents the main conclusions.

6.2 Selection of the Baseline Case

An appropriate baseline case is selected to calibrate the prediction procedure to. The baseline case will consist of a set of key factors that impact the SHOLs, as explained in subsection 2.5.2. All factors that affect SHOLs are mapped in the diagram in figure 2.11 in chapter 2. For each key factor it is discussed to what extend it is included in the baseline case.

Ship and Helicopter

The objective of this project is to contribute to a better design of an amphibious transport ship. As such, a Dutch amphibious transport ship is selected for the baseline case: the **LPD2** (Johan de Witt). The Johan de Witt is considered relevant as this is an amphibious transport ship currently in operation. In addition, there is a lot of data available for the Johan de Witt and multiple research projects are already performed with the LPD2 as subject. This makes this ship suitable for the calibration and testing of the prediction procedure. The **NH90 NFH** is selected as helicopter type. The NH90 is relevant as it is a modern helicopter type currently widely used in the Dutch Royal Navy.

Weight

For the LPD 2 NH90 combination, SHOLs are constructed for three reference weight scenarios: 10.000 kg, 11.000 kg and 11.600 kg. The choice of weight is not expected to be of importance for testing of the prediction procedure. The 11.000 kg scenario is selected as it is expected that this weight occurs mostly during operations which is relevant when using the prediction procedure on new ship designs.

Landing Spot

Landing spot 1 is assumed for the baseline case. The SHOLs for the Johan de Witt are often the same for landing spot 1 and spot 2, however the envelope for spot 2 is sometimes slightly more extended. Near landing spot 1 more problematic wind variations are experienced compared to spot 2, which makes this is the suitable spot for the baseline case.

Pilot

Regarding the helicopter pilot, there are two scenarios possible which affect the operational availability. Scenario 1 is operating in the presence of only 1 pilot, seated on the right side of the helicopter. Scenario 2 is operating in the presence of a second deck qualified pilot in the left seat or operating with 1 pilot seated on the left. When operating in pilot scenario 1, all starboard operations cannot be performed aboard an amphibious transport ship (due to limited visual). The pilot scenario 2 is assumed to allow the validation of the prediction procedure to be as complete as possible[1].

---

[1] When evaluating operational effectiveness of new ship designs, it is important to investigate how frequent each scenario occurs.

Relative Wind Speed and Direction

The SHOLs for the LPD 2 NH90 NFH combination indicate the safe envelope for each approach procedure in a polar plot. This polar plot extends 360° and to a specific maximum relative wind speed. During calibration and testing of LightPink, a relevant selection is made of wind speeds and angles for evaluation, depending on the approach procedure.

Approach Procedure

For the present amphibious transport ships of the Royal Netherlands Navy there are three approach procedures: the fore-aft procedure, the oblique procedure and the cross procedure. The relative wind direction usually dictates which procedure is used. For the larger ships, the relative wind direction also dictates for all procedures from which side the approach must be performed. In the present study, the SHOLs are analysed for all procedures currently used on the LPDs. It is assumed that for red winds, always a port procedure will be applied and for green winds always a starboard procedure.

Ship Motion

The limits to the maximum ship motion in pitch and roll for the LPD 2 NH90 NFH combination at 11.000 kg by day are as follows[2]:

- *Fore-aft:* A maximum roll angle of 7° and a maximum pitch angle of 3°.
- *Oblique*: A maximum roll angle of 6° and a maximum pitch angle of 2°.
- *Cross:* A maximum roll angle of 5° and a maximum pitch angle of 2°.

Selected Baseline Case

Below, it is summarized which set of scenarios are included in the baseline case:

- Helicopter and ship type: NH90 NFH and LPD2
- Helicopter reference weight: 11.000 kg
- Time of day: daytime
- Landing spot: spot 1
- Number of deck qualified pilots: 2
- Range of wind speed: set of relevant velocities, dependent on approach procedure
- Range of relative wind angles: set of relevant angles, dependent on approach procedure

---

[2] More about the effect of ship motion on the ship helicopter operational limits can be found in section 2.5.2.

- Maximum ship roll angle for respectively the fore-aft, oblique and cross procedure: 7°, 6°, 5°
- Maximum ship pitch angle for respectively the fore-aft, oblique and cross procedure: 3°, 2°, 2°

6.3 Calibration of Prediction Procedure

The LightPink base formulas, which were presented in chapter 5, are calibrated to the baseline case. Per type of LightPink base formula[3] it is explained which data is used for the calibration and the final calibrated formula is presented.

In 6.3.1 the models which are used in DeepPurple during the calibration are introduced. The relevant locations in the ship domain, where mean flow data is retrieved for the evaluation of different types of limits, are also presented in 6.3.1. Subsection 6.3.2 discusses the calibration of the base formulas for the angle of bank, subsection 6.3.3 for the pitch-up attitude and 6.3.4 for torque required. Finally subsection 6.3.5 discusses the calibration of the base formula for the indication of regions with likeliness of subjective limits.

6.3.1 Models used and Data Locations

The ship models which are used in DeepPurple for the simulations for calibration and validation of the prediction procedure are introduced below. This is followed by an explanation of the relevant locations in the ship domain. It is explained which locations in the domain are relevant for the each type of limit. For example, a pitch-up limit is only relevant when above the flight deck due to the risk of a tail-strike.

Ship Models

For the simulations in DeepPurple, two different simplified models of the LPD2 were used: *LPD2-Model1* and *LPD2-Model2*. LPD2-Model1 is a simplified model of the LPD2 with quite some details included and is presented in figure 6.1. This model is developed by the NLR to use for DeepPurple simulations. The LPD2-Model2 is a simplified model of the LPD2 without any details and is presented in figure 6.2. This model is developed for the purpose of the present research. Below, the choice of ship models is explained.

---

[3] Types: Angle of Bank, Pitch Attitude, Torque Required, Subjective limit risk area

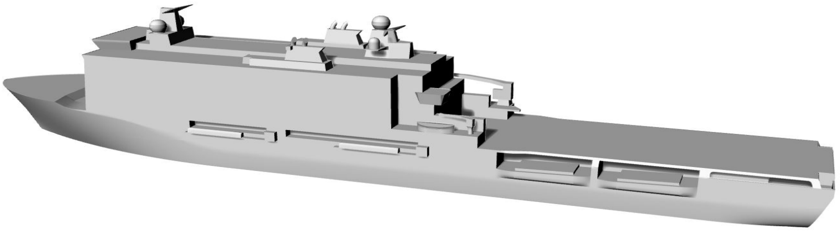

Figure 6.1: LPD2-Model1 (developed by the NLR)

DeepPurple has trouble meshing a geometry with too many details so a full detailed geometry of the LPD 2 could not be used. As the correlation (for calibration) will be established with data from sea-trials, as much detail as possible is desired for the model in DeepPurple. The LPD2-Model1 has quite some detail but is simplified enough for DeepPurple to mesh. After performing multiple test-runs with the LPD2-Model1, it was found that DeepPurple can successfully perform simulations for relative wind angles from R15 to G15, however for larger inflow angles the solution cannot converge. This is as expected as the DeepPurple mesh is designed for small relative wind angles as explained in 4.2.3. For relative wind angles larger than R15 and G15 the LPD2-Model2 was created in Rhino. This model is based on the LPD2 dimensions but does not include any details. Simulations with this model converge for all relative wind angles in DeepPurple.

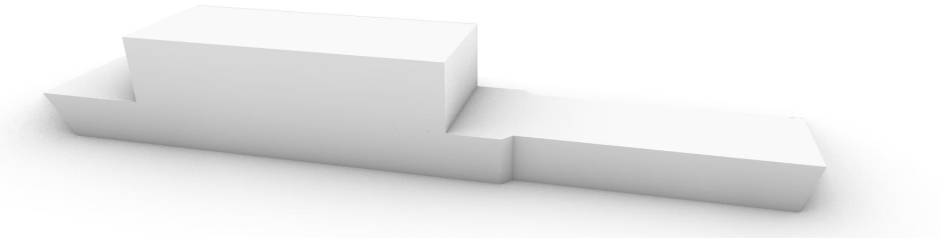

Figure 6.2: LPD2-Model2 (developed for the present research)

The correlation for calibration is mainly based on the relative wind angles from R15 to G15, using the LPD2-Model2. During the correlation establishment it was found that with this range of relative wind angles not enough information was obtained to find a correlation for all the rejection criteria. For this reason, limits occurring in larger relative wind angles were also used for the correlation establishment with the LPD2-Model2.

Two situations can be distinguished when evaluating different relative wind angles of the flow over the ship and are illustrated in figure 6.3. In situation 1 the flow reaching the helicopter has a strong interaction with the superstructure of the ship, creating regions of strong downwash and significantly slowed-down flow in the helicopter path. In situation 2 the flow reaching the helicopter has not interacted strongly with the superstructure but interacts with the edge of the flight deck. The relative wind angles for which situation 1 or 2 occur are dependent on the landing procedure in question, as the helicopter path during landing differs per procedure.

- **Situation 1**: The helicopter path during landing intersects with airflow that is disturbed by the superstructure in front of the flight deck. To establish a correlation for scenarios in situation 1, it is relevant to use the LPD2-Model1 which includes as much detail on the superstructure as possible. The correlation for situations with flow interaction with the superstructure is established based as much as possible on scenarios with relative wind angles from R15 to G15.
- **Situation 2**: The helicopter path during landing does not intersect with flow disturbed by the superstructure in front of the flight deck, but intersects with flow disturbed by the flight deck edges. To establish a correlation for scenarios in situation 2, the LPD2-Model2 is used as larger relative wind angles need to be evaluated.

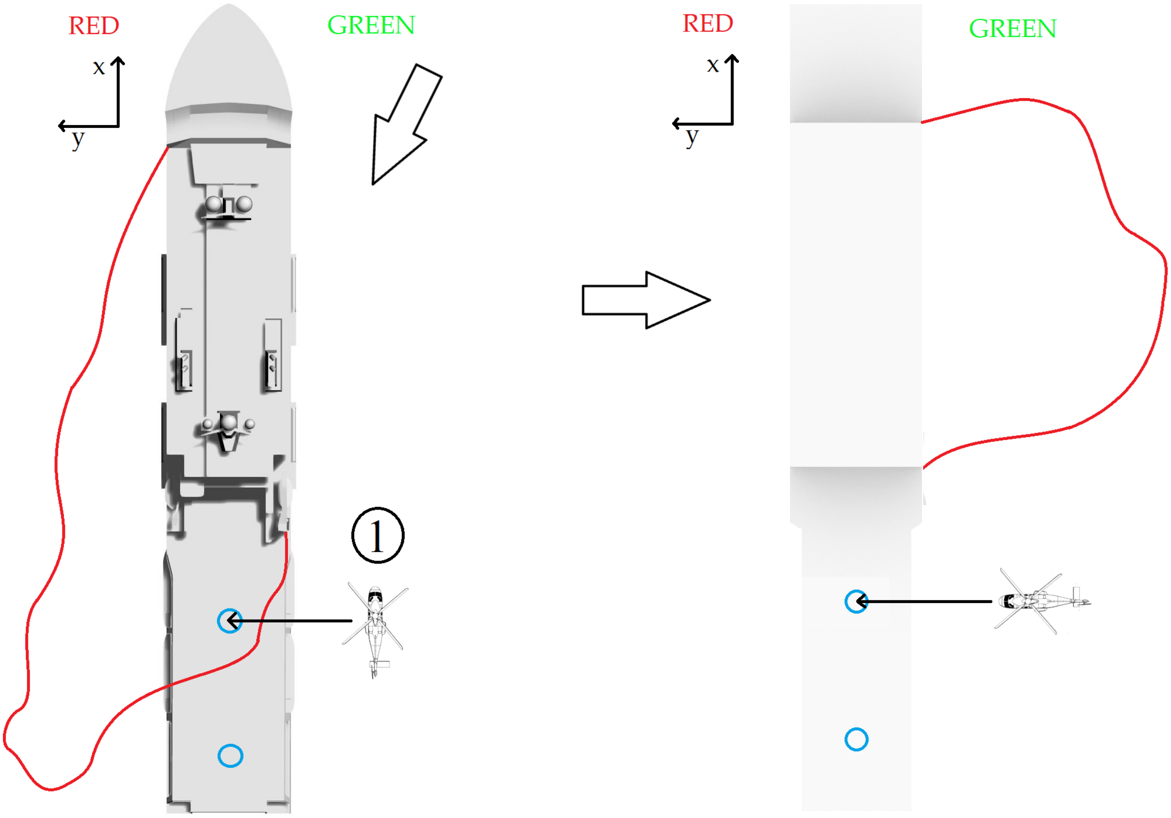

Figure 6.3: Left: situation 1 fore-aft starboard procedure. Right: situation 2 cross facing starboard procedure.

Data Locations in Domain

Depending on the type of rejection criterion, flow data from the domain needs to be retrieved at a specific location. For example, the AoB1 LightPink formula is only relevant at hover height above the landing spot. It is chosen to retrieve information about the airflow in DeepPurple from the rotor disk location at three locations per procedure. These locations are indicated with: Disk A, Disk B and Disk C. The disks are different for the various landing procedures. Each disk is located at rotor height and the diameter of the disk is the diameter of the rotor[4]:

- **Rotor height NH90 NFH:** 4.230 [m] and hover above the flight deck is 3[m]. Total rotor height above flight deck: $4.320 + 3 = 7.320[m]$.
- **Diameter NH90 NFH rotor:** 16.3 [m].

To determine the average flow components (U, V and W) at the rotor disk, 21 data points are taken, distributed across the disk (at the same height in the domain) and the average of the components is calculated. The distribution of the points is illustrated in figure 6.4. A short evaluation was performed to find the effect of taking more or less data points, at different heights. Averaging 21 data points at 1 height was deemed sufficiently accurate whilst keeping the post-processing time within boundaries (TecPlot takes significant time to retrieve data at a specific coordinate in the domain).

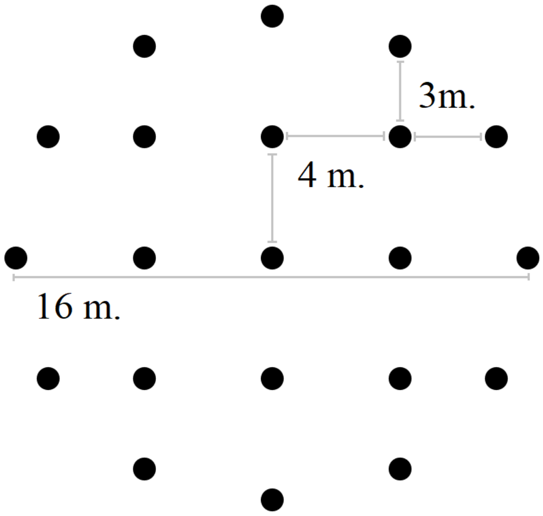

Figure 6.4: Distribution of 21 data points, taken to determine the average flow velocities in a rotor disk.

---

[4] https://www.airbus.com [cited 21 July 2020]

Below, it is indicated where the disks are located and which types of LightPink rejection criteria are evaluated in each disk. Not all criteria are evaluated in every disk as some rejection criteria are only valid/relevant at specific locations in the domain. Additionally, to keep post-processing time as low as possible, in some cases a criteria is not evaluated in a disk when it is expected that this criteria will seldom be critical at this location[5].

- **Disk A:** Rotor height during hover above landing spot. At this location, the following LightPink formulas are evaluated: AoB1, AoB2, Torque1 (for the cross procedure), Torque2 (for the fore-aft and oblique procedure), Pitch1 and Pitch2.
- **Disk B:** Rotor height during hover above edge of the flight deck. The helicopter moves here above the flight deck causing a risk of tail-strike to become relevant. The following LightPink formulas are evaluated: Pitch1 and Pitch2.
- **Disk C:** Rotor height at 1 rotor diameter next to Disk B. This location is relevant as the helicopter needs to be already aligned with the ship according to the specific landing procedure at this location. During the fore-aft procedure, the helicopter is expected to fly in (almost) free-stream wind conditions at Disk C. During the cross and oblique procedure, this region can contain disturbed flow. The following LightPink formulas are evaluated: Torque1 (for the fore-aft and oblique procedure), Torque2 (for the cross procedure) and the subjective criterion (for the cross and oblique procedure).

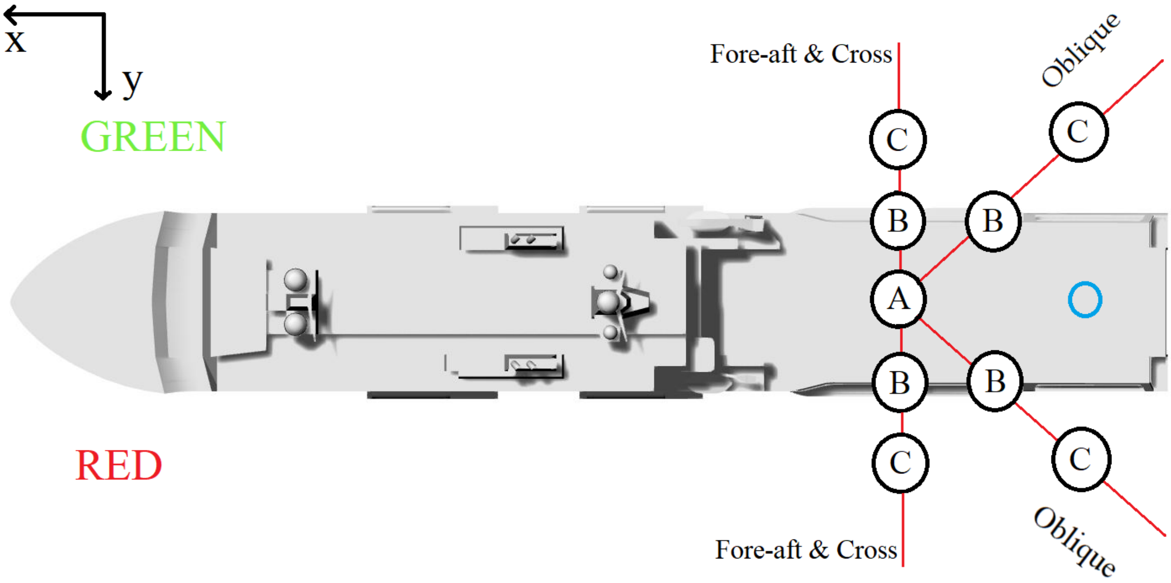

Figure 6.5: Disk A, B and C, port and starboard

---

[5] In future research, more locations in the domain may be included where the criteria are evaluated given that they are relevant at these locations.

When using LightPink for new superstructure concepts, it is advised to evaluate the criteria as stated below[6].

AOB1 and AOB2: Disk A (relevant above landing spot)

Pitch1 and Pitch2: Disk A and Disk B (relevant above flight deck)

Torque1 and Torque2: Disk A, Disk B and Disk C (relevant everywhere during approach for landing)

6.3.2 Angle of Bank Calibration

The calibration of the base formula for *AoB1* is done by combining shore-based hover trial data and sea-trail data. The calibration of base formula *AoB2* is solely based on sea-trial data.

Calibration AoB1

The LightPink base formula for **AoB1** is presented in 6.1.

$$L_{perp} < P_1(-)\ [m/s] \tag{6.1}$$

This rejection criteria gives a maximum for the R90 component towards the helicopter. Parameter P_1 is found from shore-based hover-trial data and is checked by correlation to sea-trail data. From the hover trials, on the top of figure 5.7 it can be seen that this is the velocity at which R90 will cause the angle of bank to exceed the safety margin. This value for P_1 is compared to one data point from the existing SHOLs of the baseline case. This data point must be one where an angle of bank limit is experienced by a strong cross-wind, where downwash does not play a role and where the reason for a limit is not a loss in visual cues but the risk that one main wheel touches the flight deck early. In figure 6.6 the data point is presented and the value of L_{perp}, obtained from DeepPurple, at this point is given.

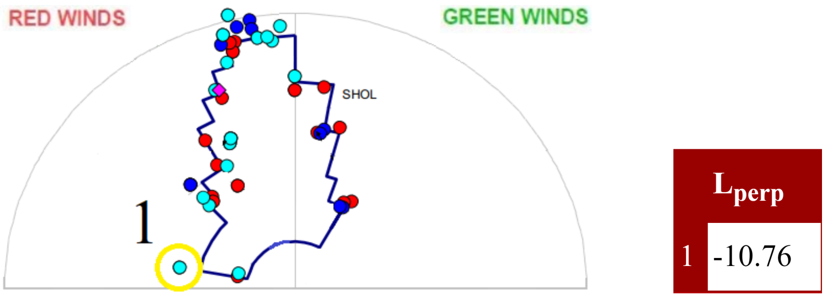

	L_{perp}
1	-10.76

Figure 6.6: Left: data point used for calibration of AoB1. Right: DeepPurple velocity component L_{perp} at Disk A in [m/s].

---

[6] For new superstructure designs, it is important to evaluate all relevant locations in the domain as the flow around these concepts is still completely unknown.

The average of the velocity of L_{perp} from the hover trial data and L_{perp} found from the data point presented in figure 6.6 is rounded to a P_1 of 10 [m/s]. This results in the calibrated LightPink formula **AoB1** presented in 6.2.

$$L_{perp} < 10[m/s] \ (-) \tag{6.2}$$

Calibration AoB2

The LightPink base formula for **AoB2** is presented in 6.3.

$$P_2 \cdot \frac{1}{U_{tot}} + P_3 \cdot L_{perp} + |W|^{P_4} > \alpha_{max} \ [°] \tag{6.3}$$

The parameters P_2, P_3 and P_4 are found by correlating to sea-trial data. The Nelder-Mead least-squares method is used to determine the individual parameters, as explained in subsection 5.6.2. The maximum reference angle of bank is set to 10.5°[7]. In figure 6.7 the data points which are used to find the parameters are indicated and the magnitudes of the mean flow components found from DeepPurple at the relevant location are presented.

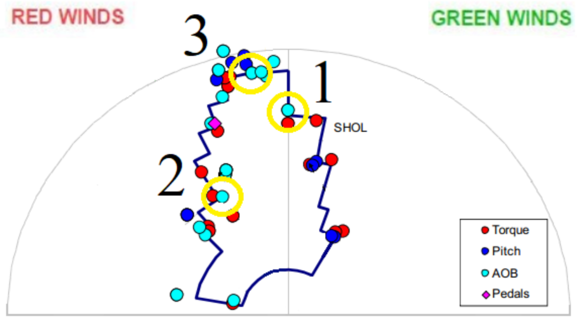

	U_{tot}	L_{perp}	W
1	5.09	-0.38	-1.93
2	4.81	-2.03	-0.16
3	7.07	-0.87	-1.74

Figure 6.7: Left: data points used for calibration of AoB2. Right: DeepPurple velocity components U_{tot}, L_{perp} and W at Disk A in [m/s].

Using the Nelder-Mead method, the magnitudes of the parameters are as follows: $P_2 = 2$, $P_3 = -5$, $P_4 = 3.2$. This results in the calibrated LightPink formula **AoB2** presented in 6.4.

$$2 \cdot \frac{1}{U_{tot}} - 5 \cdot L_{perp} + |W|^{3.2} > 10.5° \tag{6.4}$$

6.3.3 Pitch Attitude Calibration

The calibration of both *Pitch1* and *Pitch2* is done by correlation to sea-trials. After the calibration it is tested how the calibration results compare to the shore-based hover-trial data. The data points for larger angles for the oblique and cross procedure are not used as it is expected that turbulence plays a role here in causing pitch limits.

---

[7] A maximum angle of bank of 12° as stated in the flight manual and an assumed standard angle of bank of 1.5°, due to minimal tail rotor torque, gives 10.5° as reference maximum angle of bank. The exact assumed magnitudes of the angle at which a limit occurs is not of influence on the results, as the parameters are established by a correlation with known SHOLs.

Calibration Pitch1

The LightPink base formulas for **Pitch1** is presented in 6.5.

$$U_{head} > P_5 \; [m/s] \tag{6.5}$$

To calibrate parameter P_5, one data point is used of the existing SHOL where the LPD2-Model1 could be used in DeepPurple. In figure 6.8 the data point is presented and the local value of U_{head}, obtained with DeepPurple, at this point is given.

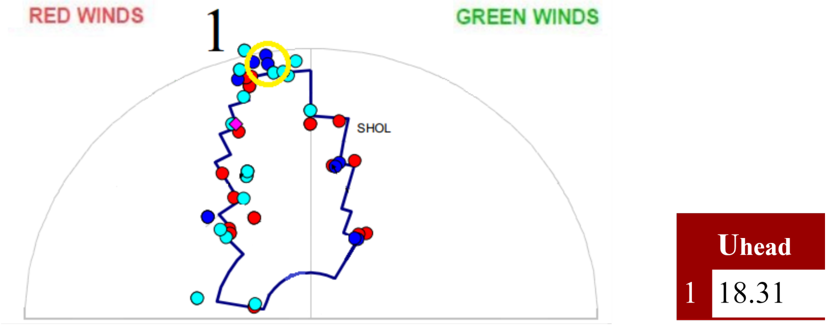

	Uhead
1	18.31

Figure 6.8: Left: data point used for calibration of Pitch1. Right: DeepPurple velocity component U_{head} at Disk B in [m/s].

P_5 is set to 18 [m/s], which results in the calibrated LightPink formula **Pitch1** in 6.6.

$$U_{head} > 18 \; [m/s] \tag{6.6}$$

When looking at the shore-based hover trial data, the pitch-up angle comes near the safety margin at a higher magnitude of U_{head} compared to 18 [m/s] (around 23 [m/s]). This suggests that for the LightPink formula *Pitch1* in the ship environment, turbulent flow components play a role. The uncertainty of the role that turbulence plays for this rejection criteria indicates that the LightPink formula *Pitch1* needs to be evaluated carefully during prediction of limits for new ship designs. In low turbulence regions this criteria may be too strict, in high turbulence regions this criteria may be too forgiving.

Calibration Pitch2

The LightPink base formula for **Pitch2** is presented in 6.7.

$$\left(\frac{G30}{U_{tot}}\right)^{P_6} \cdot G30 > P_7 \; [m/s] \tag{6.7}$$

When the relative wind (U_{tot}) comes exactly from the G30 direction then 6.7 reduces to: $G30 > P_7$. In figure 6.9, the sea-trial data point used for calibration is presented and the value of $G30$ at Disk B obtained with DeepPurple is given.

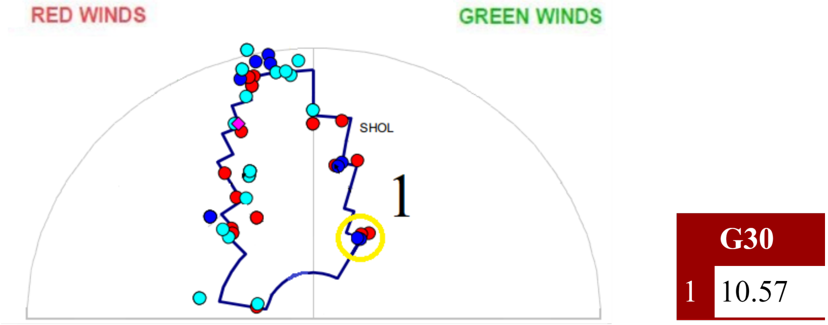

	G30
1	10.57

Figure 6.9: Left: data point used for calibration of Pitch2. Right: the DeepPurple velocity component $G30$ at Disk B in [m/s].

This leads to $P_7 = 10.5$ [m/s]. When looking at the shore-based hover trial data, the pitch-up angle comes near the safety margin at a higher magnitude of $G30$ compared to 10.5 [m/s] (around 15 [m/s]). This suggests, similar to the *Pitch1* criteria, that for the rejection criteria *Pitch2* turbulent flow components may play a role which makes the criteria in the ship environment more strict compared to a shore-based situation.

Using the calibrated *Pitch1* LightPink formula where the limit to U_{head} is set to 18 [m/s], P_6 can be found as presented in equation 6.8 where a relative wind angle of 0° is assumed so $U_{head} = U_{tot}$.

$$\left(\frac{G30}{U_{tot}}\right)^{P_6} \cdot G30 > P_7 \rightarrow \cos(30)^{P_6} \cdot \cos(30) \cdot 18 = 10.5 \rightarrow then\ P_6 = 2.75 \tag{6.8}$$

This results in the calibrated LightPink formula **Pitch2** presented in 6.9.

$$\left(\frac{G30}{U_{tot}}\right)^{2.75} \cdot G30 > 10.5\ [m/s] \tag{6.9}$$

6.3.4 Torque Required Calibration

The calibration of *Torque1* is done by correlation to the sea-trial data of the baseline case. The calibration of *Torque2* is done both using the shore-based hover trial data and sea-trial data.

Calibration Torque1

The LightPink base formula for **Torque1** is presented in 6.10.

$$P_8(-) > L_{perp} > P_9(+)\ [m/s] \tag{6.10}$$

Parameter P_8 is found by correlation to data points from the sea-trials in red winds and P_9 is found with data points in green winds. The data points are chosen in areas in the domain where no downwash is expected. The data points used and the magnitude of L_{perp} obtained with DeepPurple in Disk C are indicated in figure 6.10.

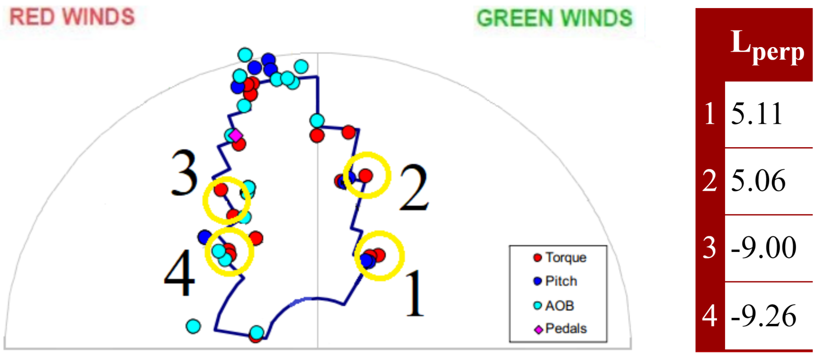

	L_{perp}
1	5.11
2	5.06
3	-9.00
4	-9.26

Figure 6.10: Left: data point used for calibration of Torque1. Right: DeepPurple velocity component L_{perp} at Disk C in [m/s].

The parameter P_8 is set to -9 [m/s] and the parameter P_9 is set to 5 [m/s]. $|P_8| > |P_9|$ which is as expected as noted in section 5.4.3 due to the direction of the tail rotor torque. This results in the calibrated LightPink formula **Torque1** presented in 6.11.

$$-9 > L_{perp} > 5 \; [m/s] \tag{6.11}$$

Calibration Torque2

The LightPink base formula for **Torque2a** is presented in 6.12.

$$P_{10} \cdot \frac{1}{U_{tot}^{P_{11}}} + P_{12} \cdot |W|_{13}^{P} + P_{14} \cdot L_{perp} + P_{15} > T_{req,max}[\%] \tag{6.12}$$

The base formula for *Torque2b* is similar to *Torque2a*, but without a W component and with a variable $T_{req,max}$ magnitude. *Torque2a* and *Torque2b* are separate formulas, as different $T_{req,max}$ magnitudes are related to these formulas. The maximum torque percentage depends on the scenario. The maximum continuous torque allowed is 98% and the maximum transient torque allowed is 113% as explained in 2.5.3. In the present research, all scenarios in the ship environment are considered transient except for the case of minimum environmental relative wind velocity. The inner circular boundary in the envelop as seen in e.g. 6.10 indicates the inner limit where wind velocities are continuously too low. *Torque2b* can be calibrated without performing a correlation, so this base formula will be considered first. Then calibrated parameters of *Torque2b* are incorporated in *Torque2a*, and the remaining uncalibrated parameters are found by a correlation to sea-trial data.

Parameters P_{10}, P_{14} and P_{15} are obtained with shore-based hover trial data. Parameter P_{10} is calibrated to 65% for the baseline case. When the rotors are at their most efficient, there is a minimum torque required. This magnitude is retrieved from the graph for torque required at a higher relative wind speed in the bottom graph in 5.11. The lowest point in the graph, at a 0° relative wind angle, indicates the minimum torque required.

Parameter P_{14} is calibrated to 1. A limit due to *Torque2b* occurs in low wind speeds and the effect of the tail rotor torque can be seen when looking at a low wind speed graph as presented at the top of figure 5.11. Looking at the data in table 6.1 it can be seen that with an increase of 10 [kts] in L_{perp} the torque required increases with 5%. As 1 [kts] is equal to 0.514 [m/s], this indicates an approximate direct relationship between the torque required and the L_{perp} flow component leading to a parameter P_{14} of 1.

Torque Required at 10 kts relative wind velocity		
Torque	93 %	98 %
Relative Angle	0°	G90°
Utot	10 kts	10 kts
Lperp	0 kts	10 kts

Table 6.1: Torque required at 10 kts

Parameter P_{15} is determined on basis of the assumption that the total torque required will be twice as high as the minimum torque required (P_{15}) when U_{tot} is equal to 1 [m/s]. Then, using the *Torque2b* criterion, it is found that $P_{10} = P_{15} = 65\%$.

Parameter P_{11} is found by looking at the inner circular boundary of the existing SHOLs. The minimum continuous relative wind velocity which causes the maximum continuous power of 98% to be exceeded. When looking at the formula for *Torque2b*, assuming a 0° relative wind direction and $P_{10} = P_{15} = 65\%$, then it can be found that $P_{11} = 0.414$.

To calibrate P_{12} and P_{13} from the formula for *Torque2a* a correlation is performed to the existing SHOLs of the baseline case. The data points used and the magnitude of U_{tot}, W and L_{perp} for these points in Disk A are indicated in figures 6.11 and 6.12.

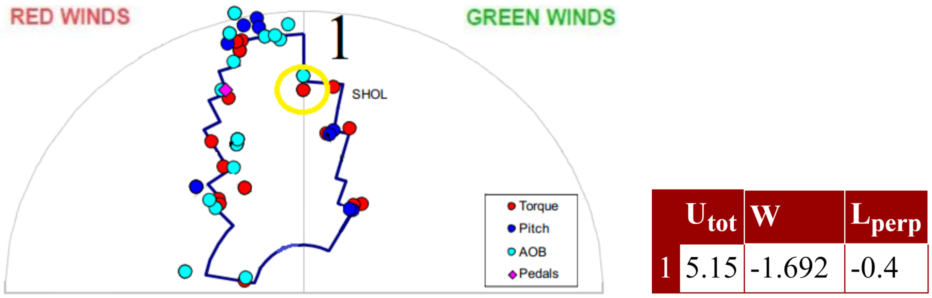

	U_{tot}	W	L_{perp}
1	5.15	-1.692	-0.4

Figure 6.11: Left: First data point used for calibration of Torque2. Right: DeepPurple velocity components U_{tot}, W and L_{perp} at Disk A in [m/s].

Setting the maximum torque required to 113% and using the Nelder-Mead least-squares method, the parameters were found as follows: $P_{12} = 6.965$ and $P_{13} = 1.511$. This results in the calibrated LightPink formula **Torque2a** presented in 6.13 and the calibrated **Torque2b** presented in 6.14. For simplicity, to establish the inner boundary of the SHOLs with *Torque2b*

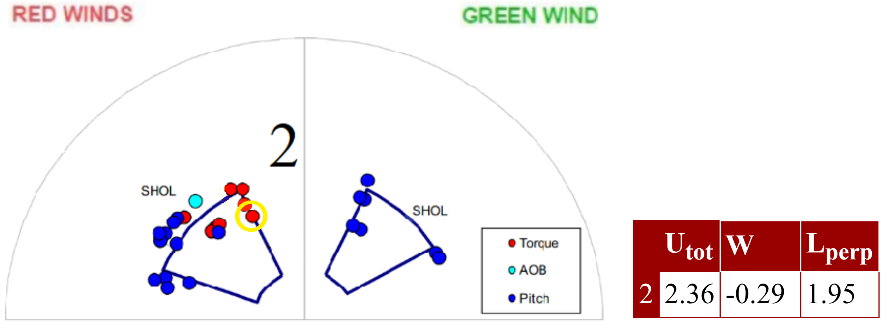

	U_{tot}	W	L_{perp}
2	2.36	-0.29	1.95

Figure 6.12: Left: Second data point used for calibration of Torque2. Right: DeepPurple velocity components U_{tot}, W and L_{perp} at Disk A in [m/s].

in continuous wind conditions, a constant minimum wind speed can be assumed[8]. This leads to the formula in 6.15, which gives a constant magnitude of the minimum acceptable U_{tot}.

$$65 \cdot \frac{1}{U_{tot}^{0.4}} + 7 \cdot |W|^{1.5} + 1 \cdot L_{perp} + 65 > 113[\%] \tag{6.13}$$

$$65 \cdot \frac{1}{U_{tot}^{0.4}} + 1 \cdot L_{perp} + 65 > 113[\%] \tag{6.14}$$

$$65 \cdot \frac{1}{U_{tot}^{0.4}} + 65 > (98[\%]) \tag{6.15}$$

6.3.5 Subjective Rejection Calibration

The LightPink base formula for subjective limits which was introduced in chapter 5 is repeated in equation 6.16. This formula indicates regions in the SHOL where a high risk is expected of limits due to a high subjective rating. This base formula is only applicable to subjective limits attributed by pilots to turbulent flow leeward of the flight deck during cross-winds, in the approach path during the oblique or cross procedure.

$$\textit{Risk Region when} \ \rightarrow \ |W| > P_{16} \tag{6.16}$$

The calibration is done by correlating DeepPurple mean flow data to the baseline existing SHOLs. There are specific regions in the SHOLs of the baseline case where limits are known to be attributed to turbulent flow leeward of the flight deck[9]. The data points which are indicated with "unacceptable" in the SHOLs are indicated in figure 6.13 by 1, 2, 3, and 4. The data points of which it is known (refer to chapter 5) that subjective limits occur which are attributed to turbulence in the approach are indicated by 5 and 6. The magnitude DeepPurple gives of W for these points in Disk C is also presented in figure 6.13. From the data points it can be seen that a slight adjustment of the base formula is in place. The calibrated LightPink formula for subjective limits is formulated in equation 6.17.

---

[8] This is also done in practice, depending on the helicopter weight.

[9] Some of these regions have an indicated subjective limit ("Unacceptable"), found during sea-trials.

$$Risk\ Region\ when\ \rightarrow\ W > 1.55[m/s]\ or\ W < -2.25[m/s] \tag{6.17}$$

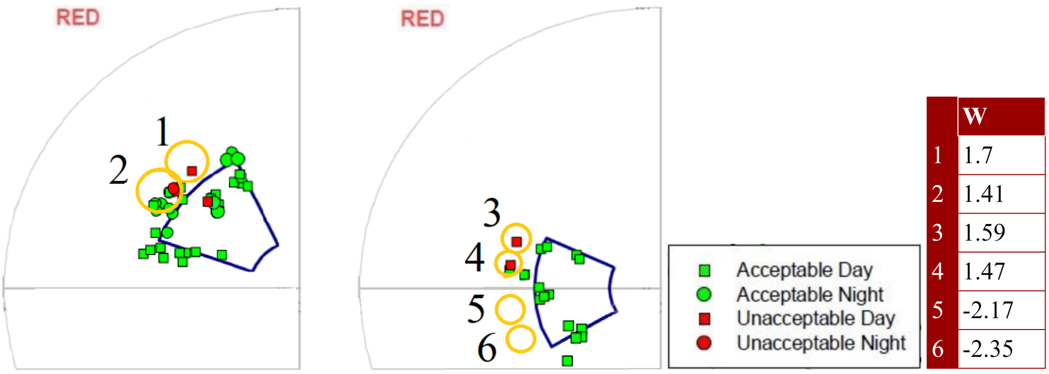

	W
1	1.7
2	1.41
3	1.59
4	1.47
5	-2.17
6	-2.35

Figure 6.13: Left: data points used for calibration of the subjective criterion. Right: DeepPurple velocity component W at Disk C in [m/s].

6.4 Validation of Prediction Procedure

To validate the prediction procedure, the predicted SHOLs of the baseline case for the fore-aft, oblique and cross procedures are compared to the existing SHOLs of the baseline case.

In subsection 6.4.1 the comparisons of the SHOLs are presented and discussed. Subsection 6.4.2 presents a sensitivity analysis of the prediction procedure. Subsection 6.4.3 gives a final assessment of the prediction procedure and presents notes on how to use the prediction procedure for new ship designs.

A number of things are important to understand about the predicted and existing SHOL diagrams. The existing SHOL diagrams of the baseline case contain in reality more limits than are indicated specifically with dots in the diagrams. Limits obtained with the prediction procedure are found by evaluating a bounded range (indicated by the dotted lines in the diagrams) of relative wind angles and velocities. Limits occurring outside of these bounds are not presented in the diagrams. Upper limits indicated in the diagrams are found by searching for the maximum allowable wind speed at a specific relative wind angle for a type of limit. Lower limits for Torque2b are found by assuming environmental wind conditions. Finally, it is assumed that subjective limits are symmetric for Red and Green winds[10], so the subjective limits are mirrored for Red and Green winds.

---

[10] This is also done in practice when establishing the SHOLs, as explained in 2.5.4

6.4.1 Comparisons Existing and Predicted SHOLs

Comparison SHOLs Fore-Aft Procedure

Figure 6.14 presents the existing and predicted SHOLs for the fore-aft procedure of the baseline case. The limits that are circled in yellow are the limits which were used for the calibration of the base formulas. Each yellow circle is related to only 1 limit. The dotted lines in the SHOL developed with the prediction procedure indicate the range of relative wind angles and velocities which were analysed.

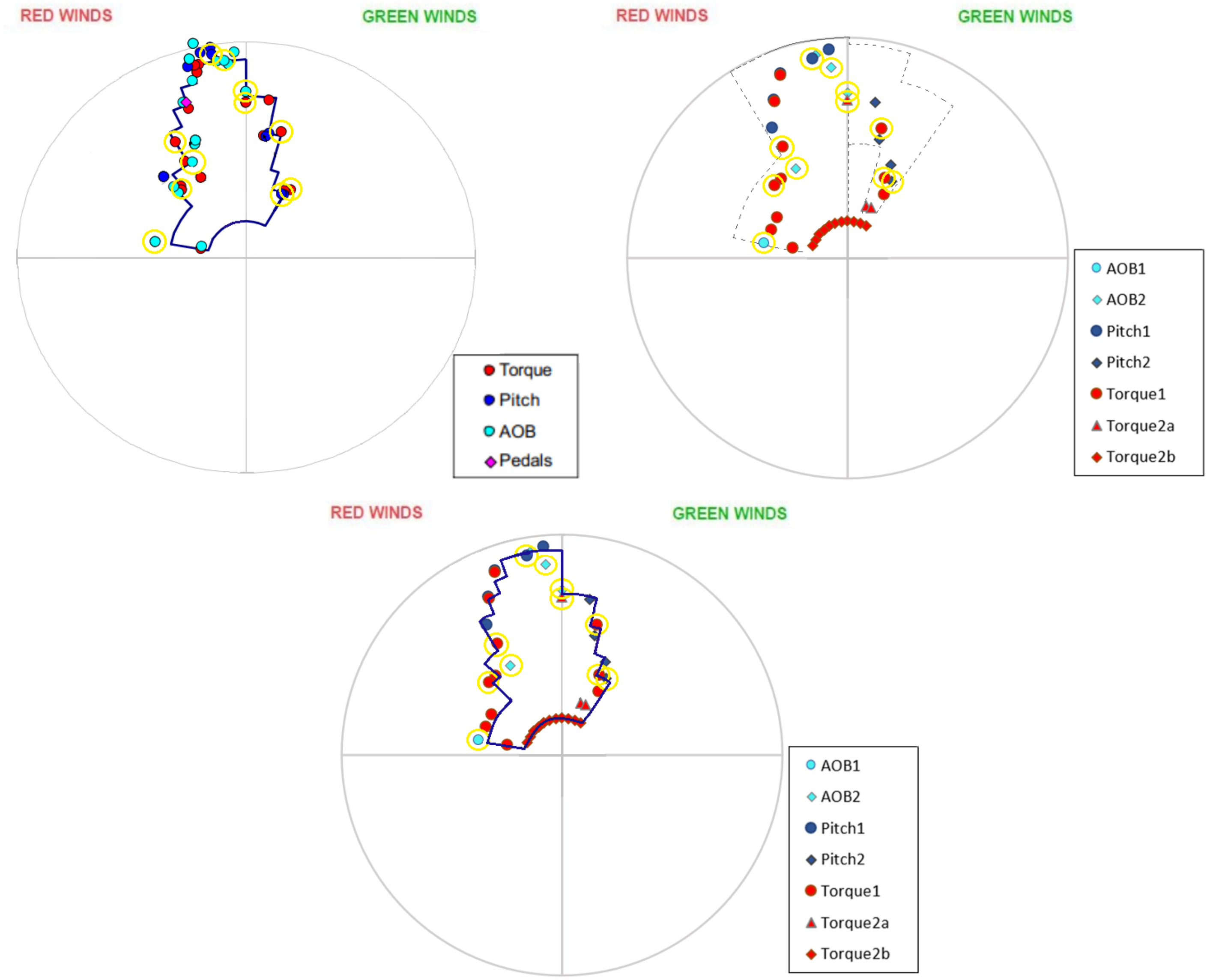

Figure 6.14: Top left: existing SHOL fore-aft procedure. Top right: predicted SHOL fore-aft procedure. Bottom: predicted SHOL with exsiting envelope included. Circled in yellow: data points used for calibration.

Comparison SHOL Oblique Procedure

Figure 6.15 presents the existing and predicted SHOLs for the oblique procedure of the baseline case. The limits that are circled in yellow are the limits which were used for the calibration of the base formulas. Each yellow circle is related to only 1 limit. The dotted lines in the SHOL developed with the prediction procedure indicate the range of relative wind angles and velocities which were analysed. Circled in purple are areas where the prediction procedure misses pitch-up limits, most likely caused by *flapback*.

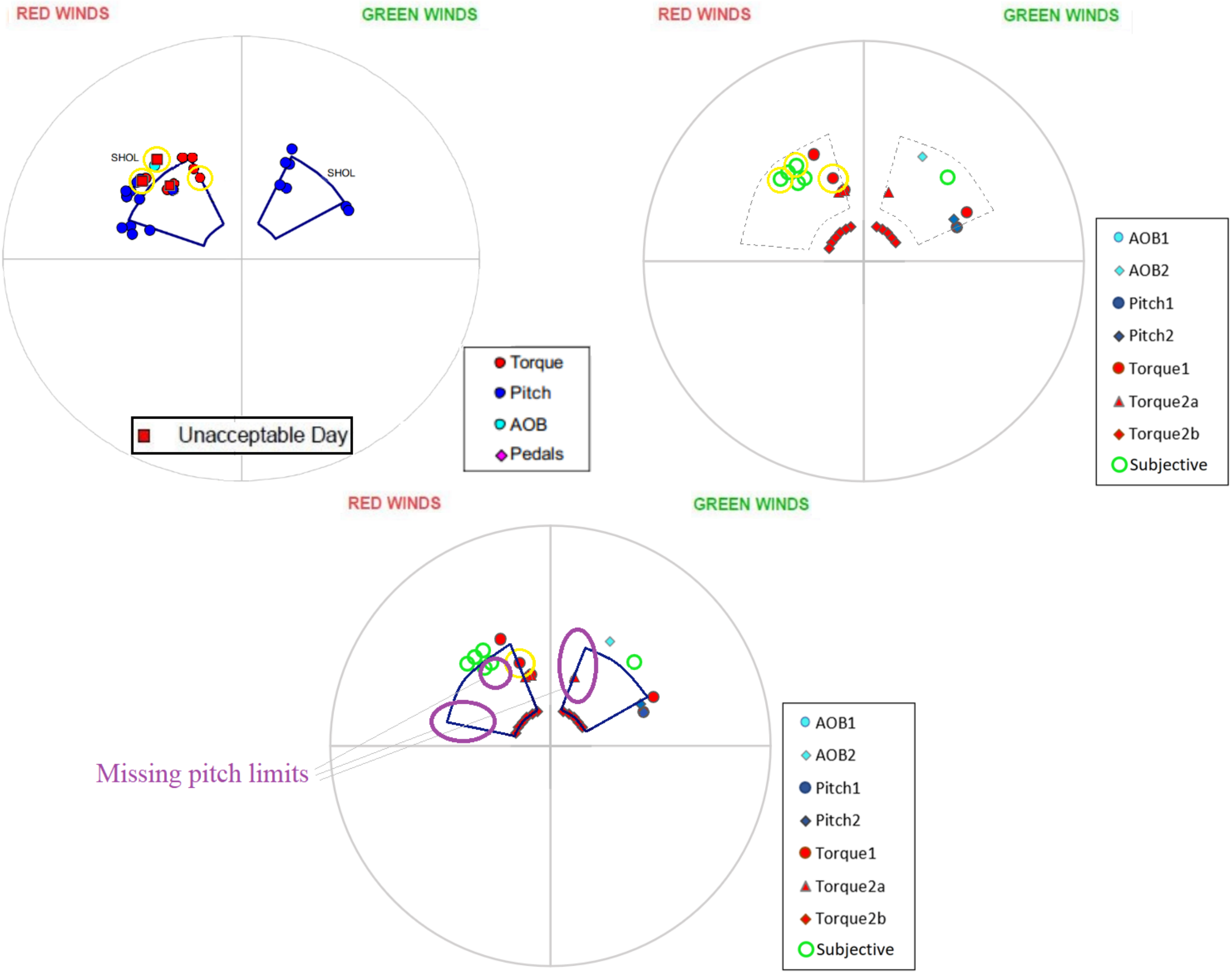

Figure 6.15: Top left: existing SHOL oblique procedure. Top right: predicted SHOL oblique procedure. Bottom: predicted SHOL with exsiting envelope included. Circled in yellow: data points used for calibration.

Comparison Cross Procedure

Figure 6.16 presents the existing and predicted SHOLs for the cross procedure of the baseline case. The limits that are circled in yellow are the limits which were used for the calibration of the base formulas. From the existing SHOL only the subjective limits were used for calibration, of which two were indicated by ”unacceptable” and two are known to be there by the analysis presented in 5.5. The dotted lines in the SHOL developed with the prediction procedure indicate the range of relative wind angles and velocities which were analysed.

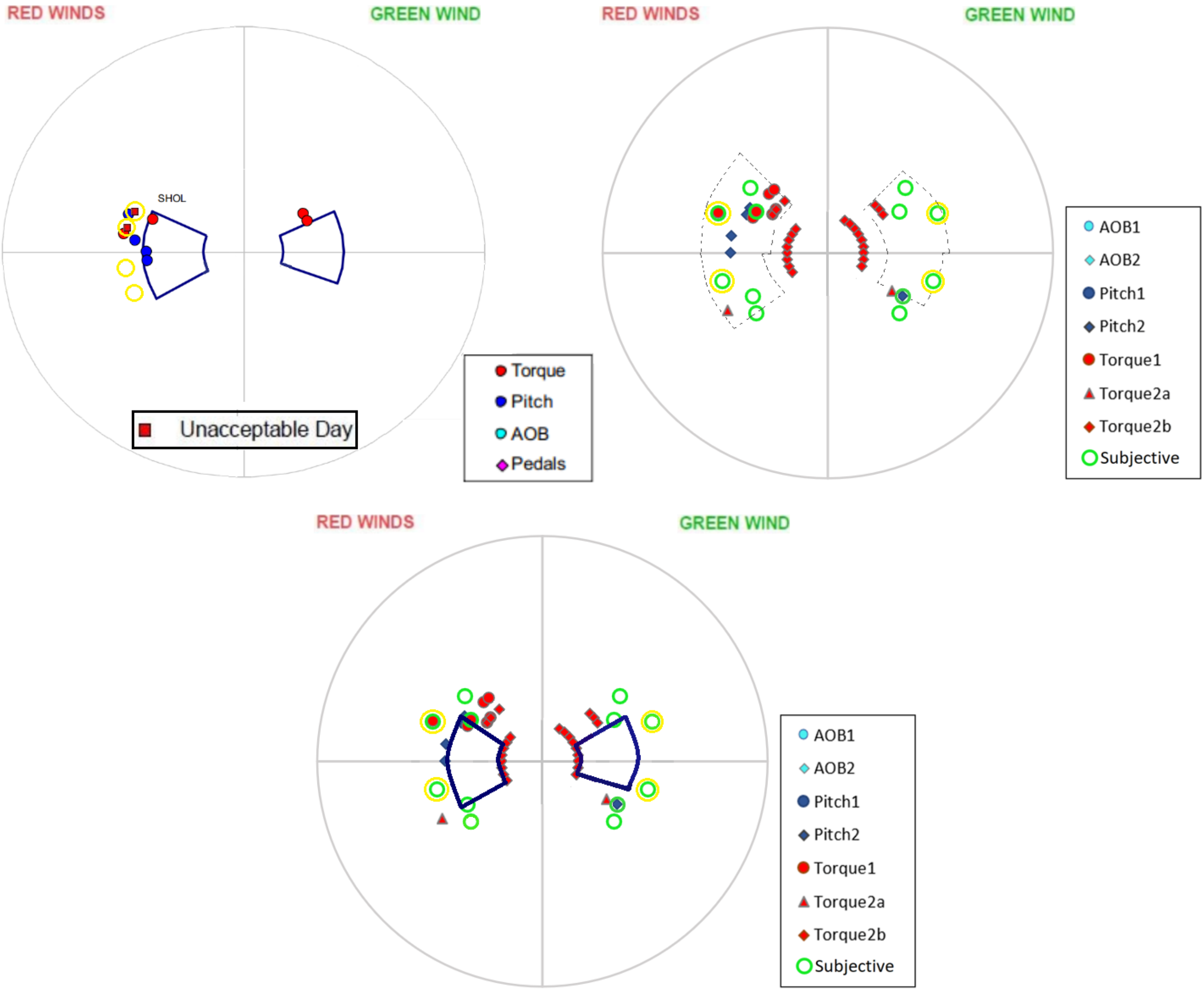

Figure 6.16: Top left: existing SHOL cross procedure. Top right: predicted SHOL cross procedure. Bottom: predicted SHOL with exsiting envelope included. Circled in yellow: data points used for calibration.

Discussion of Comparisons

From the comparisons between the existing SHOLs and the predicted SHOLs for the baseline case multiple observations can be made. Below these are discussed per landing procedure.

Fore-aft Procedure:
It can be seen from figure 6.14 that the envelope of the fore-aft procedure can be quite accurately reconstructed with the prediction procedure. The types of limits that cause the boundary of the envelope are not always similar for the existing SHOL and the predicted SHOL. Approximately, 95% of the outline can be predicted by LightPink. A small part of the outline of the SHOL is expected to depend on turbulent flow components causing pitch-up limits. The following can be observed and explained:

- In the regions of the relative wind angle from R30 to R15 and G15 to G30 some deviations between the diagrams is observed. These are expected to be partly caused by the fact that the LPD2-Model1 could not be used here, while there is a lot of interaction with the superstructure for these relative wind angles.
- It can be observed that quite some limits for the angle of bank are missed by the prediction procedure. It is expected that this is because the contribution of low wind speeds to the *AOB2* criteria is too little. An improvement might be possible by calibrating the *AOB2* formula with more suitable calibration data points.
- For Red winds, a few *Pitch1* limits are predicted which do not occur in the existing SHOL. This means that the *Pitch1* criteria is too strict for a R30 component to the helicopter. This suggests that the *Pitch1* base formula cannot be purely related to a R30 component, but might depend quite strongly on turbulent flow components.
- Quite some limits from the existing SHOLs are used as calibration data points. The effect on the predicted SHOL, when using less (and/or different) existing limits as data points for calibration is investigated in subsection 6.4.2.

Oblique Procedure:
It can be seen from figure 6.15 that the envelope of the oblique procedure can be quite accurately reconstructed with the prediction procedure, except for one part of the boundary. Approximately, 70% of the outline can be predicted by LightPink. A part of the outline which cannot be predicted is expected to depend on turbulent flow components causing mainly pitch-up limits. The following can be observed and explained:

- The majority of the pitch-up limits are missed by the prediction procedure. This is most likely because turbulent flow features play a role in the causation of pitch limits (due to *flapback*) and this is not taken into account in the LightPink formulas. This effect is significant for the oblique procedure as the combination of the relative wind angles and the flight path for this procedure result in a disturbed flow above the flight deck, which the helicopter crosses. This is different for the cross procedure, where the disturbed flow is for most relative wind angles for the greater part located leeward of the flight deck (and not above), where pitch-up attitudes are not relevant yet.

- The two boundaries of the existing envelope which are caused by pitch-limits and cannot be found by the prediction procedure are in the region of small Green relative wind angles and larger Red relative wind angles. These are circled in the bottom diagram of figure 6.15. It can be seen in DeepPurple flow data, that for these relative wind angles, strong upwash occurs in Disk A and Disk B. This suggests that pitch-limits occur here due to *flapback*, which is not predicted by the prediction procedure.
- Differences in the existing SHOL and the predicted SHOL can also be attributed to the fact that for the prediction procedure, limits are analysed at specific locations along the landing path. It might be the case that a limit occurs at a location along the landing path which is not analysed during the prediction procedure.

Cross Procedure:
It can be seen from figure 6.16 that with the combination of the predicted objective and subjective limits, approximately 90% of the outline can be predicted by LightPink. A part of the outline which cannot be predicted is expected to depend on turbulent flow components causing mainly pitch-up limits and on limited visual cues for the pilot. The following can be observed and explained:

- A large part of this SHOL is - both in reality and in the predicted SHOL - determined by subjective limits. It can be seen that the predicted subjective limits quite accurately indicate the borders of the existing envelope. The yellow circled subjective limits were used to calibrate the LightPink base formula for subjective limits, so these cannot say a lot about the correctness of the prediction. To test the subjective prediction more thoroughly, the procedure should be analysed for another ship with known SHOLs.
- The limits for a pitch attitude differ slightly for the existing SHOL compared to the predicted SHOL. This is most likely because turbulent flow features play a role in the causation of pitch limits.
- Differences in the existing SHOL and the predicted SHOL can also be attributed to the fact that for the prediction procedure, limits are analysed at specific locations along the landing path. For the cross procedure, this is expected to have especially an effect on the subjective limits for relative wind angles beyond 100°, which are analysed in Disk C only.

6.4.2 Sensitivity Analysis

In this subsection, it is analysed how sensitive the prediction procedure for the baseline case is to the data points taken for the calibration. In section 6.3 a calibration (*calibration 1*) of the LightPink formulas is performed with data from shore-based hover-trials and specific data points from the existing SHOLs of the baseline case. In this section, a second calibration (*calibration 2*) is performed using different and less data points taken from the existing SHOL. Table 6.2 presents the calibrated formulas found from *calibration 1* and table 6.3 presents the calibrated formulas found with *calibration 2*. The data points which are used for the calibration are circled in yellow in the SHOL diagrams and the same shore-based hover-trial data is used for the second calibration.

In 6.4.2 the SHOL diagrams of the fore-aft procedure are presented. Then 6.4.2 presents the diagrams for the oblique procedure and 6.4.2 for the cross procedure. In 6.4.2 the conclusions are discussed. The following is adjusted for *calibration 2* in comparison to *calibration 1*:

AOB1: The AOB1 base formula is now only calibrated with data from the shore-based hover trials.

AOB2: The AOB2 base formula is still calibrated with 3 data points from the existing SHOL, with 1 adjusted data point compared to *calibration 1*.

Pitch1 and Pitch2: No adjustments are made for these formulas, as there are no suitable data points in the existing SHOL other than the ones already used for *calibration 1*.

Torque1: The Torque1 formula is now calibrated with only 2 data points in contrast to the 4 data points used for *calibration 1*.

Torque2: The Torque2 formula is still calibrated with the same shore-based hover trial data and 2 data points from the existing SHOL, with 1 adjusted data point compared to *calibration 1*.

Subjective Criterion: The LightPink formula for subjective limits is not included in the sensitivity analysis.

LightPink Formulas by Calibration 1			
Type	Name	Condition	Base Formula
Angle of Bank	AoB1	-	$L_{perp} < 10(-)[m/s]$
	AoB2	W <0	$2 \cdot \frac{1}{U_{tot}} - 5 \cdot L_{perp} + \lvert W\rvert^{3.2} > 10.5[°]$
Pitch Attitude	Pitch1	RED wind	$U_{head} > 18[m/s]$
	Pitch2	GREEN wind	${\frac{G30}{U_{tot}}}^{2.75} \cdot G30 > 10.5[m/s]$
Torque Required	Torque1	-	$9(-) > L_{perp} > 5(+)\ [m/s]$
	Torque2a	W <0	$65 \cdot \frac{1}{U_{tot}^{0.4}} + 7 \cdot \lvert W\rvert^{1.5} + 1 \cdot L_{perp} + 65 > 113[\%]$
	Torque2b	W >= 0	$65 \cdot \frac{1}{U_{tot}^{0.4}} + 1 \cdot L_{perp} + 65 > 113\%\ or\ 98\%$

Table 6.2: LightPink formulas for objective limits by calibration 1

LightPink Formulas by Calibration 2			
Type	Name	Condition	Base Formula
Angle of Bank	AoB1	-	$L_{perp} < 10.28(-)[m/s]$
	AoB2	W <0	$20.45 \cdot \frac{1}{U_{tot}} - 1.28 \cdot L_{perp} + \lvert W\rvert^{2.93} > 10.5[°]$
Pitch Attitude	Pitch1	RED wind	$U_{head} > 18[m/s]$
	Pitch2	GREEN wind	${\frac{G30}{U_{tot}}}^{2.75} \cdot G30 > 10.5[m/s]$
Torque Required	Torque1	-	$9.26(-) > L_{perp} > 5.11(+)\ [m/s]$
	Torque2a	W <0	$65 \cdot \frac{1}{U_{tot}^{0.4}} + 9.15 \cdot \lvert W\rvert^{0.99} + 1 \cdot L_{perp} + 65 > 113[\%]$
	Torque2b	W >= 0	$65 \cdot \frac{1}{U_{tot}^{0.4}} + 1 \cdot L_{perp} + 65 > 113\%\ or\ 98\%$

Table 6.3: LightPink formulas for objective limits by calibration 2

Sensitivity Fore-Aft Procedure

Figure 6.17 presents three SHOL diagrams for the fore-aft procedure: the original SHOL of the baseline case, the predicted SHOL with *calibration 1* and the predicted SHOL with *calibration 2* (both including the existing SHOL indicated by the blue line). It can be seen that the AOB2 criterion from *calibration 2* results in a bit more limits for AOB2 compared to *calibration 1* and slightly better in accordance with the original SHOL. The Torque1 criterion does not show large differences from *calibration1* to *calibration2*. The Torque2 criterion shows two incorrect outliers (circled in purple) for *calibration2*.

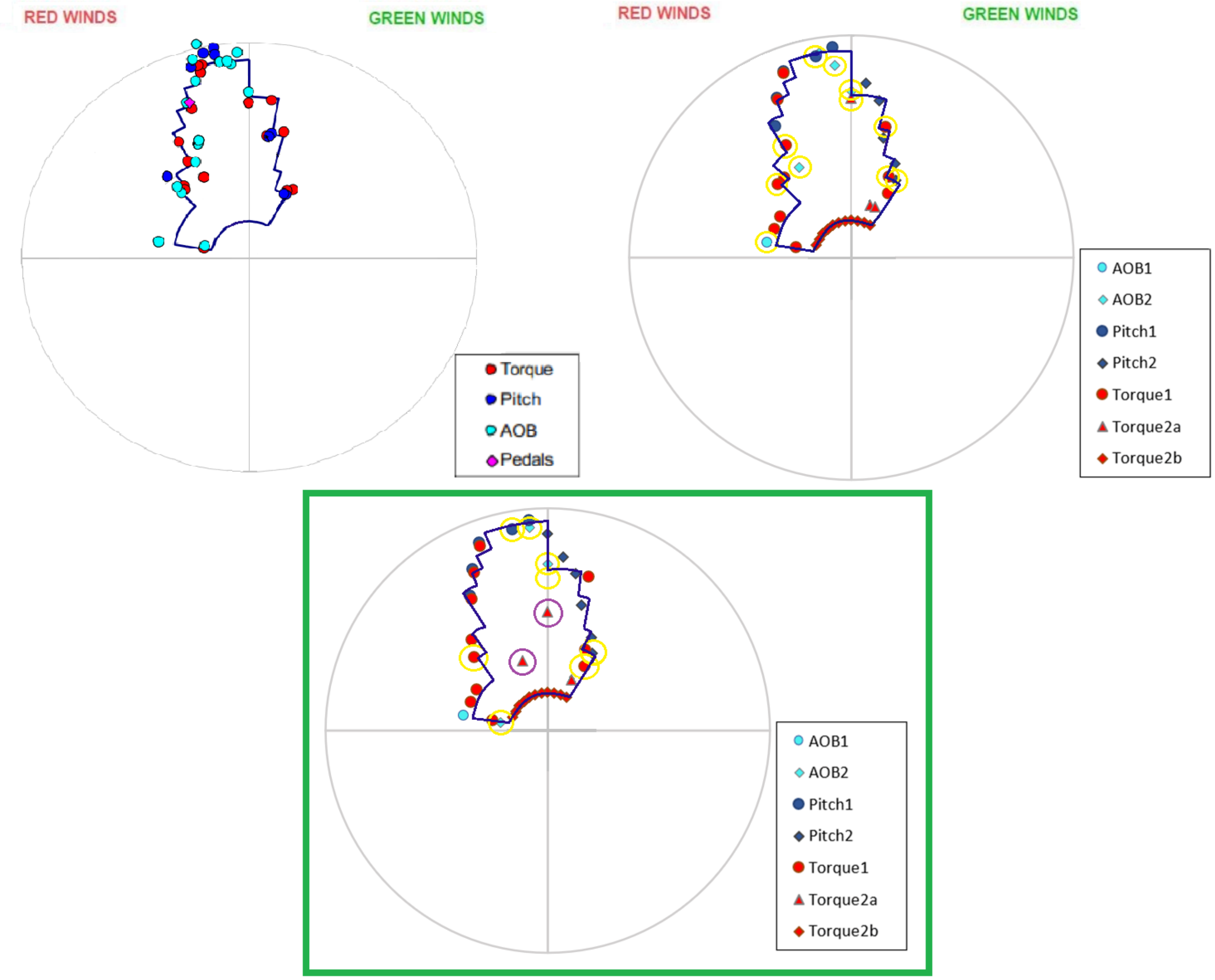

Figure 6.17: Top left: existing SHOL fore-aft procedure. Top right: predicted SHOL with *calibration1*. Bottom: predicted SHOL with *calibration2*. Circled in yellow: data points used for calibration. Circled in purple: outliers. Blue line: existing SHOL.

Sensitivity Oblique Procedure

Figure 6.18 presents three SHOL diagrams for the oblique procedure: the original SHOL of the baseline case, the predicted SHOL with *calibration 1* and the predicted SHOL with *calibration 2* (both including the existing SHOL indicated by the blue line). It can be seen that no significant changes occur for the Torque limits when comparing the predicted SHOLs of *calibration1* to *calibration2*. The AOB2 limits occur in the same regions of the diagram, however are slightly different for *calibration1* compared to *calibration2*.

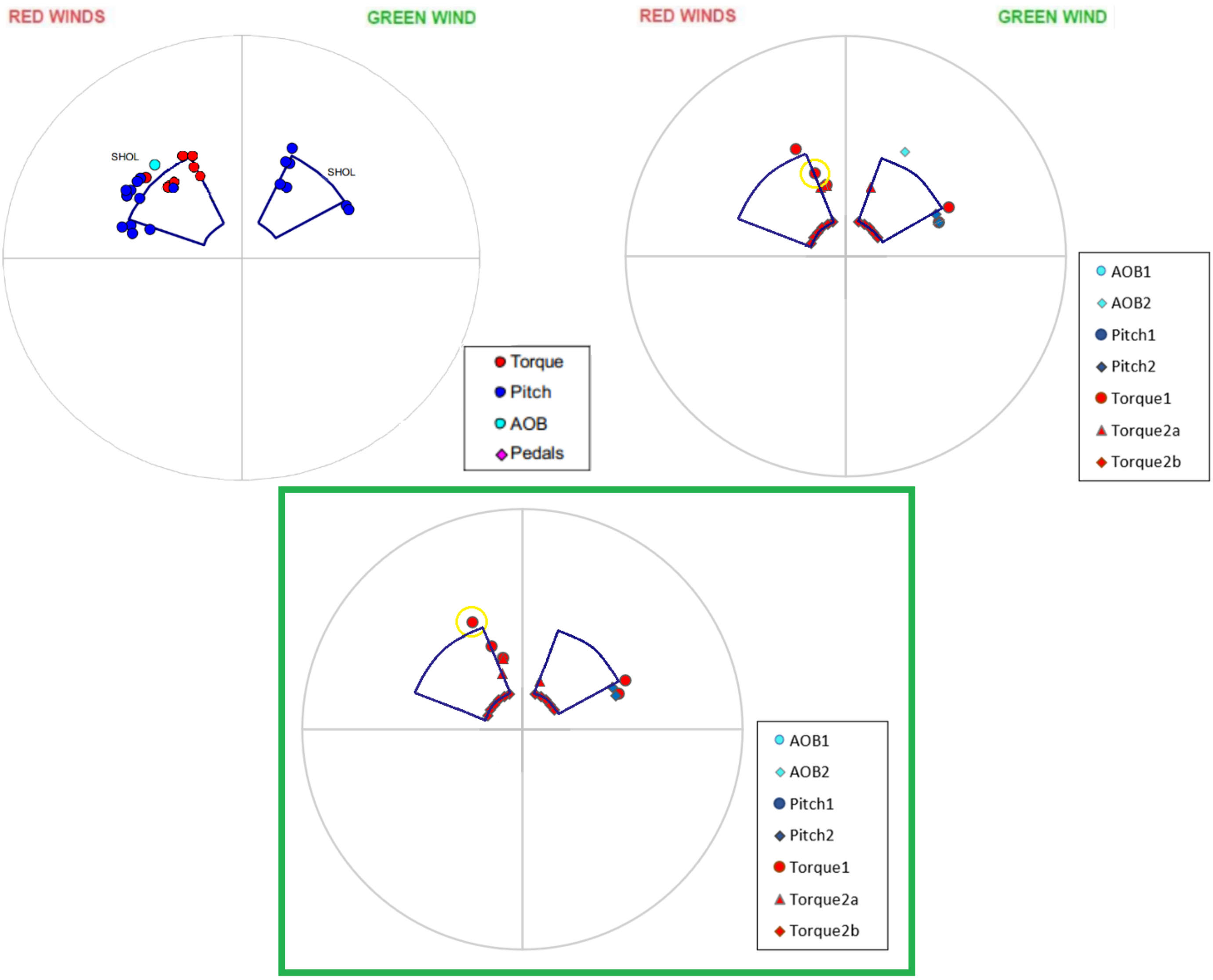

Figure 6.18: Top left: existing SHOL oblique procedure. Top right: predicted SHOL with *calibration1*. Bottom: predicted SHOL with *calibration2*. Circled in yellow: data points used for calibration. Blue line: existing SHOL.

Sensitivity Cross Procedure

Figure 6.19 presents three SHOL diagrams for the cross procedure: the original SHOL of the baseline case, the predicted SHOL with *calibration 1* and the predicted SHOL with *calibration 2* (both including the existing SHOL indicated by the blue line). It can be seen that for both the Torque criteria, nothing has changed comparing the limits of *calibration1* to *calibration2*.

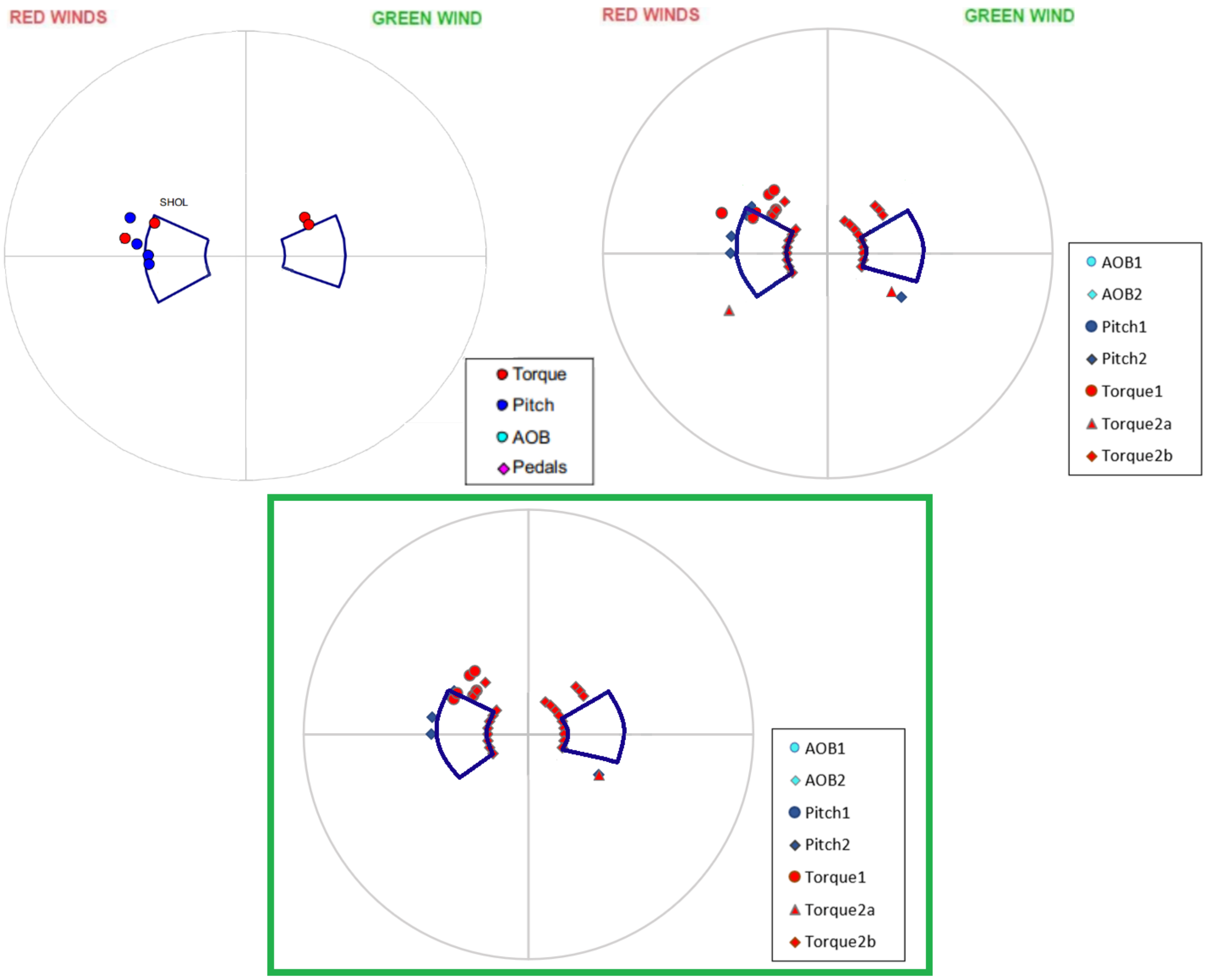

Figure 6.19: Top left: existing SHOL cross procedure. Top right: predicted SHOL with *calibration1*. Bottom: predicted SHOL with *calibration2*. Circled in yellow: data points used for calibration. Blue line: existing SHOL.

Discussion Sensitivity Analysis

The main conclusions that can be drawn from the sensitivity analysis are the following:

- The parameters from the base formulas of AOB2 and Torque2 are sensitive to the data points chosen to calibrate these to. It is important to select data points for calibration which are fitting for the criterion in question. In table 6.4 guidelines are presented for selection of suitable data points for calibration.
- The *calibration2* applied to the AOB2 criteria gives an improvement in the amount of correctly predicted angle of bank limits, however a significant amount of angle of bank limits can still not be predicted. A change in the base formula might improve this. It is not expected that the lack of AOB prediction is purely due to environmental elements which DeepPurple cannot simulate. It is expected that a change in the relation between the mean flow velocity and the angle of bank may bring improvement.
- A change in parameter magnitude does not necessarily mean a significant change in the final predicted SHOL. The SHOLs predicted with *calibration1* and *calibration2* have the same overall prediction of the envelope, except for 2 Torque2a outliers.
- The sensitivity analysis is restricted because of the limited data available. It would be valuable to test the sensitivity of the prediction procedure for another ship type.

Guideline Suitable Data Points for Calibration	
LightPink Formula	Guideline
AOB1	An AOB limit which is caused by a strong cross wind, which occurs when no/little downwash is experienced.
AOB2	An AOB limit which is caused by low wind speed, in combination with downwash.
Pitch1	A pitch limit which occurs for Red winds, where no strong turbulence is expected to be experienced by the pilot.
Pitch2	A pitch limit which occurs for Green winds, where no strong turbulence is expected to be experienced by the pilot.
Torque1	A torque limit which is caused by a strong cross component, which occurs when no/little downwash is experienced.
Torque2a	A torque limit which is caused by low wind speed, in combination with downwash.
Torque2b	*Can be calibrated purely with shore-based hover trial data.*

Table 6.4: Guidelines for calibration of LightPink formulas.

6.4.3 Assessment and Proposed Improvements

With the results from the validation and sensitivity analysis of LightPink, an assessment can be made of the prediction procedure. The following can be concluded:

- All the types of objective limits of the baseline case can be predicted to an extend with the prediction procedure. The predicted objective limits for the baseline case occur in correct regions of the SHOL but not all are captured.
- Only 1 type of subjective limit can be predicted with the prediction procedure: subjective limits attributed by pilots to turbulence in the approach of the cross- or oblique procedure. For the baseline case this type of subjective limit can be captured well by the prediction procedure, however this might be different for other ship types. It is deemed valuable to validate the prediction of subjective limits with another ship.
- For Red winds during the fore-aft procedure, *Pitch1* limits are predicted by the procedure which do not occur in the existing SHOL. This means that the *Pitch1* criteria is too strict for a R30 component to the helicopter. This suggests that for improved prediction, turbulent flow components should be included in the LightPink formula.
- Pitch limits caused by turbulent flow components cannot be predicted by the procedure. These types of pitch limits are especially apparent during oblique procedures.
- The AOB2 and Torque2 LightPink formulas are sensitive to the data points taken for the calibration. It is important to evaluate the calibrated criteria for their physical meaning.
- The sensitivity of the parameters of the LightPink formulas to data points taken for the calibration does not largely affect the overall predicted SHOLs for the baseline case. However, parameters which are calibrated with 'less suitable' data points, can cause outliers in the predicted SHOLs.
- Inaccuracies of the predicted limits can in some cases be caused by the fact that discrete locations in the ship domain are evaluated (i.e. Disk A, Disk B and Disk C).

All together, it can be learned from this chapter that LightPink is able to predict sufficient limits and risk areas to give an outline of the SHOLs for the known case. Approximately 85% of the SHOLs of the baseline case can be predicted with LightPink[11]. The remaining 15% is expected to depend on turbulent flow components or subjective limits caused by limited visual cues of the pilot. Before applying the *LightPink* prediction procedure - calibrated with the baseline case - to new ship designs, the following is important to understand about the expected predictive capabilities of LightPink:

- The calibration of most of the parameters of the LightPink formulas are obtained by correlating DeepPurple mean-flow data to a selected set of existing limits of the baseline case. Due to the correlation, elements of the ship environment which are not experienced during shore-based hover trials, are included in the LightPink model. This makes the LightPink formulas specific for the environment of the baseline ship. It is anticipated that this does not prevent the prediction procedure having a predictive function for new ship designs, when in the same size-range as the baseline case. It is expected that the ship environment elements are sufficiently comparable for these ship types, however further validation of the tool is advised to confirm this.

---

[11] Combining the results of the three landing procedures: $(95\% + 70\% + 90\%) \cdot \frac{1}{3} = 85\%$

- When using the tool LightPink, it is important to keep in mind that LightPink cannot predict a complete SHOL diagram. The outcomes need to be viewed with an engineering judgement, keeping in mind which limits LightPink does not (accurately) capture.
- A limited validation of the prediction tool was performed in this study, as only 1 ship type is studied. This causes difficulty in quantifying potential inaccuracies when using the tool for new/other ship designs. Before using the tool, it is recommended to validate the tool - calibrated to the baseline case - for another ship type with known limits. In this way it can also be analysed how dependent the predictive methodology is on the ship-type it is calibrated to.

By means of the validation performed in this study, an approximation of the accuracy of the predicted limits by the tool can be made as presented in table 6.5.

LightPink Capturing of Limits			
Captured	Approximately	Rough Estimate	Not Captured
Objective - Pitch2 Objective - Torque	Objective - Pitch1 Objective - AOB	Subjective - Turbulence in Approach	Subjective - Visual Cues Subjective - Ship Motions Subjective - Turbulence above Flight Deck

Table 6.5: Limits which are captured and not captured by LightPink

The following improvements of LightPink are recommended for future research:

- The relation between the mean flow velocity and the angle of bank in the LightPink base formula for *AOB2* may be improved.
- The calibration of the subjective base formula may be improved by analysing more locations in the approach path, instead of solely Disk C.
- Turbulent flow features appear to cause limits in specific regions in the SHOL (subjective and objective), which cannot be predicted with LightPink. It is advised to investigate the possibility of incorporating modelled turbulence intensity from DeepPurple into the base formulas (especially for the *Pitch1* formula and for subjective limits due to turbulence above the flight deck).

6.5 Summary and Conclusions

LightPink is calibrated, tested and assessed for a baseline case. The calibration of the LightPink base formulas to the baseline case is done by using data from NH90 NFH shore-based hover trials and by correlating sea-trial limits of the baseline case to mean flow data obtained with DeepPurple. A selected number of sea-trial limits is used for the calibration of LightPink. To validate LightPink, the prediction SHOLs are compared to the complete set of existing limits. The sensitivity of the predicted SHOLs to the data points used for calibration is also tested. From the validation and sensitivity analysis of the prediction procedure, the following conclusions can be drawn:

- All together, it can be concluded that LightPink is able to predict sufficient limits and risk areas to give an outline of the SHOLs for the known case, after a suitable calibration. Approximately 85% of the SHOLs of the baseline case can be predicted with LightPink.
- For the calibration of LightPink, it is important to use suitable data points. Using unsuitable data points can cause outliers in predicted SHOLs. This may be prevented by evaluating the calibrated formulas for their physical meaning.
- The use of the *LPD2-Model2* (where the more detailed *LPD2-Model1* could not be used) is most likely the cause of slight deviations between the existing SHOL and the predicted SHOL for the fore-aft procedure for angles in the range of R15 to R30 and G30 to G15.
- Limits which cannot be predicted with LightPink for the baseline case include: objective limits caused by sudden velocity/directional changes in relative wind flow (most relevant for pitch limits during the oblique procedure), a number of angle of bank limits occurring in Red winds during the fore-aft procedure, subjective limits due to restricted visual cues, subjective limits due to ship motions and subjective limits due to turbulence above the flight deck.
- It is expected that the prediction procedure which is calibrated with the baseline case, is capable of providing valuable information on the impact of (broad) ship design choices on specific types of limits. It is key that LightPink is used to identify *trends* and not for investigation of quantitative results.

The following improvements could be made to LightPink in future research:

- The prediction of *AOB2* limits may be improved by adjusting the relation between the mean flow velocity and the angle of bank in the LightPink base formula.
- Turbulent flow features appear to cause limits in specific regions in the SHOL (subjective and objective), which cannot be predicted with LightPink. It is advised to investigate the possibility of incorporating modelled turbulence intensity (from DeepPurple) into the base formulas.

Chapter 7

Preview Proposed Ship Concepts

Impact of Superstructure Design
Proposed Ship Designs
LightPink Analysis Concept A

> Quality without results is pointless.
> Results without quality is boring.
>
> *Johan Cruijff*

7.1 Introduction

A preview is given of a proposed set of conceptual ship designs which are considered relevant to investigate in future research for the impact of superstructure design choices on the ship helicopter operational availability. The use of LightPink is demonstrated by analysing one new ship concept.

Section 7.2 evaluates the sources of the ship helicopter operational limits of the baseline case[1], and the impact of specific superstructure design features on the sources. Section 7.3 discusses the design philosophy which leads to a set of conceptual superstructure designs proposed to be studied in future research. Section 7.4 presents the results of the LightPink analysis of 1 new ship concept.

---

[1] The baseline case: a combination of the LPD2 with a NH90 NFH of 11.000 kg ref. weight.

7.2 Impact of Superstructure Design

The type of limits that cause specific parts of the boundaries of the baseline case are explained below. It is analysed what the expected impact of superstructure design features on the type of limits are.

The red areas in the diagram in figure 7.1 present the total ship helicopter envelope of the baseline case for all the landing and take-off procedures. The yellow areas indicate regions for potential improvements to the envelope. Each yellow are is separately discussed, using the knowledge obtained in the course of this research.

Two terms will be used to indicate boundaries in the SHOL: *velocity boundaries*, which indicate a boundary which prevents higher relative wind velocities to be included in the envelope, and *angle boundaries*, which indicate a boundary which prevents smaller or larger relative wind angles.

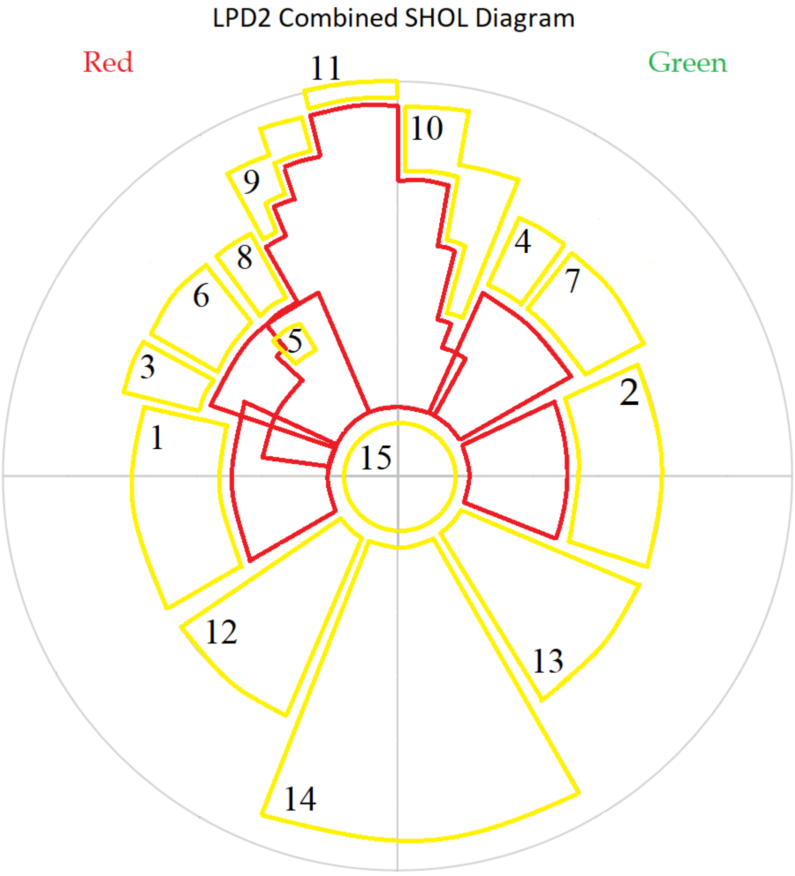

Figure 7.1: Red: LPD2 SHOL diagrams for the fore-aft, oblique and cross procedure both port and starboard. Yellow: areas for potential improvements in the envelope.

- **Area 1, 2:** The velocity boundaries in area 1 and 2 corresponds to the cross procedure and are caused by an excessive *subjective rating* attributed by the pilot to *turbulence in approach*. The turbulence experienced by the pilot here is most likely related to upwash and downwash over the flight deck during cross winds to the ship. *Pitch* limits occur during the cross procedure. The angle boundaries for smaller relative wind angles are caused by *torque required* limits. The torque limits are likely due to a strong cross-flow component towards the helicopter when above the flight deck (L_{perp}) and sudden low wind speeds or strong downwash in the approach when flying in the wake of the superstructure.

  Impact of superstructure: The current flight deck design allows for an airflow over the flight deck which is almost at the undisturbed relative wind speed, which causes strong upwash and downwash regions close to the flight deck. A change in the design of the flight deck edges can be investigated to reduce the turbulent region leeward of the flight deck. Also, a superstructure and flight deck layout that allows for more different approach paths for landing can potentially allow the envelope to extend to area 1 and 2.

- **Area 3, 4, 5:** The velocity boundaries in area 3 and 4 (and 5) correspond to the oblique procedure and are caused by *pitch* limits. These are limits due to an excessive pitch-up attitude above the flight deck which are most likely caused by *flapback* due to sudden velocity/directional changes in relative wind flow. Especially in area 5, excessive *subjective ratings* which are attributed to *turbulence in approach* by the pilot occur.

  Impact of superstructure: Almost undisturbed flow over the flight deck causes strong upwash and downwash regions. Especially during oblique procedures, this flow over the flight deck also causes sudden velocity/directional changes in relative wind flow in the helicopter path above the flight deck. A change in the design of the flight deck edges can be investigated to reduce the turbulent region leeward of the flight deck. Also, a superstructure and flight deck layout that allows for more different approach paths for landing can potentially allow the envelope to extend to area 3 and 4.

- **Area 6, 7:** The velocity boundaries in area 6 and 7 correspond to the oblique procedure and are caused by an excessive *subjective rating* attributed by the pilot to *turbulence in approach*. The turbulence experienced by the pilot here is most likely related to upwash and downwash near flight deck during cross winds to the ship. A number of *Objective* limits occur, which can most likely be attributed to sudden velocity/directional changes or peaks in relative wind flow.

  Impact of superstructure: The impact is the same as described for area 3, 4 and 5.

- **Area 8:** The velocity boundary in this area corresponds to the fore-aft procedure and is caused by *torque required* limits due to a strong cross-flow component towards the helicopter (L_{perp}).

  Impact of superstructure: A superstructure and flight deck layout that allows for a procedure that enables the helicopter to manoeuvre more head-to-wind in these situations may extend the envelope to area 8.

- **Area 9:** The velocity boundary corresponds to the (port) fore-aft procedure and is caused by *torque required* limits due to a strong cross-helicopter component, and *angle of* *bank* limits. The AOB limits are likely due to low wind velocities and strong downwash above the landing spot.

Impact of superstructure: A superstructure and flight deck layout that allows for more different approach paths for landing may allow the envelope to extend to area 9.

- **Area 10:** The velocity boundary in this area corresponds to the (starboard) fore-aft procedure and is caused by *torque required* limits and *angle of bank* limits. These limits are caused by low wind speeds and strong downwash above the landing spot, for the small relative wind angles. For the larger relative wind angles *pitch* limits (due to strong G30 components toward the helicopter) occur and *torque required* limits occur due to a strong cross-flow towards the helicopter.

  Impact of superstructure: For the small relative wind angles, a superstructure shape that reduces the downwash in the helicopter flight path can extend the boundary. For the larger relative wind angles, a superstructure and flight deck layout that allows for more different approach paths for landing may extend the envelope.

- **Area 11:** The velocity boundary in area 11 corresponds to the fore-aft procedure and is caused by *angle of bank*, *torque required* and *pitch* limits. Also, *subjective rating* limits attributed to turbulence above the flight deck occur in area 11.

  Impact of superstructure: Enlarging the superstructure in height can potentially extend the envelope to area 11.

- **Area 12, 13, 14:** These areas are not part of the envelope as there are no suitable approach paths possible on the LPD2 which allow the helicopter to land safely in the relative wind directions of area 12, 13 and 14.

  Impact of superstructure: A superstructure and flight deck layout that allows for more different approach paths for landing can potentially allow the envelope to extend to area 12, and 14. A ship with a significant superstructure and a flight deck on the rear and on the front could be an option.

- **Area 15:** The envelope does not extend to this area due to *torque required* limits. The helicopter assumed for the baseline case cannot fly at continuous relative wind velocities occurring in this area. The superstructure has no influence here.

The sources from the ship environment which can cause limits to the ship helicopter envelope are lined up below, as learned from the development and testing of LightPink. The magnitudes are related to the baseline case and obtained from LightPink relations. The magnitudes are to illustrate the relation between variables and may deviate from magnitudes in reality.

Angle of Bank: Two wind-scenarios can cause a limit: strong RED winds w.r.t. the helicopter and very weak RED winds. A R90 wind w.r.t. the helicopter, of a magnitude around 10 [m/s], causes a limit. A reduction in wind speed significantly increases the angle of bank attitude. In LightPink, a reduction of the relative wind speed from 20 [kts] to 10 [kts] causes an increase in angle of bank of 2°. Green winds are never critical for the helicopter angle of bank. In LightPink, a downwash component of 1.5 [m/s] can cause an angle of bank increase of more than 3°.

Pitch Attitude: Pitch-up attitudes can cause limits to the envelope, pitch-down attitudes are in practice never critical during ship helicopter operations. A G30 wind w.r.t. the helicopter causes extremes in the pitch-up attitude due to the fixed horizontal tailplane of the helicopter. In LigthPink, a G30 component of 10.5 [m/s] causes a limit above the flight deck. For Red winds, an U_{head} component of 18 [m/s] causes a limit. Low frequency and high intensity fluctuations in the wind environment *above the flight deck* can cause pitch-up limits due to *flapback* which can already occur for mean relative wind speeds in the range of 20 [kts] to 30 [kts].

Torque Required: Two wind-scenarios can cause a torque required limit: strong winds from G90 due to tail torque limitations and low wind speed conditions from G90 in combination with downwash due to total torque required limitations. In LightPink, a R90 wind component that exceeds 9 [m/s] or a G90 component that exceeds 5 [m/s] causes a limit. For a scenario without downwash, continuous environmental wind speeds lower than 5.4 [m/s] (or: 10.5 [kts]) cause limits. In LightPink, a downwash component of 1.5 [m/s] can cause a torque required [%] increase of more than 12%.

Subjective Rating: The subjective rating is determined by three main sources: the ship motion, limited pilot visual with the ship (and Flight Deck Officer) and turbulence experienced by the pilot. Two different types of turbulence limits can be identified for the LPD2. Firstly, strong winds cause limits for small relative wind angles (0° to 10°) due to turbulent flow behind the superstructure. Secondly, changes in mean flow velocities in the approach path can cause the pilot to experience low frequency turbulence during the oblique and cross procedure, which can cause subjective limits. Subjective limits attributed by the pilot to turbulence are the main type of subjective limits to the envelope of the LPD2. In LightPink, a high risk of these subjective limits occurs during the cross- and oblique procedure where a W of -2.25 or a W of 1.55 [m/s] is exceeded in Disk C.

7.3 Proposed Ship Concepts

The proposed set of conceptual designs is to be in line with the process of *concept exploration and definition* as applied by Defence Material Organisation. Subsection 7.3.1 explains in short how the Maritime Systems Division of DMO applies the *concept exploration and definition* process in warship design and how the present research fits into this process. Subsection 7.3.2 presents the conceptual superstructure designs. General design considerations and assumptions applied for the conceptual ship designs can be found in appendix F.

7.3.1 Concept Exploration Process DMO

The process of warship concept exploration and definition as applied by DMO, and how this fits into the design process of a warship, is described by Oers et al. (2018). The concept exploration and concept definition processes is briefly discussed below and it is explained how the present research fits into this process.

Warship Design Process

The design process of a warship in the Netherlands is a cooperation between different organisations. Iterative dialogues between these organisations are necessary to successfully complete the design of a warship. At the start of the design process an iterative dialogue between stakeholders takes place to elucidate requirements and budget. This iterative dialogue is illustrated in figure 7.2. The role of DMO in this phase is to support the iterative dialogue with technical specifications and analysis. This is done by concept exploration and concept definition.

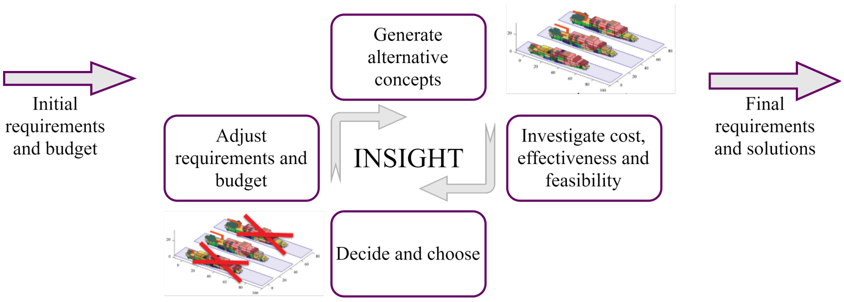
Initial requirements and budget
Generate alternative concepts
Adjust requirements and budget
INSIGHT
Investigate cost, effectiveness and feasibility
Decide and choose
Final requirements and solutions

Figure 7.2: Iterative dialogue for elucidation of requirements and budget, based on Oers et al. (2018)

The engineering support of the iterative dialogue is provided by the Bureau of Life Cycle Modelling which is part of the Maritime Systems Division of DMO. Concept exploration is a very broad study of many alternatives. Concept definition is a more detailed and less wide study of alternatives. In practice, these processes do not take place strictly subsequent but happen in synergy. During the exploration of concepts a wide range of alternatives are considered with respect to ship layout, systems and performance. For the exploration of concepts, preliminary assessments of performance are made using a limited level of detail whilst keeping sufficient fidelity of the performance predictions. From the exploration, a set of concepts is selected which are considered most suitable. These concepts are studied into more detail during the concept definition process with regard to the performance, cost, risks and the operational effectiveness.

The Present Research

In this research project, a practical and simplified method is developed for the prediction of operational limits for the NH90 NFH aboard a LPD-like navy ship. The limited level of detail of this method allows for a broad analysis. This method is expected to be a useful tool during the concept exploration phase to predict the performance of a ship concept with regard to the ship helicopter operational availability.

7.3.2 Conceptual Superstructure Designs

During the exploration process it is useful to analyse advantages and disadvantages of certain design choices with regard to the ship helicopter operations. Questions which are interesting to answer during this phase concerning the ship helicopter operational availability in comparison to the baseline case (the LPD2) are for example:

> *What is the effect of making the ship longer?*
>
> *What is the effect of making the ship higher?*
>
> *What is the effect of removing the superstructure?*

These types of questions lead to a set of conceptual superstructure designs A to K[2] which are presented the block diagram in figure 7.3 and the models are illustrated in figure 7.4. Also added, are two concepts including airwake control methods. General considerations to be taken into account when proposing a new conceptual ship design (such as the minimum size of the flight deck) are outlined in appendix F.

---

[2] For concept C and J, the factor 1.56 for a hull height increase is assumed, which approximately includes the volume of the baseline superstructure into the hull.

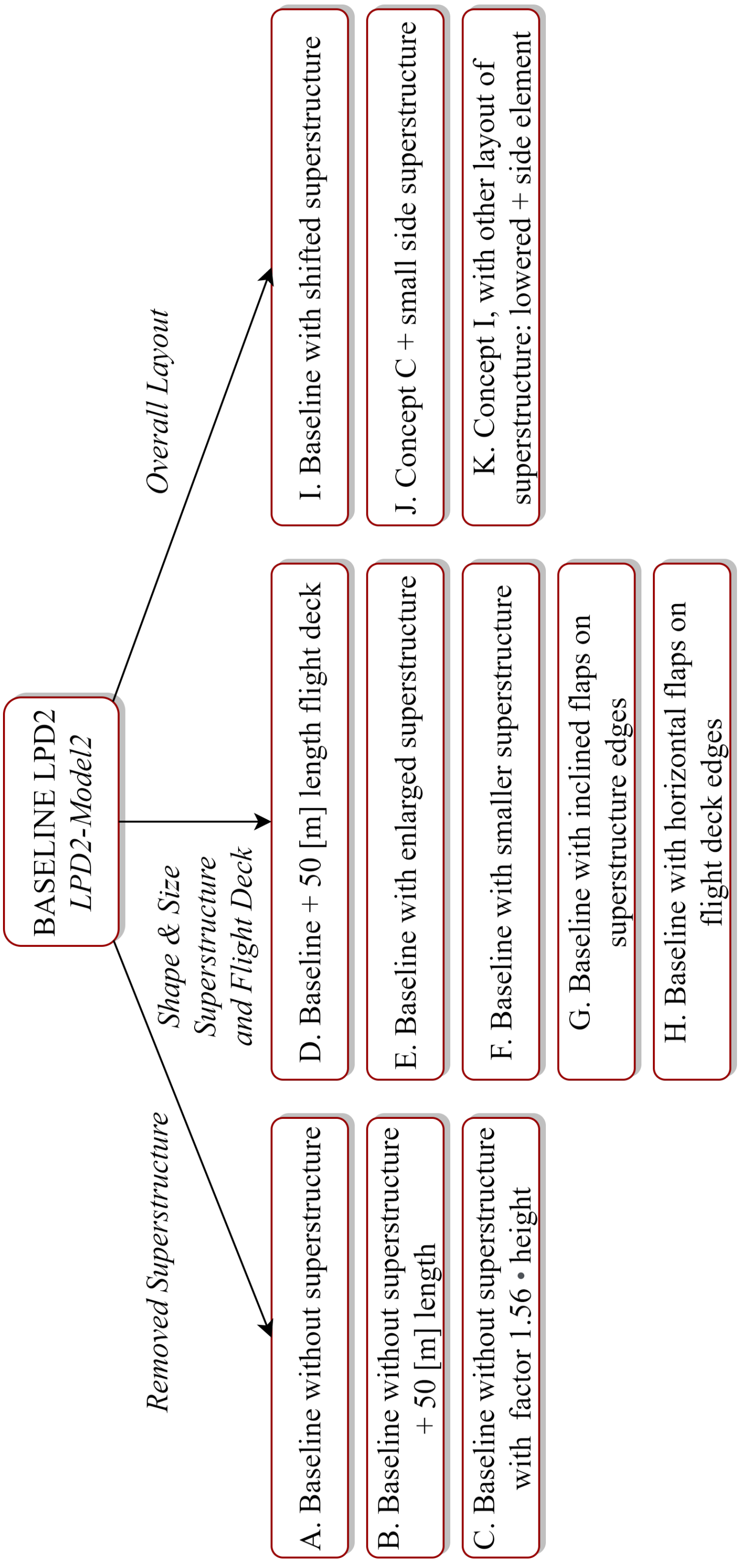
BASELINE LPD2
LPD2-Model2
Removed Superstructure
Shape & Size Superstructure and Flight Deck
Overall Layout
A. Baseline without superstructure
B. Baseline without superstructure + 50 [m] length
C. Baseline without superstructure with factor 1.56 • height
D. Baseline + 50 [m] length flight deck
E. Baseline with enlarged superstructure
F. Baseline with smaller superstructure
G. Baseline with inclined flaps on superstructure edges
H. Baseline with horizontal flaps on flight deck edges
I. Baseline with shifted superstructure
J. Concept C + small side superstructure
K. Concept I, with other layout of superstructure: lowered + side element

Figure 7.3: Blockdiagram conceptual designs with *LPD2-Model2* as baseline and conceptual design A to K.

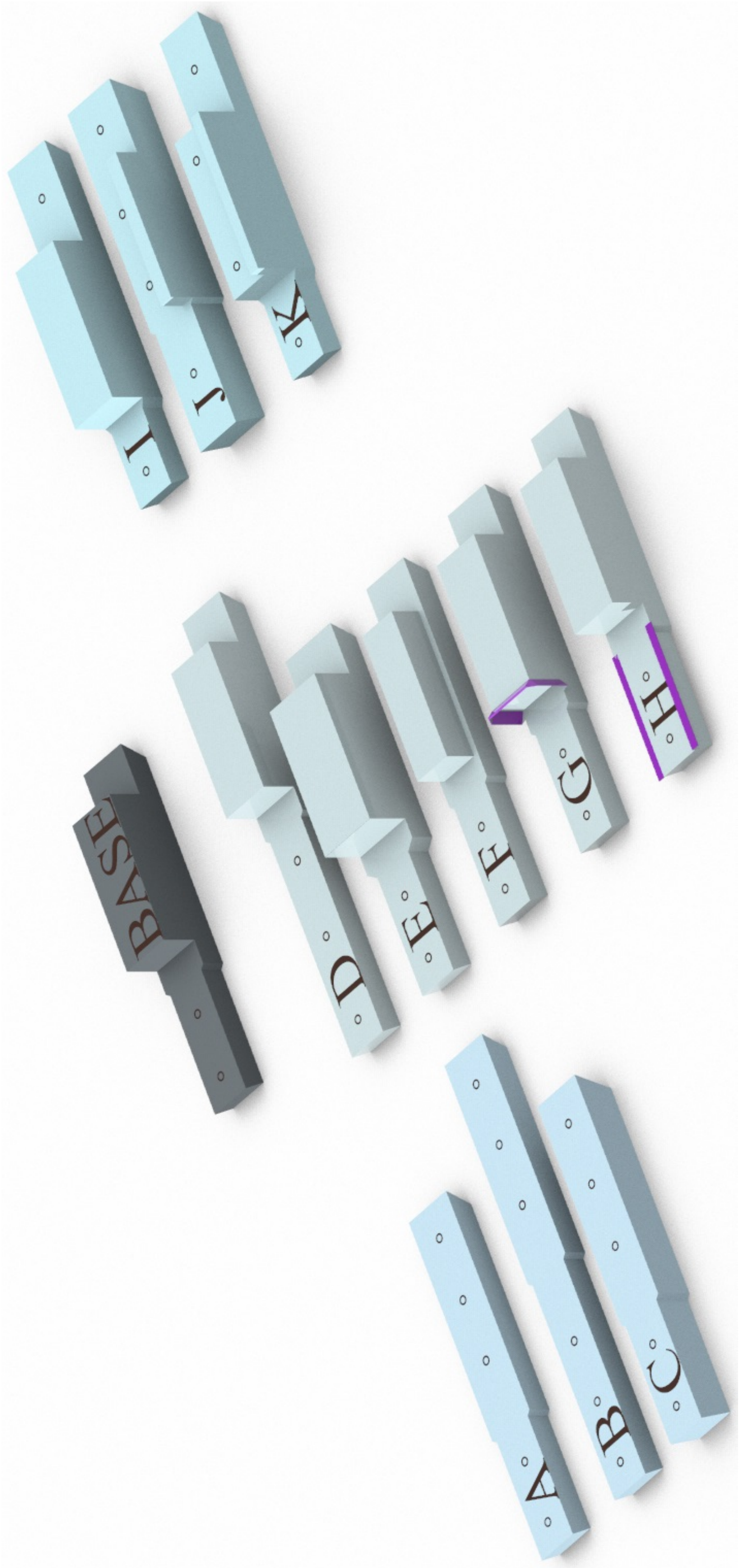
BASE
A
B
C
D
E
F
G
H
I
J
K

Figure 7.4: *LPD2-Model2* as baseline with Concept A to K 3D models.

7.4 LightPink Analysis of Concept A

To demonstrate the use of LightPink for a new conceptual ship design, this section presents the predicted SHOLs of Concept A for 1 potential landing spot on the ship. The LightPink base formulas are calibrated to the baseline case (LPD2).

7.4.1 About the Analysis

Table 7.1 presents for each LightPink formula which calibrated formula is used and in which location in the domain the formula is tested. Below, two key items about the analysis are outlined.

- The *AOB2* limits where $U_{tot} < 8kts$ are removed from the predicted SHOLs, as explained in chapter 5.4.1.
- The *Pitch1* limits are expected to be too strict (they appear for too low velocities).

LightPink Analysis of Concept A				
Formula	Calibrated with	Location Fore-Aft	Location Oblique	Location Cross
AOB1	LPD2 - Calibration 1	Disk A	Disk A	Disk A
AOB2	LPD2 - Calibration 2	Disk A	Disk A	Disk A
Pitch1	LPD2 - Calibration 1	Disk A and B	Disk A and B	Disk A and B
Pitch2	LPD2 - Calibration 1	Disk A and B	Disk A and B	Disk A and B
Torque1	LPD2 - Calibration 1	Disk A, B and C	Disk A, B and C	Disk A, B and C
Torque2a	LPD2 - Calibration 1	Disk A, B and C	Disk A, B and C	Disk A, B and C
Torque2b	*Assumed constant lower limit*			

Table 7.1: LightPink Analysis details of Concept A

7.4.2 Predicted SHOLs Concept A

Figure 7.5 presents the landing- and take-off procedures which are assumed for Concept A for landing spot 1 (the most forward landing spot).

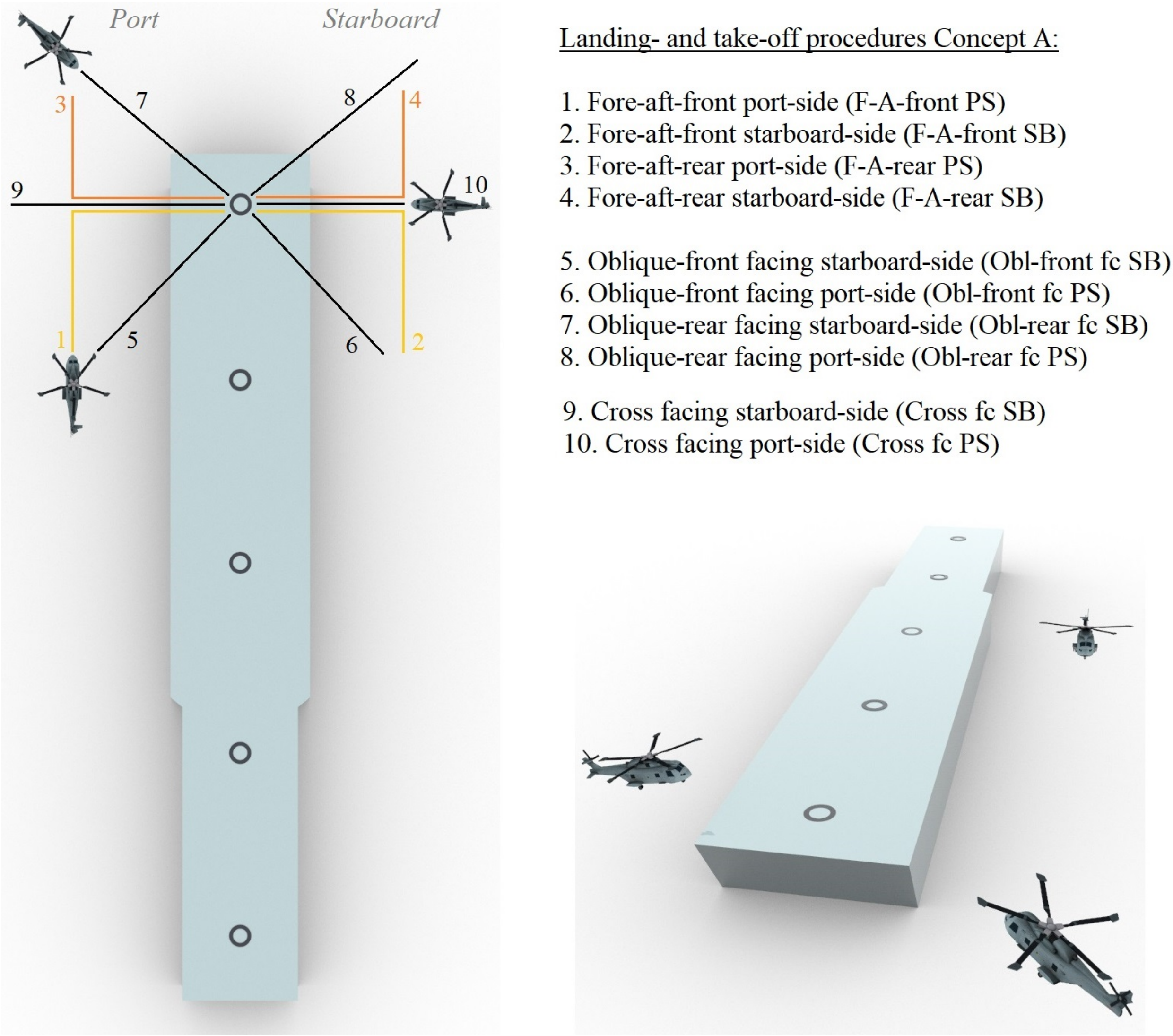

Landing- and take-off procedures Concept A:

1. Fore-aft-front port-side (F-A-front PS)
2. Fore-aft-front starboard-side (F-A-front SB)
3. Fore-aft-rear port-side (F-A-rear PS)
4. Fore-aft-rear starboard-side (F-A-rear SB)

5. Oblique-front facing starboard-side (Obl-front fc SB)
6. Oblique-front facing port-side (Obl-front fc PS)
7. Oblique-rear facing starboard-side (Obl-rear fc SB)
8. Oblique-rear facing port-side (Obl-rear fc PS)

9. Cross facing starboard-side (Cross fc SB)
10. Cross facing port-side (Cross fc PS)

Figure 7.5: Concept A: landing- and take-off procedures for Spot 1.

Figures 7.6, 7.7, 7.8 and 7.9 present the predicted SHOLs for Concept A. The SHOLs for procedure 5 and 7 (oblique-front and rear facing starboard) are not shown, these can be considered approximately mirrored along the 0° relative wind angle from procedure 6 and 8.

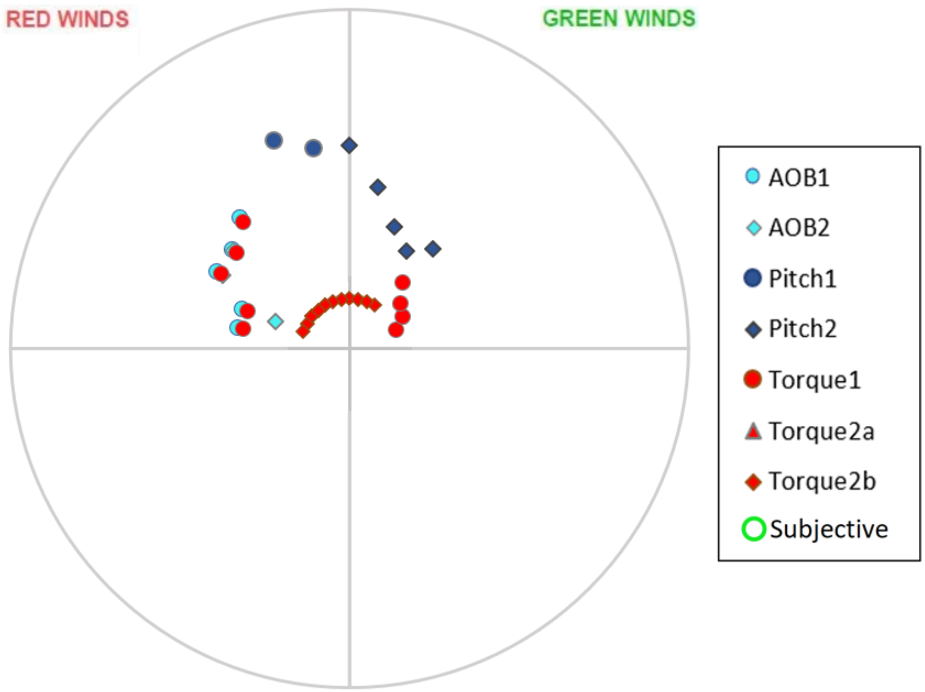

Figure 7.6: Concept A: LightPink predicted SHOL fore-aft-front port-side and starboard-side (procedure 1 and 2).

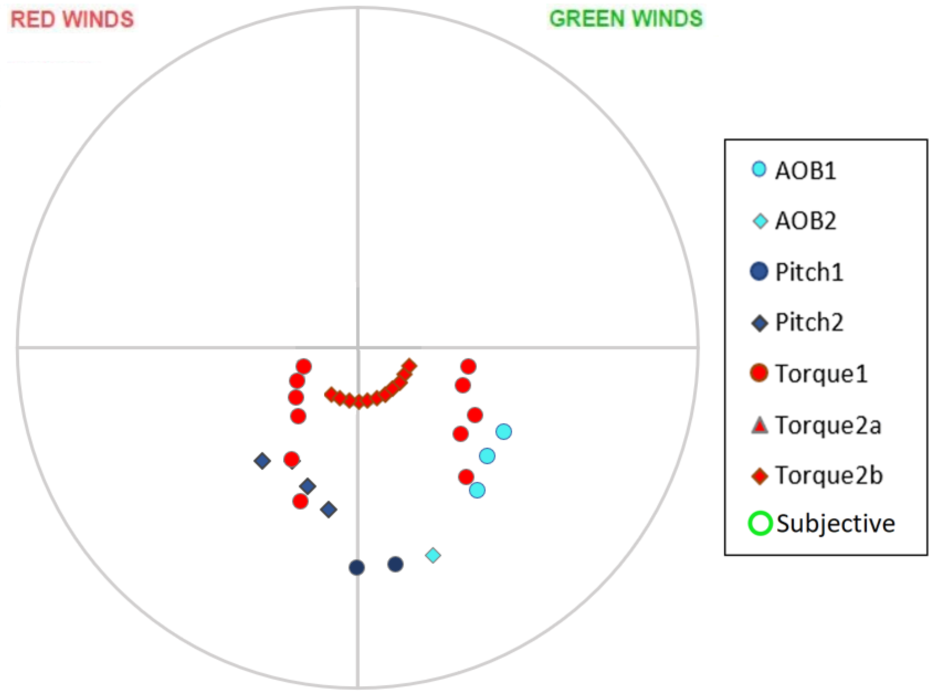

Figure 7.7: Concept A: LightPink predicted SHOL fore-aft-rear port-side and starboard-side (procedure 3 and 4).

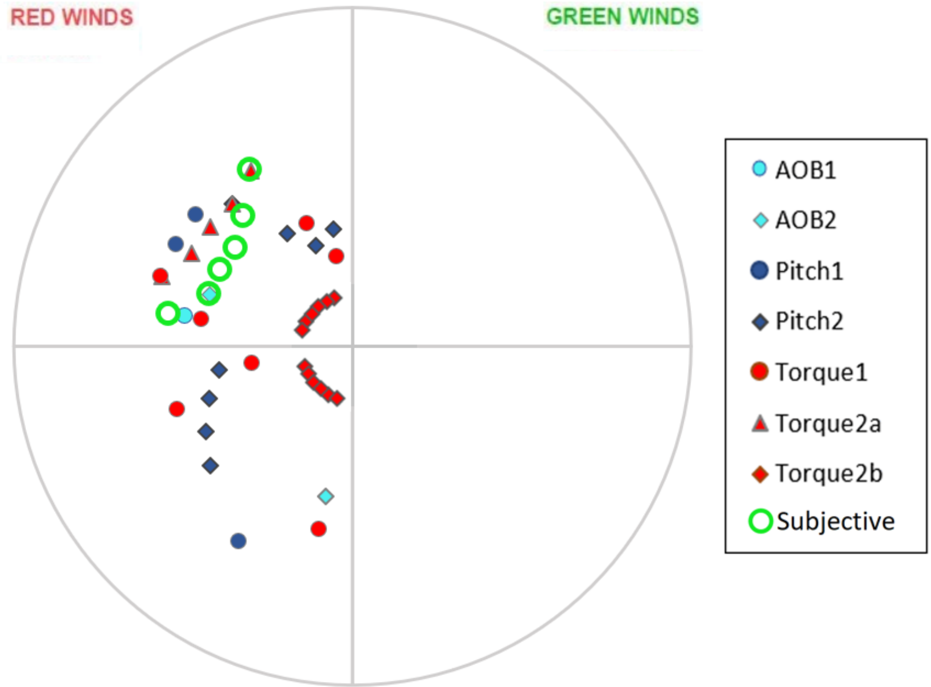

Figure 7.8: Concept A: LightPink predicted SHOL oblique-front and -rear facing port-side (procedure 6 and 8).

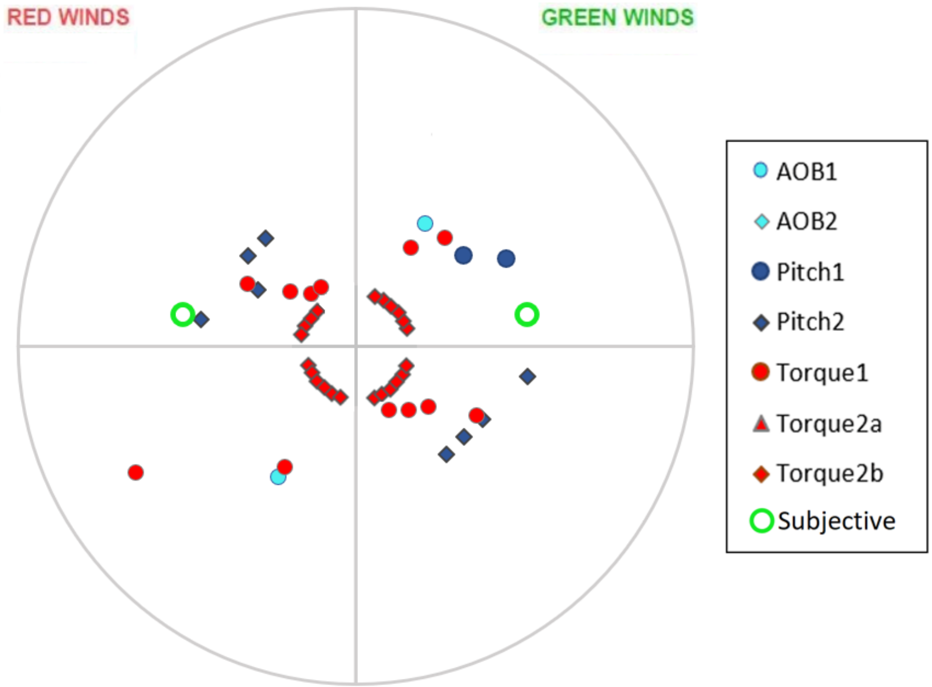

Figure 7.9: Concept A: LightPink predicted SHOL cross facing port-side and starboard-side (procedure 9 and 10).

7.4.3 Discussion

From the predicted SHOLs, the following can be observed:

- The fore-aft-front procedures are in general more restricted for Concept A compared to the baseline concept (*LPD2-model2*). Most likely, the wake created by the large superstructure on the baseline concept enables the fore-aft-front procedure to be performed in stronger wind speeds compared to Concept A.
- For the oblique-front facing port procedure (procedure 6), subjective 'risk areas' are predicted to limit the envelope. This does not play a role for the oblique-rear facing port procedure (procedure 8). This difference can be understood by looking at visualized streamlines as shown in figure 7.10. In the oblique-front procedure (top figure 7.10) the helicopter has an approach path that crosses the region circled in black (Disk C) where strong downward flow occurs. In the oblique-rear procedure (bottom figure 7.10) the helicopter has an approach path that crosses the region circled in black (Disk C) where the mean flow is mostly horizontal.

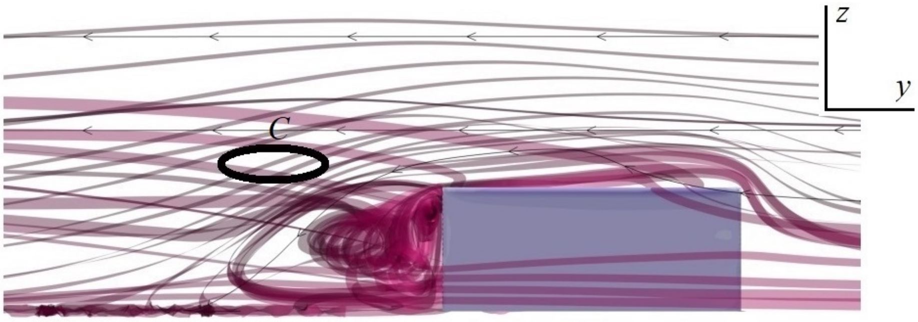

Front-view of Concept A: R50 33 kts
(procedure 6)

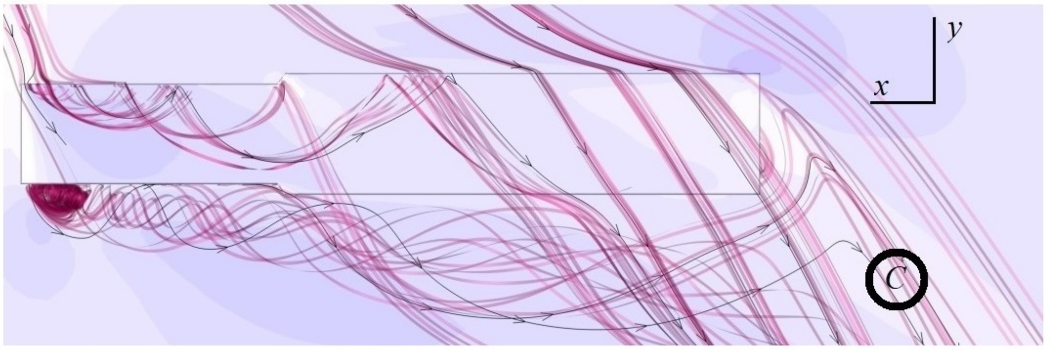

Top-view of Concept A: R120 31 kts
(procedure 8)

Figure 7.10: Top: Front-view of Concept A with partially visualized streamlines for a R50 relative wind angle and 33 kts wind speed. Bottom: Top-view of Concept A with partially visualized streamlines for a R120 relative wind and 31 kts wind speed.

- The envelope for the cross procedures is quite similar to the baseline case. It is predicted that Concept A allows for a slightly broader envelope for the cross procedure facing starboard (procedure 10). It is expected that the superstructure on the baseline ship causes large circulating flow structures which create subjective 'risk areas', for lower wind velocities than Concept A. This can be understood by comparing the visualized streamlines around the baseline ship shown in figure 7.11, to the front-view in figure 7.10 (top). It can be seen (independent of the exact relative wind angle) that the circulating flow structures leeward of the ship reach higher (into the approach path for the cross procedure) for the baseline ship due to the large superstructure.

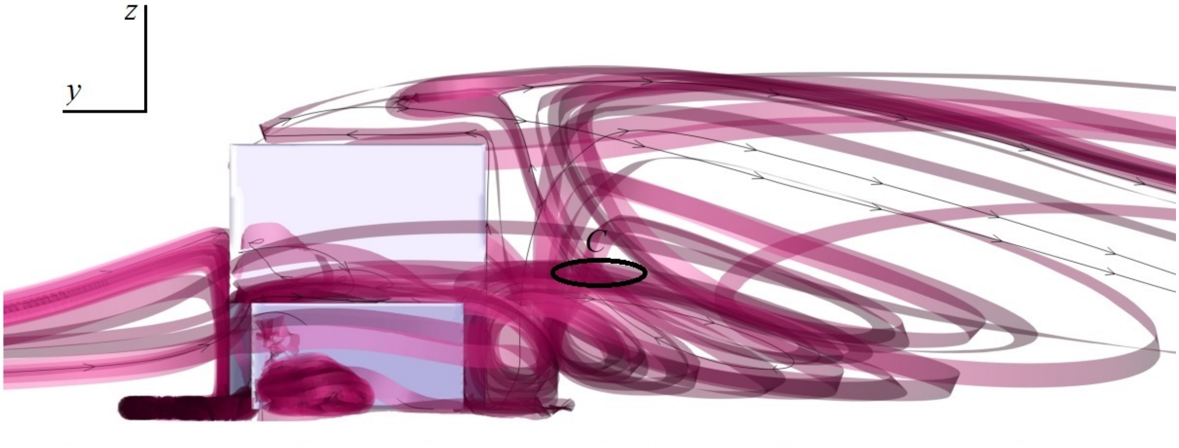

Figure 7.11: Rear-view of the baseline ship (*LPD2-Model2*) for a R105 relative wind angle and 29 kts wind speed (cross facing port procedure).

Chapter 8

Conclusions and Recommendations

> We can only see a short distance ahead, but we can see plenty there that needs to be done.
>
> *Alan Turing*

8.1 Conclusions

In light of the new amphibious transport ship to be designed for the Dutch Royal Navy and the expected increase in airborne operations from the ship, more insight is desired into the impact of ship design choices on helicopter operational availability. The research question of this study is formulated as follows:

What is a suitable tool that can be used to predict the impact of a ship design on helicopter operations in the early design phase?

This question is answered according to the scheme introduced at the beginning of this paper and repeated (minimized) in figure 8.1.

For the development of this tool, first an insight is gained into the methods that can be used to analyse the influence of the ship design on the wind environment of the ship, suitable in the early design phase. DMO is in possession of a low fidelity computational software *DeepPurple*, which can simulate flows around simple ship designs. On basis of a validation of DeepPurple performed in this study, it is anticipated that the mean flow information provided by DeepPurple is sufficiently accurate to use as input for the tool.

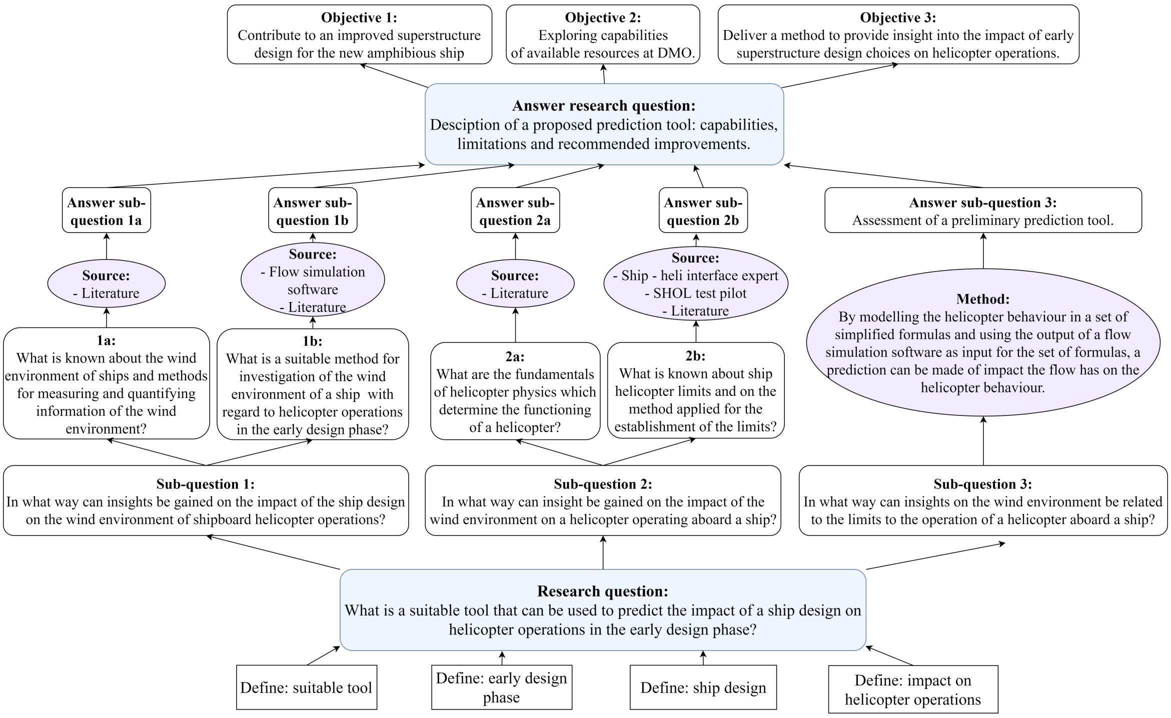
Objective 1:
Contribute to an improved superstructure design for the new amphibious ship
Objective 2:
Exploring capabilities of available resources at DMO.
Objective 3:
Deliver a method to provide insight into the impact of early superstructure design choices on helicopter operations.
Answer research question:
Desciption of a proposed prediction tool: capabilities, limitations and recommended improvements.
Answer sub-question 1a
Answer sub-question 1b
Answer sub-question 2a
Answer sub-question 2b
Answer sub-question 3:
Assessment of a preliminary prediction tool.
Source:
- Literature
Source:
- Flow simulation software
- Literature
Source:
- Literature
Source:
- Ship - heli interface expert
- SHOL test pilot
- Literature
Method:
By modelling the helicopter behaviour in a set of simplified formulas and using the output of a flow simulation software as input for the set of formulas, a prediction can be made of impact the flow has on the helicopter behaviour.
1a:
What is known about the wind environment of ships and methods for measuring and quantifying information of the wind environment?
1b:
What is a suitable method for investigation of the wind environment of a ship with regard to helicopter operations in the early design phase?
2a:
What are the fundamentals of helicopter physics which determine the functioning of a helicopter?
2b:
What is known about ship helicopter limits and on the method applied for the establishment of the limits?
Sub-question 1:
In what way can insights be gained on the impact of the ship design on the wind environment of shipboard helicopter operations?
Sub-question 2:
In what way can insight be gained on the impact of the wind environment on a helicopter operating aboard a ship?
Sub-question 3:
In what way can insights on the wind environment be related to the limits to the operation of a helicopter aboard a ship?
Research question:
What is a suitable tool that can be used to predict the impact of a ship design on helicopter operations in the early design phase?
Define: suitable tool
Define: early design phase
Define: ship design
Define: impact on helicopter operations

Figure 8.1: Research structure (for full-size refer to thesis introduction).

To be able to investigate the effect of the wind environment on a helicopter, insights were gained into helicopter physics and into the process of establishing SHOLs at the Dutch Royal Navy. Key factors influencing limits during shipboard helicopter operations can be related to helicopter attitude and performance, ship motions and pilot workload.

Insights regarding ship environment modelling and shipboard helicopter operations are related through a model. This model predicts the behaviour of a helicopter, using mean flow data as input. This model is the basis of the prediction procedure *LightPink*. LightPink relates information about the local mean flow in the ship environment to the behaviour and shipboard limits of a NH90 NFH. The data flow of LightPink is illustrated in figure 8.2.

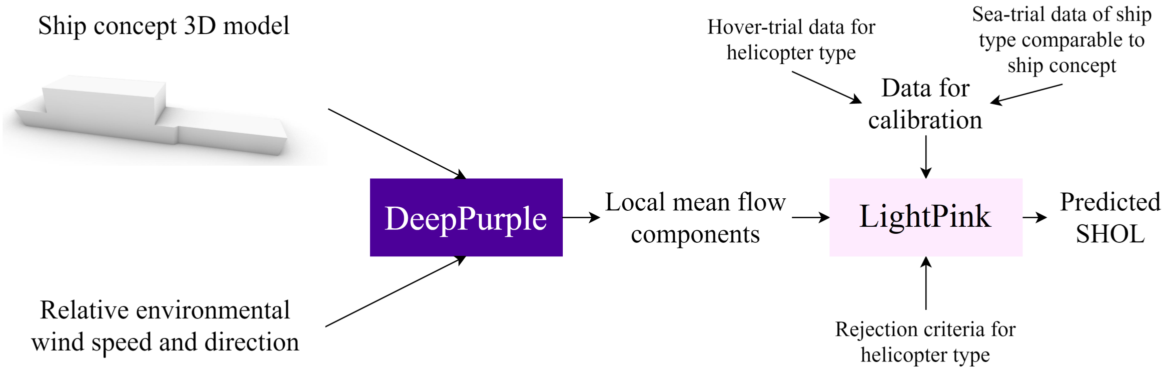
Ship concept 3D model
Hover-trial data for helicopter type
Sea-trial data of ship type comparable to ship concept
Data for calibration
DeepPurple
Local mean flow components
LightPink
Predicted SHOL
Relative environmental wind speed and direction
Rejection criteria for helicopter type

Figure 8.2: Data flow of proposed procedure for prediction of SHOLs.

The purpose of the prediction procedure is to predict helicopter limits aboard new amphibious transport ship designs. In the present research, LightPink is tested for a Dutch navy ship with known SHOLs. It was found that the limits and risk areas which can be related to mean flow components can successfully be approximated with LightPink. These limits determine up to 85% of the ship helicopter operational envelope of the Dutch navy ship. The remaining 15% of the envelope, which cannot be predicted with the tool, are most likely dependent on limits due to time-varying flow components and limited visual cues for the pilot. LightPink has shown to be able to predict sufficient limits and risk areas to give an outline of the SHOLs for the known case. The procedure is considered to be able to provide useful information about *trends* concerning the potential limits of new amphibious transport ship designs. Before applying the tool in practice, it is stressed that it is of importance to have detailed knowledge of the limitations of the method. Conclusions drawn on basis of the predicted SHOLs should be made with an engineering judgement. Before actual use of LightPink, the method requires attention in areas which are outlined in section 8.2.

The objective of this thesis is to provide insight into a suitable tool for the investigation of superstructure impact on helicopter operations in the early design phase. This is accomplished by developing a predictive method, in the form of a tool *LightPink*. This study has demonstrated a methodology for assessment of early ship designs, using inputs provided by DMO in-house software DeepPurple. The tool LightPink shows potential to predict the outline of ship helicopter limits of new conceptual ship designs, for the purpose of observing trends concerning the impact of the superstructure design choices on helicopter operations. The essence of the method lies in the *accesibility*, *low-cost* and *simplicity of inputs*. With the insights given in this thesis and the proposed prediction methodology, it is aspired to lay the basis for a practical prediction tool. This tool can lead to an improved design of the amphibious transport ship for the Dutch Royal Navy and potentially for other ship types. An additional goal of the research is to explore the capabilities and limitations of in-house resources at DMO for the present subject. This is accomplished by the verification and validation of the CFD software *DeepPurple* and by exploration of DeepPurple software elements as is documented in appendix A.

8.2 Recommendations

A number of general recommendations are presented below for DMO, for future research concerning the present research topic.

- The tool which is proposed in this research is developed for a specific type of helicopter (NH90 NFH). The tool is validated by calibrating it to a select number of existing limits for a Dutch navy ship, and predicting the remaining limits. The predicted limits, which were not used for calibration, are validated with the existing limits. Conclusions about the capabilities of the tool for prediction of limits aboard this ship were made in this study. However, limited conclusions can be drawn about the capabilities of the tool for new ship designs. The steps taken during development of the tool aim to lead to a tool which is as generic as possible within the scope of 'amphibious transport ship types', which refers to large and wide ships with spacious (and high) flight decks. However, for a well grounded validation, independent data should be used (which is not used during calibration). In the present research, the data used for calibration is not expected to be entirely independent of the data used for validation. In order to formulate better statements about the capabilities of LightPink for new ship designs, the calibrated LightPink tool from the present study should be tested for another large ship type for which helicopter limits are known by sea-trials.

- The present study has shown that it is possible to develop a simple tool for the prediction of helicopter limits based on computed mean flow information. This was done by proposing a tool for 1 type of helicopter. Potentially, the same method can be developed for other types of helicopters, when following the steps described in this report and being in possession of the relevant information[1].

- For a pilot operating a helicopter in the ship environment, predictability of the environment is crucial to keep the pilot workload within acceptable bounds. In the present study, it was found that informative images can be obtained from DeepPurple presenting streamlines of the mean wind flow in the ship environment. Potentially, this could be useful for pilots to get an idea of the wind environment and potential improved flight paths to be taken.

- As briefly discussed in the introduction of the thesis, a predictive tool for SHOLs exists within the Dutch Royal Navy. This tool *SHOL-X* is developed by A. Hoencamp. This tool was developed for the purpose of increasing the efficiency of establishing SHOLs for existing ships. This results in a detailed model, requiring accurate inputs.

  To reach the objective of the present research, using SHOL-X for the prediction of SHOLs, with inputs obtained from DeepPurple, was considered unfit. The level of complexity of *SHOL-X* is considered excessive for the present research, and does not comply with the simplicity (and limitations) of the information obtained with DeepPurple. However, in future research, improvements to the prediction method proposed in this thesis could be made by incorporating some of the details of the (helicopter) model of *SHOL-X* into the LightPink formulas.

- For future research, it will be valuable to investigate a method to connect design choices for the topside of the ship to design choices for the underwater ship. This method has to connect ship motions to the (relative) wind environment. It is recommended to study the possibility of doing this by connecting the (relative) wind environment to sea-states. When combining information about the ship sailing velocity and the relative wind speed, the related sea-state can be found by the table provided on p. 21 in the NATO *Draft STANAG* document (NATO-Naval-Armaments-Group, 1994). In turn, sea-states can be connected to ship motions.

  In addition to this, the interaction between ship motions and ship airwake can be studied. The influence of ship motions on the ship airwake and consequently on helicopter operations in the ship airwake is discussed in the recent work of Dooley et al. (2020).

---

[1] Relevant information: shore-based hover trials for the type of helicopter and a set of existing ship-heli limits found during sea-trials and a DeepPurple-friendly ship model.

By relating the wind environment to the sea-states and ship motions, and clarifying the interaction between ship motions and ship airwake, the connection can be made between choices for the topside design and design choices for the underwater ship.

If continuing research with the proposed first version of LightPink, a number of improvements are recommended:

- The relation between the mean flow velocity and the angle of bank in the LightPink base formula *AOB2* may be improved.
- The base formula for *Pitch1* may be improved by including turbulent flow features in the formula. It would be valuable to investigate if turbulence intensity modelled by DeepPurple can be incorporated into this base formula.
- In general, turbulent flow features appear to have more influence on the objective limits than anticipated. It would be valuable to investigate the incorporation of modelled turbulence intensity (from DeepPurple) into the LightPink base formulas (subjective and objective). A further validation of turbulence intensity modelled by DeepPurple is advised. It could be investigated if a correlation can be found between turbulence rating given by test-pilots during sea-trials and turbulence intensity modelled by DeepPurple.
- In the present research, specific locations in the domain along the helicopter flight path were selected to retrieve data from. LightPink may be improved by selecting more locations along the flight path for data evaluation.

Bibliography

P. J. A. Booij, H. van der Ven, and K. D. S. Zeilstra. The use of cfd modelling of a ship's air wake for the generation of candidate flight envelopes, 2016.

A. R. S. Bramwell, D. Balmford, and G. Done. *Bramwell's Helicopter Dynamics*. Butterworth-Heinemann, second edition, 2001.

G.D. Carico, R. Fang, R.S. Finch, Jr. W.P. Geyer, Cdr. (Ret.) H.W. Krijns, and K. Long. *Helicopter/Ship Qualification Testing*. NATO, rto-ag-3000 vol. 22 edition, 2003.

S. Coyle. *The art and science of flying helicopters*. Arnold, 1996.

G. Dooley, J. E. Martin, J.H.J. Buchholz, and P.M. Carrica. Ship airwakes in waves and motions and effects on helicopter operation. *Computers and Fluids*, 208, 2020.

M. D. Driver, H. L. Seegmiller, and J. G. Marvin. Time-dependent behavior of a reattaching shear layer. *AIAA Journal*, 25, 1986.

M. Eijkman. The ship airwake influence on airborne shipboard operations, 2020.

R. Fang and P.J.A. Booij. *Helicopter-Ship Qualification Testing*. Nationaal Lucht- en Ruimtevaartlaboratorium, 2006.

D. B. Findlay and T. Ghee. Experimental investigation of ship airwake flow control for a us navy flight ii-a class destroyer (ddg). *3rd AIAA Flow Control Conference*, 2006.

S. J. Forrest and I. Owen. An investigation of ship airwakes using detached-eddy simulation. *Computers Fluids*, 39:656–673, 2010.

S. J. Forrest, I. Owen, G. D. Padfield, and S. J. Hodge. Ship-helicopter operating limits prediction using piloted flight simulation and time-accurate airwakes. *Journal of Aircraft*, 49, 2012.

D. I. Greenwell and R. V. Barrett. Inclined screens for control of ship air wakes. *3rd AIAA Flow Control Conference*, 2006.

A. Hoencamp. Helicopter-ship qualification testing: the theory and application of a novel test methodology optimizing for cost and time efficiency. *Technical University of Delft, Netherlands*, 106, 2015.

A. Hoencamp, M.D. Pavel, and D. Stapersma. The key facts of ship helicopter operational limitation development. *Annual Forum Proceedings - AHS International*, 3:1903–1916, 2013.

A. Hoencamp, D. Lee, M. D. Pavel, and D. Stapersma. Lessons learned from nh90 nfh helicopter-ship interface: Testing across the complete dutch fleet. 2014.

LTZ2OC A. Hoencamp. *Report CLSK Directive 11-32 Part 6; NH90 NFH Shore-Based Hover Trials Hot Heavy.* Ministerie van Defensie Royal Netherlands Air Force, version 1 edition, 2012.

LTZ2OC A. Hoencamp and LTZ1 R. van Kralingen. *Report CLSK Directive 11-32 Part 12; NH90 NFH sea trials LPD2 ”Zr.Ms. Johan de Witt”.* Ministerie van Defensie Royal Netherlands Air Force, version 1 edition, 2014.

C. S. van Holstein. Influence of ship design variation on wind climate around the ship, 2014.

J.H. Hulsker. *Voorschrift CZSK Algemeen 010 Opereren met helikopters aan boord van CZSK-eenheden.* Ministerie van Defensie, 2019.

M. L. Johnson and L. M. Faunt. Parameter estimation by least-squares methods. *Elsevier*, 210:1–37, 1992. doi: 10.1016/0076-6879(92)10003-V.

J. Kamp. The effects of cfd modelling on helicopter flight envelopes, 2015.

C. H. Kääriä, S. J. Forrest, and I. Owen. Using flight simulation to improve ship design for helicopter operations. *RINA-ICCAS*, 2011.

R. B. Mora. Experimental investigation of the flow on a simple frigate shape (sfs). *The Scientific World Journal*, 2014.

NATO-Naval-Armaments-Group. On standardized wave and wind environments and shipboard reporting of sea conditions. *Sub-Group 5 on Seakeeping*, page 21, 1994.

B. van Oers, E. Takken, E. Duchateau, R. Zandstra, S. Cieraad, W. Broek-de Bruin, and M. Janssen. Warship concept exploration and definition at the netherlands defence materiel organisation. *Naval Engineers Journal*, 130-2:31–82, 2018.

R. Oliveira. Comparison of computational fluid dynamics generated aerodynamic ship data against wind tunnel data, 2017.

S. A. Polsky. Cfd prediction of airwake flowfields for ships experiencing beam winds. *21st Applied Aerodynamics Conference*, 2003.

B. Praveen. Study of the ship airwake-helodeck flow field for safe helo operations. *Indian Institute of Technology Delhi*, New Delhi, 2018.

Z. Rui, R. Ji-Li, L. Hai-Xu, and Z. Peng-Cheng. Entropy-based detached-eddy simulation of the airwake over a simple frigate shape. *Advances in Mechanical Engineering*, 7:1–13, 2015.

D. M. Shafer and T. A. Ghee. Active and passive flow control over the flight deck of small naval vessels. *35th AIAA Fluid Dynamics Conference and Exhibit*, 2005.

S. Shukla, S. N. Singh, and B. Srinivasan. A computational study of modified ttcp/sfs ship airwakes. *Proceedings of the 4th Internional Conference on Ship and Offshore Technology ICSOT*, 2015.

S. Shukla, S. S. Sinha, and S. N. Singh. Ship-helo coupled airwake aerodynamics: A comprehensive review. *Progress in Aerospace Sciences*, 106:71–107, 2019.

Inc. Tecplot. *tecplot.360 2013 User's Manual*. Tecplot, Inc., release 1 edition, 2013a.

Inc. Tecplot. *tecplot.360 2013 Scripting Guide*. Tecplot, Inc., release 1 edition, 2013b.

N. S. Uzol, A. Sharma, and L. N. Long. Computational fluid dynamics simulations of ship airwake. *Journal of Aerospace Engineering*, 219:369–392, 2005.

H. van der Ven and E. H. Baalbergen. *Gebruik van een rekenmethodiek voor de bepaling van het windklimaat rond schepen in de voorontwerpfase NLR-CR-2013-092-Hzv-1 - Gebruikershandleiding van Deep Purple 2019*. Nationaal Lucht- en Ruimtevaartcentrum, 2019.

H. van der Ven, J. van Muijden, and O. J. Boelens. Fysische modellering van het windklimaat rond schepen ten behoeve van het voorontwerp nlr-cr-2012-413, 2012.

H. van der Ven, J. van Muijden, and E. H. Baalbergen. Rekenmethodiek voor de bepaling van het windklimaat rond schepen in de voorontwerpfase nlr-cr-2013-093, 2013.

R. E. Whitbread and S. A. Coleman. *Research on Offshore Helideck Environmental Issues*. Civil Aviation Authority, 2000.

R. B. Wit. Assessment of fidelity of candidate flight envelopes developed using computational fluid dynamics, 2017.

S. J. Zan. On aerodynamic modelling and simulation of the dynamic interface. *Journal of Aerospace Engineering*, 219:393–410, 2005.

Appendix A

DeepPurple Software Elements

A.1 Background

DeepPurple is a computational fluid dynamics (CFD) software program which is developed and used by the NLR. The NLR has installed DeepPurple at DMO in 2013, where it is used to analyse the wind climate around navy ships to optimise the exhaust design for minimization of smoke nuisance. DeepPurple is designed such that the user interface is as straightforward as possible, allowing users to run a lot of simulations in little time without needing a lot of knowledge of computational fluid dynamics. This results in a very easy to use, but "closed" software, making it difficult to adjust certain inputs and boundary conditions to the computations. DeepPurple uses the open source CFD software OpenFoam to run a standard case (computational method and boundary conditions) which is pre-defined in DeepPurple and cannot be altered in the user-interface.

For the extended user manual of DeepPurple refer to Ven and Baalbergen (2019). Below, the main set-up of DeepPurple and the DeepPurple computer is described. This includes an outline of the input variables, the flow of the software and the type and location of certain files. On the computer where DeepPurple is installed, two operating systems are ran: Windows and Linux. On the Linux system, you can log on on different user accounts. The two relevant user accounts are "DeepPurple" and "eCFD".

A.2 Windows User Interface

The Windows system contains the user interface which consists of an excel sheet ("DeepPurple Dashboard") where a set of input variables can be specified. The inputs for the DeepPurple Dashboard are as follows:

- Model geometry in the shape of stereolithography (Stl) files. The geometry files should include at least 1 exhaust and 1 hull file.
- Exhaust flow velocity, direction and smoke concentration.
- Flow velocity and temperature.
- Inflow angles (relative wind angles) to be analysed, multiple angles can be given as input in the Dashboard for one computation (DeepPurple will compute them consecutively).
- Settings for the planes above the flight deck which will be visualized in the results.

A.3 Linux Computation Steps

The Linux operating system contains the computational part of DeepPurple, this is where OpenFoam is installed and ran. The steps (flow of information) which are undertaken by DeepPurple for a single computation are visualised in figure A.1 and described below.

1. The inputs are given to the DeepPurple Dashboard on Windows and the computation is confirmed and started by the user.
2. The NLR middleware product ”Brics” Ven et al. (2013) is activated and communicates with the NLR software product ”eCFD” which is installed and works on the Linux operating system.
3. ”eCFD” will receive the input variables and the geometry information from ”Brics” and will call, with the eCFD run file *preproc.sh*, specific OpenFoam input and run files.
4. A specific OpenFoam case is called by eCFD.
5. The OpenFoam computation progress can be followed during the computation in the file *simpleFoam.out* where the computation iterations are written.
6. When the computation is successfully completed the raw data can be found in the *controlDict* file which is saved on two locations. The raw data can be viewed by the software ”Tecplot” by opening the *controlDict* file.
7. The pre-defined visualization planes (input in the DeepPurple Dashboard) can be found both on the Linux system and on the Windows system. In Windows they are saved on the shared Data Server ://T in a ZipFile.

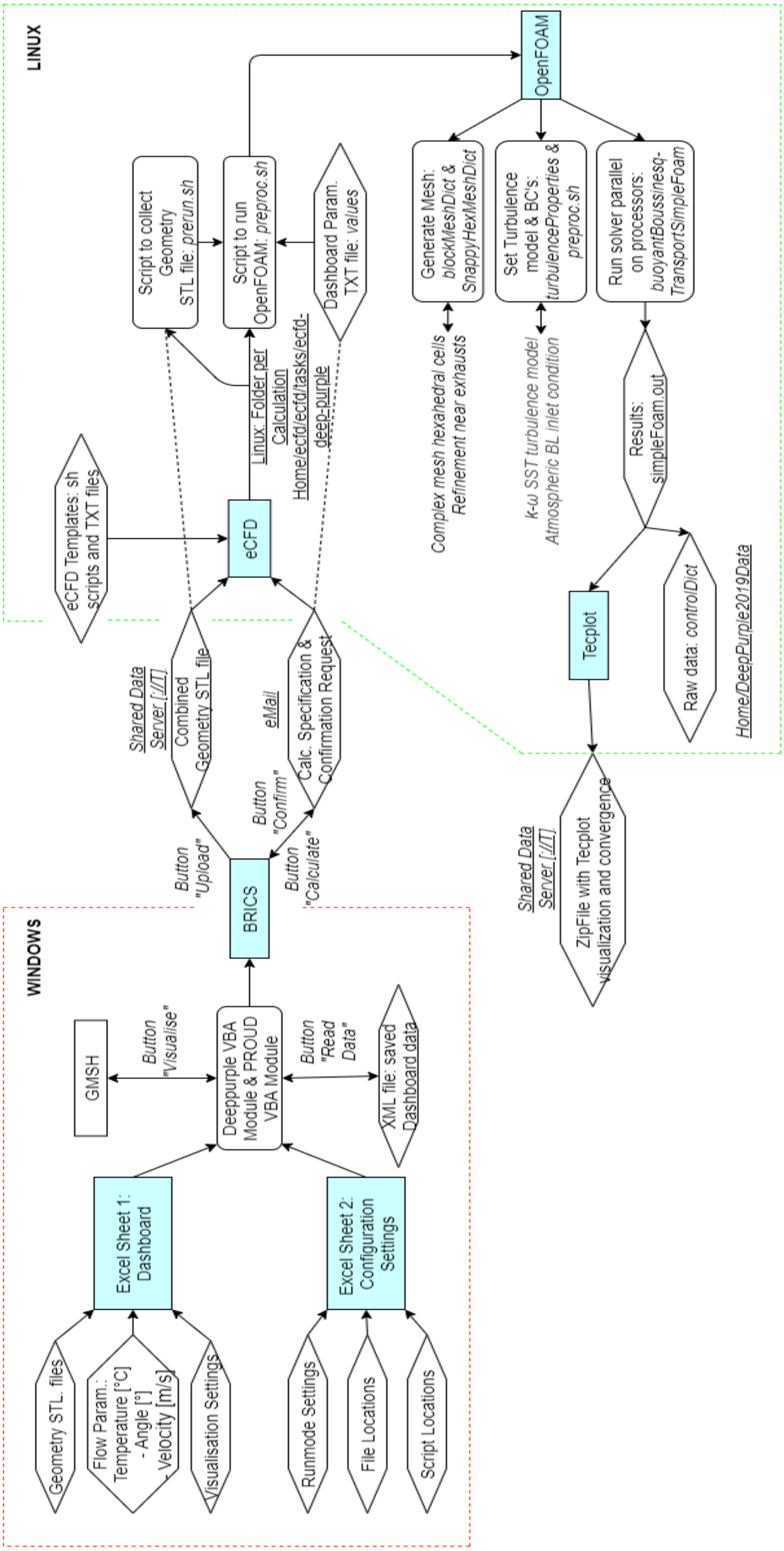
WINDOWS
Geometry STL. files
Flow Param.: Temperature [°C] - Angle [°] - Velocity [m/s]
Visualisation Settings
Excel Sheet 1: Dashboard
Runmode Settings
File Locations
Script Locations
Excel Sheet 2: Configuration Settings
GMSH
Button "Visualise"
Deeppurple VBA Module & PROUD VBA Module
Button "Read Data"
XML file: saved Dashboard data
BRICS
Button "Upload"
Button "Calculate"
Button "Confirm"
Shared Data Server [://T]
Combined Geometry STL file
eMail
Calc. Specification & Confirmation Request
LINUX
eCFD Templates: sh scripts and TXT files
eCFD
Linux: Folder per Calculation Home/ecfd/ecfd/tasks/ecfd-deep-purple
Script to collect Geometry STL file: prerun.sh
Script to run OpenFOAM: preproc.sh
Dashboard Param. TXT file: values
OpenFOAM
Generate Mesh: blockMeshDict & SnappyHexMeshDict
Complex mesh hexahedral cells Refinement near exhausts
Set Turbulence model & BC's: turbulenceProperties & preproc.sh
k-ω SST turbulence model Atmospheric BL inlet condition
Run solver parallel on processors: buoyantBoussinesq-TransportSimpleFoam
Results: simpleFoam.out
Tecplot
Raw data: controlDict
Home/DeepPurple2019Data
Shared Data Server [://T]
ZipFile with Tecplot visualization and convergence

Figure A.1: DeepPurple data flow

A.4 Relevant Files and Locations

In table A.1 the most relevant files are described and their names and locations are given. For each computation, templates of "eCFD" run files are retrieved and complemented with the specific inputs for the computation at hand. For each computation a "task file" is made on the Linux system with the task number in the name. Each task file consists of different files for the inflow angles specified in the DeepPurple Dashboard which then contain the complemented eCFD template files for that specific computation.

DEEPPURPLE FILES AND LOCATION		
File Name	Content	OS - Account - Location
”DeepPurple 2019Dashboard.xls”	DeepPurple Dashboard template	Windows - DeepPurple - :C/DeepPurple2019
”preproc.sh”	Template of eCFD run file	Linux - eCFD - Home/ecfd/templates/ecfd-deep-purple
”ofdirs.tar”	OpenFoam template files	Linux - eCFD - Home/ecfd/templates/ecfd-deep-purple
e.g. ”64”	Task file, made for each Dashboard confirmation	1. Linux - eCFD - Home/ecfd/tasks/ecfd-deep-purple/64 2. Linux - DeepPurple - Home/DeepPurple2019Data/64
e.g. ”000001”	Computation file, made for each inflow angle per task	1. Linux - eCFD - Home/ecfd/tasks/ecfd-deep-purple/64/000001 2. Linux - DeepPurple - Home/DeepPurple2019Data/64/000001
”simpleFoam.out”	Contains ’live’ info on the iterations, deleted when computation is completed	Linux - eCFD - Home/ecfd/tasks/ecfd-deep-purple/64/000001/Results
”controlDict”	For each successfully completed computation, this file contains the raw data of computation	1.Linux - eCFD - Home/ecfd/tasks/ecfd-deep-purple/64/000001/System 2. Linux - DeepPurple - Home/DeepPurple2019Data/64/000001/System

Table A.1: DeepPurple main files and location

A.5 Practical Notes on the Use of DeepPurple

A few practical notes on the use of DeepPurple are described below.

- **Setting up a new computation task in the Dashboard:** Each computation should be prepared in a new DeepPurple Dashboard excel sheet, copied from the Dashboard template. The name of the ship specified in the Dashboard should not be the same as for a previous calculation. When the ship name was used before, DeepPurple re-uses a mesh which was already created and this may lead to errors.
- **Confirming multiple computations in Windows:** In Windows the user can prepare multiple computations in DeepPurple Dashboards and confirm them. For each confirmed Dashboard, in Linux a task file will be created which contains separate files for each inflow angle. Each inflow angle will be a separate computation which is performed parallel on the 8 processors of the DeepPurple computer. All computations (i.e. per task, a specific inflow angle) are computed consecutively (not at the same time) in the order at which the Dashboard were confirmed in Windows.
- **Making adjustments to OpenFoam method and BC's:** To make alterations in the OpenFoam method, the *preproc.sh* template file should be edited. For example, the inflow boundary condition (uniform inflow or Atmospheric Boundary Layer) can be changed in *preproc.sh.* This is also where the height of the atmospheric boundary layer can be adjusted.
- **Deleting a task which is already confirmed in Windows:** If you delete a task file on the eCFD account on Linux before it is executed in OpenFoam, the task will not be performed.
- **Analysing the raw data in Tecplot:** The raw results data for a computation can be opened by going to the DeepPurple account on Linux. There the task file should be opened and with a right mouse click on the specific computation in the task (for an inflow angle, e.g. "000001") choose "open in terminal". In the terminal Tecplot can be opened by typing "tec360" and pressing enter. Then in Tecplot go to "load file" and choose the *controlDict* file from the "Systems" directory.

Appendix B

Overview NLR Reports - DeepPurple

In table B.1 an overview is given of the reports of NLR studies into the use of DeepPurple. Information is included about the validations performed in these studies.

NLR DEEPPURPLE RESEARCH - VALIDATION						
Nr.	Year	Type	Ship	Data	Validated Data	Flow Angles
1	2012	NLR Report	SFS-NLR	NLR PIV data 2009	- Velocity contours - Streamlines	- 0 - 45
2	2013	NLR Report	LCF	NLR exhaust data 2006	- Visual contours exhaust gas	- 0 - 20
3	2014	InHolland Thesis	SFS-NLR	NLR LPD visual data	- Velocity coeff. - u flow deviation - w flow deviation	- 0 to 360
4	2015	InHolland Thesis	LPD2 NLR	NLR LPD2 data 2012	- Velocity coeff. - u flow deviation - w flow deviation	- 0 to 360
5	2016	NLR Report	LPD2 NLR	NLR LPD2 data 2012	- Velocity coeff. - u flow deviation - w flow deviation	- 0 to 360
6	2017	TU Delft Thesis	LPD2 NLR	NLR LPD2 data 2010	- Velocity coeff. - u flow deviation - w flow deviation	- 0 to 360
7	2018	TU Delft Internship	Generic model ONERA	ONERA data 2018	- Velocity coeff. - u flow deviation - w flow deviation	- RED50 to GREEN50

Table B.1: NLR Research with DeepPurple: Validation Approaches

Appendix C

Additional Validation and Verification of DeepPurple

C.1 DeepPurple Validation - Atmospheric Boundary Layer

It is evaluated what effect an atmospheric boundary layer inflow[1] has on the airwake data obtained from DeepPurple compared to an uniform inflow.

From the graphs in figure C.1 the following can be observed:

- For a headwind condition as well as for a green 45 condition the atmospheric boundary only has a minor effect on the results.
- Taking the ABL into account will give slightly lower velocity values.
- From the graphs in figure 4.12 and figure 4.14 it can be seen that the effect of an ABL on the turbulence intensity is also very small.

---

[1] The atmospheric boundary layer has a reference height in OpenFoam of 10 [m].

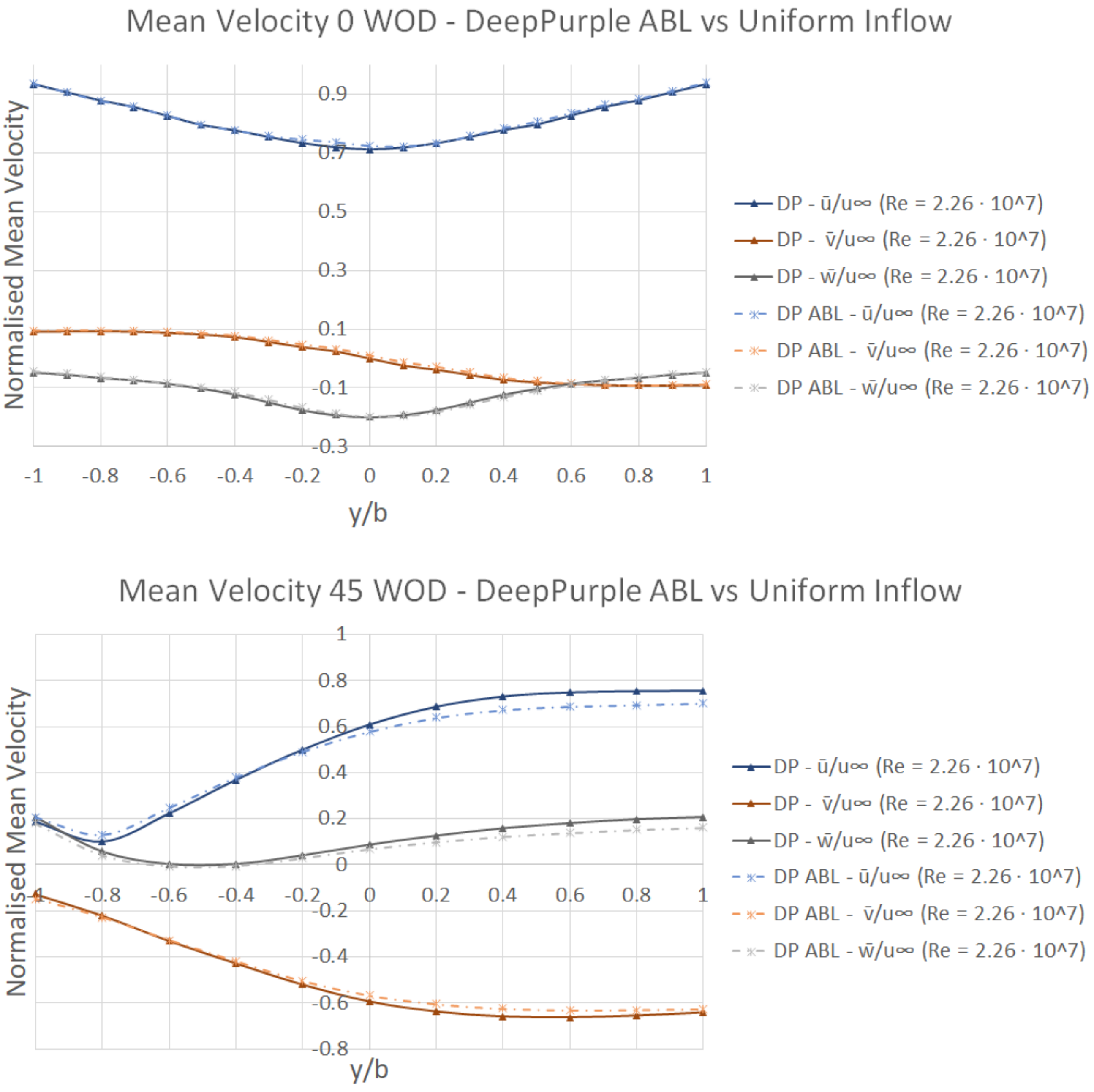

Figure C.1: Headwind (top) and G45 (bottom) mean velocity of experiment- (Forrest and Owen, 2010) and DeepPurple data at different Reynolds nr. at 50% deck length measured at hangar height with the lateral position normalized by ship beam b.

C.2 DeepPurple - RANS Comparison

The mean flow and turbulent intensity results from DeepPurple are compared to results obtained with a RANS model from Praveen (2018). In the thesis by Praveen (2018) a RANS simulation is performed with a modified SFS 2 model. The modification entails the removal of the exhaust. The turbulence model that was used by Praveen (2018) is a Transition SST turbulence model, which is a combination of a transformed k-ϵ model and a standard k-ω model. DeepPurple uses a standard k-ω turbulence model. The simulation cases which are compared are presented in table C.1.

Validation Simulations						
Name	Model	Scale	Reynold Nr.	Inflow	Rel. Wind Angle	Method
Praveen	SFS2 - Mod.	-	+/- $1.3 \cdot 10^7$	Uniform	0	RANS
DP3	SFS2 - Mod.	Full	$1.33 \cdot 10^7$	Uniform	0	RANS

Table C.1: Simulations used for the Validation of DeepPurple

Below, contour plots of mean and turbulent flow components are compared. It should be noted that although the contour colour legend of the results of B. Praveen is mimicked as accurately as possible in DeepPurple, deviations in the colours in the figures may occur. The comparison of the results is done by looking at the magnitudes, not the colours. The cases used can be found in table 4.2. The results of B. Praveen contain the normalized mean velocities in the x- and z-direction and the total turbulence intensity in contour plots at planes located at different heights above the flight deck. The planes which are compared to DeepPurple results are presented in figure C.2.

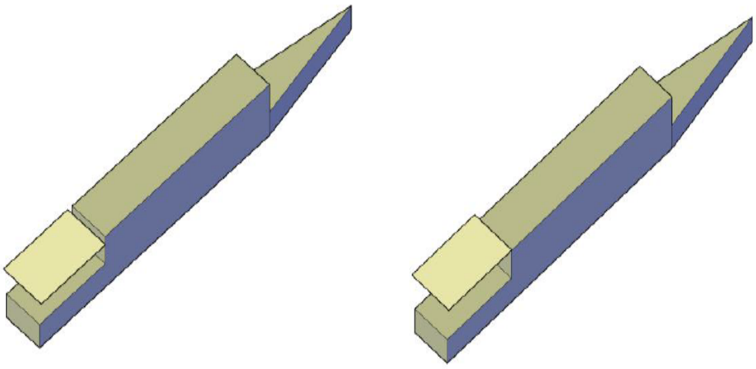

Figure C.2: Modified SFS 2, left: plane L at 9.88 [m] above the flight deck (just below hangar height). Right: plane M at 11.77 [m] above the flight deck (just above hangar height).

In figure C.3 the region where a negative normalised velocity in x (blue) occurs can be considered the recirculation region. It can be seen that the recirculation region in the DeepPurple results (right) is slightly smaller than the recirculation region from Praveen (left). In figure C.4 the results from Praveen show a slightly less strong downwash compared to the DeepPurple results at plane L. From figure C.5 it can be seen that the shape of the contours is fairly comparable, however DeepPurple gives slightly larger values for the turbulence intensity in a slightly smaller region compared to the results from Praveen.

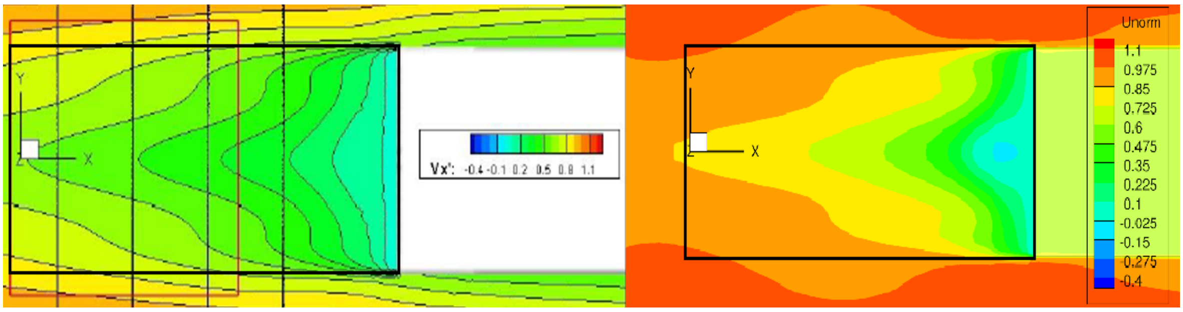

Figure C.3: Contour plot of x-component of the mean velocity normalised with freestream velocity on the L plane. Left: results from Praveen (2018). Right: DeepPurple results.

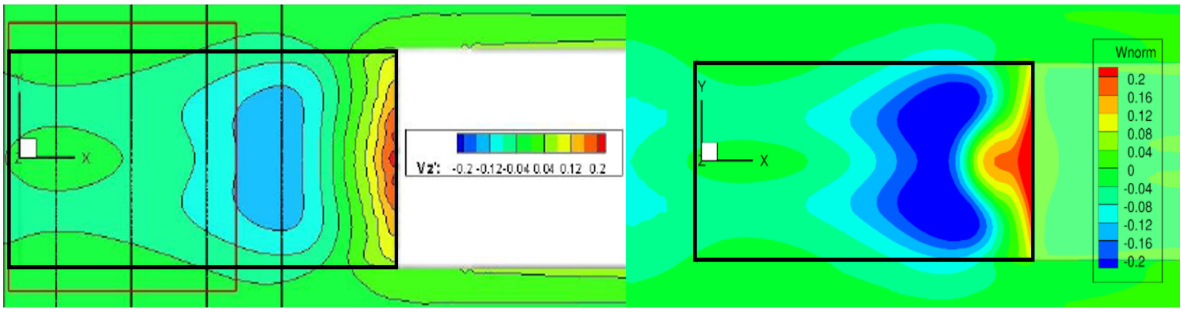

Figure C.4: Contour plot of z-component of the mean velocity normalised with freestream velocity on the L plane. Left: results from Praveen (2018). Right: DeepPurple results.

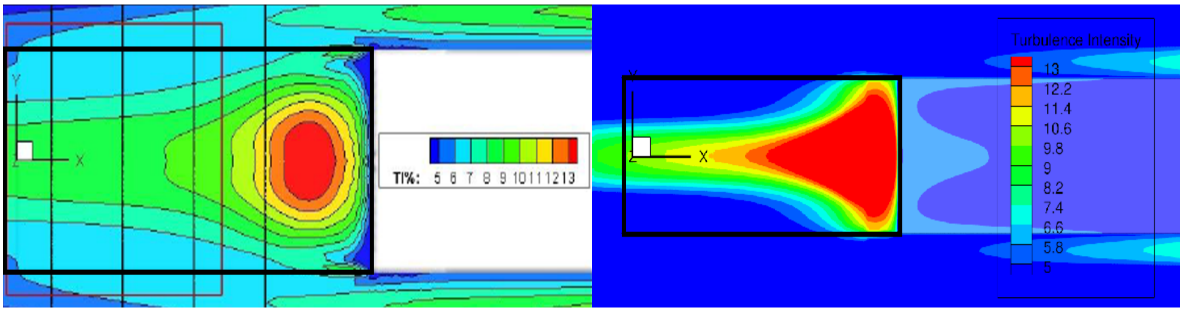

Figure C.5: Contour plot of turbulence intensity normalised with the freestream velocity on the L plane. Left: results from Praveen (2018). Right: DeepPurple results.

In figure C.6 it can be seen that DeepPurple returns more quickly to the freestream condition where the results from Praveen are still influenced by the ship. From this it can be concluded that the recirculation region in DeepPurple is smaller than the region from Praveen. In figure C.7, negative values for the z-component of the velocity should not be confused with an indication of the recirculation bubble which is not necessarily the case. DeepPurple shows stronger downwash values compared to results from Praveen. From figure C.8 it can be seen that the main shape of the contours is slightly comparable, however DeepPurple gives lower values for the turbulence intensity and in a smaller region compared to results from Praveen. This confirms the smaller recirculation region in DeepPurple. The differences between DeepPurple and results from Praveen can most likely be attributed to the different turbulence model used, but may also be caused by different grid settings in the model.

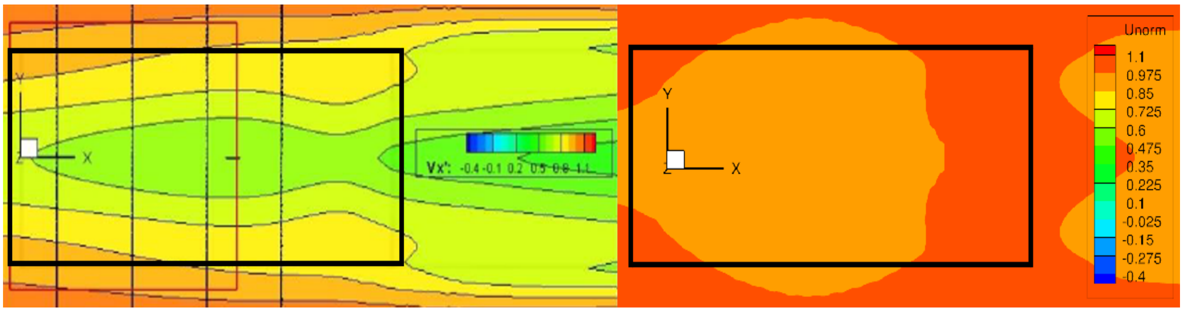

Figure C.6: Contour plot of x-component of the mean velocity normalised with freestream velocity on the M plane. Left: results from Praveen (2018). Right: DeepPurple results.

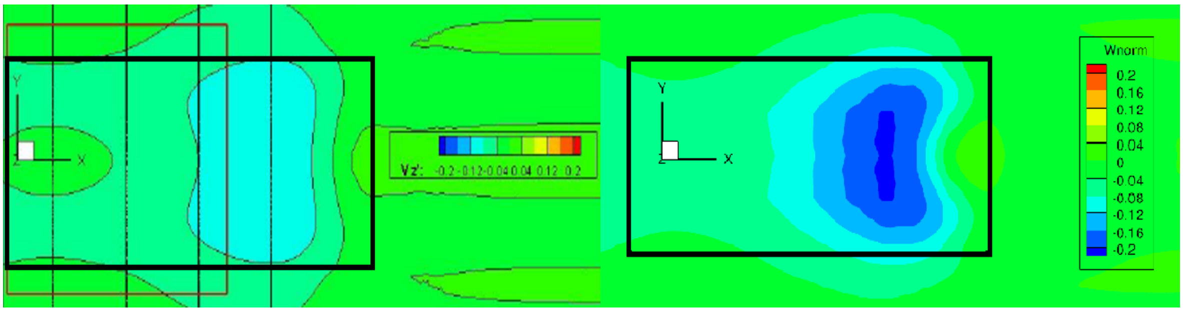

Figure C.7: Contour plot of z-component of the mean velocity normalised with freestream velocity on the M plane. Left: results from Praveen (2018). Right: DeepPurple results.

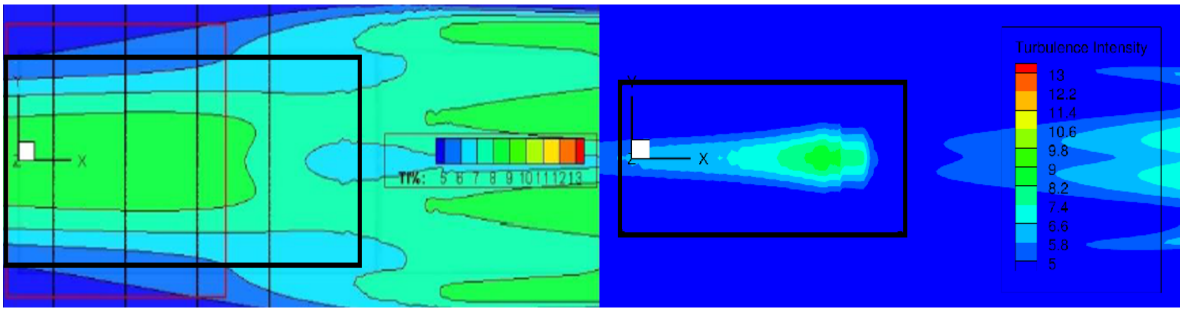

Figure C.8: Contour plot of turbulence intensity normalised with the freestream velocity on the M plane. Left: results from Praveen (2018). Right: DeepPurple results.

C.3 DeepPurple Verification - Test 2 and Test 3

Table C.2 presents the test cases. In *Test2* grid3 is compared to the original grid (total elements 9071370). Grid3 has a refinement of a lesser degree towards the ship geometry and a total number of 2780492 elements. In *Test3* grid4 is compared to the original grid. Grid4 has one level less refinement in the prismatic boundary layer and a total number of 7624442 elements. The following can be concluded from Test 2 in graphs in C.10, C.9 and C.11 and Test 3 in C.12, C.13 and C.14:

- The mean flow solution for *grid3* is less accurate than the *baseline grid*. The differences for the *baseline grid* and the *grid3* is quite significant, which indicates the importance of a sufficient degree of refinement towards the ship.

- The convergence of *grid3* is slightly faster than the convergence of the *baseline grid*.

- The difference between the mean flow solution obtained with *grid4* and obtained with the *baseline grid* is very small which indicates that one level of refinement less in the boundary layer does not influence the mean flow solution significantly when taking data at hangar height at 50% of the flight deck.

- The differences between the convergence of *grid3* and the *baseline grid* is negligible.

Verification Simulations					
Name	Model	Scale	Reynold Nr.	Nr. of Elements	Test
EXP	SFS2	1:100	$6.58{\cdot}10^5$	-	-
DP2 - Grid0	SFS2	Full	$6.58{\cdot}10^5$	9071370	Baseline
DP2 - Coarse	SFS2	Full	$6.58{\cdot}10^5$	1903852	Test 1
DP2 - Fine	SFS2	Full	$6.58{\cdot}10^5$	19100062	Test 1
DP2 - Grid3	SFS2	Full	$6.58{\cdot}10^5$	2780492	Test 2
DP2 - Grid4	SFS2	Full	$6.58{\cdot}10^5$	7624442	Test 3

Table C.2: Simulation used for the Verification of DeepPurple

C.3.1 Test 2: Refinement Levels

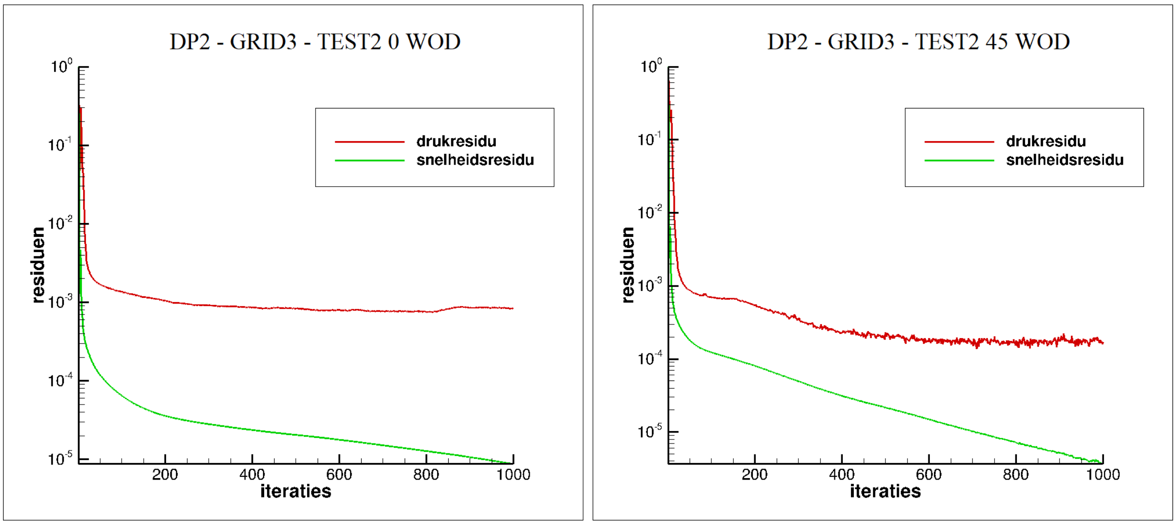

Figure C.9: Convergence Plots from DeepPurple for *DP2- Grid0*, *DP2 - Grid1* and *DP2 - Grid2* for a headwind.

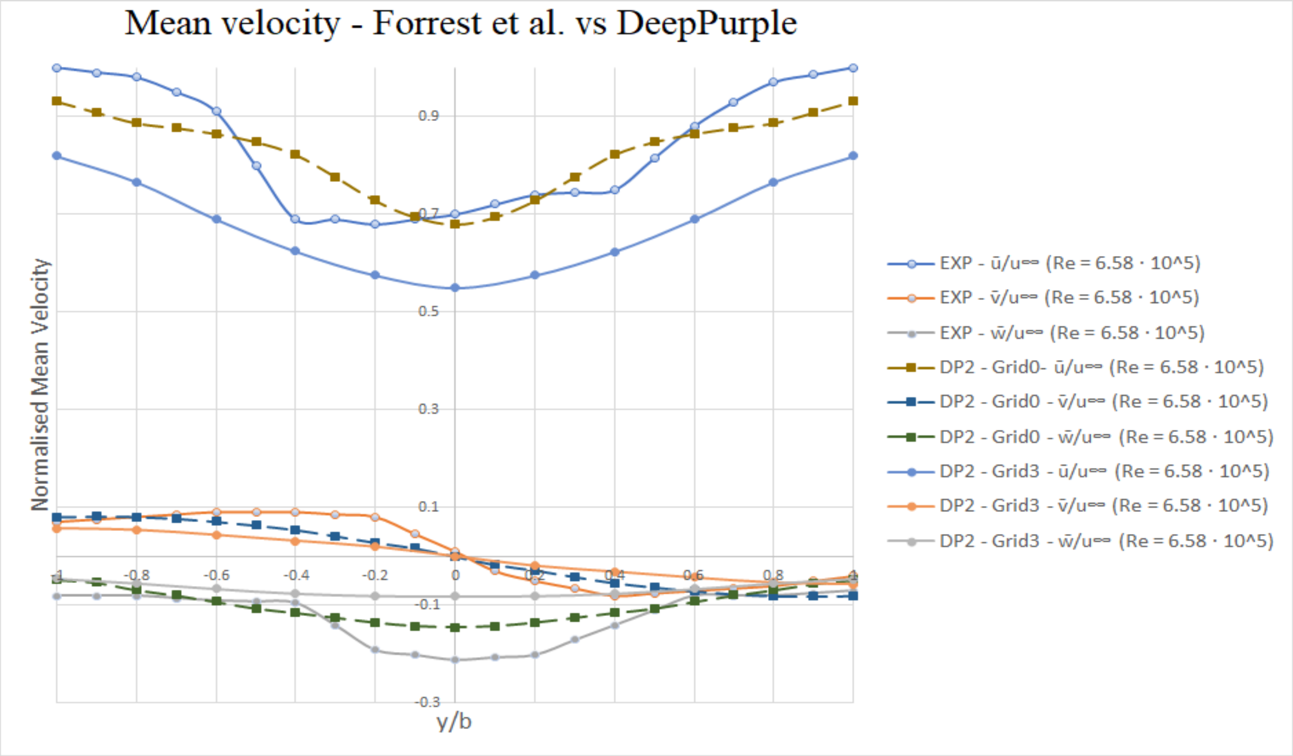

Figure C.10: Headwind condition mean velocity of experiment- (Forrest and Owen, 2010) and DeepPurple data for different grids at 50% deck length measured at hangar height with the lateral position normalized by ship beam b and an uniform inflow.

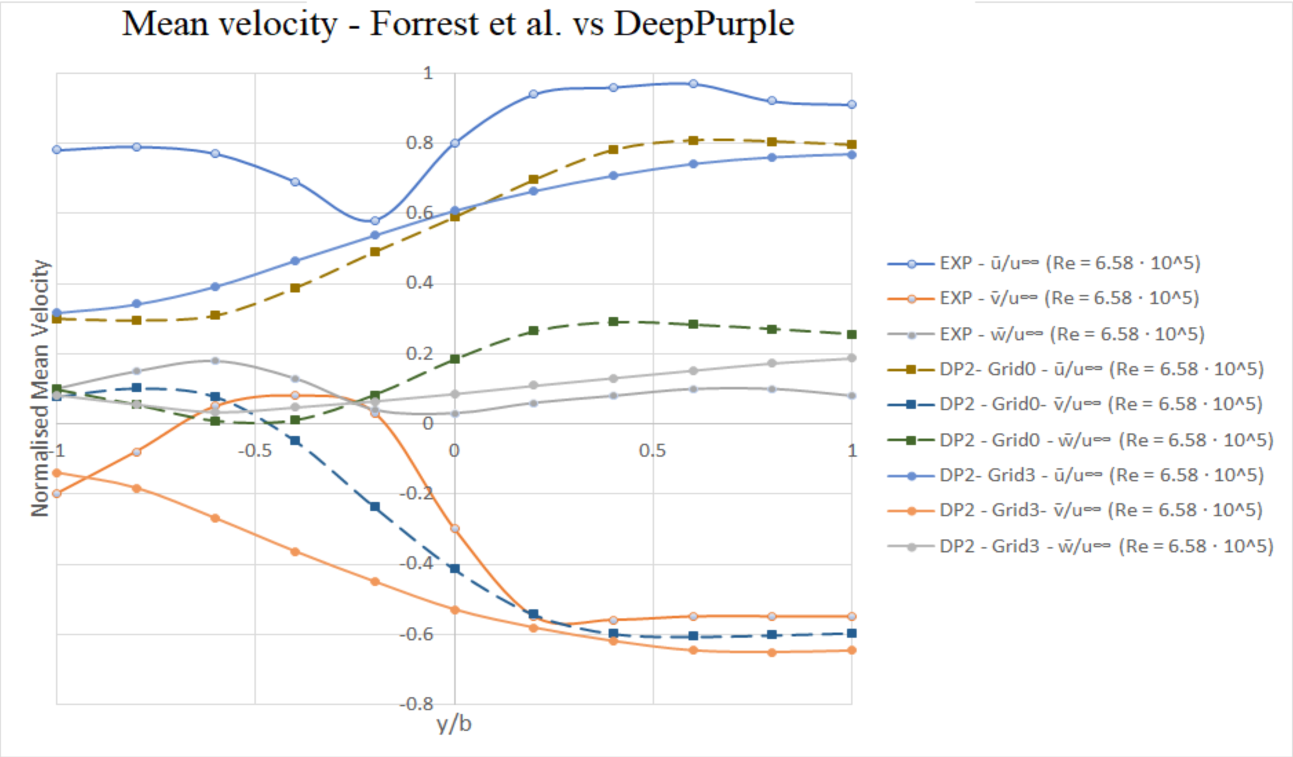

Figure C.11: G45 mean velocity of experiment- (Forrest and Owen, 2010) and DeepPurple data for different grids at 50% deck length measured at hangar height with the lateral position normalized by ship beam b and an uniform inflow.

C.3.2 Test 3: Prismatic Boundary Layer Refinement

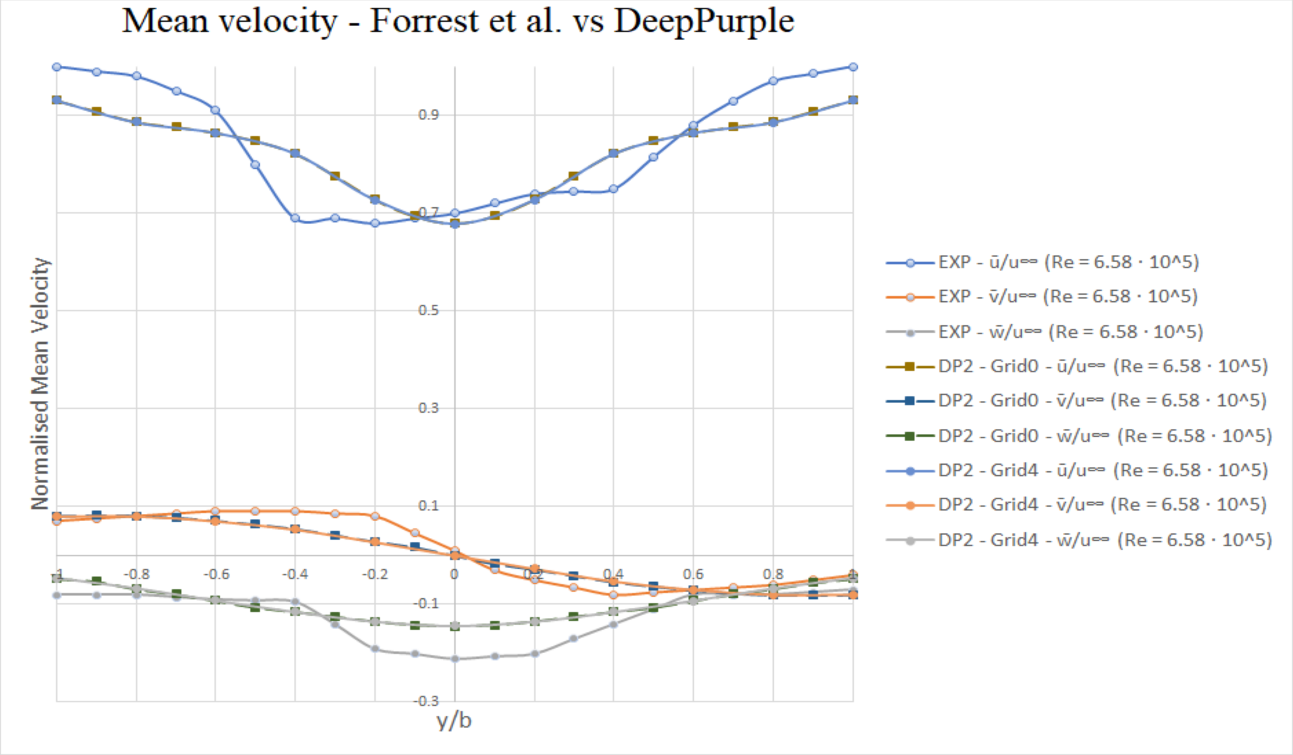

Figure C.12: Headwind condition mean velocity of experiment- (Forrest and Owen, 2010) and DeepPurple data for different grids at 50% deck length measured at hangar height with the lateral position normalized by ship beam b and an uniform inflow.

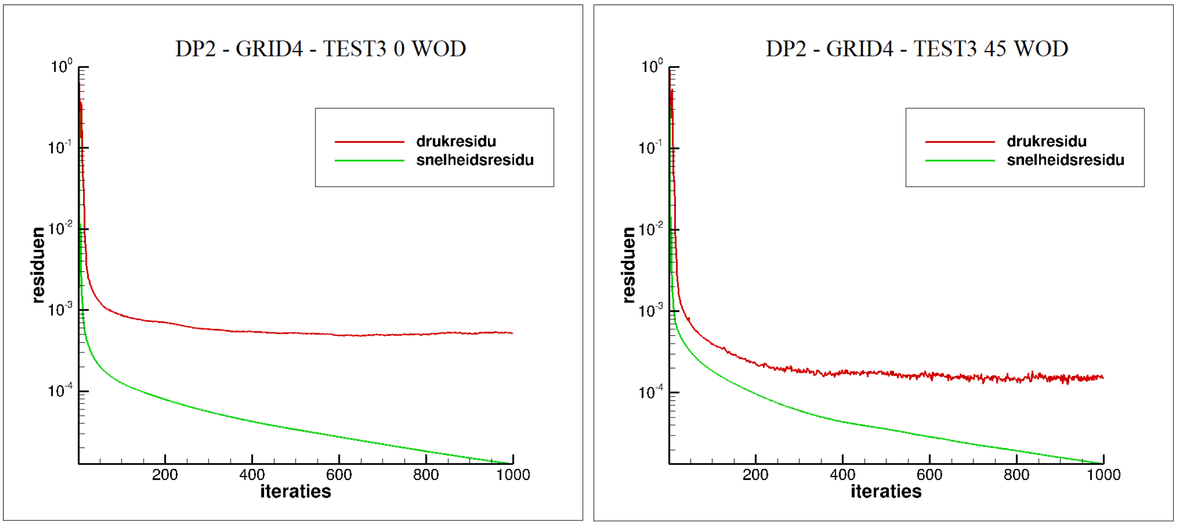

Figure C.13: Convergence Plots from DeepPurple for *DP2- Grid0*, *DP2 - Grid1* and *DP2 - Grid2* for a headwind.

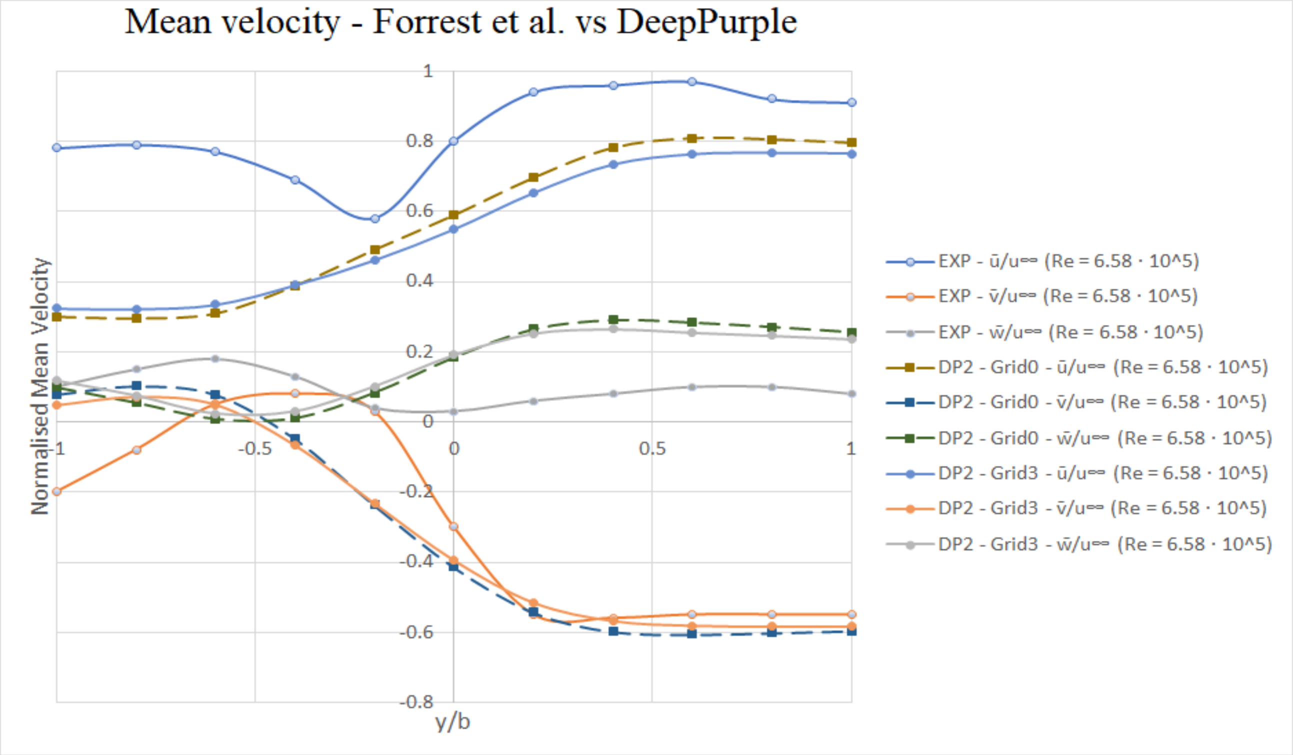

Figure C.14: 45° WOD condition mean velocity of experiment- (Forrest and Owen, 2010) and DeepPurple data for different grids at 50% deck length measured at hangar height with the lateral position normalized by ship beam b and an uniform inflow.

Appendix D

Sea-Trial Pilot Scales

D.1 Deck Interface Pilot Effort Scale

Deck Interface Pilot Effort Scale		
Scale	Effort	Guidance
1	Slight to Moderate	Reasonable compensation required. Tracking and position accuracy is constantly maintained throughout the operation. Fleet pilots will have enough spare capacity to conduct ancillary tasks.
2	Considerable	Significant compensation required. Tracking and position accuracy occasionally degrades during peaks in ship motion, turbulence or sea state. Fleet pilots will have difficulty conducting ancillary tasks.
3	Highest Tolerable	Highest tolerable compensation required. Tracking and positioning accuracy degrades regularly during peaks in ship motion, turbulence or sea state. Fleet pilots will be able to keep up with task requirements but no more. Degraded operations (ship or aircraft) will probably require an abort. Repeated safe operations are achievable.

ACCEPTABLE

UNACCEPTABLE

4	Excessive	Excessive compensation required. Accuracy is poor in one or more axes. Fleet pilots will be purely reacting to external influences rather than anticipating them. A safe abort may not be possible if an aircraft or ship system is lost during a critical phase of the evolution. Fleet pilots under operational conditions could not consistently repeat these evolutions safely.
5	Dangerous	Extreme compensation required. Repeated safe evolutions are not possible even under controlled test conditions with fully proficient pilot.

Table D.1: Deck Interface Pilot Effort Scale modified from Hoencamp (2015)

D.2 Vibration Assessment Rating Scale

Vibration Assessment Rating Scale		
Scale	Definition	Description
0	No vibration	No discernible vibration
1 2 3	Slight	Not apparent to experienced aircrew fully occupied by their task, but noticeable if their attention is directed to it if not otherwise occupied.
4 5 6	Moderate	Experienced aircrew is aware of the vibration but is does not affect their work, at least over short period.
7 8 9	Severe	Vibration is immediately apparent to experienced aircrew even when fully occupied. Performance of primary task is affected of tasks can only be done with difficulty.
10	Intolerable	Sole preoccupation of aircrew is to reduce vibration level.

Table D.2: Vibration Assessment Rating Scale modified Hoencamp (2015)

D.3 Turbulence Rating Scale

Turbulence Rating Scale		
Scale	Definition	Description
1		Flat calm.
2 3	Light	Fairly smooth, occasional gentle displacement. Small movements requiring correction if in manual control.
4 5 6	Moderate	Continuous small bumps. Continuous medium bumps. Medium bumps with occasional heavy ones.
7 8	Severe	Continuous heavy bumps. Occasional negative 'g'.
9 10	Extreme	Rotorcraft difficult to control. Rotorcraft lifted violently several hundreds of feet.

Table D.3: Turbulence rating scale modified from Hoencamp (2015)

Appendix E

More on Ship Helicopter Physics

E.1 Additional Helicopter Physics

E.1.1 Main Controls

The main controls that the pilot has to operate almost continuously are the following: cyclic, collective and pedals. These controls all take effect at the rotor head. In this section a fully articulated rotor head is taken as example as this is the most common rotor head type. In figure E.1 a fully articulated system is presented with three types of hinges.

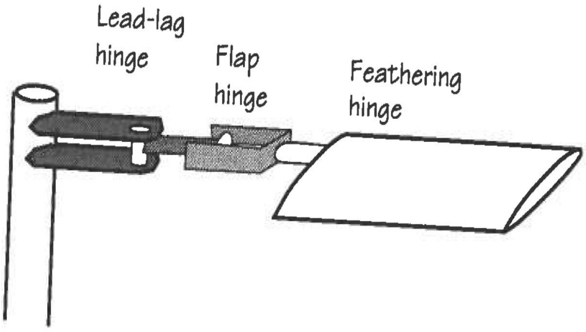

Figure E.1: Fully articulated rotor head (Coyle, 1996)

In order to transmit control inputs to a rotating mass the swashplate system is introduced. The swashplate consists of two main parts, one is fixed to the airframe and one is fixed to the rotor, see figure E.2. The swashplate controls the pitch angle of the rotor blades. The swashplate can introduce a cyclic input to the rotor blades and/or a collective input. A cyclic input to the pitch of the blades will change the pitch of a blade with every cycle, in this way the tilt of the blade-tip path plane (or: direction of the total lift vector) can be controlled. By giving each rotor blade a higher pitch on one side of the cycle and a lower pitch on the other side of the cycle, more lift is created on one side. When more lift is created by a blade, the blade will bend upwards and in this way the blade-tip path is tilted by a cyclic input. When inputting cyclic, the phenomenon gyroscopic precession will play an important role, this will be explained later in this section.

A collective input will alter the pitch angle of the blades equally everywhere, with this the magnitude of the total lift vector can be controlled. Figure E.3 presents a visualisation of the pitch changing system with swashplate. The pitch change rod is connected to a extension of the blade in order to provide leverage against the aerodynamic forces acting on the rotor blade. By tilting the swashplate, a cyclic pitch input is given. By moving the entire swashplate up or down, a collective pitch input is given. Note that, when controlling the helicopter, in general no changes are made to the rotational speed of the blades. Power is controlled by the amount of collective given. Lastly, the pedals are used to control the collective pitch angle of the tail rotor and in this way control the thrust produced by the tail rotor.

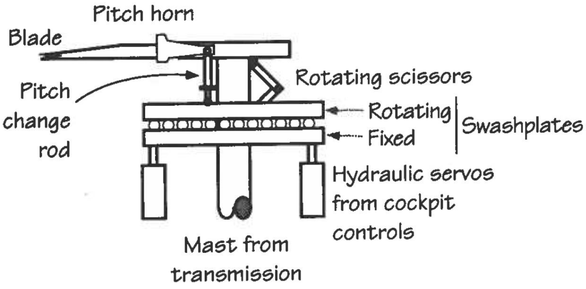
Pitch horn
Blade
Pitch change rod
Rotating scissors
Rotating
Fixed
Swashplates
Hydraulic servos from cockpit controls
Mast from transmission

Figure E.2: The swashplate (Coyle, 1996)

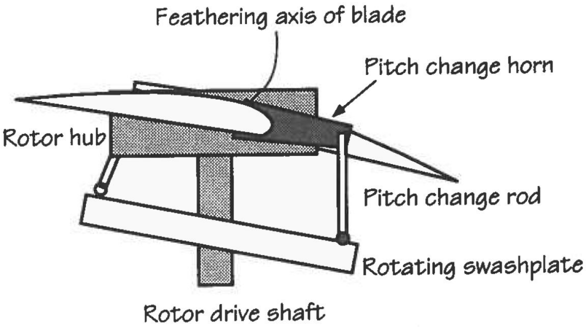
Feathering axis of blade
Pitch change horn
Rotor hub
Pitch change rod
Rotating swashplate
Rotor drive shaft

Figure E.3: Cyclic pitch input (Coyle, 1996)

E.1.2 Helicopter Airwake Features

The rotor wake of a helicopter is very complex, even more so in vicinity of the ground. In this section a concise description is given of the main elements of a rotor wake in stationary hover and away from any influence of the ground. The lift created on the blades of the rotor induce a velocity to the airflow. The flow field that is created due to the induced velocity is also called the slipstream of the rotor. The slipstream is characterised by three main elements: wake contraction, inner vortex sheet and tip vortex.

After the airflow passes the rotor blades, the wake contracts as it propagates downwards. This can be explained by the conservation of mass and a constant mass flow within the boundaries of the wake. The rotor blades accelerate the airflow passing through, and the airflow keeps accelerating further for a bit when propagating downwards in the rotor wake, as is illustrated in figure E.4. As long as the flow within the wake is still accelerating, the wake keeps contracting. For a detailed explanation on the development of these vortices refer to (Eijkman, 2020).

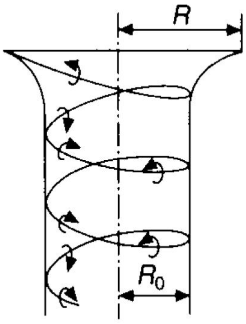

Figure E.4: Wake contraction (Bramwell et al., 2001)

Appendix F

Ship Concept Analysis - General Considerations

There are a few general aspects of the conceptual ship designs presented in 7.4 which are presented below. This involves guidelines for minimum flight deck size and a number of (practical) rules for the location of landing spots.

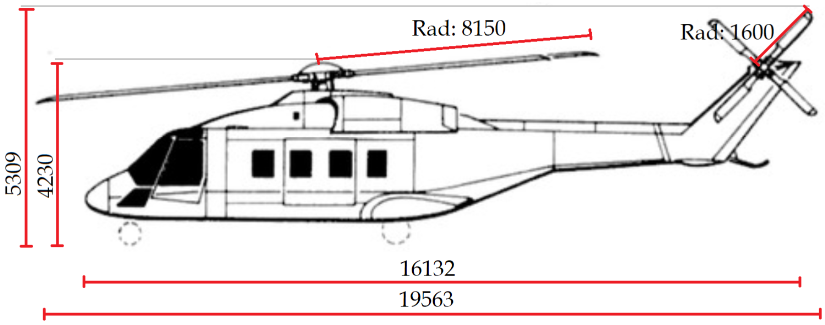

Figure F.1: NH90 NFH dimensions

- In practice, it will be necessary to have deck lines on the flight deck for NH90 operations to guide the helicopter to the grid during landing. Three types of procedures (for each procedure both starboard approach and port approach) per flight deck will be considered, which are: fore-aft procedure, oblique procedure and cross procedure.

- For the cross procedure to be possible, the flight deck needs to have a width of at least 18.8 [m]. This is based on the LCF which is the most slender ship of the Royal Netherlands Navy which still allows for cross-procedures. Ships with flight decks smaller in width than the LCF do not allow for cross-procedures, such as an OPV or an M-Fregat.

- For flight decks behind a large superstructure (+/- 18 [m] height) the minimum distance of the first landing spot to the superstructure is 30 [m]. This is based on the Dutch LPD 1 and LPD 2 design.

- For flight decks behind a small superstructure (+/- 9 [m] height) the (first) landing spot should be at least 15 [m] behind the superstructure. This is based on the current Dutch LCF design.
- The length of the flight deck behind the landing spot has to be at least 10 [m], such that the helicopter is in all cases fully above the flight deck when locked on the grid. The length of the deck lock to the tip of the tail for the NH90 NFH is approximately 10 [m], see figure F.1[1].
- The narrowing of the flight deck of the LPD 2, as can be seen in figure F.2 will also be incorporated in the new designs for the purpose of comparing the limits of the new designs to the LPD2. The narrowing of the flight deck of the LPD 2 does not have any specific functional reason. This became as such because the flight deck design of the LPD 1 was taken, and the LPD 2 ship became larger in width than the LPD 1.
- The landing spots are slightly shifted to the left on the LPD 2 which can be seen in figure F.2. This is to allow a walking lane for crew to get to landing spot 2. In the current research, the walking lane will be left out of the design for simplicity and the landing spots will be placed in the middle of the flight deck.

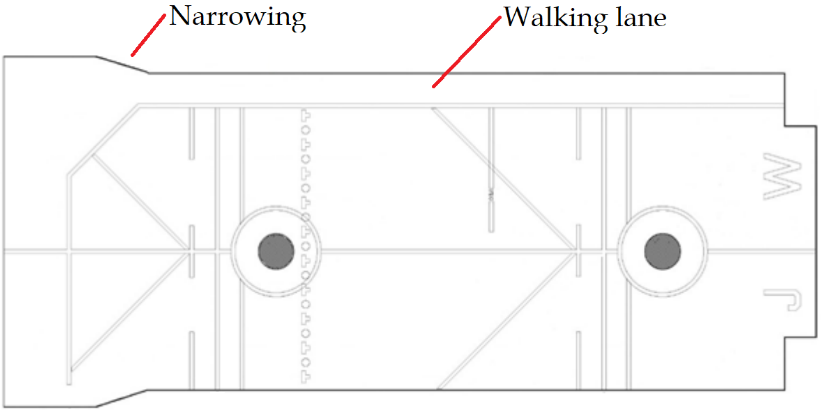

Figure F.2: LPD 2 flight deck design

---

[1] https://www.the-blueprints.com [cited 18 August 2020]